Digital control techniques for electro-hydraulic servosystems

Plummer, Andrew

Award date:
1991

Awarding institution:
University of Bath

DIGITAL CONTROL TECHNIQUES FOR ELECTRO-HYDRAULIC SERVOSYSTEMS

Submitted by
ANDREW ROBERT PLUMMER
for the degree of Ph.D.
of the University of Bath
1991

Copyright

Summary

The research presented in this thesis concerns the application of digital modelling and control techniques to electro-hydraulic servosystems. Some of the techniques are known, but have not been assessed practically for such servosystems before. Other techniques have been developed in order to tackle practical difficulties encountered.

As part of this study, system identification has been shown to be a good way of determining a linear model for digital controller design. A variety of model parameter estimators and structure selection techniques have been evaluated. Using least squares processing filtered data for parameter estimation, and comparing prediction errors to determine the best model order, has been found to be particularly effective. This is despite the non-linear nature of the plant.

Identified models have been successfully used for pole-placement controller design. The desired closed-loop pole positions are chosen with controller robustness and noise response properties in mind. These properties are further enhanced with the addition of a demand filter. Such a filter is particularly important to counteract the destabilising effect of adding integral action to the controller. However for the system under test a new integral control scheme had also to be devised to overcome problems resulting from servovalve saturation.

By combining the lessons learnt from off-line system identification and fixed-coefficient pole-placement control, a very effective indirect adaptive controller has been developed. After comparing several forgetting strategies, a novel covariance trace limiting algorithm was adopted to ensure reliability whatever the demand signal. Adaptation to a variety of plant changes is shown to be rapid, and free from large tuning transients.

The SISO system identification and pole-placement control techniques have been extended to handle multi-channel electro-hydraulic servosystems. The controller extension allows complete dynamic decoupling, and an integral version has been successfully applied to a highly non-linear interacting 2-channel servosystem.

Acknowledgements

I wish to thank the following for their assistance whilst undertaking the research embodied in this thesis:

Dr. Nick Vaughan for his invaluable advice in performing his supervisory role. Other members of the Fluid Power Centre staff under Professor Cliff Burrows for providing a friendly and stimulating working environment. Special thanks to fellow postgraduates Jonathan Gamble, Tony Mercer and Fernando Gomes de Almeida for practical assistance and many useful suggestions.

Thanks also to Dowty Aerospace Gloucester Ltd. for financial support and access to facilities, and to Gilbert Turner and Peter Heffer of that company for their help and co-operation.

Contents

Notation

The following notation is used in this thesis. Frequently symbols are only used in one chapter, in which case the relevant chapter is noted. A different set of notation is used in Appendix 1, and it is described therein.

a_i	Coefficient in $A(z^{-1})$
$a_{ij,k}$	Coefficient k in polynomial element ij in $\boldsymbol{A}(z^{-1})$ (Chapter 9)
$\hat{a}_i(\hat{n})$	Estimated value of a_i based on estimated plant order (Chapter 5)
a_{mi}	Coefficient in $A_m(z^{-1})$
$A(z^{-1})$ or A	Plant model denominator polynomial: $A(z^{-1}) = 1 + a_1z^{-1} + a_2z^{-2} +...+ a_nz^{-n}$
$\boldsymbol{A}(z^{-1})$	Denominator polynomial matrix in left matrix fraction model of multivariable plant (Chapter 9)
$\tilde{\boldsymbol{A}}(z^{-1})$	Denominator polynomial matrix in right matrix fraction model of multivariable plant (Chapter 9)
A_i	Matrix coefficient in $\boldsymbol{A}(z^{-1})$ (Chapter 9)
$A_m(z^{-1})$ or A_m	Desired closed-loop characteristic polynomial: $A_m(z^{-1}) = a_{m0} + a_{m1}z^{-1} + a_{m2}z^{-2} +...$
$\boldsymbol{A}_m(z^{-1})$	Desired denominator polynomial matrix in left matrix fraction model of multivariable plant (Chapter 9)
b_i	Coefficient in $B(z^{-1})$
$b_{ij,k}$	Coefficient k in polynomial element ij in $\boldsymbol{B}(z^{-1})$ (Chapter 9)
$\hat{b}_i(\hat{n})$	Estimated value of b_i based on estimated plant order (Chapter 5)
b_{di}	Coefficient in $B_d(z^{-1})$ (Chapter 9)
$B(z^{-1})$ or B	Plant model numerator polynomial: $B(z^{-1}) = b_1z^{-1} + b_2z^{-2} +...+ b_mz^{-m}$
$\boldsymbol{B}(z^{-1})$	Numerator polynomial matrix in left matrix fraction model of multivariable plant (Chapter 9)
$\tilde{\boldsymbol{B}}(z^{-1})$	Numerator polynomial matrix in right matrix fraction model of multivariable

	plant (Chapter 9)
B_i	Matrix coefficient in $\boldsymbol{B}(z^{-1})$ (Chapter 9)
$B_d(z^{-1})$	Shifted determinant of $\boldsymbol{B}(z^{-1})$ (Chapter 9)
c_i	Coefficient in $C(z^{-1})$
c_t	Part of square root update algorithm (Appendix 4)
C	Matrix formed from controller coefficients (Chapter 9)
$C(z^{-1})$	Plant model numerator polynomial: $C(z^{-1}) = c_1z^{-1} + c_2z^{-2} +...+ c_qz^{-q}$
d	Maximum of n and m
deg	Degree of polynomial, i.e. highest power
D	Matrix used to calculate integral multivariable pole-placement controller filters (Chapter 9)
$D(z^{-1})$	Estimation filter (Chapter 8)
e	Vector of noise samples e_t
e^*	Vector of weighted noise samples e_t (Appendix 4)
$e_{i,t}$	Element i in $\boldsymbol{e}_t$ (Chapter 9)
$e^{-j\omega T}$	Frequency domain equivalent of z^{-1}
e_t	Noise signal (forming equation error) at sample instant t
e'_t	Noise signal (forming output error) at sample instant t
$\boldsymbol{e}_t$	Noise vector (forming equation error) at sample instant t (Chapter 9)
$\boldsymbol{e}'_t$	Noise vector (forming output error) at sample instant t (Chapter 9)
E	Expectation operator
$\boldsymbol{E}(z^{-1})$	Additional polynomial matrix in forward path of multivariable controller (Chapter 9)
f_i	Coefficient in $F(z^{-1})$
$F(z^{-1})$ or F	Controller forward path filter reciprocal: $F(z^{-1}) = f_0 + f_1z^{-1} + f_2z^{-2} +...$
$\boldsymbol{F}(z^{-1})$	Polynomial matrix equivalent of $F(z^{-1})$ for multivariable plant (Chapter 9)
F_i	Matrix coefficient in $\boldsymbol{F}(z^{-1})$ (Chapter 9)
$F_1(z^{-1})$	Factor of $F(z^{-1})$ (Chapter 7)
g_i	Coefficient in $G(z^{-1})$
$G(z^{-1})$ or G	Controller feedback path filter: $G(z^{-1}) = g_0 + g_1z^{-1} + g_2z^{-2} +...$

$\boldsymbol{G}(z^{-1})$	Polynomial matrix equivalent of $G(z^{-1})$ for multivariable plant (Chapter 9)
G_i	Matrix coefficient in $\boldsymbol{G}(z^{-1})$ (Chapter 9)
h_i	Coefficient in $H(z^{-1})$
$H(z^{-1})$ or H	Controller demand filter: $H(z^{-1}) = 1 + h_1 z^{-1} + h_2 z^{-2} + \ldots$
$\boldsymbol{H}(z^{-1})$	Polynomial matrix equivalent of $H(z^{-1})$ for multivariable plant (Chapter 9)
i	An integer
I	Identity matrix
j	Square root of -1
J	Weighted least squares cost function (Appendix 4)
k	Scaling factor for characteristic polynomial (Chapter 5)
k_i	Integral gain (Chapter 7)
k_t	Recursive estimator gain
K	Proportional controller gain (Chapter 3)
$L(z^{-1})$ or L	Open-loop transfer function (Chapter 6)
m	Degree of $B(z^{-1})$ polynomial
$M(z^{-1})$ or M	Plant transfer function (Chapter 6)
$\overline{M}$	Complex conjugate of M (Chapter 6)
n	Degree of $A(z^{-1})$ polynomial or plant order
N	Number of sample points in data set
p	Number of channels (Chapter 9)
$p_{ii}(\hat{n})$	Leading diagonal element in $P(\hat{n})$
P'	Covariance matrix of model parameter estimates
$P(\hat{n})$	Normalized covariance matrix based on estimated plant order (Chapter 5)
$\boldsymbol{P}(z^{-1})$	Integral controller equivalent of $\boldsymbol{F}(z^{-1})$ (Chapter 9)
$\boldsymbol{P}_1(z^{-1})$	Factor of $\boldsymbol{P}(z^{-1})$ (Chapter 9)
P_t	Normalized covariance matrix of estimates at sample instant t
P^*_t	Factor in batch weighted least squares solution (Appendix 4)
q	Degree of $C(z^{-1})$ polynomial
q_t	Factor in batch weighted least squares solution (Appendix 4)
Q	Square root of weighting matrix W (Appendix 4)
$\boldsymbol{Q}(z^{-1})$	Integral controller equivalent of $\boldsymbol{G}(z^{-1})$ (Chapter 9)
r_t	Demand signal at sample instant t

r_t	Demand vector at sample instant t (Chapter 9)
$r_{xy}(\tau)$	Cross-correlation between x_t and y_t at lag τ (Chapter 4)
$R(z^{-1})$ or R	Quantity used in robustness criterion
R_A	Root of piston over area ratio (Chapter 3)
s	Laplace or differential operator
S	Matrix formed from plant model parameters (Chapter 9)
S_t	Square root of P_t (Appendix 4)
t	Time as a number of sample intervals
tr	Trace of a matrix
T	Sample interval
$T(z^{-1})$	Desired characteristic polynomial for all channels (Chapter 9)
T_A	All-pass compensator time constant (Chapter 3)
T_D	Derivative time constant in PD or PID controller (Chapter 3)
T_I	Integral time constant in PID controller (Chapter 3)
$u_{i,t}$	Element i in $\boldsymbol{u}_t$ (Chapter 9)
u_{ct}	Combined control signal in model-reference integral control (Chapter 7)
u_{ft}	Pole-placement control signal, before saturation limits are applied
u_{it}	Integral control signal in model-reference integral control (Chapter 7)
u_{sat-}	Negative valve saturation limit
u_{sat+}	Positive valve saturation limit
u_t	Control signal at sample instant t
u'_t	Filtered version of u_t
$\boldsymbol{u}_t$	Control vector at sample instant t (Chapter 9)
$\boldsymbol{u}'_t$	Filtered version of $\boldsymbol{u}_t$ (Chapter 9)
u_{vt}	Actual valve drive signal (Chapter 3)
$U(s)$	Laplace transform of plant control signal
v_t	White noise signal at sample instant t
$\boldsymbol{V}(z^{-1})$	Product of $\boldsymbol{H}(z^{-1})$ and $\boldsymbol{A}_m(z^{-1})$ (Chapter 9)
V_i	Matrix coefficient in $\boldsymbol{V}(z^{-1})$ (Chapter 9)
w_i	Element ii in matrix W (Appendix 4)
w_t	Noise signal added to plant input at sample instant t
W	Matrix of weights (Appendix 4)
$W(t)$	Matrix of weights up to and including that for sample instant t (Appendix 4)

x_t	Any signal at sample instant t (Chapter 4)
X	Matrix formed from $V(z^{-1})$ coefficients (Chapter 9)
y	Vector of plant output samples y_t
y^*	Vector of weighted plant output samples y_t (Appendix 4)
$y(t)$	Vector of plant output samples up to and including instant t (Appendix 4)
$y_{i,t}$	Element i in $\boldsymbol{y}_t$ (Chapter 9)
y_t	Plant output signal at sample instant t
y'_t	Filtered version of y_t
$\boldsymbol{y}_t$	Plant output vector at sample instant t (Chapter 9)
$\boldsymbol{y}'_t$	Filtered version of $\boldsymbol{y}_t$ (Chapter 9)
$\hat{y}_t(\hat{n})$	Output of plant model using estimated order (Chapter 5)
$Y(s)$	Laplace transform of plant output signal
z^{-1}	Backward shift operator
z^d	Maximum forward shift of $\boldsymbol{B}(z^{-1})$ determinant without making it non-causal (Chapter 9)
z_t	Vector of instruments at sample instant t
$z_t(\hat{n})$	Instrument vector based on estimated plant order (Chapter 5)
Z	Instrument matrix
$Z(\hat{n})$	Instrument matrix based on estimated plant order (Chapter 5)

Greek

α	Trace limit in trace limiting algorithm (Chapter 8)
Δx	(where x is any variable) Estimation error in x (Chapter 6)
ε_L	Limiting *a priori* prediction error in estimator jacketting (Chapter 8)
ε_t	*A posteriori* prediction error (Chapter 8)
ς	Damping ratio
θ	Model parameter vector
$\hat{\theta}(\hat{n})$	Parameter vector estimate based on estimated plant order (Chapter 5)
θ_i	Parameter vector to model output of channel i (Chapter 9)
$\hat{\theta}_{IV}$	Instrumental variable parameter vector estimate (Chapter 4)
$\hat{\theta}_{LS}$	Least squares parameter vector estimate (Chapter 4)

κ	Plant gain (Chapter 4)
λ	Forgetting factor (Chapter 8)
λ_1 and λ_2	Forgetting strategy parameters (Chapter 8)
λ_{min}	Minimum bound on λ_t (Chapter 8)
λ_t	Variable forgetting factor (Chapter 8)
ρ	A root of a polynomial in z (Chapter 5)
σ	Frequency domain modelling error
$\sigma(\hat{n})$	RMS prediction error (Chapter 5)
Σ_0	Required information content of variable forgetting factor estimator (Chapter 8)
Σ_t	Information content of variable forgetting factor estimator at sample instant t (Chapter 8)
τ	Cross-correlation lag (Chapter 4)
ψ_t	Regressor vector at sample instant t
$\psi_t(\hat{n})$	Regressor vector for estimated plant order (Chapter 5)
Ψ	Regressor matrix
Ψ^*	Weighted regressor matrix (Appendix 4)
$\Psi(\hat{n})$	Regressor matrix based on estimated plant order (Chapter 5)
$\Psi(t)$	Regressor matrix based on samples up to instant t (Appendix 4)
ω	Frequency
ω_n	Natural frequency

Superscripts

T	Transpose

Diacritical marks

$\hat{}$	Estimate
$\bar{}$	Simulated value (Chapter 4)

Acronyms

ADC	Analogue to Digital Converter
BLS	Batch Least Squares
DAC	Digital to Analogue Converter
DR	Determinant Ratio
ELS	Extended Least Squares
EVN	Error Variance Norm
GMV	Generalized Minimum Variance
IPM	Instrumental Product-moment Matrix
LQG	Linear Quadratic Gaussian
LVDT	Linear Variable Differential Transformer
MIMO	Multi-Input Multi-Output
PD	Proportional Derivative
PE	Prediction Error
PID	Proportional Integral Derivative
PM	Product-moment Matrix
PRBS	Pseudo-Random Binary Sequence
RIV	Recursive Instrumental Variable
RLS	Recursive Least Squares
RMS	Root Mean Square
SISO	Single-Input Single-Output

1. Introduction

1.1 Motivation

Electro-hydraulic systems combine the high power density of hydraulic actuation with the versatility of electronic control. In many applications feedback is required, often with some form of dynamic compensation, in order to achieve adequate transient and steady-state performance. At present it is common industrial practice to use a classical compensation technique for this purpose, typically a proportional-integral-derivative (PID) controller. This is often manually-tuned to improve transient response and tracking behaviour in the time-domain, or sometimes designed from frequency response data. Although in some circumstances such a controller is perfectly adequate, in many it is difficult to tune and will not extract the full performance potential from the hydraulic plant. The controller can seldom cope with the low damping intrinsic in numerous hydraulic systems, and so an additional leakage path is frequently introduced across the hydraulic actuator which increases damping but compromises the performance in other respects.

Considerable research effort in the control theory field during the last few decades has resulted in a plethora of alternative techniques being proposed for generic (usually linear) plant. Although some of these have been applied to real systems, they have not been widely adopted for industrial control systems. One hinderance is that these more sophisticated controllers are not easy to implement using traditional analogue hardware. However recent years have seen rapid progress in digital electronics, providing increased speed with ever decreasing cost and size. Digital control theory has developed in parallel, allowing straightforward design and

implementation of control schemes within a digital framework. Whereas digital control has been a cost-effective option for slow systems (e.g. those often encountered in the process industries) for some time, it is now also viable for the fast servosystems which are the subject of this study. A digital controller has the additional advantage that it can be part of a computer system which incorporates facilities to improve ease of set up and monitoring, and to allow controller modifications to be carried out in software.

The potential improvements offered by applying modern digital control methods to electro-hydraulic servosystems have motivated several research programmes in this field, some of which are surveyed in Section 1.3. These have shown that there are indeed significant performance benefits to be had. However many difficulties still remain, including how to choose controller design parameters and the best way to obtain a plant model from which the controller can be designed. A particular area of interest in previous research has been adaptive control, where the controller is designed to adapt to unforeseen changes in the behaviour of the hydraulic plant. Although much has been achieved, the ability of such controllers to adapt rapidly to all types of changes, and their reliability under a variety of operating conditions, are still questionable. These problems have been tackled as part of this study.

The ease by which complex control strategies can be implemented digitally also encourages the use of multivariable controllers. Where interacting servosystems have been controlled as individual entities in the past, the application of modern multivariable control theory allows them to be integrated into a single multi-input multi-output system. Thus the interaction between the separate channels can be taken into account by the controller. Multivariable extensions of the digital control techniques investigated in this study are presented.

1.2 Electro-hydraulic servosystems

Electro-hydraulic servosystems were first used in the aerospace industry in the 1950's. Since then they have been adopted widely within many industries where demanded positions, forces or speeds have to be tracked accurately. The common component of all these systems is a

valve which can alter the rate and direction of flow in response to an electrical signal. The servovalve is the device normally used for this purpose in high performance systems. Servovalve design has largely become standardised, consisting of a nozzle-flapper first stage driven by an electric torque motor, and a spool valve main stage. The servovalve requires precision manufacture but gives accuracy and fast dynamic response. A cheaper equivalent is the proportional valve, in which the spool is directly driven by a solenoid. Currently such valves are of lower bandwidth, and have not been used in this work.

Electro-hydraulic servosystems come in many forms. They can have linear or rotary actuation in order to control linear or angular displacement, velocity, or force. The aim of this study has been to investigate the applicability of advanced control methods to such servosystems in general, rather than to a specific system. To achieve this a variety of systems have been tested, including both control of force and displacement. However for consistency and comparison purposes the single-input single-output (SISO) methods are illustrated by application to one electro-hydraulic position control system. This exhibits many of the problems typical of hydraulic systems, including non-linearities and low damping. Another typical system, with one position and one force control channel, is used to show the multivariable work.

1.3 Background

Previous research into advanced controllers for electro-hydraulic servosystems is briefly surveyed in this Section. More specific and detailed accounts of some of the papers are given in the later chapters to which they are relevant.

The traditional closed-loop control methods used for electro-hydraulic servosystems — be they simply proportional controllers or have other compensation terms as well — have been known for many years to have deficiencies. Early attempts to improve controller performance used an adjustable controller gain to adapt to plant changes (Porter and Tatnall, 1970; Hesse, 1973). Although these studies showed promise, they used large and costly analogue controllers, and

proved impractical to develop further. However the importance of accurate modelling of electro-hydraulic plant had also been realised by this time, with parametric models in the form of continuous-time transfer functions being derived from experimental data (Parker and Desjardins, 1973).

The prospects for the application of advanced controllers to real systems greatly improved when the use of microprocessors became widespread during the 1970's. The microprocessor enabled sophisticated digital electronic devices to be constructed relatively cheaply. However unlike their analogue counterparts, digital controllers are limited in bandwidth by their sampling rate. This limitation was thought to preclude the use of digital controllers for all but the slowest servosystems. For example reviews by Maskrey (1978) and Huckvale (1984) suggested that some of the best ways of harnessing the power of the microprocessor were in sequence controllers, pre-loop processing, and "smart" redundancy. Closing the loop digitally was largely dismissed on the grounds of bandwidth limitation. Thus whilst a number of applications of advanced digital control techniques to slower systems were made in other industries, little was done for electro-hydraulic servos. However in more recent years the substantial increase in microprocessor speed has invalidated the objections to direct digital control. Whereas the conclusions of Maskrey (1978) were based on an 8-bit microprocessor running at 2MHz, nowadays 32-bit microprocessors running at 20MHz or more are widely available. Thus an upsurge of interest in applying advanced digital control techniques to electro-hydraulic servosystems is now apparent.

Many studies have presented simulation results only, particularly in the field of adaptive control — such as Panossian (1986), Kulkarni *et al* (1984), and Keller and Jiashi (1983). In some cases a linear model has been used to simulate the electro-hydraulic plant (Watton, 1988), even though this is unlikely to be a realistic representation. These simulation studies have not convinced sceptical practitioners in the electro-hydraulic field of the merits of digital control.

However a number of successful applications have been reported. These include fixed-coefficient model-following schemes described by Hori *et al* (1989), Parkkinen *et al* (1988), and Pietola and Vilenius (1989). Saffe and Feigel (1988) relate some non-linear controller applications. Much emphasis has been placed on adaptive control though, with work by Takahashi (1985), Vaughan and Whiting (1986), Edge and Figueredo (1987), Daley (1987 and

1989), Hori *et al* (1988a and b), Unbehauen *et al* (1988) and Köckemann (1990). Some of these are reviewed in more detail in Section 8.1. Surprisingly few applications of multivariable controllers to interacting multi-channel electro-hydraulic servos have been reported, Pannala *et al* (1989) being an exception. This promises to be an important growth area in the future.

Despite the existence of some successful applications, commercial interest remains low. Although electro-hydraulic servosystems with digital controllers are now becoming available (Henke, 1987), concentration is on discretized versions of traditional control methods. Uncertainty still remains about the reliability of the more advanced methods, and their applicability to a wide range of different systems. This study aims to build on previous research to take a step towards solving these problems.

1.4 Thesis outline

Chapter 2 describes the electro-hydraulic positioning system which was the main test bed for the control methods, and for which results are presented. A physical analysis of the system is presented in Appendix A. The computer system is also described, including the processor and interfacing hardware, and supporting software tools.

Chapter 3 introduces a variety of controller design techniques. The inadequacies of a PID controller are demonstrated, and alternative strategies discussed. The basic pole-placement controller is presented in more detail as it is the mainstay of subsequent chapters. It is seen that an accurate mathematical model of the plant behaviour is the key to designing better controllers. Thus system identification, which is the process of estimating a plant model from input-output data, is an important part of the controller design process. Methods of combining model estimation and controller design on-line to form an adaptive controller are also briefly reviewed, as is the need for integral control action.

System identification is the subject of Chapter 4. In particular a number of model parameter

estimators are compared, assuming a certain model structure to be correct. The success of each estimator is assessed by designing a pole-placement controller from the estimated model and comparing the resulting system response with the desired response: the error is a measure of model inaccuracy. The results are contrasted with those of a similar procedure based on a digital plant simulation, which allows actual and estimated plant parameters to be directly compared.

The system identification theme is continued in Chapter 5 by comparing a variety of model structure selection techniques. The structural information required for a model which is to be used in pole-placement controller design can be reduced to one order; this is discussed first. Then three basic criteria for selecting the best structure are introduced. The controller responses for models of varying structure are presented, from which the best structure in practice can be determined. The structure selection techniques are then rated by how clearly they pick out this best structure.

Chapter 6 describes the pole-placement controller design method in more detail. Means of improving noise attenuation and robustness to modelling errors are described. These involve the inclusion of a demand filter in the controller, and careful choice of closed-loop pole positions. The theoretical results are also used to show that increasing the sample rate can have a detrimental effect on controller robustness. This is confirmed in practice.

Extending the pole-placement controller to endow it with integral action is covered in Chapter 7. Two ways of achieving this are presented, the first of which is unsuccessful in practice. This lack of success can be traced to inferior robustness and noise characteristics by using the techniques introduced in Chapter 6. The second method gives much improved closed-loop performance.

Two areas described in earlier chapters — parameter estimation and pole-placement control — have been combined to form an indirect (self-tuning) adaptive controller, presented in Chapter 8. Methods of allowing the estimator to forget old data, and thus adapt to variations in plant characteristics, are compared. A method is adopted which exhibits rapid adaptation and yet prevents the parameter estimates from drifting when the plant dynamics are not fully excited. The response of the adaptive controller is shown under various operating conditions and plant parameter changes.

Multivariable modelling and control are considered in Chapter 9. Some of the techniques presented in earlier chapters are extended to enable decoupling control of multi-channel servosystems. The extension of system identification to find a polynomial matrix fraction model for the plant is quite straightforward. However multivariable pole-placement design raises new issues which are discussed, and a new method is proposed. The method is validated using a simple simulation, and then applied to a 2-channel electro-hydraulic servosystem.

Conclusions and suggestions for further work are contained in Chapter 10.

2. Position control system hardware

2.1 Introduction

An advantage of digital control is that control methods can be implemented and improved relatively easily in software. Thus the hardware — both electronic (computer, interfacing etc.) and hydraulic — can remain the same whilst performance is improved purely by enhancing software control algorithms. Of course the hardware will limit the ultimate performance of the system, and it is this limit which a good control algorithm should approach.

In this Chapter the hardware which forms an electro-hydraulic position control system is described. This is the system used to test the modelling and control techniques presented in later chapters. Included are the hydraulic and mechanical aspects of the actuation system and load, and the computer system on which the control algorithms are developed and implemented.

2.2 Hydraulic actuation and load

2.2.1 Description

The main two constituents of the plant are the load and the actuation system, shown diagrammatically in Figure 2.1. The load consists of a 890kg mass mounted on a low friction

trolley allowing 0.6m of horizontal movement. The requirement is to move the mass accurately and quickly to any demanded position within this range. The actuator is a single-ended hydraulic cylinder supplied via a 2-stage nozzle-flapper servovalve connected to the cylinder by short lengths of rigid pipe. Supply pressure is controlled by a proportional electro-hydraulic pressure relief valve giving 160bar maximum. Normal operating pressure is 100bar. Extra 'dead' oil volumes can be switched into the hydraulic circuit either side of the cylinder. The increase in oil compliance changes the dynamics of the plant, and is used to test the behaviour of control strategies under such circumstances. Each oil volume is 2 litres. A wirewound potentiometer is used to measure load position. Photographs of the plant are shown in Figures 2.2a and b, and the component specifications are summarised in Table 2.1.

2.2.2 Analysis

Appendix 1 contains an analysis of the positioning system. A linear model is derived, but only by considering small perturbations about one valve opening and one actuator position. Neglecting valve dynamics, the general model is fourth order but reduces to third order at one point in the stroke (dependent on the piston area ratio) and when operating around zero valve opening. The main non-linearities are summarised below:

- the square law relating valve pressure and flow (so that only small perturbations in valve opening can be accommodated by the linearised model),
- the change in stiffness of the oil volumes either side of the piston as the piston position changes (so that only small perturbations in position can be accommodated by the linearised model) — for example giving higher natural frequencies towards the ends of the stroke,
- the difference in area between the two sides of the piston, giving a change in behaviour when the valve opening changes sign — for example the no-load steady-state velocity gain is theoretically greater by the root of the area ratio, in this case 1.21, in the extend direction as compared to the retract direction (see equation A1.25),
- valve saturation.

Other non-linearities include coulomb friction in load and actuator, and backlash in the cylinder body and piston rod mountings, both of which are neglected in formulating the linear model.

Another important feature which is highlighted in the Appendix is leakage, which is the main factor determining the damping present in the system when the valve is closed.

2.2.3 Response

Figure 2.3 shows the response of the plant (operating in open-loop) to a pulse input. The response is plotted from sampled data, with a 10ms sample interval. The actuator starts at mid-stroke, and the pulse height corresponds to full valve opening. Low damping is evident when the valve is shut off, and the integrating nature of the plant is seen by the final non-zero position. The oscillatory response is typical of such systems in which the relatively large mass 'bounces' on the oil volumes in the cylinder. The natural frequency is about 12Hz, with a damping ratio in the region of 0.03. The natural frequency is sufficiently lower than the bandwidth of the valve for the dynamics of the latter to be neglected. A plant frequency response (near mid-stroke), derived from a closed-loop swept sine test, is shown in Figure 2.4.

Figure 2.5 shows the response to a negative going pulse, illustrating the larger gain in the extend direction.

Figure 2.6 shows the response when the actuator is nearly fully retracted. The natural frequency has increased to about 14Hz, which is the maximum frequency given by any stroke position. Note that the downward drift in position shown by the Figure is due to inexact nulling of the valve spool, possibly due to spool friction.

Figure 2.7 is a pulse response carried out with the dead oil volumes switched into the system. The natural frequency has been reduced to 7Hz, and the damping ratio is about 0.07.

Further response tests of the same plant, albeit with a different valve, are contained in Whiting (1987).

2.3 Computer system and interfacing

The computer system on which the control software is implemented is based around an Inmos T800 transputer microprocessor. The transputer and 2Mbytes of RAM are resident on an expansion card in an IBM AT-compatible computer. The user interface software runs on the AT, accessing screen and keyboard, and communicating with the transputer via one of the latter's four serial links. Two of the remaining links are used for analogue interfacing, one connected to an analogue to digital converter (ADC) and the other to a digital to analogue converter (DAC). The arrangement is depicted in Figure 2.8. There are eight ADC channels and four DAC channels, all of which are 12-bit. One channel of the ADC is used to read the potentiometer voltage via a buffer, giving a resolution of about 0.15mm. One DAC channel is connected to a voltage to current conversion amplifier which drives the servovalve. The specifications for the various parts of the system are summarised in Table 2.2.

The T800 transputer is capable of fast floating-point computation (as it has an on-chip floating-point unit), allowing sophisticated control algorithms to be applied to systems requiring rapid sampling. It is also designed for use as a building block in parallel computers, so by connecting additional transputers via the spare link, the computational power can be further increased. The transputer is programmed using 3L Parallel C, which is a standard C language implementation with extensions to allow parallel programming. 64-bit floating-point arithmetic is used throughout.

Valve:	Zero-lap
	Bandwidth greater than 50 Hz
	Flow gain at 70 bar, 3.8(L/min)/mA
	Saturation at 9mA
Cylinder:	Stroke 610mm
	Piston area 2025mm^2
	Annulus area 1380mm^2
Load:	890kg mass
	Very low coulomb and viscous friction
Position feedback:	Wirewound potentiometer
	Zero at centre stroke
	Retract is positive direction
Supply pressure:	variable to 160bar

Table 2.1 Electro-hydraulic positioning system specification

Main processor card:	20MHz 32-bit T800 Inmos Transputer (10Mbits/s links) plus 2Mbytes DRAM.
Host:	IBM AT-compatible (with 12MHz 80286 microprocessor plus 80287 co-processor) providing user interface.
ADC:	12-bit, 8-channel, 5µs conversion, 10µs communication (via transputer link), no anti-aliasing filters, -10V to +10V range.
DAC:	12-bit, 4-channel, 8µs settling time, 10µs communication (via transputer link), -10V to +10V range.
Potentiometer:	approx 0.3V/cm.
Valve drive amplifier:	approx 3.3mA/V.

Table 2.2 Computer system and interfacing

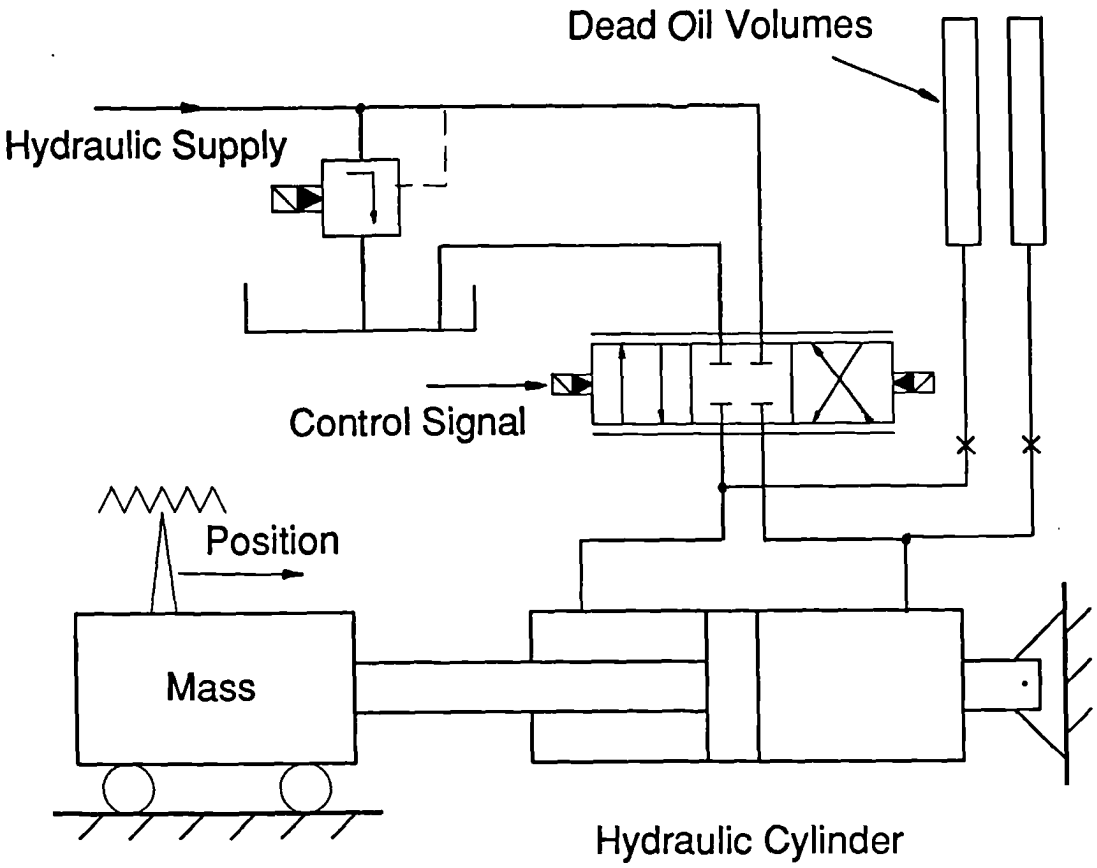

Figure 2.1 Electro-hydraulic position control system
(see Figure A1.1 for a valve schematic)

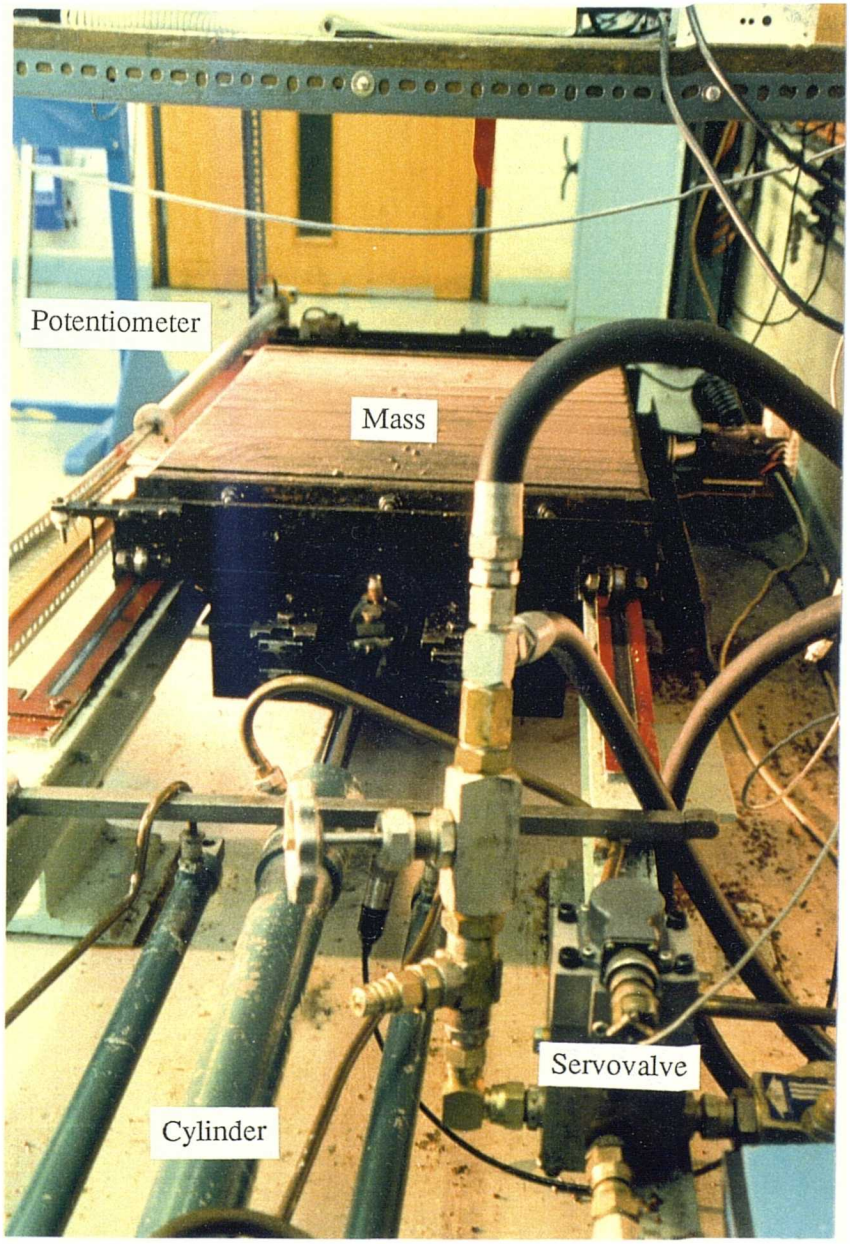

Figure 2.2a Electro-hydraulic position control test rig

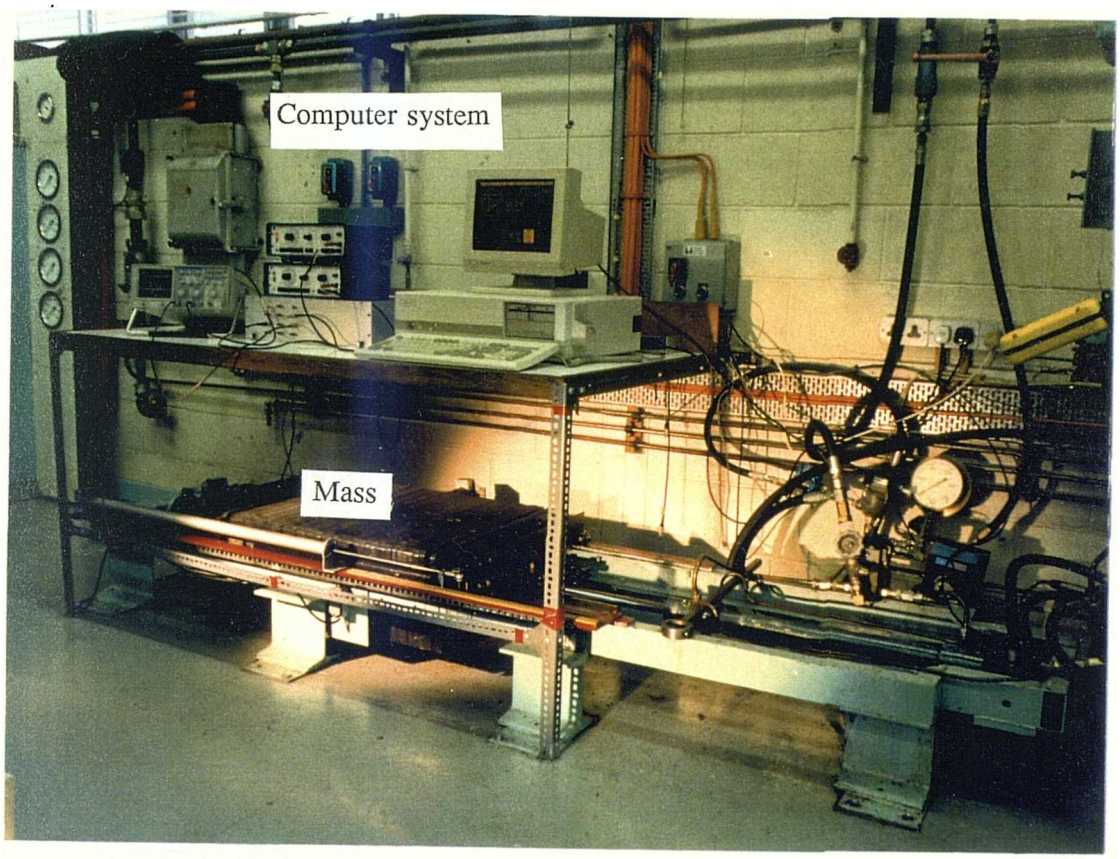

Figure 2.2b Electro-hydraulic position control test rig

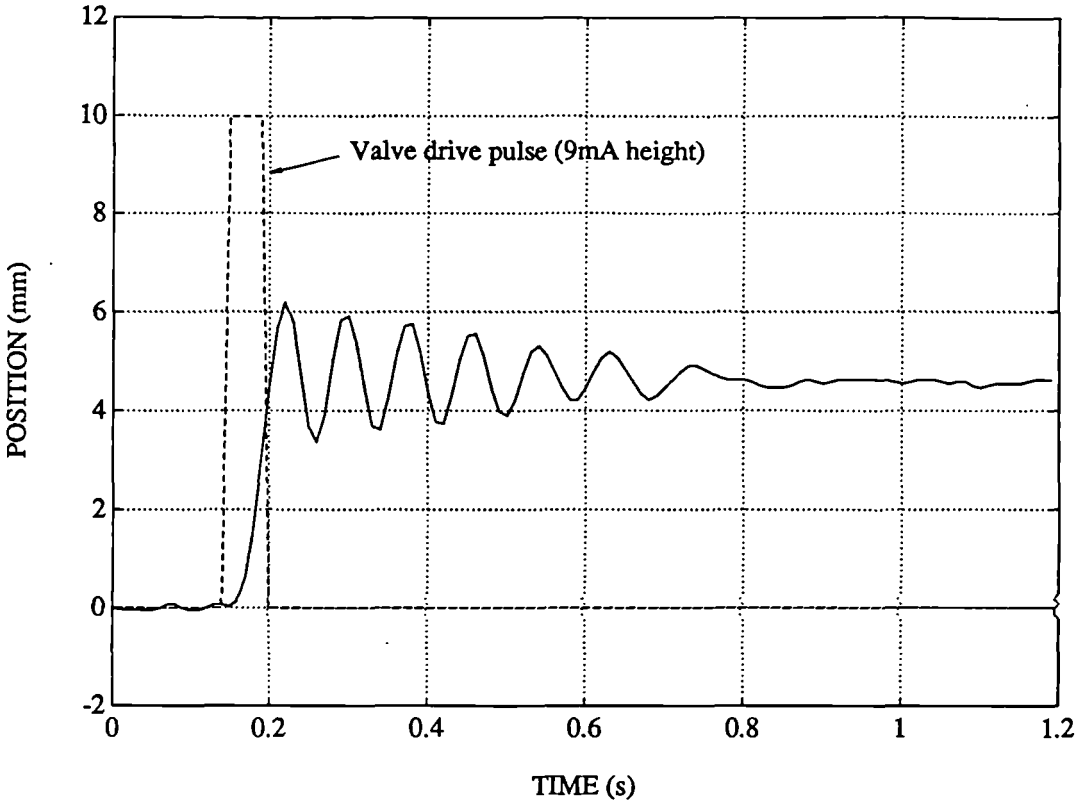

Figure 2.3 Pulse response (retract direction)

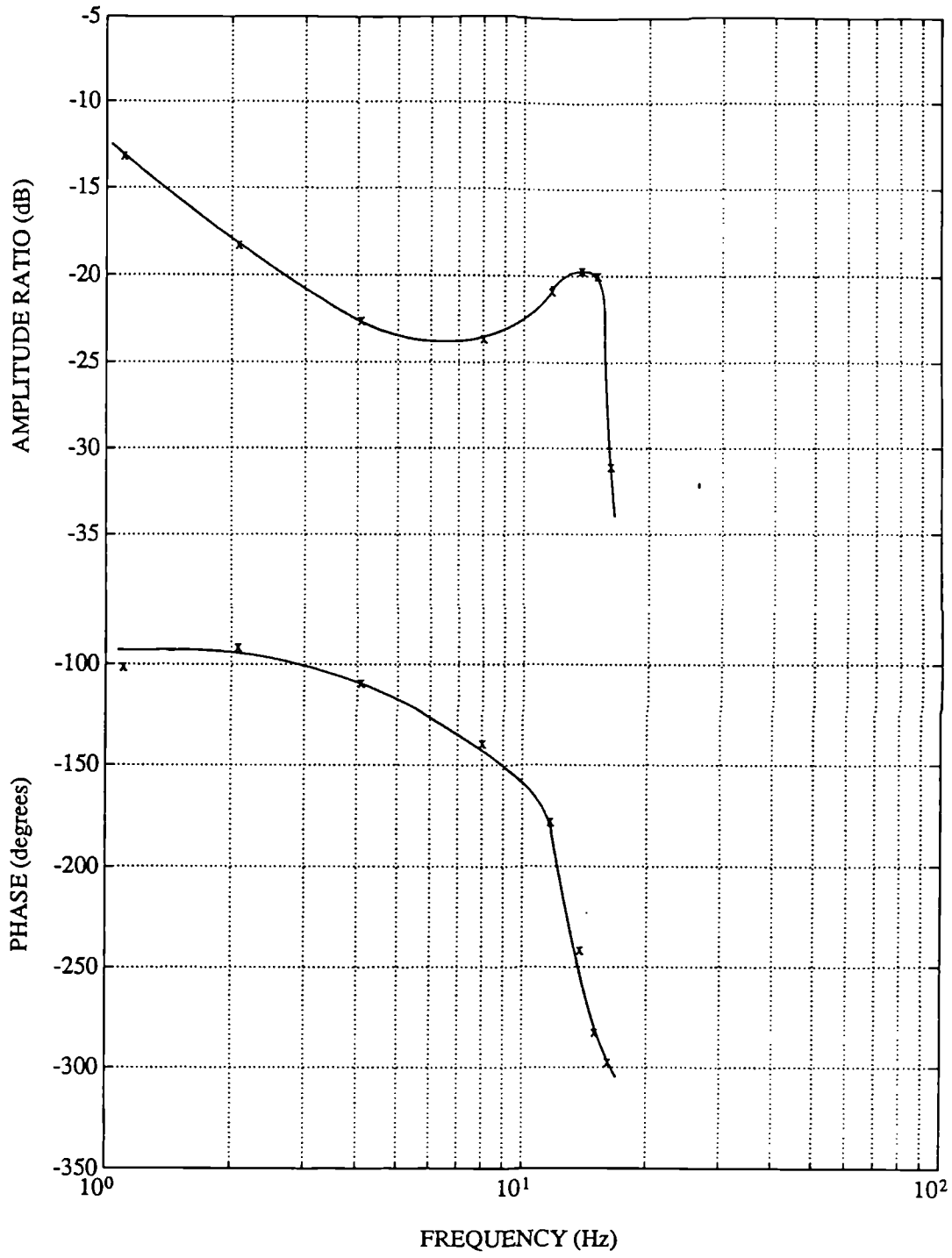

Figure 2.4 Plant frequency response

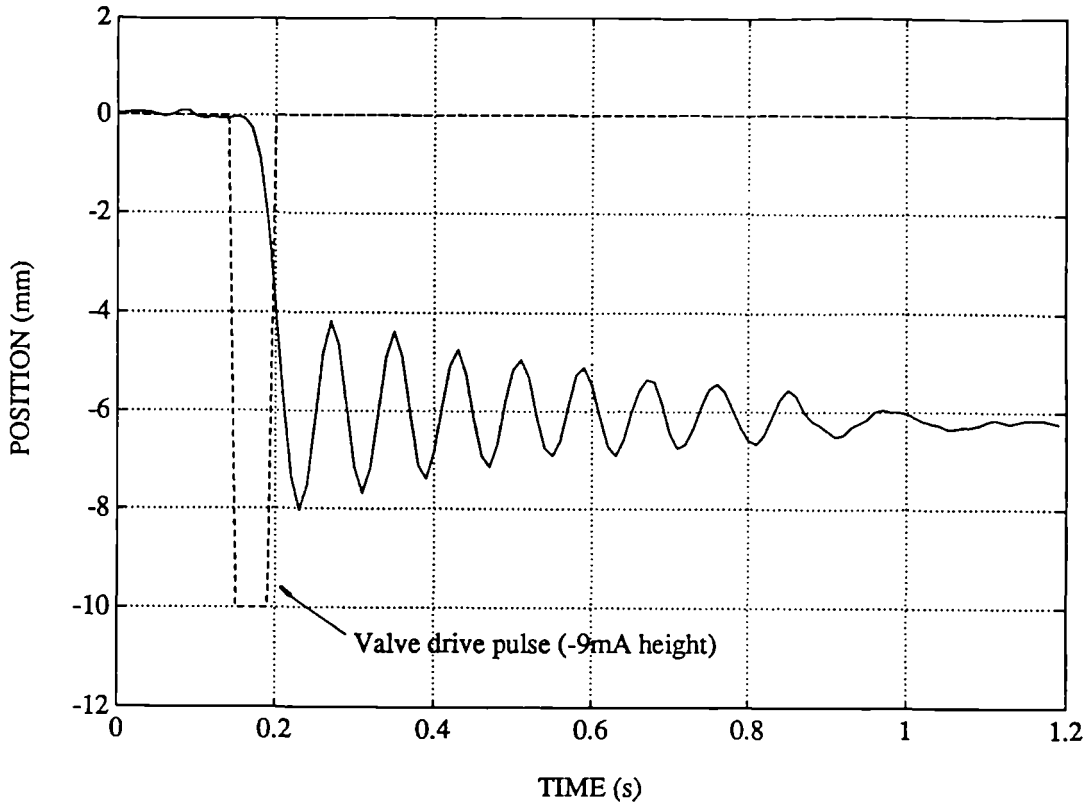

Figure 2.5 Pulse response (extend direction)

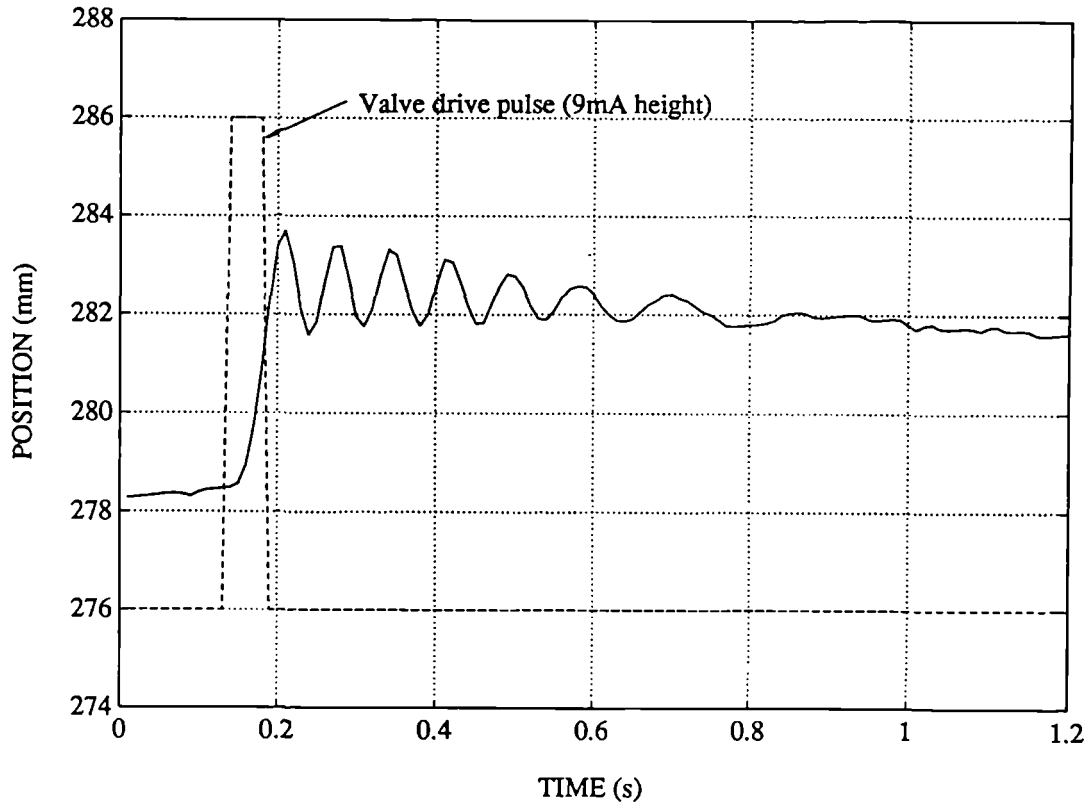

Figure 2.6 Pulse response (nearly fully retracted)

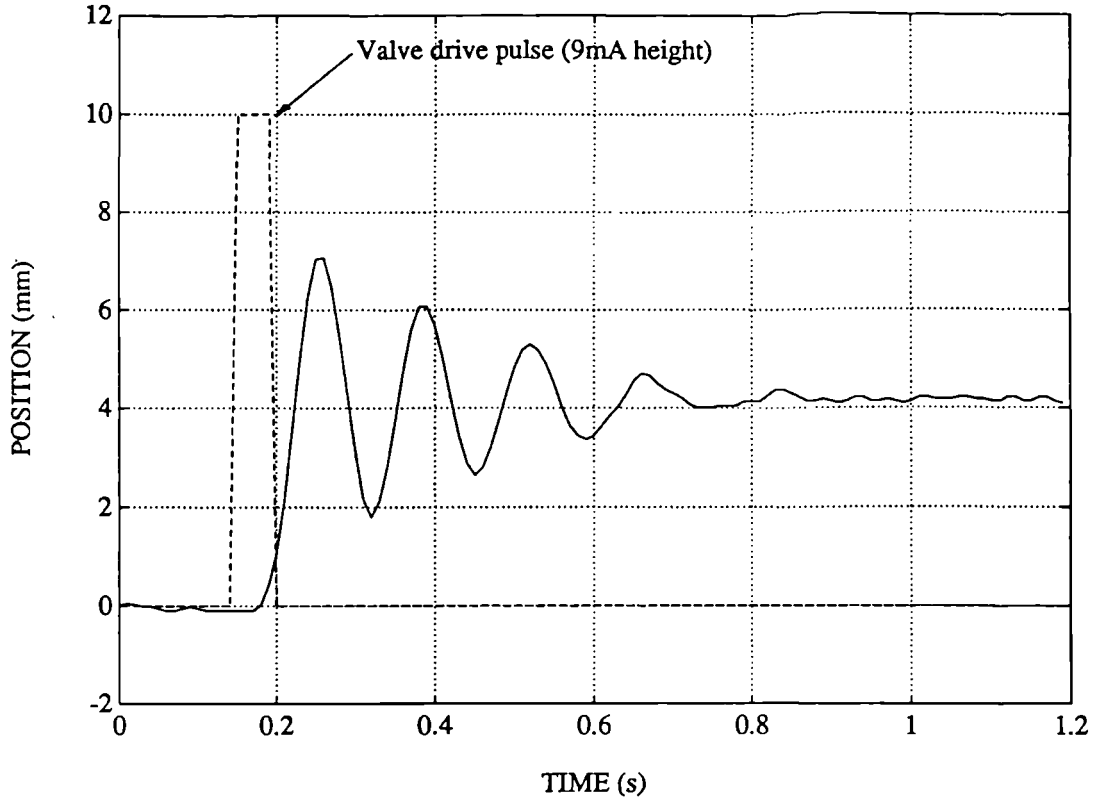

Figure 2.7 Pulse response (with dead oil volumes connected)

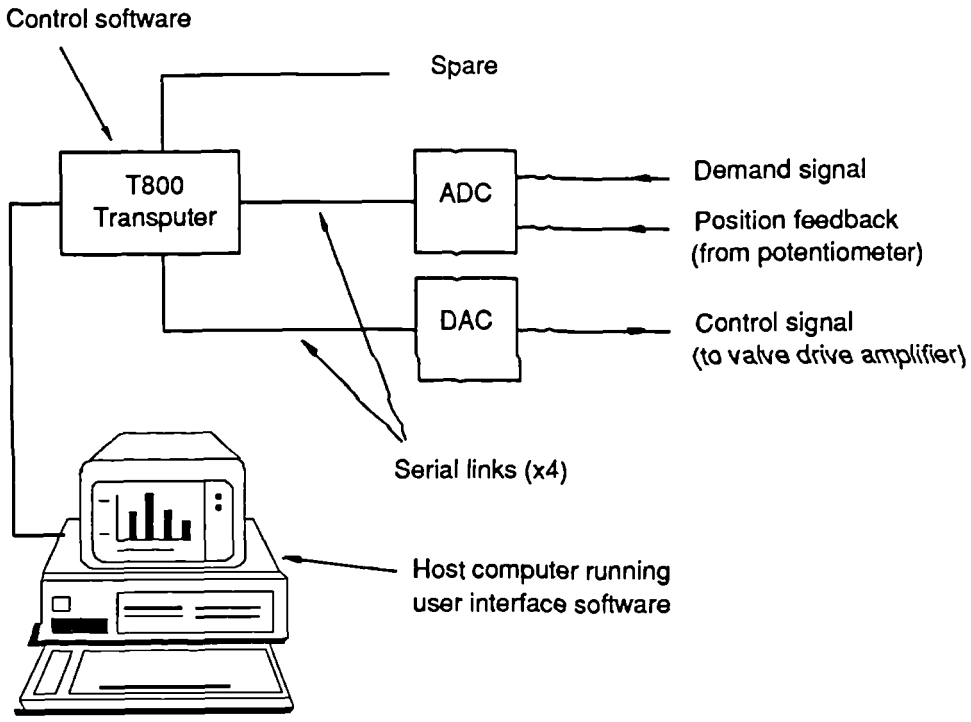

Figure 2.8 Computer system

3. Review of control methods

3.1 Introduction

A variety of possible control strategies for electro-hydraulic servosystems are reviewed in this Chapter. A conventional proportional plus derivative (PD) controller is applied to the electro-hydraulic positioning system, but design difficulties are encountered, and the closed-loop performance is not very good. More sophisticated controllers potentially offer better tracking of the demand position in the following ways:

- improved transient response in terms of greater speed and reduced oscillation,
- insensitivity to disturbances, such as low frequency load forces, or high frequency sensor noise,
- insensitivity to changes in plant parameters, ideally minimizing changes in performance but most importantly maintaining stability,

They may also offer easier controller design.

Adaptive schemes are among the controllers reviewed, as is the need for integral control, and the latter is illustrated in Section 3.4 by application of a PID controller to the positioning system of Chapter 2. Pole-placement control is described in more detail than the other methods, in preparation for its use in Chapters 4 and 5. An in-depth analysis can be found in Chapter 6.

The controller must be able to perform well despite the non-linearities inherent in most electro-hydraulic servosystems, and ways of coping with two particular non-linearities are

discussed in Section 3.6. These are the directional gain change associated with single-ended cylinders, and servovalve input saturation.

3.2 PD controller

Figure 3.1 shows the response of the positioning system using a unity gain proportional controller. By adding some form of dynamic compensation it should be possible to improve the speed of response yet reduce the oscillation. Hydraulic modifications to increase damping are one solution, either by adding a bleed orifice across the actuator or using an underlapped valve. However these can significantly reduce the actuator bandwidth and promote steady-state error (Mcloy and Martin, 1980). Another solution is to mechanically damp the load, but apart from the additional cost involved this will reduce the maximum load velocity. If these alternatives are rejected, a solution must be sought by changing the electronic controller. The use of additional feedback signals (including velocity, acceleration and actuator differential pressure), which are scaled and summed to form the servovalve drive signal, is quite successful though adds to the cost (Bell and de Pennington, 1969). A cheaper alternative is to keep just positional feedback and modify the control algorithm itself, and one of the simplest ways of doing this is to add a derivative term to the proportional controller.

The classical PD controller can be designed in the frequency domain to achieve acceptable stability margins. As shown in Figure 3.2, a gain margin of 6dB can be maintained whilst increasing the proportional gain to 6 if a derivative time constant of -0.01s is used, giving a 16Hz breakpoint for the derivative action. The negative derivative term introduces additional phase lag, moving the -180° phase point from the resonant peak to a lower frequency corresponding to the preceding trough, thus improving the gain margin. Note that the final controller gains are fairly arbitrary, not only because of the range of acceptable stability margins, but also because a wide range of different frequency response characteristics can be obtained from a non-linear plant at different operating conditions. Ideally the operating conditions should be in some way representative of the conditions expected during eventual normal operation, but a swept sine test obviously constrains the signal type to be sinusoidal.

Another problem is that designing for stability margins gives little information about the shape of the resulting time response.

The PD controller is implemented digitally as shown in Figure 3.3. Figure 3.4 shows the resulting step response. Although the speed of response has been increased significantly, the shape of the transient response is still not ideal. The following Section introduces alternative controllers which could further improve the transient response, and provide some of the other advantages listed in the introduction.

3.3 Alternative control methods

Other classical control methods are sometimes used for electro-hydraulic servosystems. For example the all-pass compensator consists of the following transfer function in the forward path:

$$\frac{1 - T_A S}{1 + T_A S} \tag{3.1}$$

This does not change the amplitude but gives additional phase lag increasing from 0° to 180° with increasing frequency. Thus it is applicable to plant such as the positioning system described, where stability margins can be improved by having more phase lag.

It is usual for classical methods to require a plant model in the form of a frequency response, and to be designed to achieve certain stability margins. For digital implementation the compensator transfer function is usually discretized approximately, but by using a fast sample rate errors are small. All the problems described for the PD controller still remain.

More recently developed digital controllers are mostly designed from parametric plant models, either in the form of an input-output equation (such as a transfer function), or a state-space model. A model of the disturbances affecting the plant can sometimes be employed as well.

One fundamental method is pole-placement, in which, given a plant model, the closed-loop poles can be positioned anywhere on the z-plane, whilst maintaining the original plant zeros. Extensions of the method place the zeros as well (Åström and Wittenmark, 1980). The method gives no indication as to where to put the closed-loop poles, and the search for the 'best' achievable response has lead to the development of optimal control methods. The minimum variance controller is one of the simpler optimal techniques. It uses an optimal prediction of the plant output at the next sample instant (if the plant has no dead time). The control law is designed to generate a control signal which equates the output prediction to the demand signal. Several problems exist with this method, including a vigorous, high amplitude, control signal, a heavy reliance on plant model accuracy, and an inability to handle non-minimum phase plant. Improvements, such as including a weighting on control signal size in the optimization problem, have lead to other methods, principally generalized minimum variance (GMV) and linear quadratic gaussian (LQG). Optimal control methods have not always been successful in practice; Finney (1982) favoured pole-placement in a comparison with GMV for an electro-hydraulic position control system. A remaining problem is robustness in the presence of modelling errors (Doyle, 1978), so that considerable theoretical research is currently directed toward robust optimal methods, of which H_∞ control is the main contender.

Many other control techniques have been suggested. The following are just a few:

- controllers with a non-linear control action, such as variable structure control,
- predictive controllers which can make use of future demand values (if known), for example generalised predictive control,
- controllers emanating from artificial intelligence related research into fuzzy sets, neural networks, and intelligent knowledge-based systems.

Pole-placement control has been chosen as the basis of the control work undertaken in this study. It has the advantages of relative simplicity and proven reliability. The design algorithm is introduced in Section 3.5.

Any controller design method based on a linear parametric model of the plant will be compromised if the model is very inaccurate. The model can be derived from physical analysis, such as that carried out in Appendix 1 for the positioning system. The continuous time-transfer function given in the Appendix can be converted to discrete-time by one of

several available methods (Franklin and Powell, 1980). However the simplifications and assumptions required to obtain the model are substantial, and the likelihood that it is the best linear model to describe the plant behaviour over a suitable operating range (including at any valve opening) is small. An alternative approach is system identification, whereby the model is estimated from experimental data. This includes determining the order of the plant model, values for unknown coefficients, and perhaps a disturbance model as well. Many alternative techniques are available for system identification, and some are tested and compared in Chapters 4 and 5.

The ability to estimate unknown model parameters from normal input-output data leads to the possibility of adaptive control. By running the estimator on-line, an updated plant model is calculated every sample instant, and the controller can be repeatedly re-designed accordingly. Thus the controller adapts to changes in plant parameters. The method can be implemented as described (known as indirect, explicit or self-tuning adaptive control), or the estimation and controller design stages can be combined so that the controller coefficients are estimated directly (known as direct, implicit, or model-reference adaptive control).

3.4 Integral Control

Servosystems often require integral action to drive the error between output and demand to zero in the presence of offsets or low-frequency disturbances. It has been shown in Appendix 1 that despite the integrating characteristic of the plant itself, an external load force will require a non-zero valve drive signal to resist it in the steady-state due to leakage effects. The resulting position error introduced is illustrated in Figure 3.5 using the PD controller described earlier in the Chapter. After 2.5s an offset is added into the control signal to simulate the application of a steady load force. Adding integral action — i.e. using a proportional-integral-derivative (PID) controller — allows a non-zero valve drive signal to be maintained with zero position error. The response of a PID controller is shown in Figure 3.6. The integral time constant (T_I) is 0.23s, a value found by manual tuning to give an acceptable rate of integration without being too detrimental to the transient response. The overall performance is far from

ideal, and improved integral control methods are investigated in Chapter 7. The digital implementation of the PID controller is shown in Figure 3.7.

3.5 Pole-placement control

The design calculations for a basic digital pole-placement controller are given in this Section. The controller can be designed in terms of input-output equations or state-variable feedback. As only output feedback is used in this study, an observer is required to estimate the states for the latter formulation. Thus the input-output equation approach is used here, which also ties in with the greater concentration on input-output equation models within the system identification field.

The controller is implemented using two digital filters as shown in Figure 3.8. The control signal is generated thus:

$$u_t = \frac{r_t - G(z^{-1})y_t}{F(z^{-1})} \tag{3.2}$$

and the plant is represented by:

$$y_t = \frac{B(z^{-1})}{A(z^{-1})} u_t \tag{3.3}$$

where:

$$\left.\begin{aligned} A(z^{-1}) &= 1 + a_1 z^{-1} + \ldots + a_n z^{-n} \\ B(z^{-1}) &= b_1 z^{-1} + b_2 z^{-2} + \ldots + b_m z^{-m} \end{aligned}\right\} \tag{3.4}$$

The resulting closed-loop response is:

$$y_t = \frac{B(z^{-1})}{F(z^{-1})A(z^{-1}) + G(z^{-1})B(z^{-1})} r_t \tag{3.5}$$

If $A(z^{-1})$ and $B(z^{-1})$ are known exactly, then $F(z^{-1})$ and $G(z^{-1})$ can be calculated to satisfy:

$$F(z^{-1})A(z^{-1}) + G(z^{-1})B(z^{-1}) = A_m(z^{-1}) \tag{3.6}$$

where $A_m(z^{-1})$ is the desired closed-loop characteristic polynomial. It has roots which are the system poles specified by the user, and a steady-state gain calculated to give unity gain in the closed-loop, i.e.:

$$A_m(1) = B(1) \tag{3.7}$$

A solution to (3.6), known as the diophantine equation, is achieved by multiplying out the polynomials and equating terms with equal powers of z^{-1}. The degrees of polynomials $F(z^{-1})$ and $G(z^{-1})$ are dictated by the need to have the same number of equations as unknowns. If:

$$\left.\begin{aligned} \deg F(z^{-1}) &= m - 1 \\ \deg G(z^{-1}) &= n - 1 \\ \deg A_m(z^{-1}) &= n + m - 1 \end{aligned}\right\} \tag{3.8}$$

there are both $n+m$ equations and $n+m$ unknown $F(z^{-1})$ and $G(z^{-1})$ coefficients. This is the minimal degree solution, i.e. if the degree of $F(z^{-1})$ or $G(z^{-1})$ were to be reduced in any way there would be more equations than unknowns, so no solution would exist.

Thus solving the diophantine equation is equivalent to solving the following matrix equation:

$$\begin{bmatrix} 1 & 0 & 0 & \cdots & & 0 & 0 & 0 & \cdots & \\ a_1 & 1 & 0 & & & b_1 & 0 & 0 & & \\ a_2 & a_1 & 1 & & & b_2 & b_1 & 0 & & \\ \vdots & & & & & \vdots & & & & \\ & & & & & b_m & b_{m-1} & b_{m-2} & \cdots & b_{m-n+1} \\ a_n & a_{n-1} & a_{n-2} & \cdots & a_{n-m+1} & 0 & b_m & b_{m-1} & \cdots & b_{m-n+2} \\ 0 & a_n & a_{n-1} & \cdots & a_{n-m+2} & \vdots & & & & \vdots \\ \vdots & & & & \vdots & & & & & \\ 0 & 0 & 0 & \cdots & a_n & 0 & 0 & 0 & \cdots & b_m \end{bmatrix} \begin{bmatrix} f_0 \\ f_1 \\ f_2 \\ \vdots \\ f_{m-1} \\ g_0 \\ g_1 \\ g_2 \\ \vdots \\ g_{n-1} \end{bmatrix} = \begin{bmatrix} a_{m0} \\ a_{m1} \\ a_{m2} \\ \vdots \\ \\ \\ \\ \\ \\ \end{bmatrix} \tag{3.9}$$

where these definitions apply:

$$\left.\begin{aligned} & a_0 = 1, \quad a_i = 0 \quad \text{for } i = -1,-2,-3... \\ \text{and} \quad & b_i = 0 \quad \text{for } i = 0,-1,-2... \end{aligned}\right\} \tag{3.10}$$

Other methods for solving the diophantine equation are reviewed in Warwick (1988).

3.6 Non-linear compensation

As has been highlighted in Chapter 2, electro-hydraulic servosytems are highly non-linear. However nearly all established control methods, including the pole-placement controller just presented, assume that the plant is linear. This mismatch has caused serious concern as to the applicability of advanced controller design methods to electro-hydraulic servosystems.

The problem can be ameliorated a little by attempting to cancel out any static non-linearities. The analysis of the positioning system in Appendix 1 has shown that the steady-state velocity gain is greater in the extend (negative) direction than the retract direction by a factor equal to the root of the piston area ratio, denoted R_A. This can be compensated for in software by scaling the valve control signal differently according to its sign. So where u_t is the signal generated by the controller and u_w is the actual valve drive signal:

$$\left.\begin{aligned} u_w &= u_t \qquad \text{for} \quad u_t < 0 \\ u_w &= R_A u_t \qquad \text{for} \quad u_t > 0 \end{aligned}\right\} \tag{3.11}$$

Note that this non-linear compensation is undertaken just before the control signal is sent to the plant. Thus for control and modelling purposes the compensation can be considered to be part of the plant itself; this is assumed in the following chapters. If the valve had a deadband around the null position due to being overlapped, or other gain change characteristics, these could be cancelled out in a similar way (Whiting, 1987).

Another non-linear aspect which warrants special attention is servovalve saturation. This can be largely neglected if the valve is never allowed to saturate. Hence the control signal should be limited in software to be just within the level which saturates the valve. This saturated value will always be closely related to the actual opening of the valve and can be considered as the actual plant input for modelling and control purposes. So in the case of the pole-placement controller, where u_{ft} is the control signal before the limits have been applied, equation (3.2) should be rewritten:

$$\left.\begin{aligned} u_{ft} &= \frac{r_t - G(z^{-1})y_t - (F(z^{-1}) - f_0)u_t}{f_0} \\ u_t &= u_{ft} \qquad \text{for } u_{sat-} < u_{ft} < u_{sat+} \\ u_t &= u_{sat-} \qquad \text{for } u_{ft} \leq u_{sat-} \\ u_t &= u_{sat+} \qquad \text{for } u_{ft} \geq u_{sat+} \end{aligned}\right\} \tag{3.12}$$

Using both a directional gain change and control signal saturation, the block diagram of Figure 3.8 becomes that of Figure 3.9.

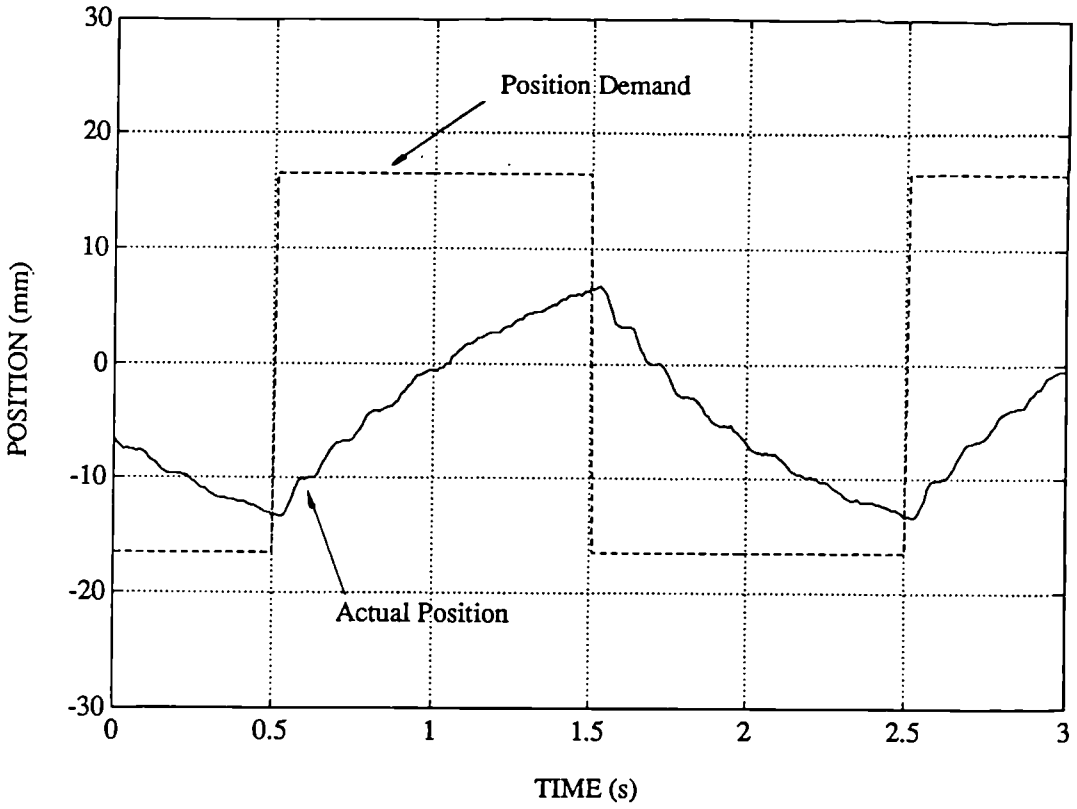

Figure 3.1 Closed-loop response, unity gain proportional control

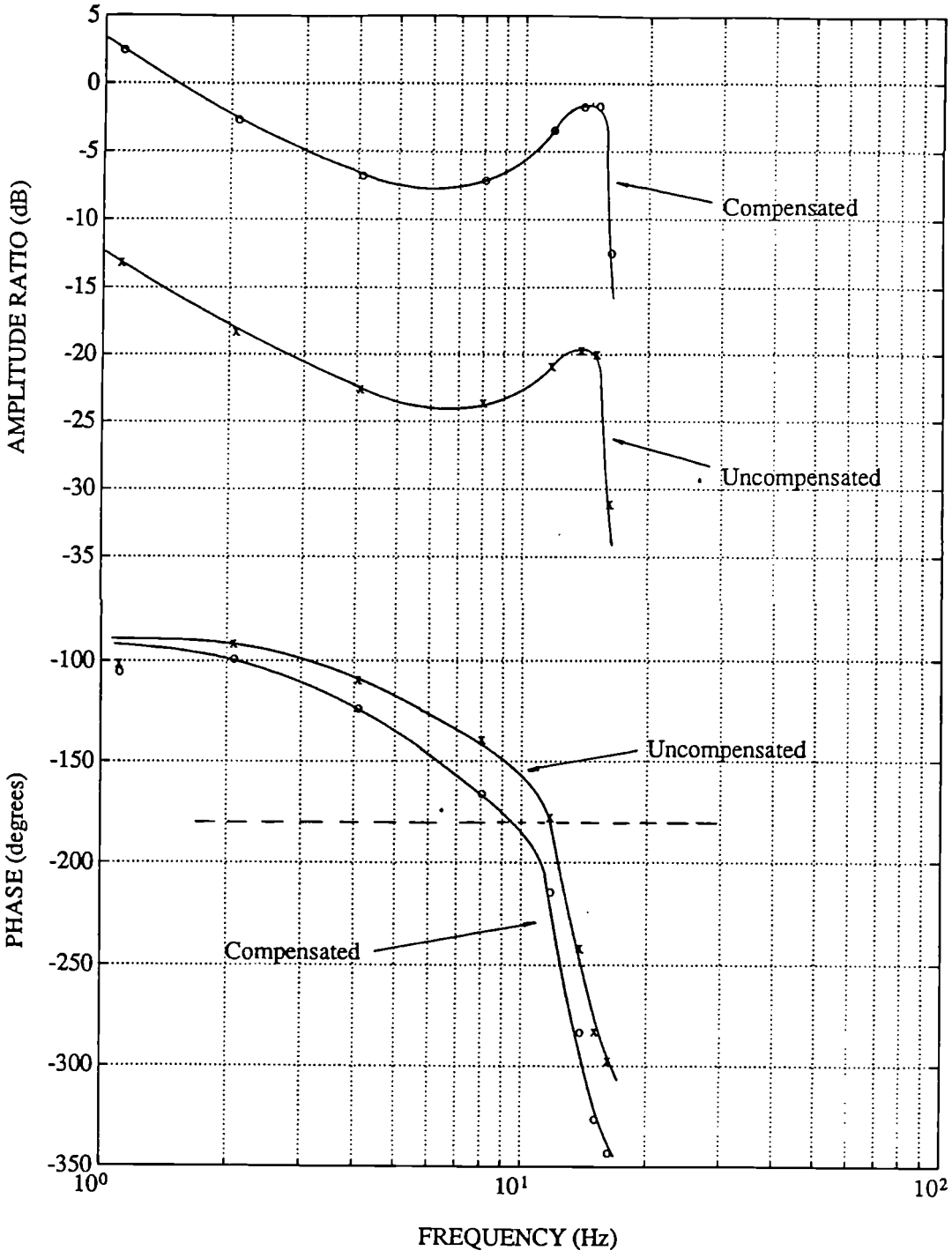

Figure 3.2 Open-loop frequency response, with and without $6(1-0.01s)$ compensator

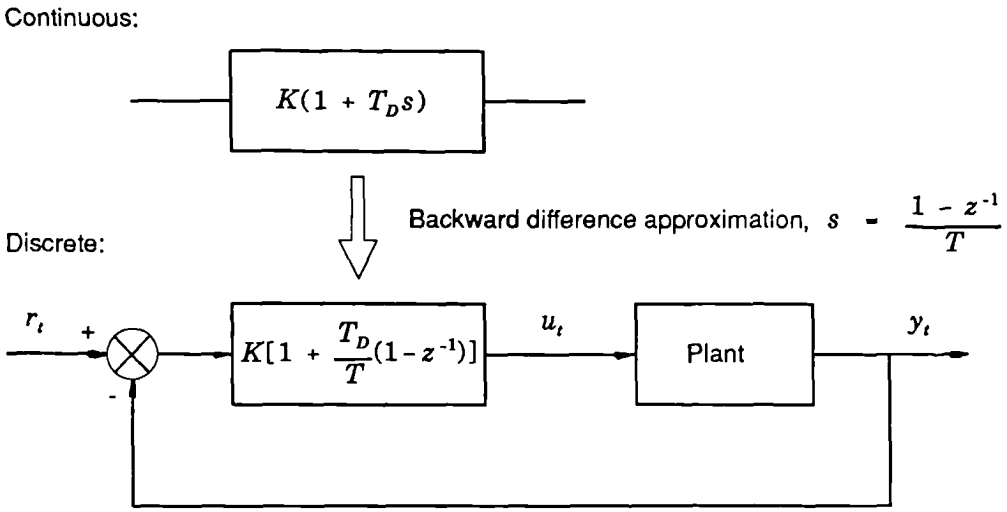

Figure 3.3 Implementation of PD controller

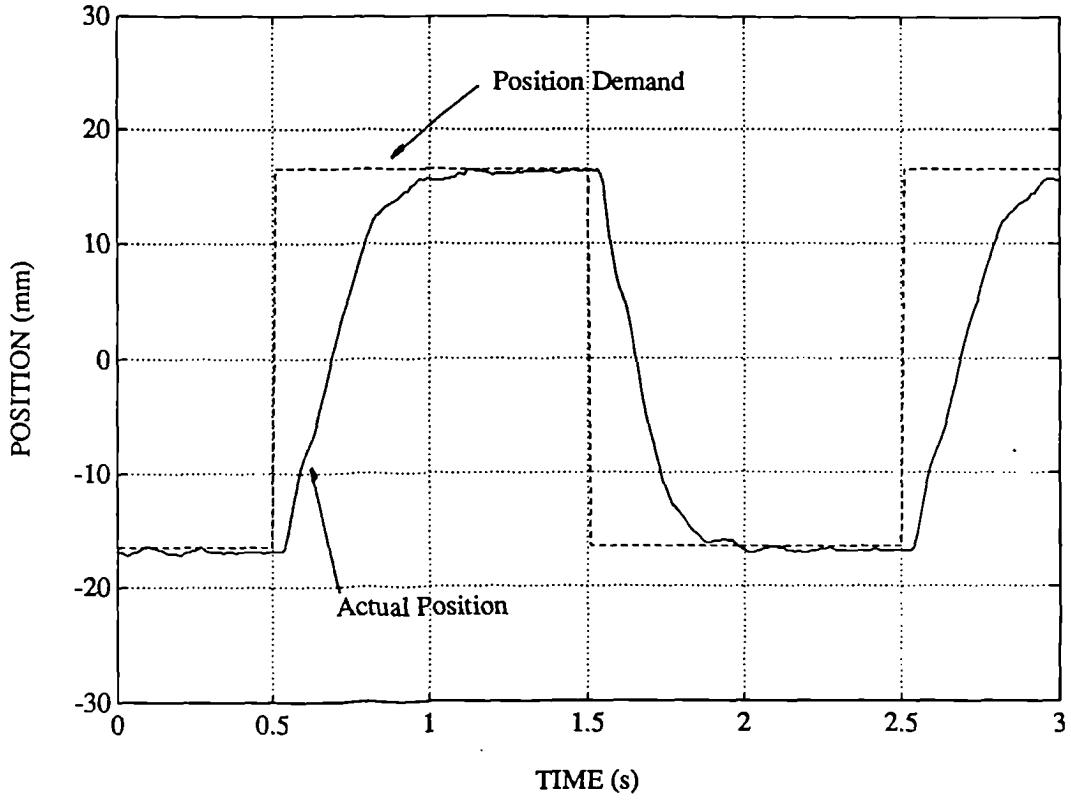

Figure 3.4 PD controller response

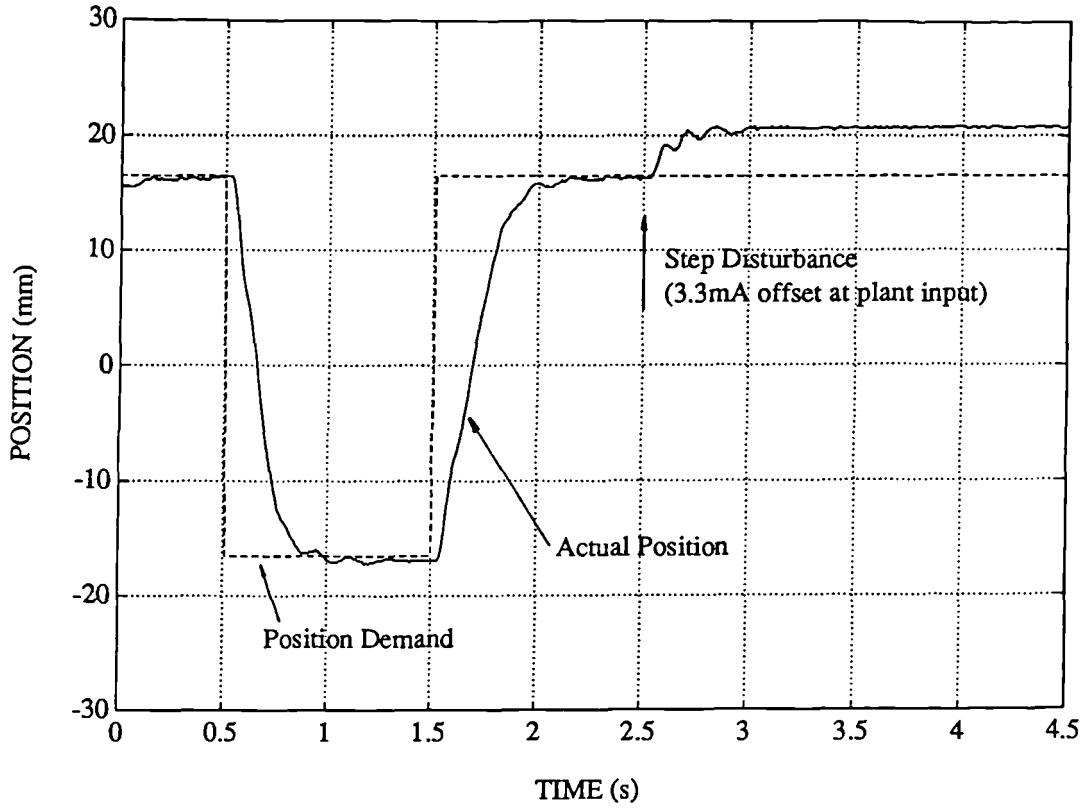

Figure 3.5 PD controller, with step disturbance

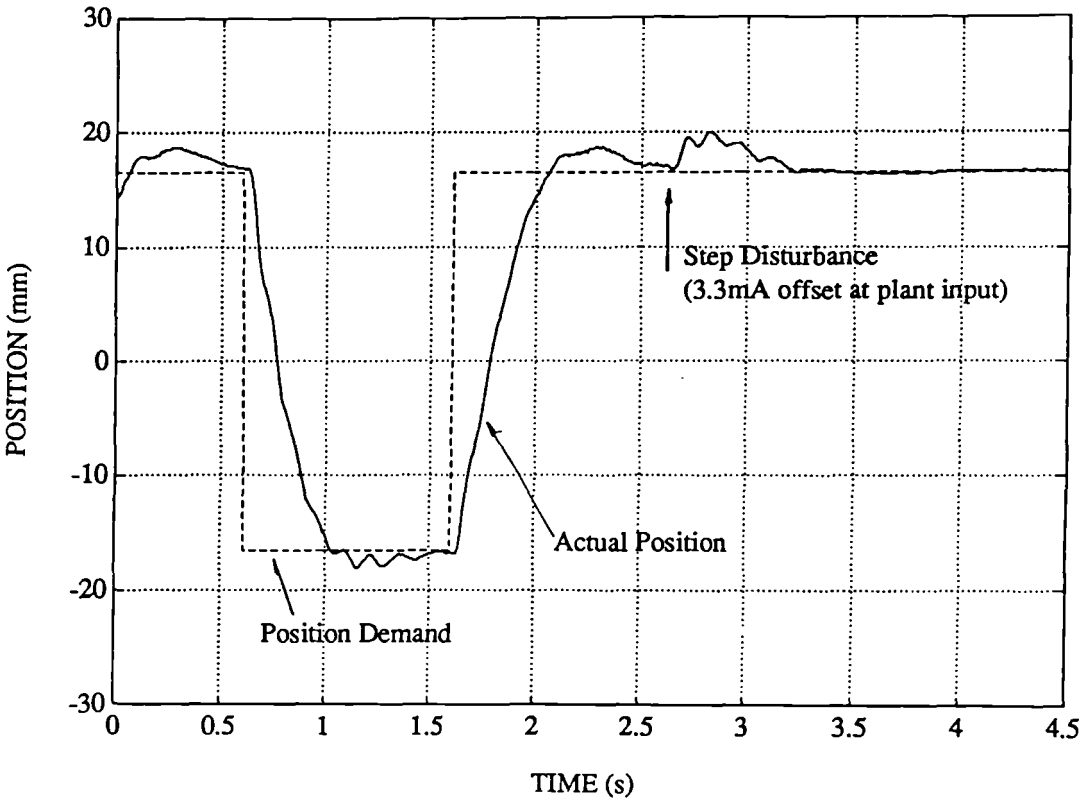

Figure 3.6 PID controller response

Continuous:

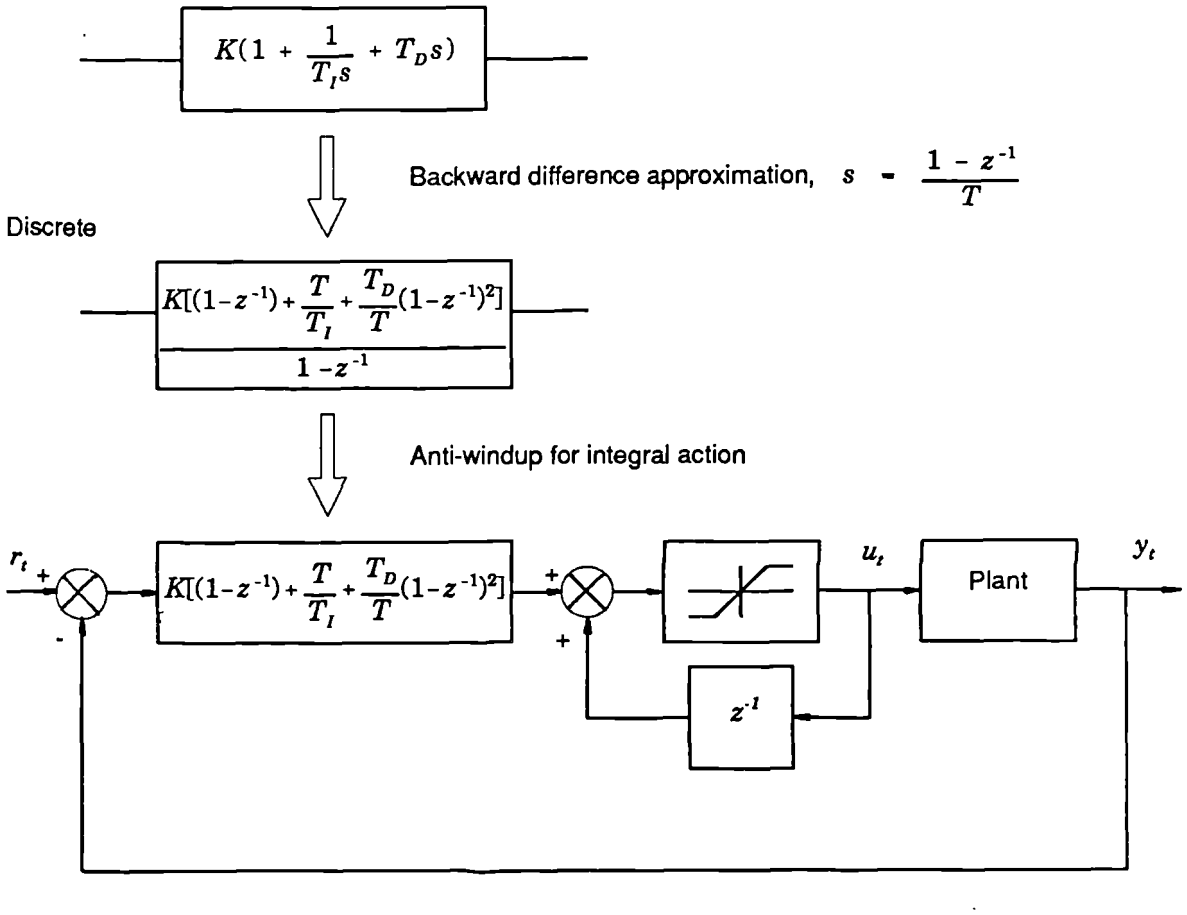

Figure 3.7 Implementation of PID controller

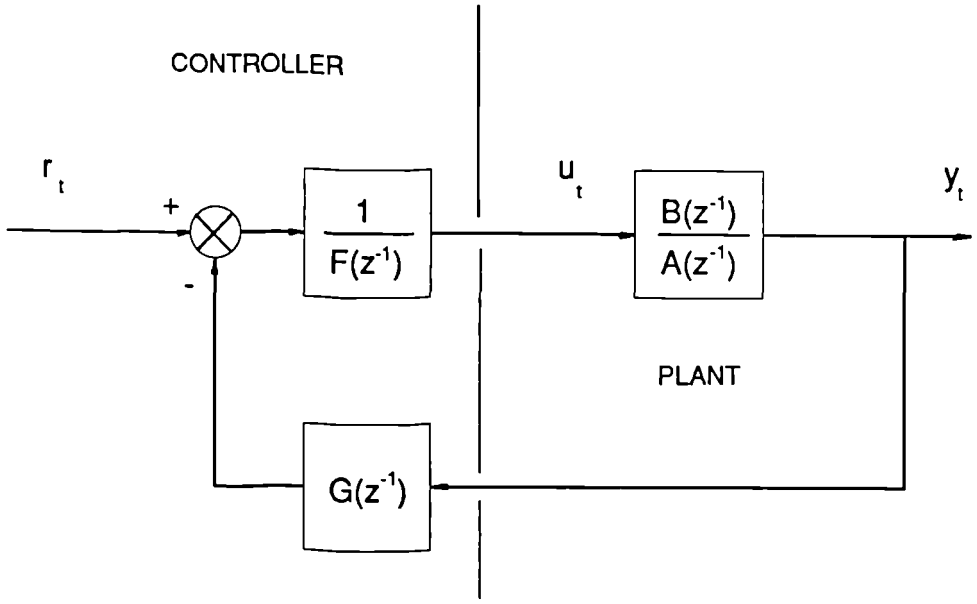

Figure 3.8 Pole-placement controller

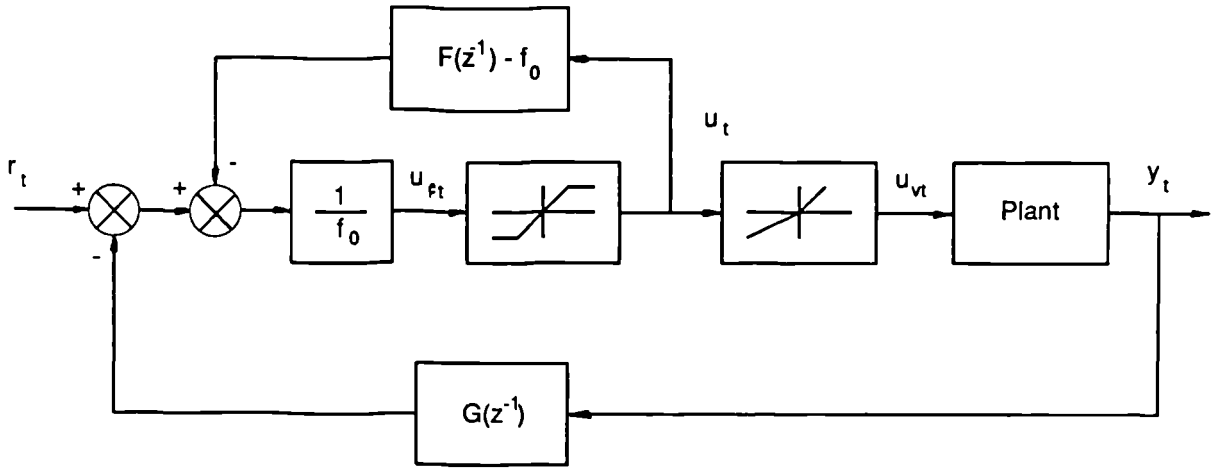

Figure 3.9 Pole-placement with non-linear compensation

4. System identification: parameter estimation

4.1 Introduction

System identification is the process of constructing a mathematical model of a dynamic system from observed input and output signals. As has been suggested in Chapter 3, system identification may provide a better alternative to physical analysis for deriving a model of an electro-hydraulic servosystem. Ideally, however, a model should be based on as much knowledge about the servosystem as possible, combining both analytical and experimental information, forming a so-called hybrid or grey-box model. The analysis of the electro-hydraulic positioning system in Appendix 1 highlights the difficulties with trying to derive a linear model with such methods. However some lessons can be learnt from the analysis, for example about the presence of a directional gain change due to using a single-ended cylinder. This gain change can then be compensated for, as described in Section 3.6. Applying system identification techniques to the combined plant and non-linear compensator is more likely to lead to an acceptable linear model. Similarly, using a plant input signal which saturates in software, mimicking the saturation of the servovalve, is another way in which knowledge of the plant is utilized. A further example – making use of the known integrating nature of the plant – is described in Section 4.4.

A procedure for system identification is shown in Figure 4.1. Some of the decisions shown in the Figure are dictated by the eventual use for the identified model. The model required for pole-placement controller design is a discrete-time transfer function between plant input and output of the form (see Section 3.5):

$$\frac{b_1 z^{-1} + b_2 z^{-2} + \ldots + b_m z^{-m}}{1 + a_1 z^{-1} + a_2 z^{-2} + \ldots + a_n z^{-n}} \tag{4.1}$$

Any dead-time in the plant can be incorporated into the numerator polynomial.

The system identification problem is one of finding the unknown parameters in the model. The problem can be divided into two areas:

- structure selection, i.e. determining values for the structural parameters n and m, which is addressed in Chapter 5,
- parameter estimation, i.e. estimating the a_i and b_i coefficients, which is addressed in this Chapter.

In both Chapters a variety of alternative techniques are presented and compared by application to the electro-hydraulic positioning system. Another important step in the identification of a discrete-time model is the choice of a sample rate. As this has bearing on control as well as identification, a discussion of sample rate selection is left until Chapter 6.

The different parameter estimation techniques to be compared are introduced in the next Section. Some of the basic theoretical results are simply quoted, and derivations can be found in a number of texts, including Ljung and Söderström (1983), Norton (1986), Ljung (1987), and Söderström and Stoica (1989).

4.2 Parameter estimators: theory

4.2.1 Modelling

In order to present methods of estimating the parameters in a discrete-time model, it is useful to represent the plant by a regression equation:

$$y_t = \psi_t^T \theta + e_t \tag{4.2}$$

where ψ is a vector of input-output data (— the regressor vector), and θ is a vector of model

parameters:

$$\left.\begin{aligned} \psi_t^T &= [y_{t-1}, \ldots, y_{t-n}, u_{t-1}, \ldots, u_{t-m}] \\ \theta &= [-a_1, \ldots, -a_n, b_1, \ldots, b_m]^T \end{aligned}\right\} \tag{4.3}$$

and e_t is a noise signal.

An estimate of θ must be found from N pairs of input-output samples. Equation (4.2) can be written for each sample instant, and combined as follows:

$$y = \Psi\theta + e \tag{4.4}$$

where

$$y = \begin{bmatrix} y_{d+1} \\ \vdots \\ y_N \end{bmatrix} \qquad \Psi = \begin{bmatrix} \psi_{d+1}^T \\ \vdots \\ \psi_N^T \end{bmatrix} \qquad e = \begin{bmatrix} e_{d+1} \\ \vdots \\ e_N \end{bmatrix} \tag{4.5}$$

and d is the largest of n and m.

4.2.2 Least Squares

The basis of many parameter estimation techniques is the method of least squares. The least squares estimator finds the parameters which minimize the sum of the squares of the errors between the actual plant output and the output predicted by the model. The least squares estimate of the parameter vector θ is given by:

$$\hat{\theta}_{LS} = (\Psi^T\Psi)^{-1}\,\Psi^T y \tag{4.6}$$

This is the batch form of the estimator, in which all the data are required before the parameters can be estimated. A recursive form of the estimator can be derived. This processes the data from each sample instant in turn, improving the estimates on each occasion. The recursive least squares (RLS) estimates should converge to the same values given by the batch version (BLS), with a small error depending on the start-up conditions. The RLS parameter vector estimate based on data up to sample time t is given by:

$$
\left.
\begin{aligned}
\hat{\theta}_t &= \hat{\theta}_{t-1} + k_t(y_t - \psi_t^T \hat{\theta}_{t-1}) && (a)\\
\text{where} \quad k_t &= \frac{P_{t-1}\psi_t}{1 + \psi_t^T P_{t-1}\psi_t} && (b)\\
\text{and} \quad P_t &= P_{t-1} - k_t \psi_t^T P_{t-1} && (c)
\end{aligned}
\right\} \tag{4.7}
$$

P_t is a normalised version of the covariance matrix of the estimates.

Estimator bias is defined as:

$$E[\hat{\theta}] - \theta \tag{4.8}$$

where E is the expectation operator. Bias is the mean error of the parameter vector estimate, regarding the estimate as a random variable due to the influence of noise. In the case of least squares, substituting for y in equation (4.6) using equation (4.4):

$$\hat{\theta}_{LS} = \theta + (\Psi^T\Psi)^{-1}\Psi^T e \tag{4.9}$$

and so the bias in the least squares estimate is given by:

$$E[\ (\Psi^T\Psi)^{-1}\Psi^T e\ ] \tag{4.10}$$

If all the regressors are uncorrelated with e_t, and e_t is zero mean, then the estimates are unbiased. However e_t is usually autocorrelated, and hence also correlated with the past values of output which appear as regressors. In the presence of feedback the past values of input which appear as regressors will also be correlated with an autocorrelated e_t. These issues are widely discussed in the literature (e.g. Norton, 1986).

4.2.3 Choice of alternative techniques

Many techniques for overcoming the problem of biased estimates have been proposed over the last 30 years, and most of them can be viewed as extensions of least squares. Several

have been selected for comparison as part of this study, mainly on the basis of good performance in comparative tests; see Isermann *et al* (1974), Gustavsson (1972), Saridis (1974). These techniques are instrumental variables, extended least squares and correlation analysis, although the latter method has been modified to yield a parametric plant model directly. A least squares technique based on filtered data is also tried. Of these techniques, instrumental variables has been previously applied to an electro-hydraulic servosystem by Daley (1987 and 1990).

4.2.4 The instrumental variable method

The instrumental variable method does not guarantee unbiased estimates, but it does give *consistent* estimates, i.e. the estimates approach the correct parameter values as the number of samples is increased. Pre-multiplying equation (4.4) by the transpose of a matrix Z (of the same dimensions as Ψ):

$$\begin{aligned} Z^T y &= Z^T \Psi \theta + Z^T e \\ \theta &= (Z^T \Psi)^{-1} Z^T y - (Z^T \Psi)^{-1} Z^T e \end{aligned} \tag{4.11}$$

And the instrumental variable estimate is given by:

$$\hat{\theta}_{IV} = (Z^T \Psi)^{-1} Z^T y \tag{4.12}$$

Thus

$$\hat{\theta}_{IV} = \theta + (Z^T \Psi)^{-1} Z^T e \tag{4.13}$$

If Z is constructed by starting with Ψ, and then replacing any regressor which is correlated with e_t by another variable which is not, then $Z^T e$ converges to zero as the number of samples increases and the parameter estimates tend towards their true values. The new variables are called instrumental variables (or just instruments).

A recursive form of the instrumental variable method (RIV) can be formulated in a similar way to recursive least squares:

$$\left.\begin{aligned} \hat{\theta}_t &= \hat{\theta}_{t-1} + k_t(y_t - \psi_t^T \hat{\theta}_{t-1}) \\ \text{where} \quad k_t &= \frac{P_{t-1} z_t}{1 + \psi_t^T P_{t-1} z_t} \\ \text{and} \quad P_t &= P_{t-1} - k_t \psi_t^T P_{t-1} \end{aligned}\right\} \tag{4.14}$$

z_t is a vector of instruments at sample instant t, so that:

$$Z = \begin{bmatrix} z_{d+1}^T \\ \vdots \\ z_N^T \end{bmatrix} \tag{4.15}$$

A number of possibilities for the choice of the instruments exist, given that the condition of non-correlation with e_t is met, and that $Z^T\Psi$ is invertible. It can be shown that a strong correlation between the instruments and the regressors which they replace reduces the variance of the estimates (Young, 1984). A good approach is to construct z_t by replacing any regressor in ψ_t which is correlated with noise with an instrument which is a simulated version of that regressor. To simulate the behaviour of a regressor, an estimate of the parameters is required. Thus this choice of instruments is most easily implemented using the recursive form of the estimator, in which the estimate of the parameters from the previous sample instant is always available.

For data collected in open-loop, where the input is generated by the data acquisition system itself, the input samples are not correlated with noise and the outputs can be simulated thus:

$$\bar{y}_t = z_t^T \hat{\theta}_t \tag{4.16}$$

where the instrument vector is:

$$z_t^T = [\bar{y}_{t-1}, \ldots, \bar{y}_{t-n}, u_{t-1}, \ldots, u_{t-m}] \tag{4.17}$$

Under closed-loop conditions, noise is fedback as part of the output to form a component of

the input, and so the instruments should be formed from neither plant input nor output. In this case the input and output can be simulated from the demand signal by the use of suitable filters. If the data were collected whilst operating the system with a pole-placement controller (see Figure 3.8), then suitable filters would be:

$$\left.\begin{aligned} \bar{y}_t &= \frac{\hat{B}_t(z^{-1})}{F(z^{-1})\hat{A}_t(z^{-1}) + G(z^{-1})\hat{B}_t(z^{-1})}\, r_t \\ \bar{u}_t &= \frac{\hat{A}_t(z^{-1})}{F(z^{-1})\hat{A}_t(z^{-1}) + G(z^{-1})\hat{B}_t(z^{-1})}\, r_t \end{aligned}\right\} \qquad (4.18)$$

where $\hat{A}_t(z^{-1})$ and $\hat{B}_t(z^{-1})$ are the most recent estimates of the plant denominator and numerator polynomials respectively (extracted from $\hat{\theta}_t$). In this case the instrument vector is:

$$z_t^T = [\bar{y}_{t-1}, \ldots, \bar{y}_{t-n}, \bar{u}_{t-1}, \ldots, \bar{u}_{t-m}] \qquad (4.19)$$

In both open- and closed-loop cases the filters used to generate the instruments should be stable, and not too lightly damped (Söderström *et al*, 1987). This is achieved by scaling any poles in the filters with magnitudes greater than 0.9 down to that size.

4.2.5 Extended least squares

Extended least squares (ELS) is a recursive technique which explicitly estimates a noise model along with the plant model. Assume the system can be represented by:

$$A(z^{-1})y_t = B(z^{-1})u_t + C(z^{-1})v_t \qquad (4.20)$$

where v_t is a white noise sequence, and

$$C(z^{-1}) = 1 + c_1 z^{-1} + \ldots + c_q z^{-q} \qquad (4.21)$$

This can be rewritten in the normal regression equation form:

$$y_t = \psi_t^T \theta + v_t \tag{4.22}$$

but now

$$\left.\begin{aligned} \psi_t^T &= [y_{t-1}, \ldots, y_{t-n}, u_{t-1}, \ldots, u_{t-m}, v_{t-1}, \ldots, v_{t-q}] \\ \theta &= [-a_1, \ldots, -a_n, b_1, \ldots, b_m, c_1, \ldots, c_q]^T \end{aligned}\right\} \tag{4.23}$$

Recursive least squares can now be applied, using these extended regressor and parameter vectors. The v_t signal included in the regressor vector is unknown, but it can be estimated at each recursion using:

$$\hat{v}_t = y_t - \psi_t^T \hat{\theta}_t \tag{4.24}$$

In equation (4.22) the unmodelled noise v_t is white, and thus not autocorrelated, so the estimates would be unbiased if all the regressors were known exactly. However some bias will remain in practice due to the use of estimated values of v_t in the regressor vector.

4.2.6 Correlation-based estimation

Traditionally, correlation analysis has been used to find non-parametric plant models, in particular the plant impulse response. However the following method has been derived which uses correlation techniques to alleviate the effect of noise on least squares parameter estimates.

Writing equation (4.2) in full:

$$y_t = -a_1 y_{t-1} - \ldots - a_n y_{t-n} + b_1 u_{t-1} + \ldots + b_m u_{t-m} + e_t \tag{4.25}$$

The cross-correlation between any signal x_t and the output y_t at lag τ is given by:

$$r_{xy}(\tau) = E[x_t y_{t+\tau}] \tag{4.26}$$

Substituting for $y_{t+\tau}$ in equation (4.26) using equation (4.25):

$$r_{xy}(\tau) = -a_1 r_{xy}(\tau-1) -...- a_n r_{xy}(\tau-n) + b_1 r_{xu}(\tau-1) +...+ b_m r_{xu}(\tau-m) + r_{xe}(\tau) \quad (4.27)$$

If x_t is chosen to be uncorrelated with e_t then $r_{xe}(\tau) = 0$ for $\tau \neq 0$. So performing a least squares fit between $r_{xu}(\tau)$ and $r_{xy}(\tau)$ will lead to exact estimates as the error term is zero. However x_t must be well correlated with y_t and u_t as otherwise least squares will be ill-conditioned. In open-loop the input u_t is not correlated with e_t, so $x_t = u_t$ can be used. In closed-loop the demand r_t is not correlated with e_t, so $x_t = r_t$ can be used.

In practice $r_{xy}(\tau)$ is not known. It can be estimated from data of sample length N by:

$$\hat{r}_{xy}(\tau) = \frac{1}{N-\tau} \sum_{t=1}^{N-\tau} x_t y_{t+\tau} \quad (4.28)$$

4.2.7 Least squares with data filtering

Consider the system of equation (4.20). If the input and output signals were filtered by the reciprocal of the noise model, they would be related by:

$$A(z^{-1}) y_t' = B(z^{-1}) u_t' + v_t \quad (4.29)$$

where

$$\left.\begin{aligned} y_t' &= \frac{1}{C(z^{-1})} y_t \\ u_t' &= \frac{1}{C(z^{-1})} u_t \end{aligned}\right\} \quad (4.30)$$

So fitting a model between u_t' and y_t' by least squares would lead to unbiased estimates.

In practice the noise model is unknown, but using engineering judgment to design a filter to attenuate noise in the signals may be sufficient to improve the estimates. The filter will be

low-pass if noise is prevalent at high-frequency only, or bandpass if low-frequency disturbances are also present. Filtering for estimation is discussed in Middleton *et al* (1988).

4.3 Comparison of methods: simulation

A digital simulation has been undertaken as a first step in comparing the estimators. A plant is simulated by a third order linear discrete-time model; as confirmed later, this is of a similar nature to the electro-hydraulic positioning system. A noise signal is added to the output, as shown below:

$$(1-z^{-1})(1-1.4z^{-1}+0.8z^{-2})y_t = (z^{-1}+9z^{-2}+10z^{-3})10^{-3}u_t + (1-z^{-1}+0.2z^{-2})v_t \quad (4.31)$$

The white noise signal v_t is Gaussian with a standard deviation of 0.005.

The success of each estimator can be assessed by comparing the actual and estimated parameter values. However the sensitivity of the model (as a predictor) to parameter error is also important. If the model is very insensitive to variations in a particular parameter, an inaccurate estimate of this parameter is not significant. Thus an appropriate measure of estimator success which takes this into account is the error between the output of the estimated model and the noise-free simulated plant output (driven by the same input). This will be referred to as the noise-free prediction error. In the case which follows, the input signal used for this purpose is the same as that used for estimation. Both the mean and RMS noise-free prediction error are calculated.

Data were collected from the simulated plant using a pseudo-random binary sequence (PRBS) input signal. The plant was operated in open-loop, with a sample length of 200. The data is shown in Figure 4.2.

The parameter estimates and prediction errors are in Table 4.1. As the noise is correlated with past output samples, BLS and RLS give biased results. When an estimation filter is used the

estimates are good. Two filters were tried, the correct one (i.e. the inverse of the noise model):

$$\frac{1}{1 - z^{-1} + 0.2z^{-2}} \tag{4.32}$$

and a more realistic 'guessed' filter:

$$\frac{1}{1 - 0.7z^{-1}} \tag{4.33}$$

Using the guessed filter gave only marginally worse results.

The RIV, ELS, and correlation-based estimators were all successful. As ELS also estimates noise parameters, it needs to know the structure of the noise model. Correct (second) order and first order noise models were used. The latter was only slightly inferior, but this may be due to the second noise coefficient being small. For the correlation-based estimator the correlation functions up to lag 200 were calculated, using a total sample length of 400. The batch version of least squares was used to obtain the final estimates.

Note that the three numerator parameter estimates (b_1, b_2, b_3) vary greatly and are often very inaccurate (in terms of percentage error). This is due to the model's insensitivity to their individual values. However their sum is important as this directly affects the steady- state velocity gain of the model.

Figure 4.3 illustrates the convergence of a typical estimate towards its final value for each of the recursive estimators. Inspecting the convergence is useful to ensure that sufficient samples have been used for estimation. Each recursive estimator was initialised with all elements in the parameter vector set to zero, and the normalised covariance matrix set to the identity matrix scaled up by 10^6.

4.4 Comparison of methods: electro-hydraulic positioning system

4.4.1 Model structure

The techniques described in Section 4.2 have been used to estimate model parameters for the electro-hydraulic positioning system. Before the model parameters are estimated, a model structure must be selected. Experience has shown that a linearised continuous-time model of the form shown below can be suitable for this type of hydraulic plant:

$$\frac{Y(s)}{U(s)} = \frac{\kappa\omega_n^2}{s(s^2 + 2\zeta\omega_n s + \omega_n^2)} \tag{4.34}$$

This translates into a third order (i.e. n=m=3) discrete-time model with one pole at z=1:

$$y_t = \frac{b_1 z^{-1} + b_2 z^{-2} + b_3 z^{-3}}{(1 - z^{-1})(1 + a_1 z^{-1} + a_2 z^{-2})} u_t \tag{4.35}$$

Alternatively the most appropriate model structure can be selected by analyzing experimental data. This is covered in Chapter 5, in which a third order model is indeed found to be best.

In equation (4.35) one pole is fixed at z=1, indicating that the integrating nature of the plant is assumed from the outset, rather than a property which is identified with the rest of the model. Fixing the pole is not essential, but it does reduce the number of parameters to be estimated, and also ensures unity steady-state gain in the eventual pole-placement controller (see Appendix 2).

In order to force the pole at z=1, the output can be filtered by $(1 - z^{-1})$, and a model fitted between the input and this new output.

4.4.2 Results

Figure 4.4 shows data collected from the plant. The data were collected in open-loop, and sampled at 100Hz, which is about 8 times the plant bandwidth. A PRBS was used for the valve drive current, which is a signal of sufficient dynamic richness to excite all the modes of the plant. However a square wave has also been found to give acceptable results. The Figure shows the load position 'wandering' as a result of the integral nature of the plant. If operating the plant in open-loop had been unacceptable (e.g. for safety reasons), data could have been collected with the plant under proportional closed-loop control, an example of which is given later.

Table 4.2 contains the parameters estimated from the data by the various methods described in Section 4.2. A sample length of 400 was used in each case. There is a wide variation in estimate values, in particular for the numerator parameters. However the steady-state velocity gain is similar for all models.

The convergence of a typical parameter estimate towards its final value is shown in Figure 4.5 for each recursive estimator.

A third order noise model was chosen for extended least squares (i.e. q=3), as this was found to give best results. For the correlation based method, correlation functions up to a lag of 200 were calculated.

The estimation filter for filtered least squares can be designed in continuous-time and converted to discrete-time by one of the numerous methods available (Franklin and Powell, 1980). In this case a second order filter with a natural frequency of 20Hz and damping ratio of 0.5 was used. It was transformed from continuous-time by pole/zero mapping, giving the following digital filter:

$$\frac{(1 + z^{-1})^2}{(1 - (0.25 + 0.47j)z^{-1})(1 - (0.25 - 0.47j)z^{-1})} \tag{4.36}$$

A 20Hz bandwidth filter was used in order to attenuate noise and the effect of high order unmodelled dynamics above the plant bandwidth, such as the dynamics of the servovalve. Filter selection is addressed further in Section 4.5.

The results in Table 4.2 show wide discrepancies in parameter estimates between the various estimators. As there are no correct values for the parameters in the servosystem model, comparing the results from the different estimators is not straightforward. However if a pole-placement controller is designed from each model, the resulting closed-loop response can be compared with the desired response and the error used as a measure of model accuracy.

Figure 4.6 shows the desired and actual closed-loop step responses based on the model estimated by each estimator in turn. Three desired closed-loop poles were specified, all at z=0.7. The responses based on the recursive least squares models are not shown as they are (unsurprisingly) virtually identical to the corresponding batch least squares responses. Note that in generating the desired response, the fact that the valve can saturate was taken into account. The slight kink in both desired and actual responses during the initial transient after a step change in demand occurs whilst the valve is saturated.

The responses show that basic least squares does give an inaccurate model, resulting in an unacceptable intermittent oscillation of the output. Filtered least squares gives the closest model following, and the correlation method is also quite good.

To emphasize that these results are typical, another example is presented, this time using data collected with the plant operating under proportional unity-gain closed-loop control. The data used for estimation is shown in Figure 4.7, including the PRBS demand signal. The same sample length, estimation filter (for filtered least squares), and noise model order (for extended least squares) were used, leading to the estimates in Table 4.3. The convergence of the recursive estimates to their final values is illustrated in Figure 4.8. Figure 4.9 shows the desired and actual closed-loop step responses corresponding to different estimated models, using three desired closed-loop poles at z=0.7 as before.

The response given by the basic least squares model exhibits instability, and the response corresponding to filtered least squares is again best. In fact considering the non-linear nature of the plant, the actual response given by filtered least squares in both Figure 4.6 and 4.9 is very close to the desired. The rate of convergence of the filtered RLS estimator is also much greater than for the other recursive estimators (Figures 4.5 and 4.8).

4.5 Effect of the estimation filter

The sensitivity of the model and corresponding controller to the filter used in filtered least squares has been investigated experimentally for the servosystem. The frequency responses for four digital filters which have 3dB breakpoints at about 15Hz are shown in Figure 4.10. They include a moving average filter, and three recursive filters ranging from first to third order with all real poles. Models were estimated with these filters using the closed-loop data shown in Figure 4.7. Pole-placement controllers were designed as before, and the step responses are shown in Figure 4.11. Although all the responses are better than with no estimation filter, only the moving average filter gives very good results. The zeros at $z = -1$ in this filter give rapid roll-off and a gain of zero at the Nyquist frequency (50Hz).

The rapid roll-off towards zero appears to be an important feature, so four more filters, all with zeros at $z = -1$, have also been tried. As shown in the frequency responses for the filters in Figure 4.12, they have bandwidths ranging from 5 to 12Hz. The corresponding controller responses are shown in Figure 4.13, and all exhibit a close match between the actual and desired. Thus the choice of a particular estimation filter is not critical.

4.6 Computational speed

The processing times required for each estimator to produce the results described in Section 4.4 are shown in Table 4.4. For comparison the code is run on the T800 transputer and also the host (which has an 80286 processor running at 12MHz, and a 80287 maths co-processor). See Section 2.3 for a detailed description of the computer system. The times for the recursive estimators, e.g. about 2.5ms per sample for filtered RLS on the transputer, are especially interesting as estimation is the main computational burden in adaptive control.

Note that those estimators — particularly filtered RLS — which converge well within 400 samples, are really faster than the times suggest.

4.7 Conclusions

A variety of parameter estimators have been used to find models for the electro-hydraulic positioning system. The system exhibits numerous non-linear characteristics, and these have to be approximated by any linear model used to represent the plant.

Least squares is shown to give very biased results. The other estimators, which include instrumental variables, extended least squares, and a correlation-based method, all modify the least squares algorithm in some way to try to overcome the problem of bias. Results presented here and elsewhere (Plummer, 1989) show that these methods work well for a simple simulation, and can be satisfactory using real data. However only filtered least squares is consistently successful in practice. The success of the estimator is gauged by designing a pole-placement controller from the estimated model. Considering the significant plant non-linearities, the match between the desired and actual closed-loop responses using the filtered least squares model is very good.

There appears to be a wide range of filters which give good results for a particular data set, although including zeros at $z = -1$ to give zero gain at the Nyquist frequency seems to be important in practice. At present the filter is designed on a heuristic basis to attenuate high frequency noise.

The performance of the estimators for the servosystem can be attributed to the nature of the errors between plant and model. In most theoretical studies it is assumed that the errors can be modelled as a coloured noise sequence. For this system the errors are mainly due to non-linearities. Thus the robustness of an estimator to different types of error is important.

Despite the problem with the basic least squares algorithm, the majority of the previous applications of parameter estimation to electro-hydraulic servosystems have used this method. Many of these applications are adaptive controllers using on-line RLS. Parkinnen *et al* (1988) and Watton (1990) are examples of off-line use of least squares. Surprisingly little research on using the other methods has been undertaken, Daley (1987) being a notable exception.

	Model parameter estimates					S.S. Gain*	Pred'n Error RMS, Mean
	$\hat{a}_1$	$\hat{a}_2$	$\hat{b}_1$	$\hat{b}_2$	$\hat{b}_3$		
				x10^{-3}		x10^{-2}	x10^{-4}
Correct Values	-1.400	0.800	1.0	9.0	10.0	5.00	0.0 0.0
BLS	-1.154	0.641	1.7	7.4	15.6	5.10	14.0 8.7
RLS	-1.150	0.633	1.7	7.5	15.4	5.09	14.2 8.7
RIV	-1.386	0.803	3.2	5.9	11.7	5.02	3.3 1.5
ELS, noise order 2 ($\hat{C}(z^{-1})$=1-1.003z^{-1}+0.124z^{-2})	-1.401	0.803	0.0	12.7	7.4	5.00	3.9 0.8
ELS, noise order 1 ($\hat{C}(z^{-1})$=1-0.933z^{-1})	-1.386	0.785	0.6	11.5	7.8	5.02	3.0 1.2
Correlation	-1.416	0.829	0.9	9.7	9.8	4.99	2.5 1.4
Filtered BLS, $(1-z^{-1}+0.2z^{-2})^{-1}$ filter	-1.404	0.821	0.0	9.3	11.4	4.99	2.5 1.3
Filtered RLS, $(1-z^{-1}+0.2z^{-2})^{-1}$ filter	-1.406	0.823	0.0	9.3	11.4	4.99	2.6 1.3
Filtered BLS, $(1-0.7z^{-1})^{-1}$ filter	-1.372	0.799	1.0	7.9	12.4	5.00	2.9 1.6
Filtered RLS, $(1-0.7z^{-1})^{-1}$ filter	-1.372	0.801	1.0	8.0	12.4	5.00	3.0 1.6

* This is the steady-state velocity gain, given by:

$$\frac{\hat{b}_1 + \hat{b}_2 + \hat{b}_3}{1 + \hat{a}_1 + \hat{a}_2}$$

Table 4.1 Comparison of estimated parameters (simulation)

Estimator	Plant model parameter estimates $\hat{a}_1$	$\hat{a}_2$	$\hat{b}_1$ x10^{-3}	$\hat{b}_2$ x10^{-3}	$\hat{b}_3$ x10^{-3}	S.S. Gain x10^{-2}
BLS	-0.317	-0.025	1.5	4.4	5.3	1.72
RLS	-0.317	-0.026	1.4	4.4	5.3	1.72
RIV	-1.058	0.548	-0.5	7.2	1.2	1.63
ELS	-1.407	0.785	0.5	3.6	2.2	1.69
Correlation	-1.191	0.563	3.7	2.9	-0.6	1.63
Filtered BLS	-1.426	0.859	0.0	5.5	1.5	1.59
Filtered RLS	-1.426	0.859	0.0	5.3	1.6	1.59

Table 4.2 Comparison of estimated parameters (open-loop data)

Estimator	Plant model parameter estimates $\hat{a}_1$	$\hat{a}_2$	$\hat{b}_1$ x10^{-3}	$\hat{b}_2$ x10^{-3}	$\hat{b}_3$ x10^{-3}	S.S. Gain x10^{-2}
BLS	-0.590	0.157	3.2	1.3	5.7	1.83
RLS	-0.590	0.153	3.1	1.3	5.6	1.82
RIV	-1.389	0.847	2.6	1.2	4.2	1.77
ELS	-1.428	0.710	1.8	0.1	5.2	1.73
Correlation	-1.374	0.710	1.0	6.0	-1.4	1.70
Filtered BLS	-1.480	0.896	-1.3	6.9	1.0	1.61
Filtered RLS	-1.480	0.896	-1.2	6.9	1.0	1.61

Table 4.3 Comparison of estimated parameters (closed-loop data)

Estimator	Time for estimation (s)	
	AT-Compatible	Transputer
BLS	2.5	0.28
RLS	9.4	0.93
RIV	11.1	1.10
ELS	21.5	2.04
Correlation	9.2	0.83
Filtered BLS	3.1	0.34
Filtered RLS	10.2	1.01

Table 4.4 Computation times for estimation

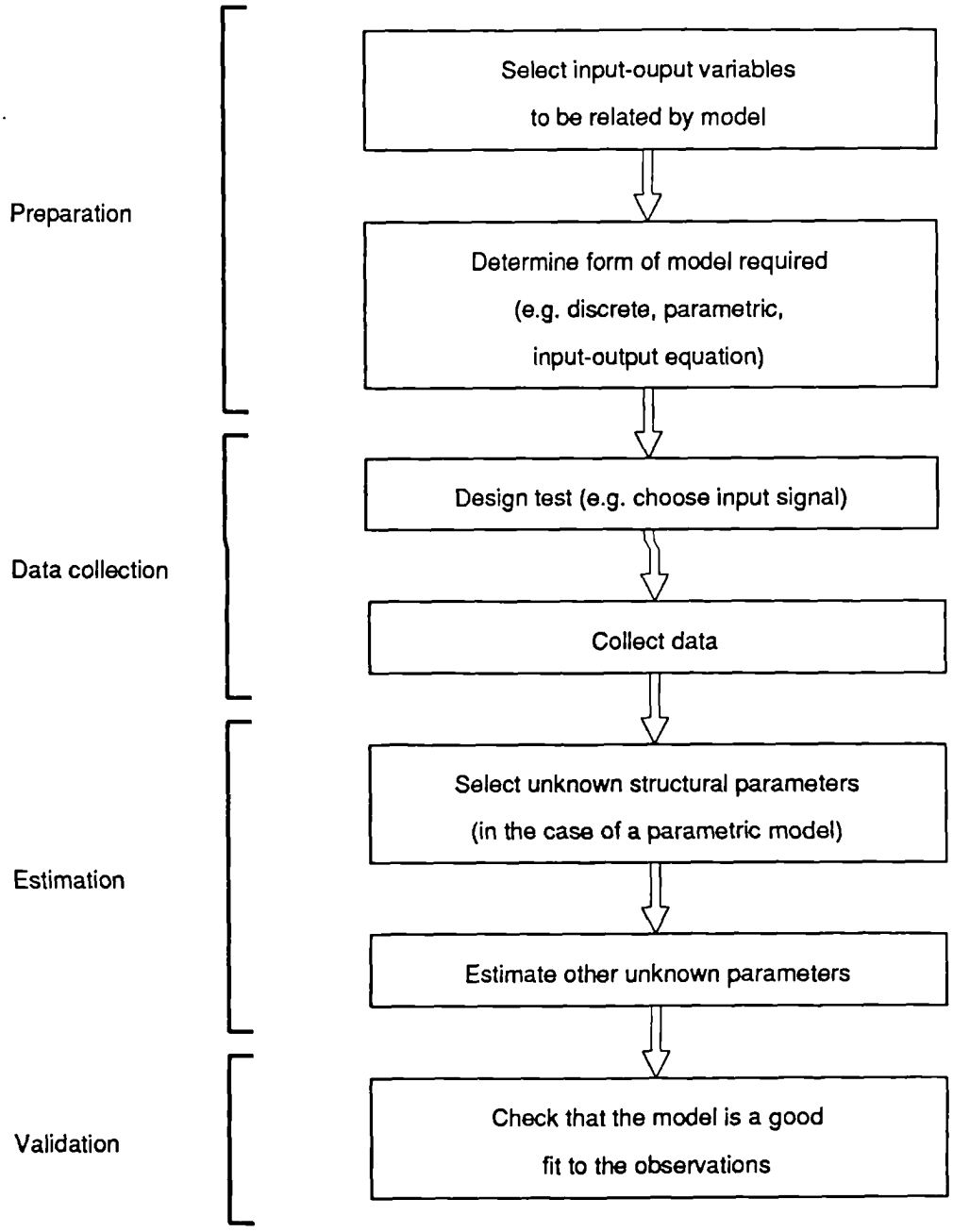

Figure 4.1 System identification procedure

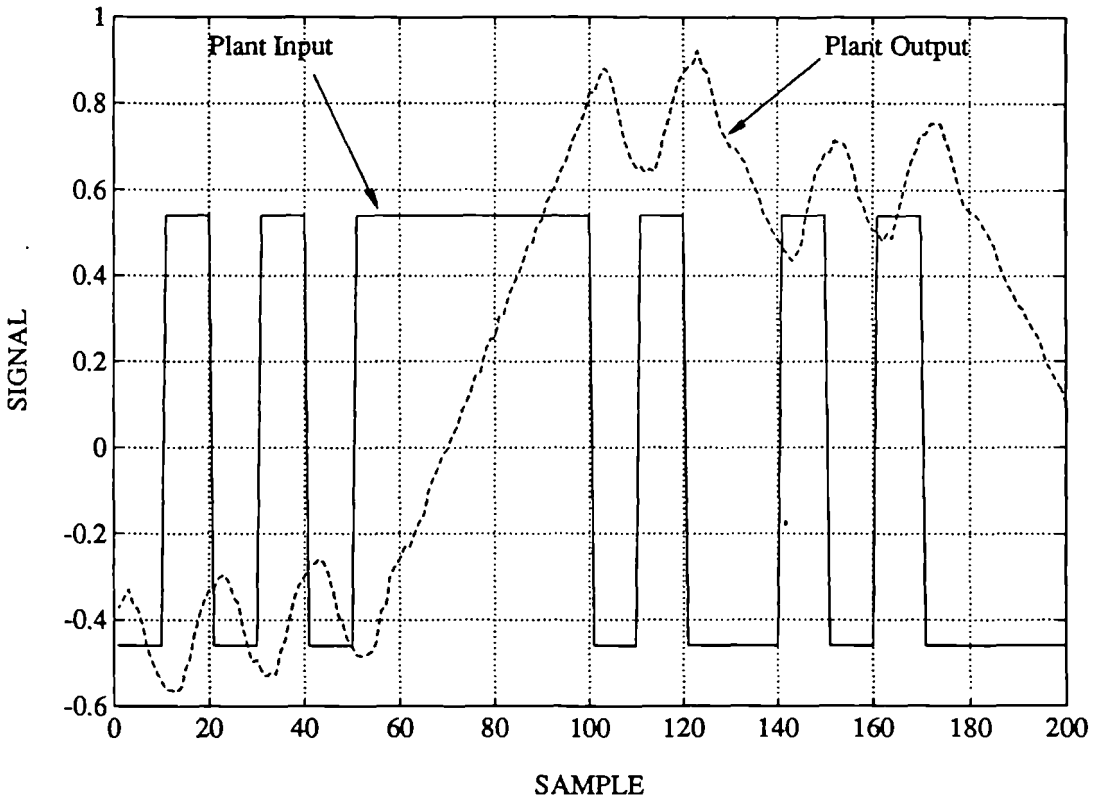

Figure 4.2 Input-output data used for estimation (simulation)

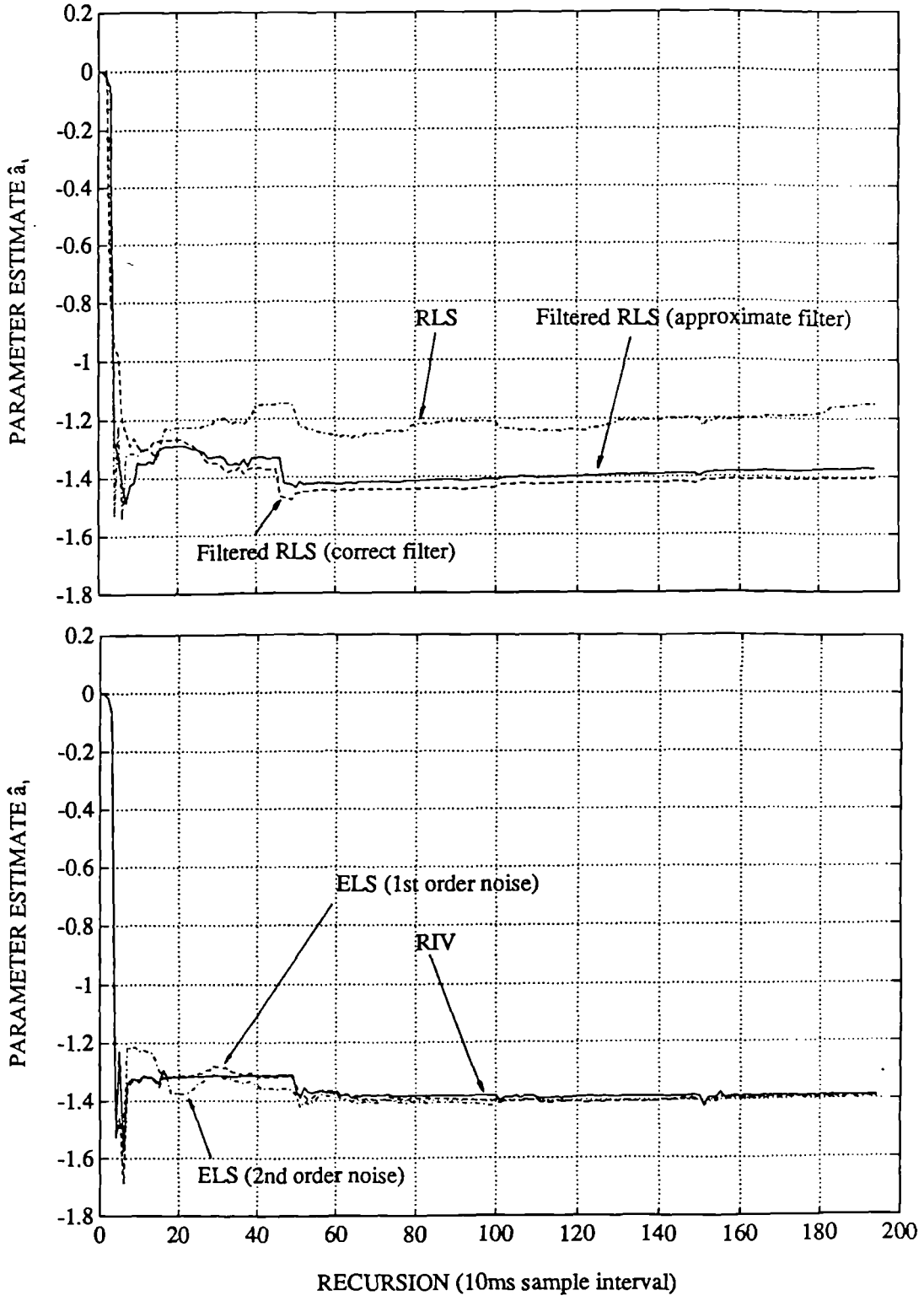

Figure 4.3 Convergence of recursive estimators (simulation data)

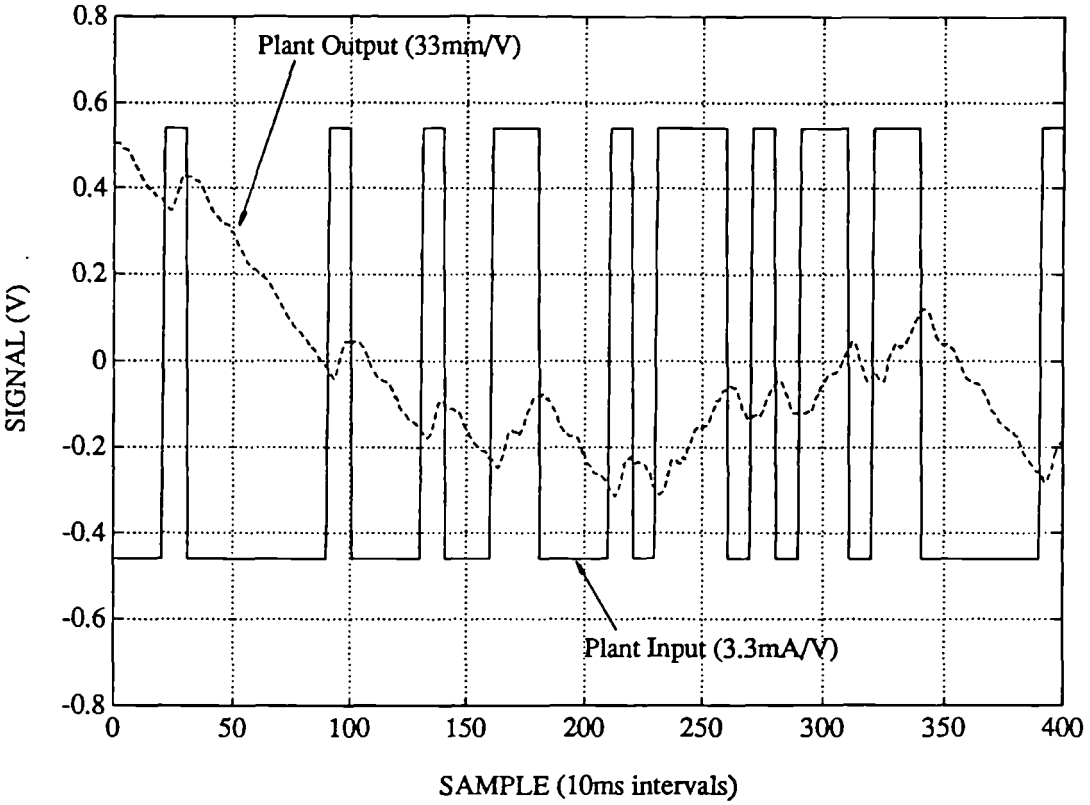

Figure 4.4 Plant input-output data used for estimation (collected with open-loop)

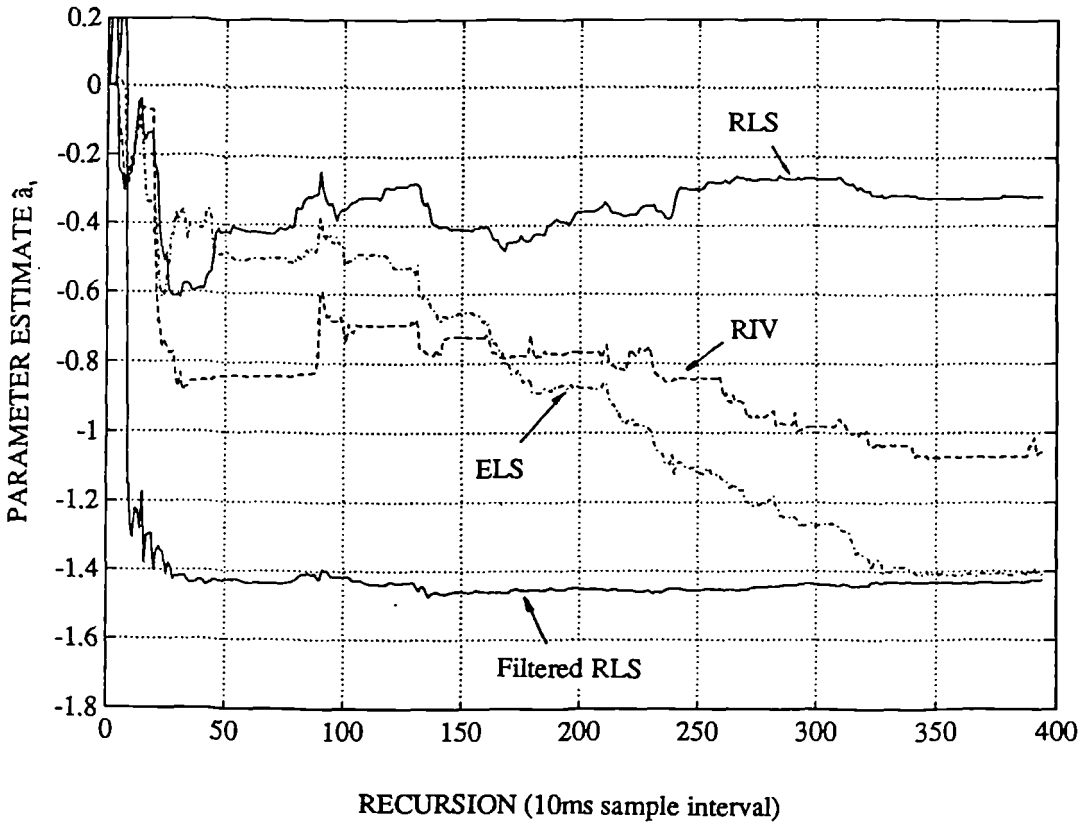

Figure 4.5 Convergence of recursive estimators (open-loop plant data)

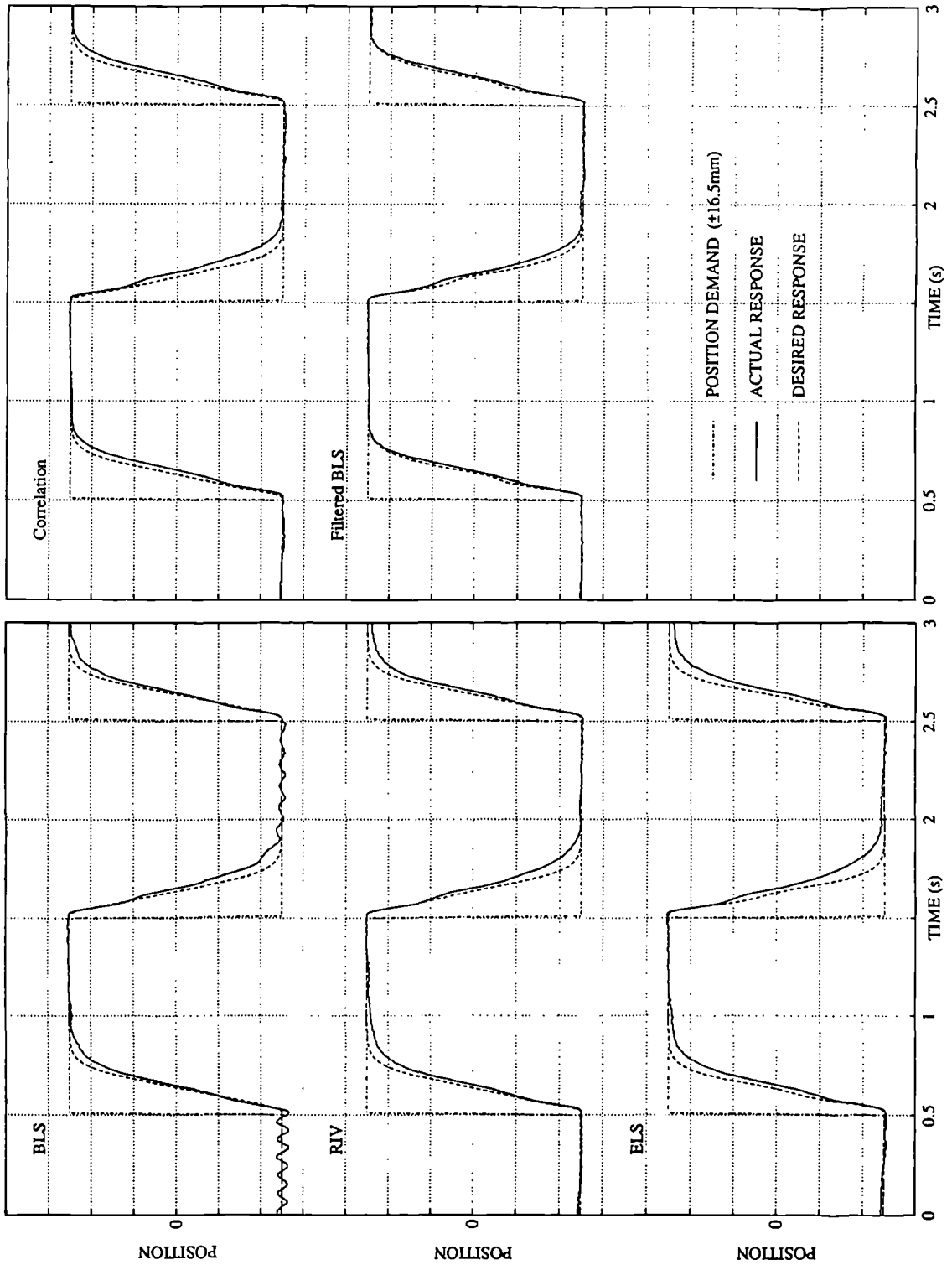

Figure 4.6 Comparison of desired and actual closed-loop responses for the various estimators (using open-loop data)

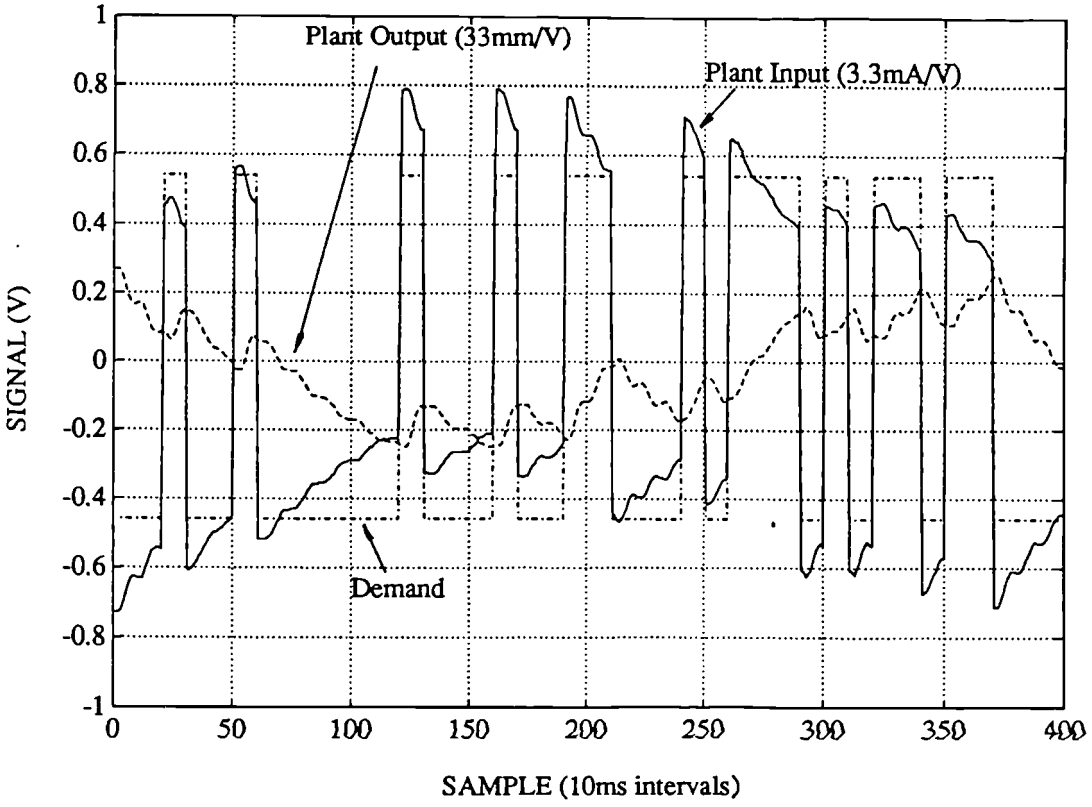

Figure 4.7 Plant data used for estimation (collected using unity-gain proportional control)

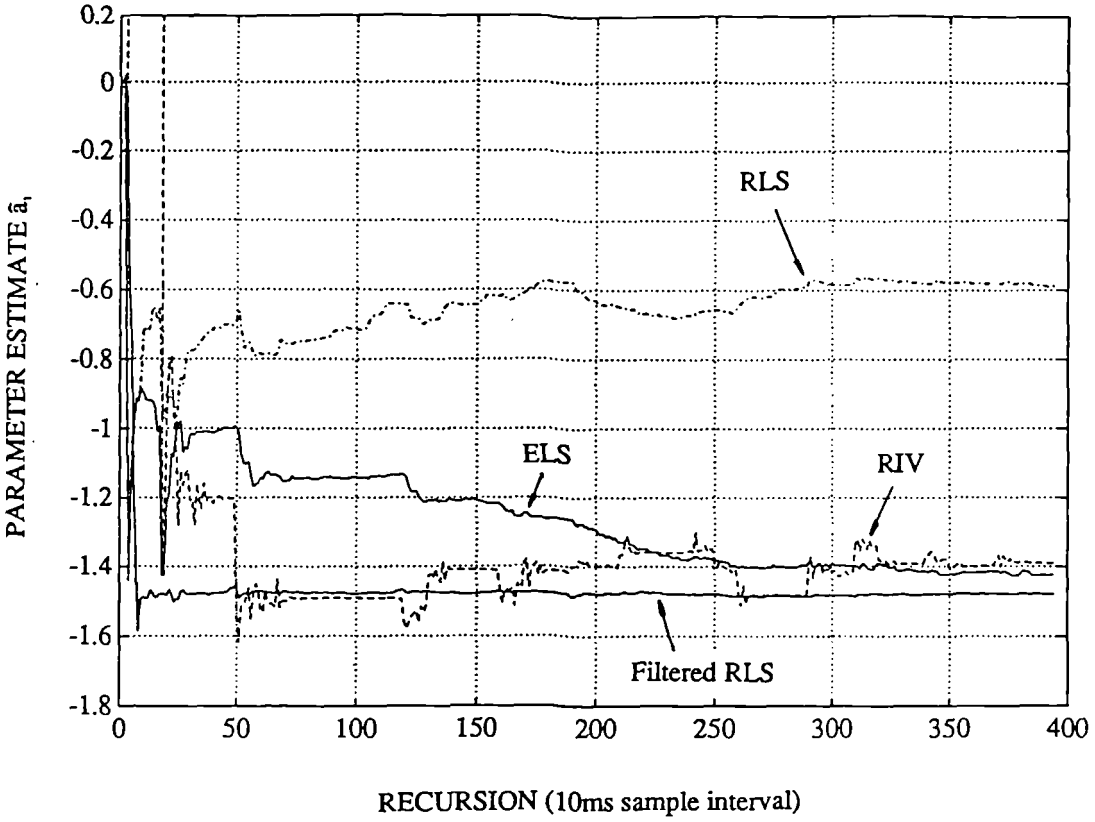

Figure 4.8 Convergence of recursive estimators (closed-loop plant data)

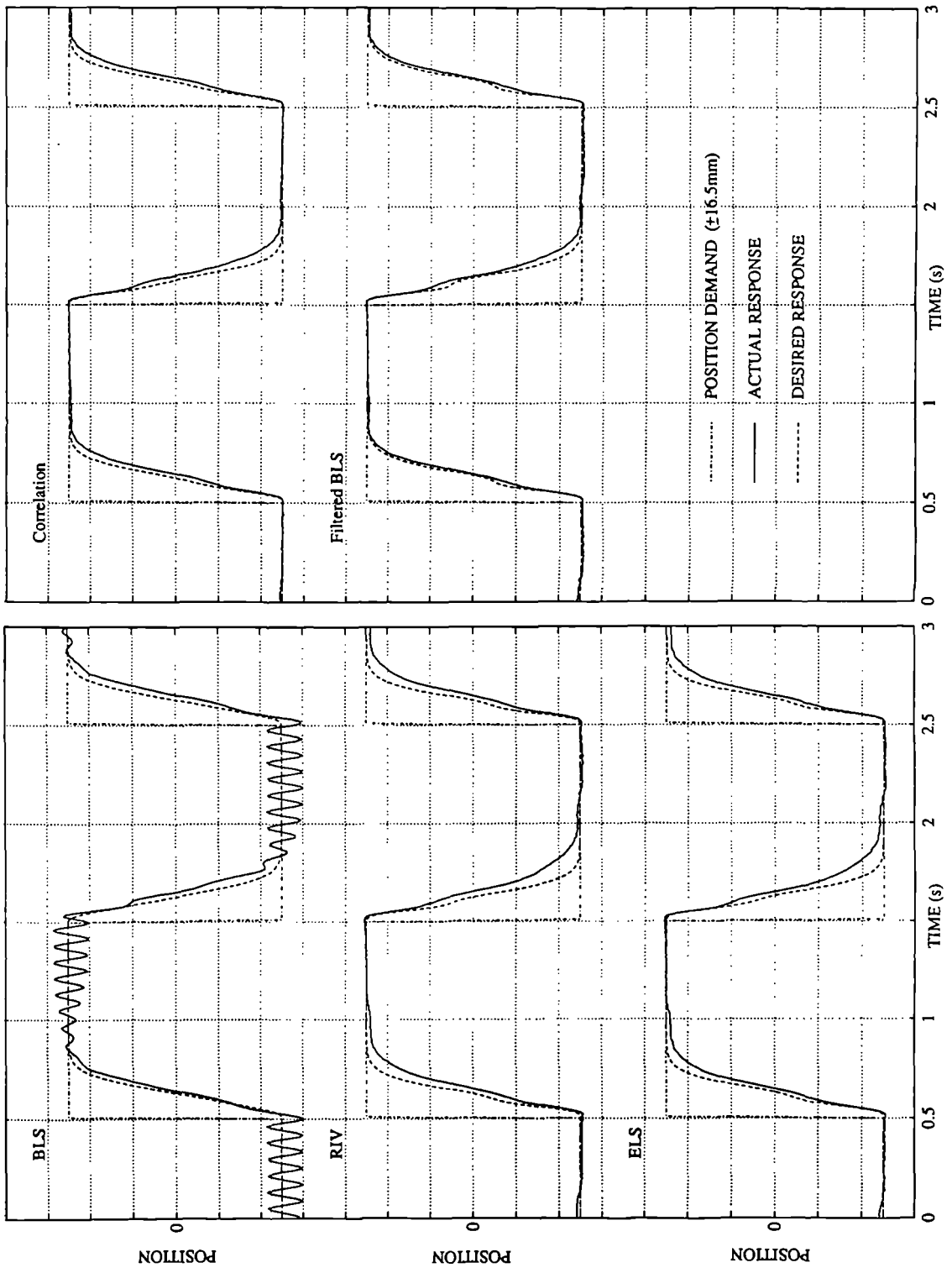

Figure 4.9 Comparison of desired and actual closed-loop responses for the various estimators (using closed-loop data)

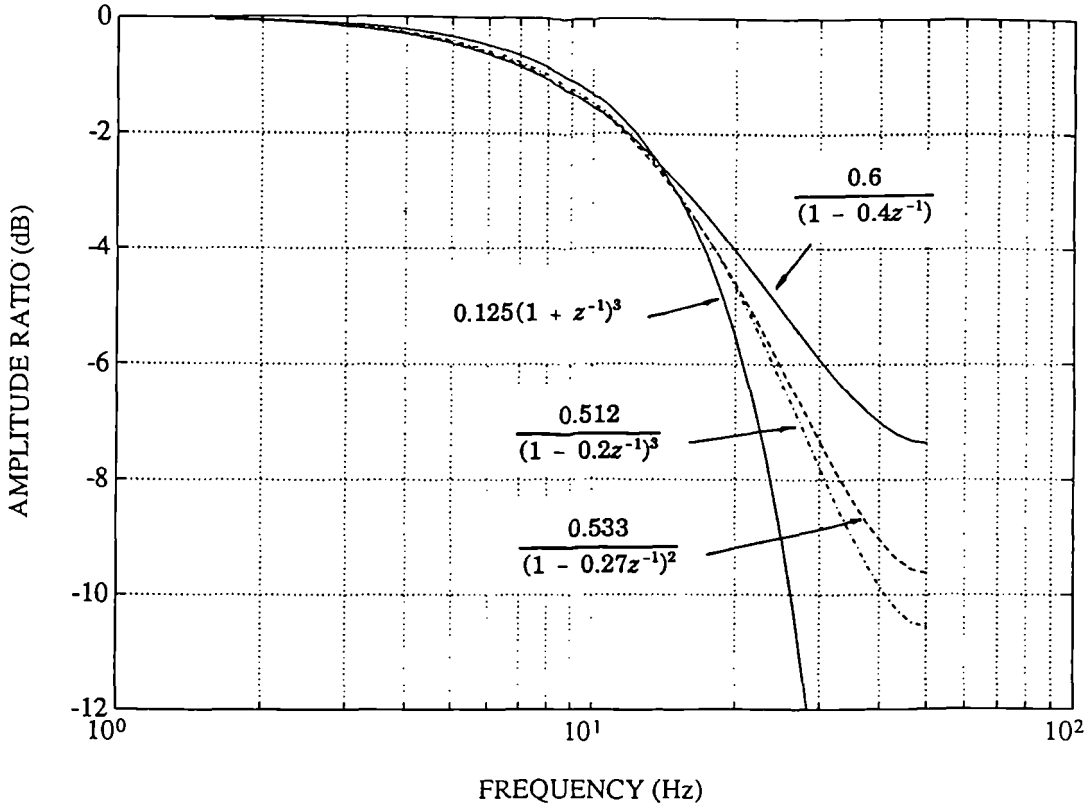

Figure 4.10 Frequency response of some digital filters with breakpoints at 15Hz (10ms sample interval)

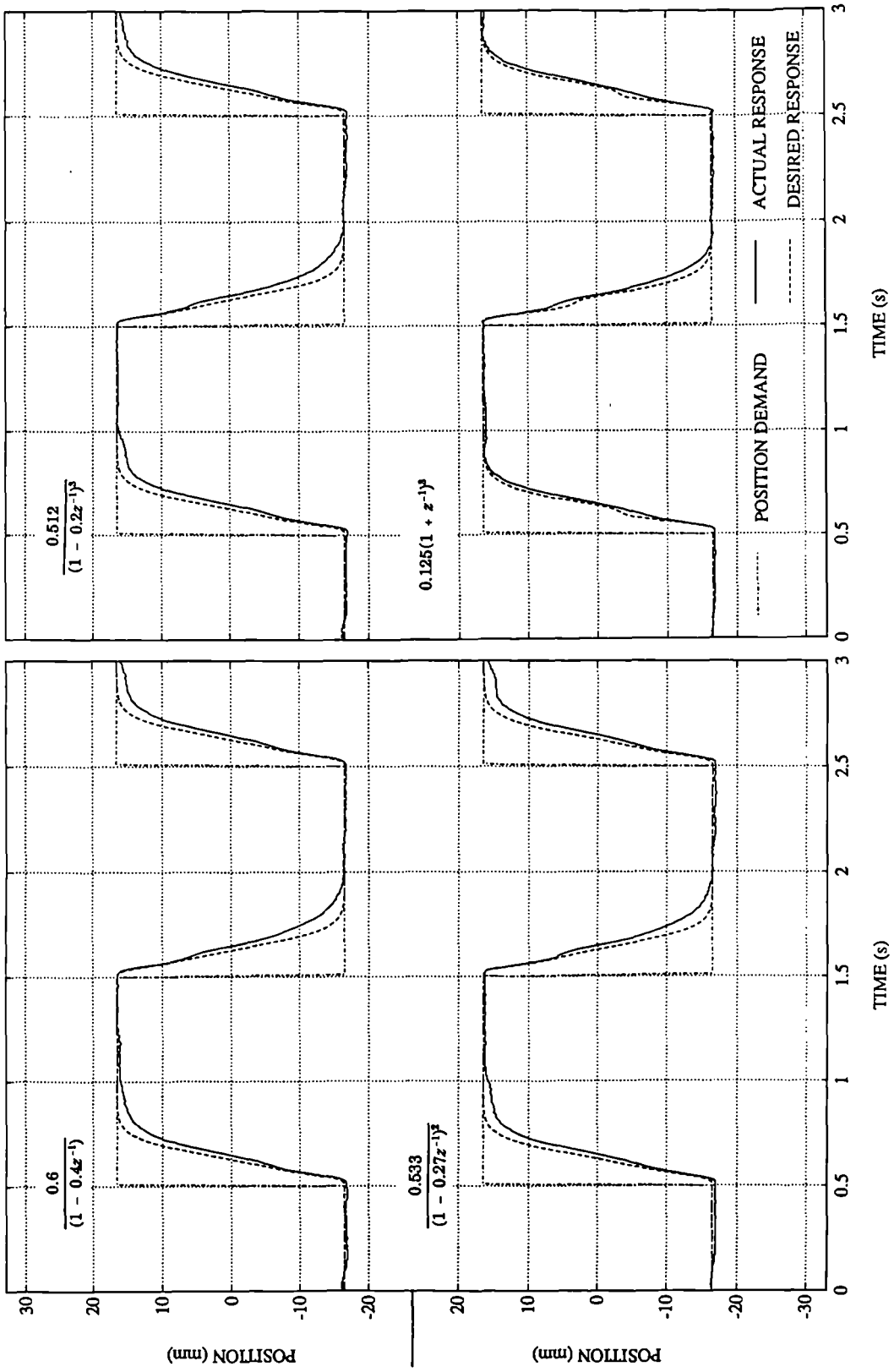

Figure 4.11 Comparison of desired and actual closed-loop responses for models estimated using filters with 15Hz breakpoints

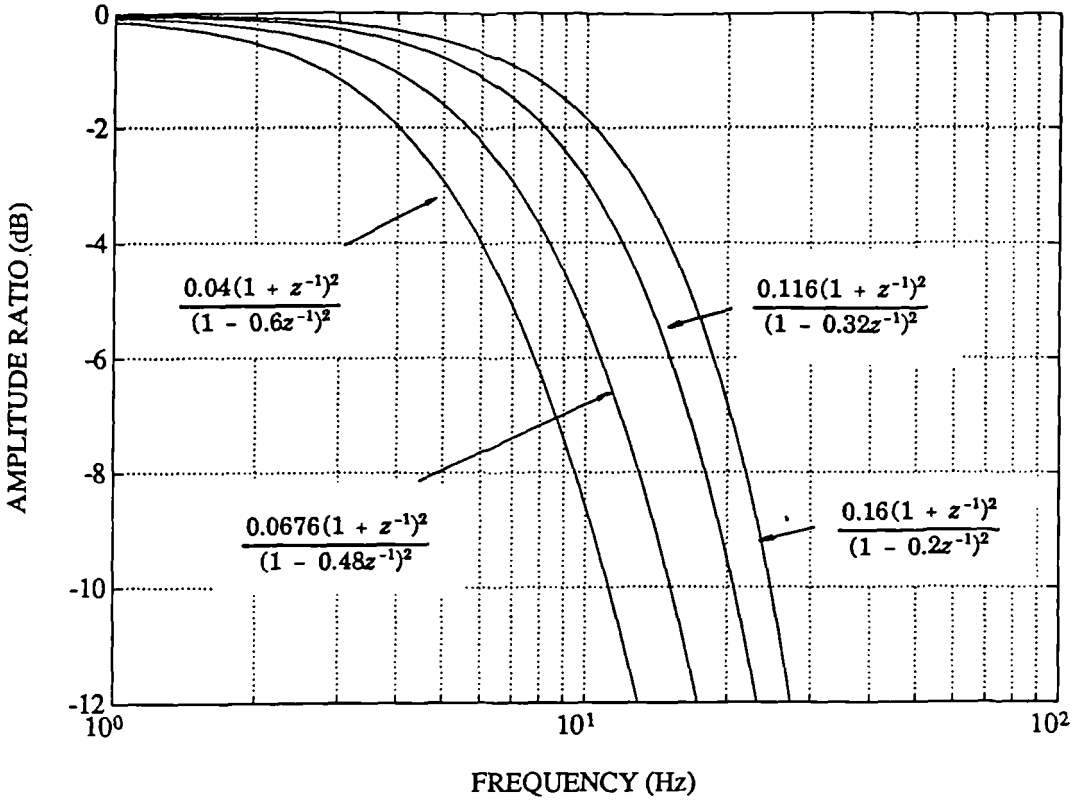

Figure 4.12 Frequency response of some digital filters, all with zeros at z=-1 (10ms sample interval)

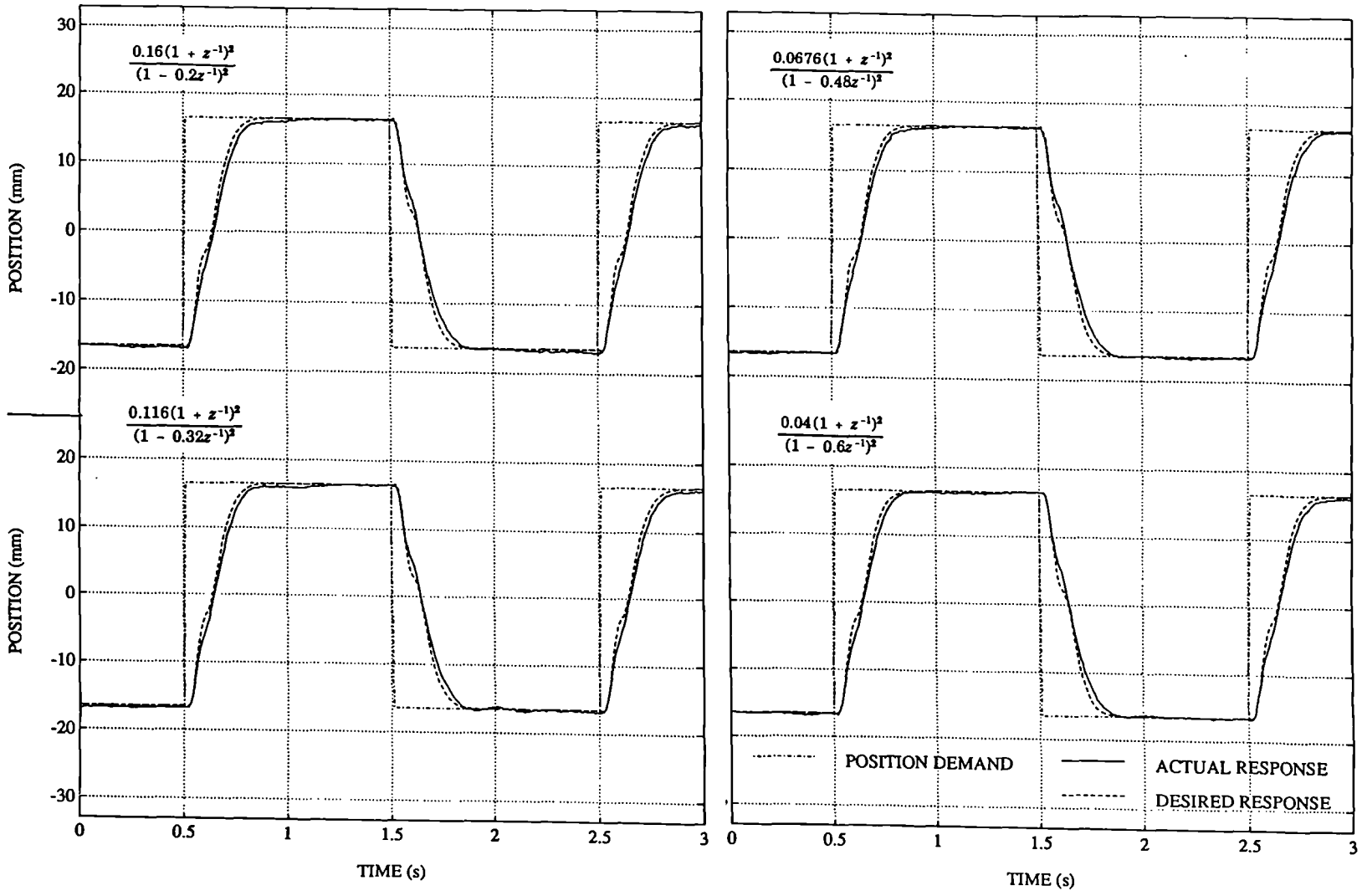

Figure 4.13 Comparison of desired and actual closed-loop responses for models estimated using filters with zeros at $z = -1$

5. System identification: structure selection

5.1 Introduction: simplifying the task

The structural parameters of a discrete-time linear model are the degrees of the numerator and denominator polynomials n and m, as seen in equation (4.1). Sometimes another structural parameter is defined: the number of whole sample intervals of dead-time. If the dead-time is large compared to the sample interval, then knowledge of its size will prevent a large number of numerator (b_i) coefficients from being unnecessarily estimated, as they can be set to zero. However for the type of servosystems under consideration, which are designed for rapid actuation, no significant dead-time is expected. So the dead-time will not be determined as a separate structural parameter. Note that although this is acceptable for pole-placement control, some other controllers (such as minimum variance) require the dead-time to be known precisely.

Model structure selection techniques are largely a matter of trial and error. For example, models can be estimated for a range of possible structures, and the goodness of fit between each model and the data can be assessed. Thus if the number of possible structures can be reduced, the work load involved in structure selection is also reduced.

Simplifications can be made by considering the lee-way which exists in choosing $\hat{n}$ and $\hat{m}$, which are the structural parameters of the estimated model. For instance, a maximum conceivable order for the plant might be guessed, and $\hat{n}$ and $\hat{m}$ equated to this order. Apart from the unnecessarily large number of controller coefficients obtained from this approach,

over-parameterising the model can result in $\hat{A}(z^{-1})$ and $\hat{B}(z^{-1})$ having common roots. If both polynomials are estimated with (say) one too many terms, the extra root in each will tend to be the same. To determine how this affects the pole-placement controller, consider the diophantine equation, equation (3.6), based on estimated model polynomials:

$$F(z^{-1})\hat{A}(z^{-1}) + G(z^{-1})\hat{B}(z^{-1}) = A_m(z^{-1}) \tag{5.1}$$

If the polynomials are over-parameterised by one degree as suggested, but are (for the sake of argument) otherwise accurate, then:

$$\left.\begin{aligned} \hat{A}(z^{-1}) &= A(z^{-1})(1 - \rho z^{-1}) \\ \hat{B}(z^{-1}) &= B(z^{-1})(1 - \rho z^{-1}) \end{aligned}\right\} \tag{5.2}$$

where $(1 - \rho z^{-1})$ is the common factor. The left hand side of the diophantine equation can now be re-written:

$$[F(z^{-1})A(z^{-1}) + G(z^{-1})B(z^{-1})](1 - \rho z^{-1}) \tag{5.3}$$

Thus equation (5.1) has no solution, assuming that the common factor is not also a factor of $A_m(z^{-1})$.

Thus if both polynomials are of too high a degree the pole-placement controller design algorithm will breakdown. However if only one of the polynomial degrees is too high, this problem does not occur. Hence only the degree of the longer polynomial need be found; the other polynomial can be made the same length (i.e. use $\hat{n} = \hat{m}$). The structure selection problem is now reduced to finding one order, and the model will be of the form:

$$\frac{\hat{b}_1 z^{-1} + \hat{b}_2 z^{-2} + \ldots + \hat{b}_{\hat{n}} z^{-\hat{n}}}{1 + \hat{a}_1 z^{-1} + \hat{a}_2 z^{-2} + \ldots + \hat{a}_{\hat{n}} z^{-\hat{n}}} \tag{5.4}$$

5.2 Model structure selection methods

5.2.1 Choice of selection methods

Several structure selection techniques have been implemented and compared. The techniques chosen were those which have performed well in tests described in the literature, especially van den Boom and van den Enden (1974), Unbehauen and Göhring (1974), and Young *et al* (1980). They involve assessing different model structures by:

- comparing the prediction errors generated by models of different structure.
- comparing the estimated parameter variances for the different structures.
- comparing the determinants of the product-moment matrices for the different structures.

Structure selection based on variants of the first two of these has been applied to electro-hydraulic servosystems by Daley (1987 and 1989) and Yufei *et al* (1988). The techniques are described in turn below.

5.2.2 Prediction error method

Estimating parameters for a range of model orders, and assessing the goodness of fit between each model and the data, can indicate the most appropriate model to use. The root-mean-square (RMS) prediction error, i.e. the error between the actual output and the output predicted by the model, is a suitable statistic for goodness of fit. The predicted output $\hat{y}_t$ for a model of order $\hat{n}$ is given by:

$$\hat{y}_t(\hat{n}) = \psi_t^T(\hat{n})\ \hat{\theta}(\hat{n}) \tag{5.5}$$

where the regressor and parameter vectors are (respectively):

$$\left.\begin{aligned} \psi_t^T(\hat{n}) &= [y_{t-1}, \ldots, y_{t-\hat{n}}, u_{t-1}, \ldots, u_{t-\hat{n}}] \\ \hat{\theta}(\hat{n}) &= [-\hat{a}_1(\hat{n}), \ldots, -\hat{a}_{\hat{n}}(\hat{n}), \hat{b}_1(\hat{n}), \ldots, \hat{b}_{\hat{n}}(\hat{n})] \end{aligned}\right\} \tag{5.6}$$

Thus the RMS prediction error based on N samples of data is given by:

$$\sigma(\hat{n}) = \left(\frac{1}{N-\hat{n}} \sum_{t=\hat{n}+1}^{N} (y_t - \hat{y}_t(\hat{n}))^2 \right)^{0.5} \tag{5.7}$$

If the model order is too low, increasing it will reduce the RMS prediction error. As the model order increases beyond the most appropriate order for the plant, no further significant reductions in the RMS prediction error would be expected. However small reductions are still likely, as the greater freedom in a higher order model would allow a better fit to the data.

Various tests have been devised to pick out automatically the correct order from this prediction error information (e.g. Akaike's Information Criterion and the F-test), but these have been found to be unreliable in practice — van den Boom and van den Enden (1974), Unbehauen and Göhring (1974), and Söderström (1977). In this study the RMS prediction errors are merely plotted against model order.

The estimator used to find the model for each order is filtered least squares, as this was found to be the most successful parameter estimator in Chapter 4. The data used for calculating the RMS prediction errors are the same as those used to estimate the models in the first place. The errors are calculated from the filtered form of the data. This is motivated by the interpretation of the filter as a means of attenuating noisy parts of the spectrum, so that the filtered data are more representative of the actual plant behaviour.

5.2.3 Parameter variance method

In this method a model is estimated for each order and the variances of the model parameter estimates are estimated. The arithmetic mean of the variances for a model is known as the error variance norm or EVN (Young *et al*, 1980). For model orders which are too high it may be expected that identifiability problems would result in large variances and thus large EVN values.

The normalised covariance matrix is defined as:

$$P(\hat{n}) = [\Psi^T(\hat{n})\Psi(\hat{n})]^{-1} \tag{5.8}$$

where $\Psi(\hat{n})$ is the matrix of regressor values given by:

$$\Psi(\hat{n}) = \begin{bmatrix} \psi_{n+1}^T(\hat{n}) \\ \vdots \\ \psi_N^T(\hat{n}) \end{bmatrix} \tag{5.9}$$

An estimate of the covariance matrix for least squares parameter estimates is the product of the normalised covariance matrix and the variance of the noise component of the data (Norton, 1986). The mean-square prediction error is an estimate of the latter. The parameter estimate variances can be extracted from the leading diagonal of the covariance matrix. Note that the normalised covariance matrix is a natural by-product of the recursive least squares estimator (see equation 4.7). Thus the EVN is given by:

$$\mathrm{EVN}(\hat{n}) = \frac{\sigma^2(\hat{n})}{2\hat{n}} \sum_{i=1}^{2n} p_{ii}(\hat{n}) \tag{5.10}$$

where $p_{ii}(\hat{n})$ is an element in the leading diagonal of $P(\hat{n})$. As with the first technique, filtered data are used throughout, the same data being used for RLS estimation as for prediction error calculation.

5.2.4 Product-moment matrix method

The final technique relies on the product-moment matrix (PM) becoming near-singular as the model order increases beyond the correct value. The product-moment matrix is defined by:

$$\mathrm{PM}(\hat{n}) = \Psi^T(\hat{n})\Psi(\hat{n}) \tag{5.11}$$

For a model order which is too great, redundancy in Ψ leads to the near-singularity in the PM, which is indicated by a small determinant. Thus the determinant ratio (DR), i.e. the determinant for order $\hat{n}$ divided by that for $\hat{n}$+1, should jump significantly when the correct

order is reached. Thus the test statistic is:

$$\text{PM DR} = \frac{|\text{PM}(\hat{n})|}{|\text{PM}(\hat{n}+1)|} \tag{5.12}$$

Unlike the other methods it is not necessary to estimate models for the different structures in order to compare them.

Three versions of the PM DR approach have been implemented. In addition to the basic technique, these are:

- calculating the PM using filtered data (called filtered PM hereafter),
- replacing the samples in one of the regressor matrices which is used to form the PM with instrumental variables (called instrumental PM or IPM).

These two approaches are intended to reduce the influence of noise on the results.

In the latter technique:

$$\text{IPM}(\hat{n}) = Z^T(\hat{n})\Psi(\hat{n}) \tag{5.13}$$

where

$$Z(\hat{n}) = \begin{bmatrix} z_{\hat{n}+1}^T(\hat{n}) \\ \vdots \\ z_N^T(\hat{n}) \end{bmatrix} \tag{5.14}$$

and $z_i(\hat{n})$ is the instrument vector for a test model of order $\hat{n}$.

The instrument vector may contain simulated input and output samples, as detailed in Section 4.2.4. The models used for simulation are estimated using filtered least squares, and are of the order currently under test. As the instruments are uncorrelated with the noise in the regressors, the noise will be 'correlated out' of the IPM (Young *et al*, 1980).

5.3 Comparison of methods: simulation

The model order selection techniques were initially compared using data generated by a digital simulation. The simulation is the same as described in Section 4.3, so the correct model order is 3. The data is shown in Figure 4.2. A sample length of 200 is used throughout, and the filter used for filtered least squares, filtered PM etc. is:

$$\frac{1}{1 - 0.7z^{-1}} \tag{5.15}$$

A range of orders from 1 to 5 were tested, and the results are illustrated in Figure 5.1. The elbow in the RMS prediction error characteristic (denoted RMS PE) clearly indicates the correct model order, but the dip in EVN at order 3 is less distinct. In fact the first order EVN is the minimum, but it appears that the EVN tends to rise with model order as a general rule, and the correct model order is only signalled by a break in this trend.

The basic PM DR gives no clear indication of model order, whereas the filtered version gives a slightly greater rise from order 2 to 3 than between the other orders. However the IPM DR give a very clear indication of a third order model.

5.4 Best structure for the electro-hydraulic positioning system

The structure selection methods have also been compared by applying them to the electro-hydraulic positioning system. As the plant exhibits non-linear behaviour, and has high order dynamics which may or may not need to be modelled (e.g. dynamics associated with the valve), there is no model order which can be called correct. So to establish the best order to use in practice, models have been estimated for orders ranging from 1 to 5. A filtered least squares estimator was used to estimate the model parameters, processing the 400 samples of open-loop input-output data illustrated in Figure 4.4. A pole-placement controller was then

designed and implemented for each model order.

Desired closed-loop pole positions have to be specified for the pole-placement controller. The degree of the closed-loop transfer function characteristic equation was chosen to be the same as the order of the plant model used for controller design. All the closed-loop poles were located at z = 0.7. Thus in each case:

$$A_m(z^{-1}) = k(1 - 0.7z^{-1})^4 \tag{5.16}$$

where k is chosen to yield unity steady-state gain.

The closed-loop response corresponding to each model order is shown in Figure 5.2. First, second and fifth order models do not give stable controllers. Third and fourth order models give acceptable responses, so assuming the simpler controller is preferable, a third order model is most appropriate. Note that these results are typical; models based on different data sets or controllers with different desired closed-loop poles give similar results.

Experience has shown that a third order model *is* often suitable for this type of plant. However another order may be more appropriate for an outwardly similar plant. For example if the load mass were less significant, a first order model can be acceptable, as shown in Hori *et al* (1988) and Vaughan and Whiting (1984). Alternatively the valve dynamics may also have to be modelled in other cases, giving a higher order. Also note that the physical analysis in Appendix 1 indicated that a fourth order model is (in general) best. Thus there is sufficient uncertainty to warrant the use of the mathematical structure selection methods of Section 5.2.

5.5 Comparison of methods: positioning system

The various structure selection methods have been tested using the open-loop data mentioned in Section 5.4. Wherever a filter is needed for filtered least squares, filtered PM etc., the following is used:

$$\frac{(1 + z^{-1})^2}{(1 - (0.25 + 0.47j)z^{-1})(1 - (0.25 - 0.47j)z^{-1})} \tag{5.17}$$

This is the same filter as used for most of Chapter 4.

The RMS prediction error, the logarithm of the error variance norm, and the various product-moment matrix methods are plotted against model order in Figure 5.3. The significant reduction in the RMS prediction error between orders 2 and 3, followed by virtually no reduction between orders 3 and 4, clearly indicates the correct model order. There is a dip in the EVN characteristic at order three, but it is not especially distinct. The basic PM DR gives no clear indication of model order, and the filtered version is little better. However the IPM DR clearly indicates that a third order model should be used.

To confirm these findings, another set of results is presented in Figure 5.4. These are based on 400 samples of data collected with the plant operating under unity gain proportional closed-loop control. The data is that shown in Figure 4.7. The RMS prediction error and IPM DR methods clearly indicate a third order model, whereas the other methods do not give a distinct indication of any particular order.

5.6 Conclusions

An appropriate order for the model to be identified can readily be found by inspecting the RMS prediction errors for a range of orders. The IPM DR (instrumental product-moment matrix determinant ratio) technique is also successful in this respect. Results using a simple linear simulation and those using the real plant are very similar.

Very few applications of any structure selection techniques to electro-hydraulic servosystems have been previously reported, let alone comparisons between several techniques. Model structure information used in control or estimation work appears to have been found by trial and error, or is sometimes justified by analytical modelling.

The results in this and the previous Chapter illustrate that the application of certain system identification techniques to an electro-hydraulic servosystem can yield a good model for controller design purposes. The techniques form a systematic modelling procedure, so there is no need to rely on physical modelling or guesswork. However some knowledge about the plant is always useful if not essential.

Note that identifying a model is important for designing adaptive as well as fixed-coefficient controllers. Although in most adaptive controllers the parameters are estimated on-line, knowledge of the model structure is still essential. Furthermore, values for the parameter estimates are required to initialise the adaptive controller.

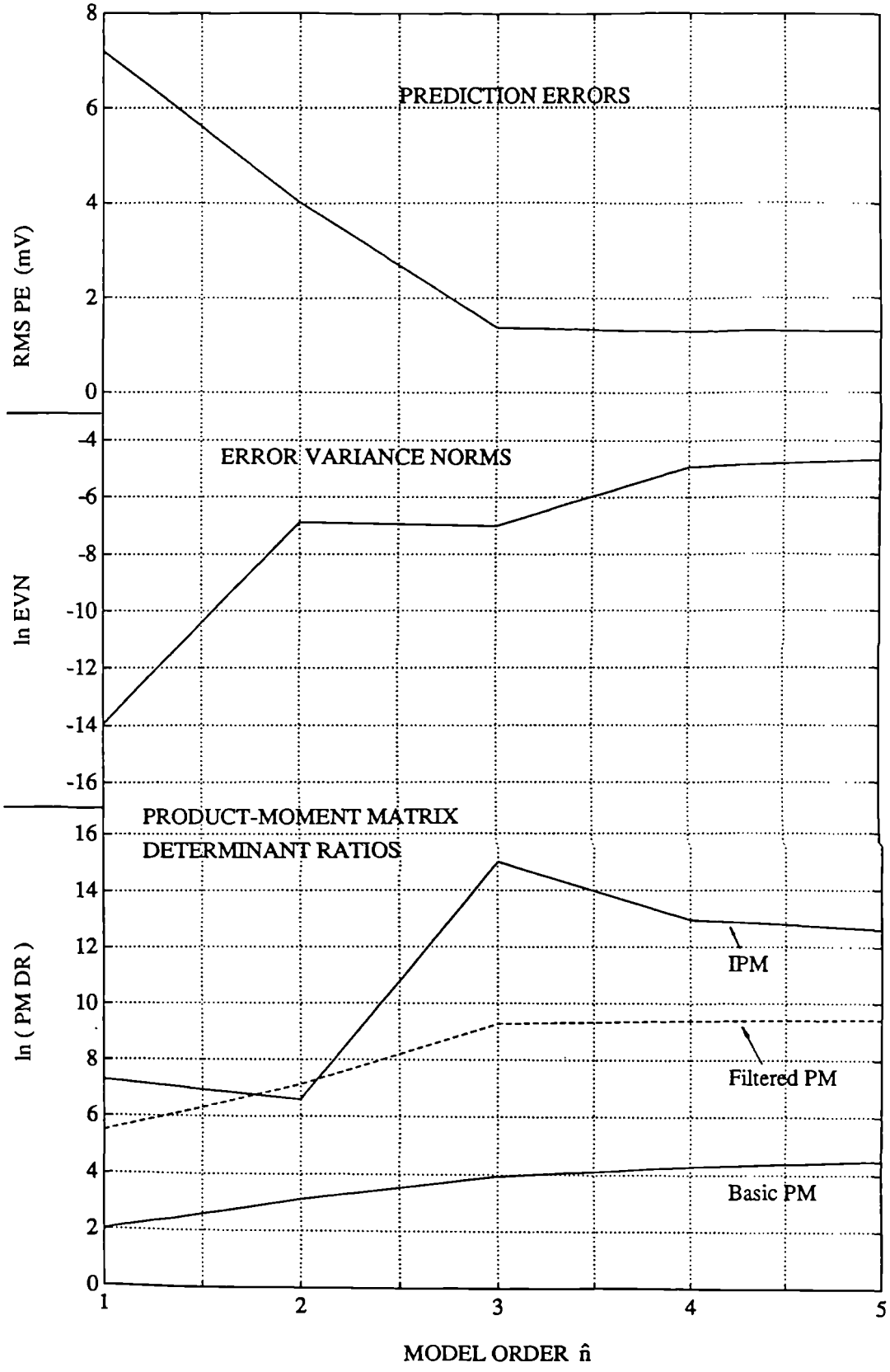

Figure 5.1 Model order selection (for simulated 3rd order plant)

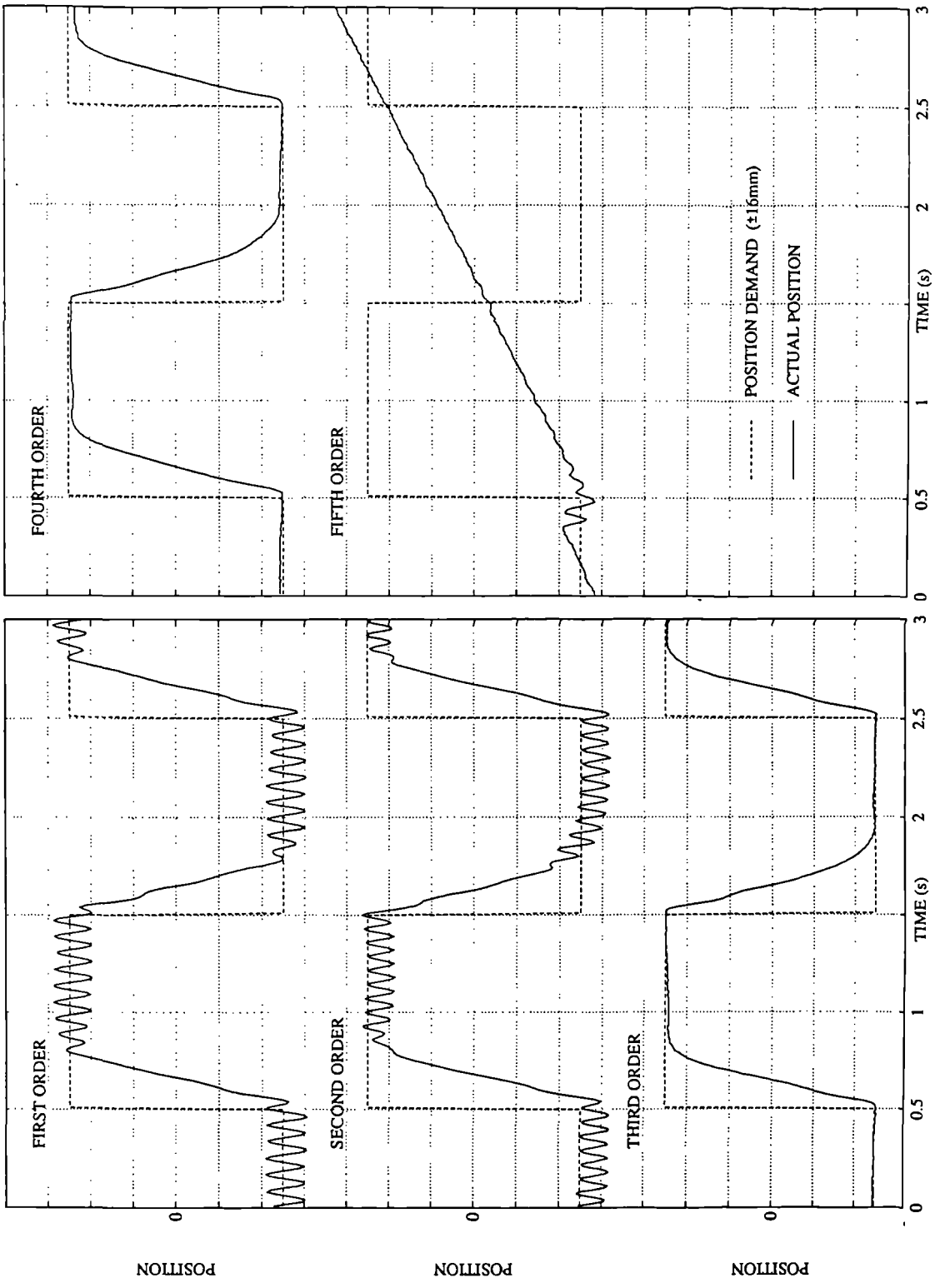

Figure 5.2 Pole-placement control of electro-hydraulic servosystem using models of different order

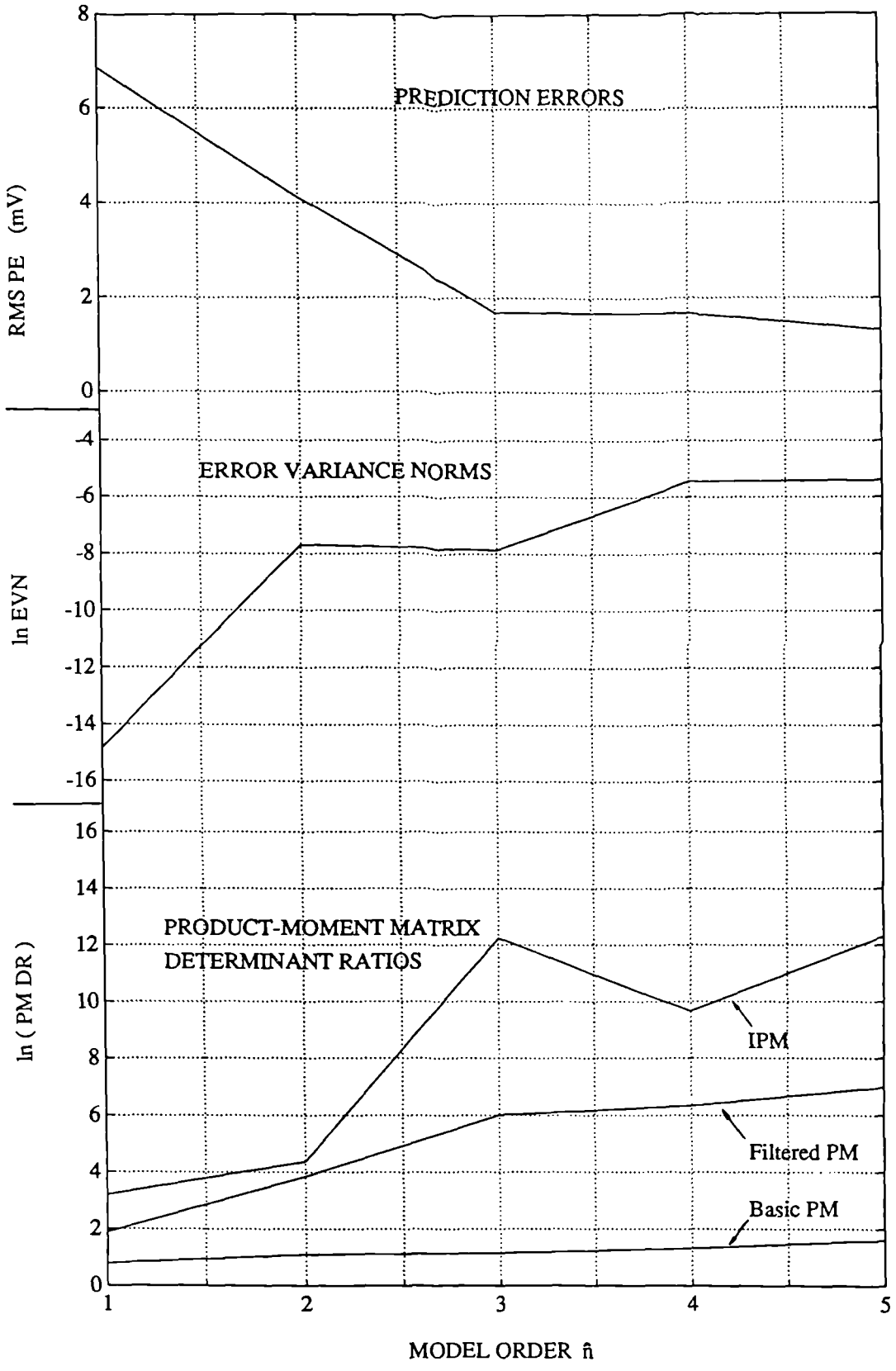

Figure 5.3 Model order selection (from open-loop plant data)

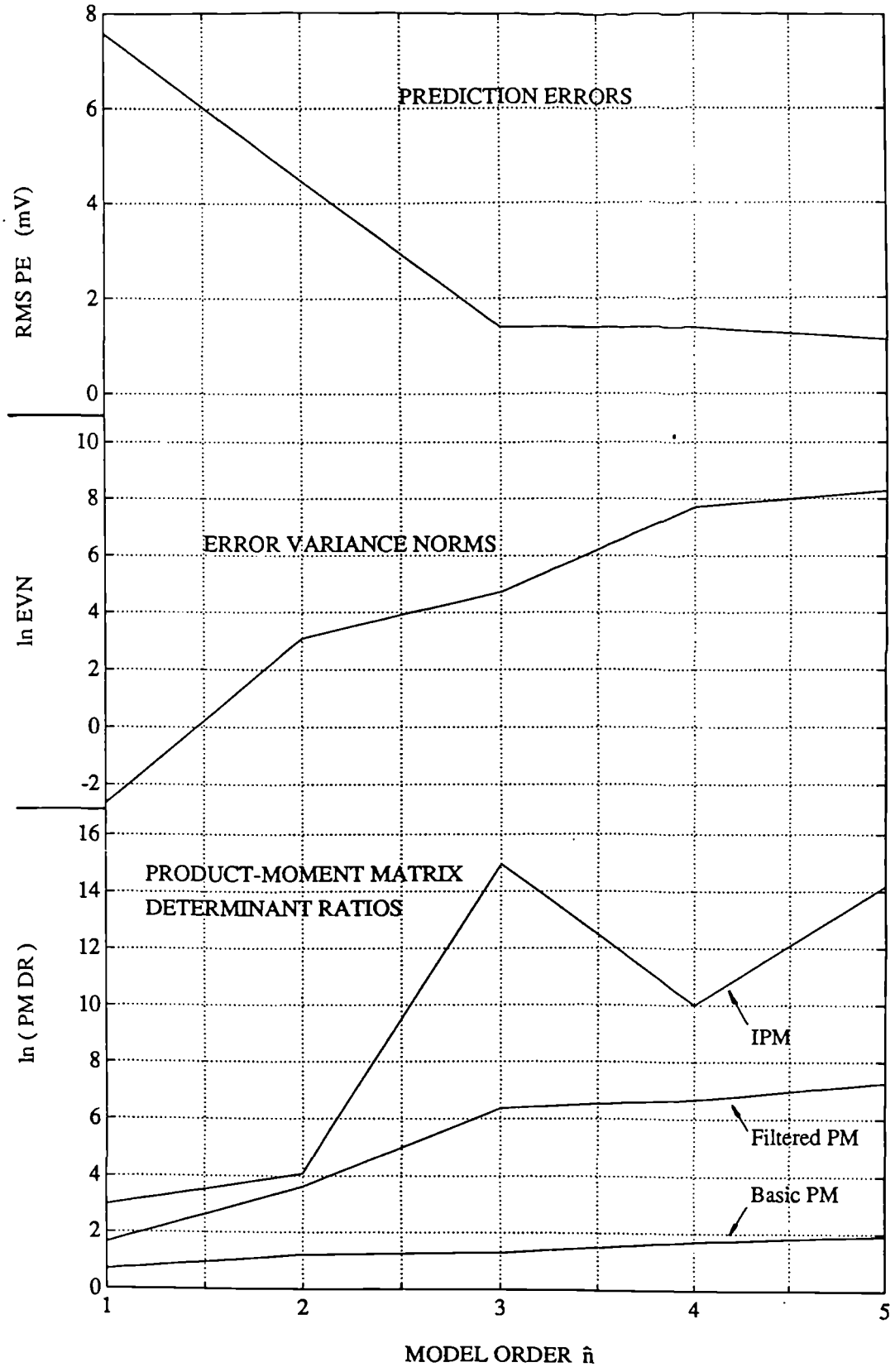

Figure 5.4 Model order selection (from closed-loop plant data)

6. Pole-placement control

6.1 Introduction

The basic pole-placement controller was introduced in Chapter 3, and used to assess the merit of system identification techniques in Chapters 4 and 5. However the analysis in Section 3.5 was purely deterministic — no consideration was given to the response of the controller to signal noise, nor to the effect of errors in the plant model. The insensitivity of a control system to both these uncertainties is an important property, and is discussed in this Chapter.

A controller giving a closed-loop response which is insensitive to modelling errors is known as robust. One measure of robustness is the size of the modelling error which can be tolerated before the onset of instability. This is stability robustness. Although this gives no direct information about the extent to which the closed-loop response deviates from the desired response as modelling errors increase (before the response becomes unstable), it has the advantage of yielding usable results.

In order to design a pole-placement controller pole positions have to be chosen for the closed-loop response. Using a purely linear deterministic analysis it appears that any pole positions could be specified. Thus all poles could be placed at $z=0$, giving the fastest possible response (i.e. a deadbeat controller). In practice the speed of response is limited by saturation of the servovalve, but such fast pole positions also place a high demand on the accuracy on the model, and may amplify noise. It is demonstrated in this Chapter that a consideration of robustness and noise attenuation serves as a useful guide to choosing pole positions. It is also

shown that the addition of a third digital filter in the controller structure, used to filter the demand signal, allows faster pole positions to be specified whilst maintaining similar levels of robustness and noise attenuation.

6.2 Controller design

The following analysis mirrors that in Section 3.5, but here a demand filter is included in the controller, and a noise signal contaminates the plant output. Hence the pole-placement controller structure is that shown in Figure 6.1. The control signal is generated thus:

$$u_t = \frac{H(z^{-1})r_t - G(z^{-1})y_t}{F(z^{-1})} \tag{6.1}$$

Note that in practice the controller is still implemented with software control signal saturation and non-linear compensation as described in Section 3.6. Let the plant be represented by:

$$y_t = \frac{B(z^{-1})}{A(z^{-1})}u_t + e_t' \tag{6.2}$$

where e'_t is a coloured noise signal. The resulting closed-loop response is:

$$y_t = \frac{B(z^{-1})H(z^{-1})}{F(z^{-1})A(z^{-1}) + G(z^{-1})B(z^{-1})}r_t + \frac{F(z^{-1})A(z^{-1})}{F(z^{-1})A(z^{-1}) + G(z^{-1})B(z^{-1})}e_t' \tag{6.3}$$

If $A(z^{-1})$ and $B(z^{-1})$ are known exactly, then $F(z^{-1})$ and $G(z^{-1})$ can be calculated to satisfy:

$$F(z^{-1})A(z^{-1}) + G(z^{-1})B(z^{-1}) = A_m(z^{-1})H(z^{-1}) \tag{6.4}$$

Substituting equation (6.4) into (6.3):

$$y_t = \frac{B(z^{-1})}{A_m(z^{-1})} r_t + \frac{F(z^{-1})A(z^{-1})}{A_m(z^{-1})H(z^{-1})} e_t' \qquad (6.5)$$

Thus $A_m(z^{-1})$ is the closed-loop characteristic polynomial relating demand to output. It has roots which are the desired system poles specified by the user, and a steady-state gain calculated to give unity gain in the closed-loop, i.e.:

$$A_m(1) = B(1) \qquad (6.6)$$

As can be seen from equation (6.5), the demand filter $H(z^{-1})$ only appears in the transfer function from noise to output, and it can be used to attenuate noise without affecting servo performance. Hence the reciprocal of $H(z^{-1})$ can be any stable filter specified by the user.

Equation (6.4) can be written as a matrix equation of the same form as equation (3.9), from which $F(z^{-1})$ and $G(z^{-1})$ are found. The polynomials in the minimal degree solution have the following degrees:

$$\left.\begin{aligned} \deg F(z^{-1}) &= m - 1 \\ \deg G(z^{-1}) &= n - 1 \\ \deg A_m(z^{-1})H(z^{-1}) &= n + m - 1 \end{aligned}\right\} \qquad (6.7)$$

6.3 Robustness to modelling errors

In practice only an approximate plant model is available. Using $\hat{A}(z^{-1})$ and $\hat{B}(z^{-1})$ to denote estimates of $A(z^{-1})$ and $B(z^{-1})$ respectively, the controller coefficients are actually calculated from the following equations, rather than equations (6.4) and (6.6):

$$\left.\begin{aligned} A_m(1) &= \hat{B}(1) \\ F(z^{-1})\hat{A}(z^{-1}) + G(z^{-1})\hat{B}(z^{-1}) &= A_m(z^{-1})H(z^{-1}) \end{aligned}\right\} \tag{6.8}$$

Thus $A_m(z^{-1})$ will not be the closed-loop characteristic polynomial exactly, and $H(z^{-1})$ will not be cancelled out of the transfer function from demand to output exactly. These inaccuracies may affect both transient and steady-state performance. An error in steady-state gain is a particularly significant failing for a servosystem, but as shown in Appendix 2, unity steady-state gain can be ensured for a plant which exhibits integral action if $\hat{A}(1)=0$.

Modelling errors will affect the transient response, potentially to the extent of causing instability. A simple test of robustness is derived by considering the modelling error which can be accommodated before the system becomes unstable. On the Nyquist plot in Figure 6.2, $L(e^{-j\omega T})$ is the true open-loop transfer function, given by:

$$L(e^{-j\omega T}) = \frac{B(e^{-j\omega T})G(e^{-j\omega T})}{A(e^{-j\omega T})F(e^{-j\omega T})} \tag{6.9}$$

and $\hat{L}(e^{-j\omega T})$ is the assumed open-loop transfer function based on approximate model polynomials $\hat{A}(z^{-1})$ and $\hat{B}(z^{-1})$. If the lengths a and b marked on the Figure are such that $a < b$ for all frequencies, the actual open-loop transfer function cannot encircle the -1 point, and the closed-loop system is stable. Note that the condition is sufficient rather than necessary. If $M(z^{-1})$ is the plant transfer function $B(z^{-1})/A(z^{-1})$, the stability condition can be related to the error in M (dropping the $e^{-j\omega T}$ argument for brevity):

$$\begin{aligned} a &< b \\ |\hat{L} - L| &< |\hat{L} + 1| \\ \left|\frac{\hat{B}}{\hat{A}} - \frac{B}{A}\right| &< \left|\frac{\hat{B}}{\hat{A}} + \frac{F}{G}\right| \\ |\hat{M} - M| &< \left|\frac{A_m H}{\hat{A} G}\right| \\ |\hat{M} - M| &< |R| \end{aligned} \tag{6.10}$$

So $|R|$, which is dependent on the choice of A_m and H, should be as large as possible at all frequencies for maximum stability robustness. Note that robustness to modelling errors is particularly important when a non-linear plant is modelled by a linear model, and when the plant characteristics may be varying with time.

The actual modelling error is unknown. However for time-invariant plant, input-output data which are used to estimate a plant model can also be used to estimate the error in that model. This modelling error is in the form of a covariance matrix for the estimate of the model parameter vector θ. For an unbiased estimator, the covariance matrix is defined as:

$$P' = E[(\hat{\theta} - \theta)(\hat{\theta} - \theta)^T] \tag{6.11}$$

This can be translated into a frequency domain modelling error as shown below. Introducing the notation:

$$\Delta M(e^{-j\omega T}) = \hat{M}(e^{-j\omega T}) - M(e^{-j\omega T}) \tag{6.12}$$

Then (dropping the $e^{-j\omega T}$ argument for brevity again):

$$\left.\begin{aligned} \Delta M &\approx \left[-\frac{\partial \hat{M}}{\partial \hat{a}_1}, \ldots -\frac{\partial \hat{M}}{\partial \hat{a}_n}, \frac{\partial \hat{M}}{\partial \hat{b}_1}, \ldots \frac{\partial \hat{M}}{\partial \hat{b}_m}\right][-\Delta a_1, \ldots -\Delta a_n, \Delta b_1, \ldots \Delta b_m]^T \\ \Delta M &\approx \frac{\partial \hat{M}^T}{\partial \hat{\theta}} \Delta\theta \\ \text{and} \quad \Delta M &\approx \Delta\theta^T \frac{\partial \hat{M}}{\partial \hat{\theta}} \end{aligned}\right\} \tag{6.13}$$

and, denoting $\Delta\bar{M}$ as the complex conjugate of ΔM,

$$
\begin{aligned}
|\Delta M|^2 &= \Delta M \Delta \overline{M} \\
|\Delta M|^2 &\approx \frac{\partial \hat{M}}{\partial \hat{\theta}}^T \Delta\theta \Delta\theta^T \frac{\partial \overline{\hat{M}}}{\partial \hat{\theta}} \\
E[\,|\Delta M|^2] &\approx \frac{\partial \hat{M}}{\partial \hat{\theta}}^T P' \frac{\partial \overline{\hat{M}}}{\partial \hat{\theta}} \\
\sigma &\approx \left(\frac{\partial \hat{M}}{\partial \hat{\theta}}^T P' \frac{\partial \overline{\hat{M}}}{\partial \hat{\theta}} \right)^{0.5}
\end{aligned}
\tag{6.14}
$$

The quantity σ, defined as $(E[\,|\Delta M|^2])^{0.5}$, is a measure of the magnitude of the frequency domain modelling error. It is akin to the standard deviation in a univariate distribution. As $\hat{M} = \hat{B}/\hat{A}$, the partial derivatives of $\hat{M}$ with respect to the model parameter estimates are given by:

$$
\frac{\partial \hat{M}}{\partial \hat{a}_i} = -e^{-ji\omega T} \hat{B} \hat{A}^{-2}, \qquad \frac{\partial \hat{M}}{\partial \hat{b}_i} = e^{-ji\omega T} \hat{A}^{-1} \tag{6.15}
$$

Inaccuracies in the value of σ given by equation (6.14) will occur if the estimator is biased, if the model parameter errors are not small, and because in practice the value can only be based on an estimate of the covariance matrix.

6.4 Application to the electro-hydraulic positioning system

A plant model was estimated using the filtered least squares technique, and the covariance matrix was estimated by the method described in Section 5.2.3. Input-output data were collected, using a pseudo-random binary sequence input signal, and with the plant operating in open-loop near mid-stroke at 100bar supply pressure. A 10ms sample interval was still used, and the estimation filter was $(1 + z^{-1})^3$. The resulting model and covariance matrix estimates are shown below:

$$\hat{y}_t = \frac{\hat{b}_1 z^{-1} + \hat{b}_2 z^{-2} + \hat{b}_3 z^{-3}}{1 + \hat{a}_1 z^{-1} + \hat{a}_2 z^{-2} + \hat{a}_3 z^{-3}} u_t \qquad (6.16)$$

$$\begin{aligned} \hat{a}_1 &= -2.37 \\ \hat{a}_2 &= 2.28 \\ \hat{a}_3 &= -0.909 \\ \hat{b}_1 &= 1.07\text{x}10^{-3} \\ \hat{b}_2 &= 3.78\text{x}10^{-3} \\ \hat{b}_3 &= 3.27\text{x}10^{-3} \end{aligned}$$

$$\hat{P}' = \begin{bmatrix} 0.656 & -1.082 & 0.425 & 0.001 & -0.004 & -0.003 \\ -1.082 & 2.103 & -1.021 & -0.010 & 0.025 & -0.012 \\ 0.425 & -1.021 & 0.596 & 0.009 & -0.022 & 0.015 \\ 0.001 & -0.010 & 0.009 & 0.003 & -0.006 & 0.003 \\ -0.004 & 0.025 & -0.022 & -0.006 & 0.011 & -0.006 \\ -0.003 & -0.012 & 0.015 & 0.003 & -0.006 & 0.004 \end{bmatrix} \text{x } 10^{-4}$$

If no demand filter is specified (i.e. $H(z\text{-}1) = 1$), only the desired closed-loop poles remain to be specified. The performance given by particular pole positions is shown on the z-plane in Figure 6.3. Some limits on the pole positions will arise from the shape of the response acceptable for any particular application. In this case, with the third order model (n=m=3), 5 closed-loop poles can be specified (see equation (6.7)). Choosing three poles coincident on the real axis, and the other two at z=0 so that they play no part in the dynamic response, gives a closed-loop system of the same order as the plant, and no overshoot. The real difficulty is to decide how fast the poles should be, i.e. how close to the origin.

Figure 6.4 indicates the stability robustness for controllers with the three coincident poles at different positions along the real axis. The robustness quantity $|R|$ for each controller, and the measure of modelling error σ given by equation (6.14), are plotted in the frequency domain. The modelling error in terms of a multiple of σ which can be accommodated before the onset of instability, i.e. before inequality (6.10) becomes false, is contained in Table 6.1 for each pole position. If, for example, the real and imaginary parts of the frequency response were independent and normally distributed with equal variance, a value of 1.73 in the Table would give a 95% confidence level of stability (Johnson and Wichern, 1990). However, with

the inaccuracy of the estimate of modelling error, and the seriousness of designing an unstable controller, a much higher buffer is desirable. This is also likely to lead to better stability robustness to plant time-variations (including those due to changing the operating point with non-linear plant), and may perhaps reduce deviations from the desired performance due to modelling errors.

From the Table, poles between about z=0.6 and z=0.8 are best for robustness. Another aspect of choosing pole positions is the effect on noise amplitude. The magnitude of the noise transfer function in equation (6.5) is plotted against frequency in Figure 6.5. At high frequencies, where noise is prevalent, there is no significant amplification, especially for poles at z=0.6 or above. However from Figure 6.1, the control signal is given by:

$$u_t = \frac{A(z^{-1})H(z^{-1})}{F(z^{-1})A(z^{-1}) + G(z^{-1})B(z^{-1})} r_t - \frac{G(z^{-1})A(z^{-1})}{F(z^{-1})A(z^{-1}) + G(z^{-1})B(z^{-1})} e_t' \quad (6.17)$$

and using equation (6.4), which assumes exact plant modelling:

$$u_t = \frac{A(z^{-1})}{A_m(z^{-1})} r_t - \frac{G(z^{-1})A(z^{-1})}{A_m(z^{-1})H(z^{-1})} e_t' \quad (6.18)$$

Thus the magnitude of the noise superimposed on the control signal is approximated by the inverse of the robustness quantity which was plotted against frequency in Figure 6.4. At high frequency noise amplification can be very large, the minimum being with poles at about z=0.7, in which case the amplification peaks at 37dB.

To show whether the best pole positions, as indicated on robustness and noise grounds, are apparent in practice, step responses were performed with the different poles. Figure 6.6 shows the results. Note that the very vigorous nature of the control signal for poles at z=0.5 and below, and at z=0.9, are unacceptable due to the excessive vibration caused to the rig structure and pipework, even though the load position is largely unaffected. Three poles at z=0.7 give better results than any of the other positions tested.

If the speed of response were found to be inadequate with poles at z=0.7, a demand filter

could be used to improve robustness and reduce noise amplification for faster pole positions. If the desired response remains as third order, $H(z^{-1})$ can be of degree two. Choosing $H(z^{-1})$ to have two coincident real roots, the theoretical effect of their position with desired closed-loop poles at z=0.4 is shown in Figure 6.7. Demand filter roots at z=0.6 show much improved robustness and noise response. The practical effect of the demand filter on step responses is shown in Figure 6.8. The influence of noise on the control signal is reduced significantly as the demand filter roots increase. However the root positions do have some effect on the closed-loop response, although this is only significant at higher root values. This is due to servovalve saturation preventing $H(z^{-1})$ from being accurately cancelled out of the transfer function from demand to output.

For this system there is little reason for requesting system poles faster than about z=0.6 as valve saturation limits the speed at which the load can move. Figure 6.9 compares the step responses of Figure 6.6, and thus assuming that the size of the steps are representative of normal operation, the robustness and noise problems associated with poles faster than z=0.6 far out-weigh the marginal speed advantage. Improvements in noise attenuation and robustness with poles at z=0.6 can still be made by introducing a demand filter. By following a similar procedure to that demonstrated above, demand filter roots at z=0.2 were chosen, and the corresponding step response is shown in Figure 6.10. The desired response, taking valve saturation into account, is also plotted in the Figure. The match between desired and actual responses is still as close as demonstrated previously (in Chapter 4), despite an extra potential source of error through inaccurate cancelling of the demand filter.

6.5 Sample rate selection

In the preceding sections, a sample interval of 10ms has been used throughout, giving a sample rate of about 8 times the plant natural frequency. The choice of sample rate influences plant model estimation as well as control, assuming that the same rate is used for both, which avoids the need to transform the estimated model to a different sample rate for control. Some of the issues which affect sample rate choice are listed below.

For control purposes, the sample rate should be fast for the following reasons (Franklin and Powell, 1980):

- for good response to demand, i.e. high closed-loop bandwidth,
- for adequate control and monitoring of the plant, i.e. the rate should be faster than the plant bandwidth to the extent that the control signal steps do not excite the plant, and sampled feedback is representative of the plant behaviour,
- for fast disturbance rejection.

For model estimation purposes, the sample rate should be sufficient to capture all relevant dynamic information (Ljung, 1987). However there are also a number of problems associated with sampling too fast:

- model fit is forced over a larger frequency range, allowing noise present at higher frequencies to have more influence — but this can be largely counteracted by appropriate data filtering,
- low frequency behaviour may not be estimated correctly due to quantisation in the analogue to digital converter, i.e. the change from one sample to the next of a slowly varying signal will fluctuate greatly (Goodwin, 1985),
- any dead time may be equivalent to many sample intervals — this will have to be recognized when the model structure is selected.

In addition, the choice of sample rate can dramatically affect the robustness and noise response of a pole-placement control system. This aspect has been investigated by applying the techniques of Section 6.3 to the electro-hydraulic position control system using different sample rates.

Figure 6.11 shows the response of the position control system to a square wave input for a variety of sample rates. In each case data were collected at the required sample rate with the plant operating under unity gain proportional closed-loop control with a PRBS demand signal. A model was estimated using filtered least squares, and the digital filter was adjusted for each sample rate to maintain the same bandwidth. At a 10ms sample interval the following filter was used:

$$\frac{0.216}{(1 - 0.4z^{-1})(1 - 0.4z^{-1})(1 - 0.4z^{-1})} \tag{6.19}$$

Three coincident closed-loop poles were specified, their location chosen to give the same equivalent continuous-time response whatever the sample rate. The poles were situated at z=0.7 for the 10ms sample interval.

The 10ms and 20ms sample intervals give best results. Interpreting the resonant frequency (at about 12Hz) as the bandwidth of the plant, these sample intervals correspond to sample rates of 8.3 and 4.2 times the plant bandwidth respectively. The controller breaks down at higher sample rates. At a 30ms sample interval, which is a rate of only 2.8 times the plant bandwidth, the control action is still quite good. However reducing the sample rate further degrades the performance as the Nyquist frequency becomes close to the plant bandwidth.

The rapid deterioration of the response as the sample interval is reduced below 10ms can be explained by studying the robustness quantity $|R|$. This is plotted, against the measure of modelling error σ, for each sample interval in Figure 6.12. The modelling errors (in terms of a multiple of σ) which can be accommodated before the onset of instability are listed in Table 6.2. This value is particularly small for sample intervals 3ms and 7ms, indicating robustness problems. Note that this is mainly due to the high sensitivity of the controller to modelling errors, i.e. low values of $|R|$, rather than the likely presence of large modelling errors (as indicated by σ).

Recalling that the inverse of the robustness quantity is the magnitude of the control signal noise response (equation 6.18), the very vigorous control signal activity for the 3ms sample interval is also explained.

6.6 Conclusions

The detailed analysis of pole-placement control undertaken in this Chapter has furnished greater insight into the overall influence of the main design freedom, i.e. the closed-loop pole positions. No definite (off-line) answer can yet be given to the fundamental question: how fast can the poles be before the controller breaks down? However the reasons for the control

action becoming unacceptable as the pole positions are altered have been investigated; they are:

- modelling errors can cause the performance to deteriorate, or even exhibit instability,
- the effect of noise on the output or control signal can increase.

In addition, valve saturation will limit the speed of response of the system.

Design guidelines can be developed from the methods demonstrated in this Chapter. Once a set of pole positions has been tried for a particular control system, the methods can be used to decide how to move the poles either to achieve better noise attenuation and robustness, or to improve the speed of response. For the best combination of properties, a demand filter can be introduced. This can improve robustness and noise properties for a particular set of closed-loop poles, perhaps to allow faster pole positions than would otherwise be used. The effect of the filter on robustness and noise can be assessed off-line for design purposes. However its root positions are constrained by valve saturation causing unacceptably inaccurate cancellation of the filter out of the closed-loop response. But this can be assessed off-line as well if required, by means of simulation, simply using the estimated plant model in place of the actual plant, and limiting the control signal to the known valve saturation level as usual.

It has also been shown that the sample rate has a significant effect on the properties of a pole-placement controller. Problems associated with sampling too slowly are well known, but the deterioration in robustness and noise response as sampling becomes faster is just as serious. For the plant under test, a sample rate greater then 10 times the plant bandwidth was unacceptable, and sampling as low as 3 or 4 times the bandwidth gave quite good results.

Robustness is not only important to allow for model estimation errors brought on by using noisy data. It is especially important for plant with non-linear characteristics as the best linear approximation of the plant changes from one operating point to another. For example, damping varies with valve opening, and natural frequency varies with piston position. There may be other changes in behaviour which are less predictable, such as changes in the load driven by the servosystem. The controller response in the presence of such time-variations is shown in detail in Chapter 8.

Position of three coincident poles	Modelling error as a multiple of σ
0.9	4.63
0.8	9.45
0.7	9.93
0.6	10.44
0.5	5.33
0.4	2.26

Table 6.1 Permissible modelling error before the onset of instability (see Figure 6.4)

Sample interval (ms)	Modelling error as a multiple of σ
3	0.919
7	1.504
10	6.10
20	9.29
30	12.94
40	14.90

Table 6.2 Permissible modelling error before the onset of instability (see Figure 6.12)

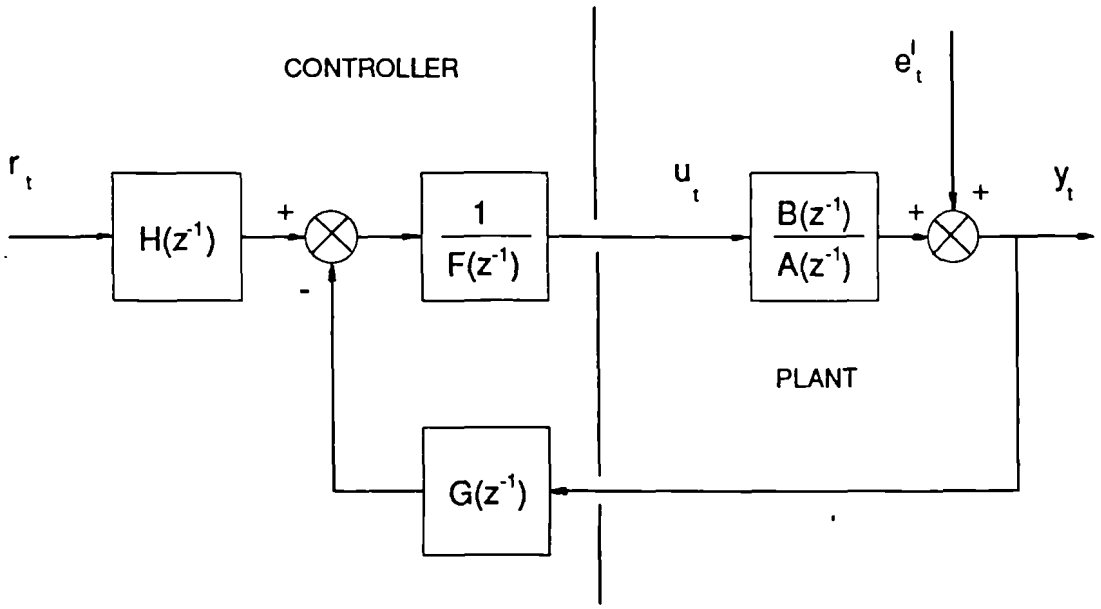

Figure 6.1 Pole-placement controller

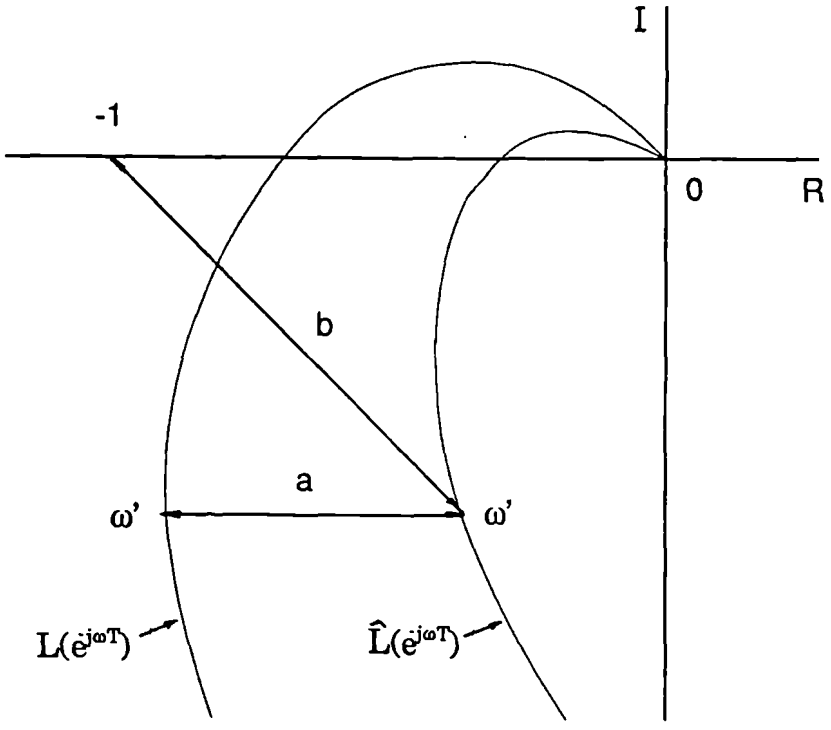

Figure 6.2 Actual and estimated Nyquist plots, with lengths *a* and *b* shown for points corresponding to frequency ω'

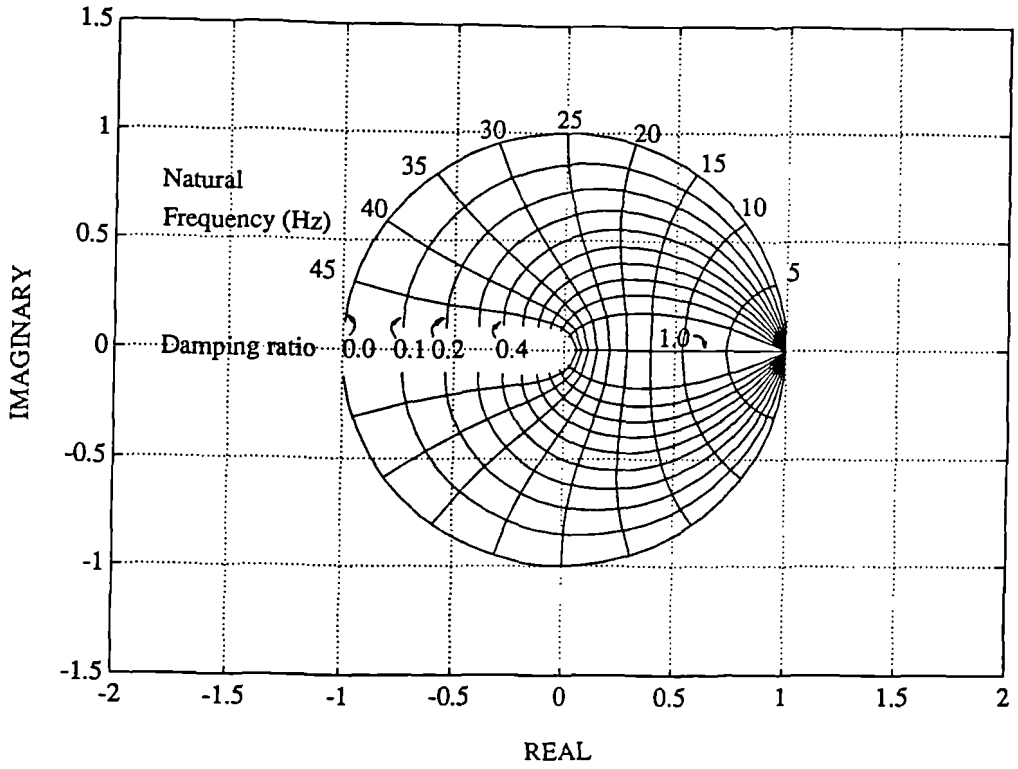

Figure 6.3 Mapping of pole position to natural frequency and damping ratio on the z-plane (for 10ms sample interval)

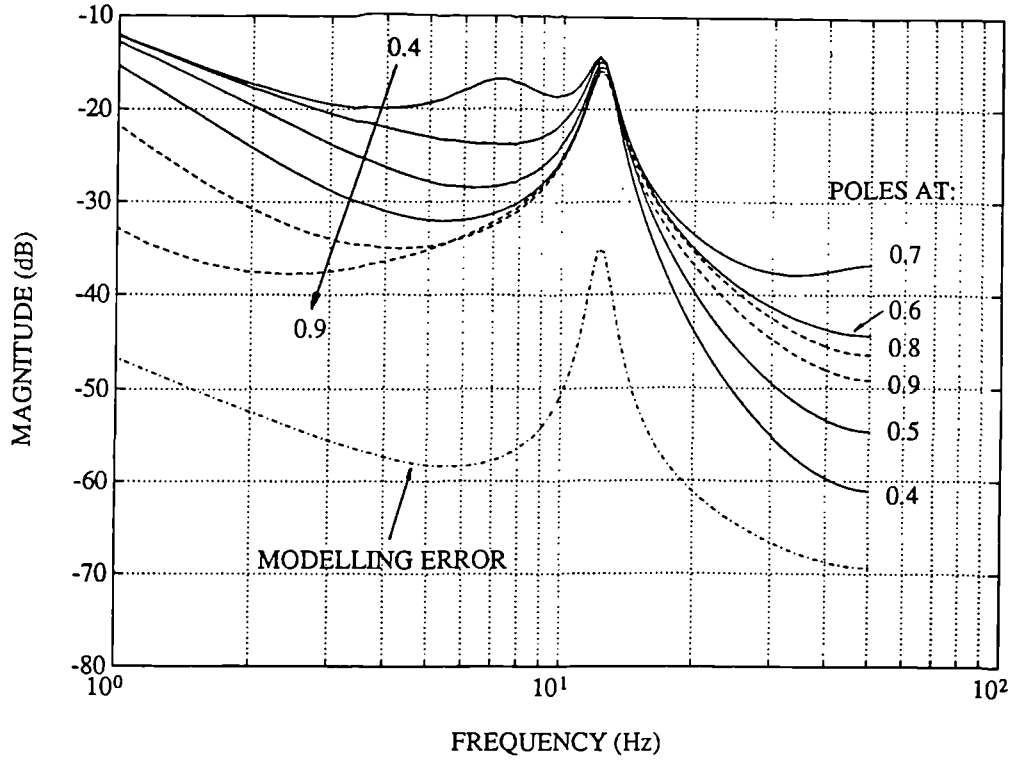

Figure 6.4 Robustness quantity $|R|$ for different closed-loop pole positions, compared to modelling error σ

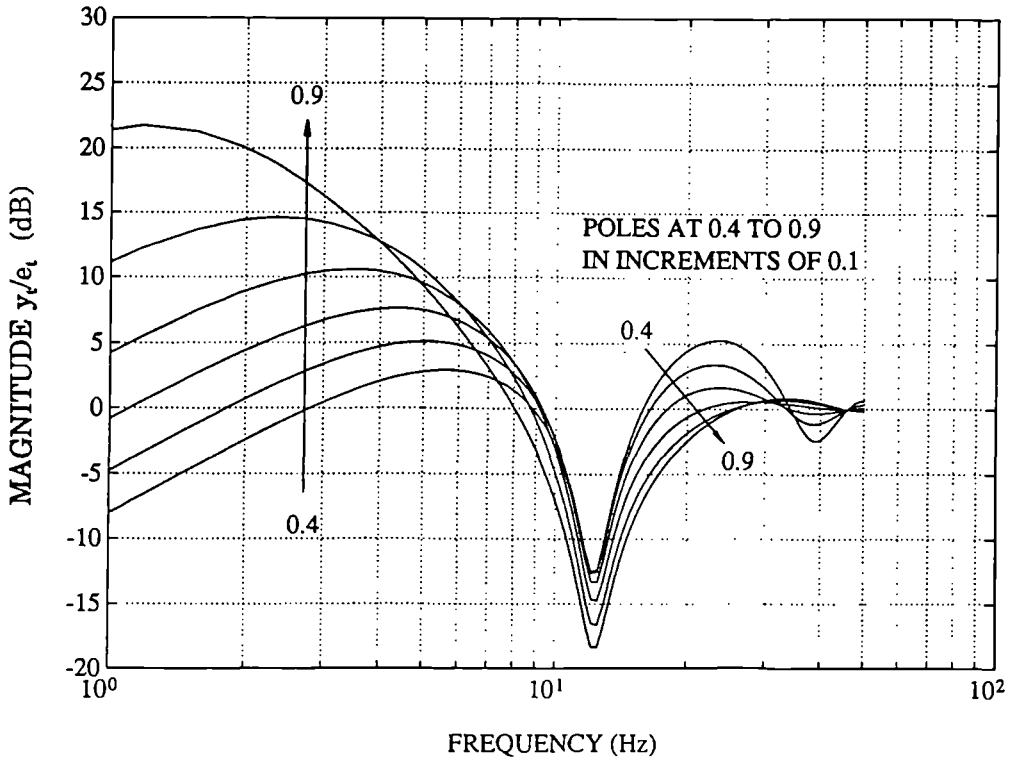

Figure 6.5 Frequency response of load position (y_t) to noise (e_t) for different closed-loop pole positions

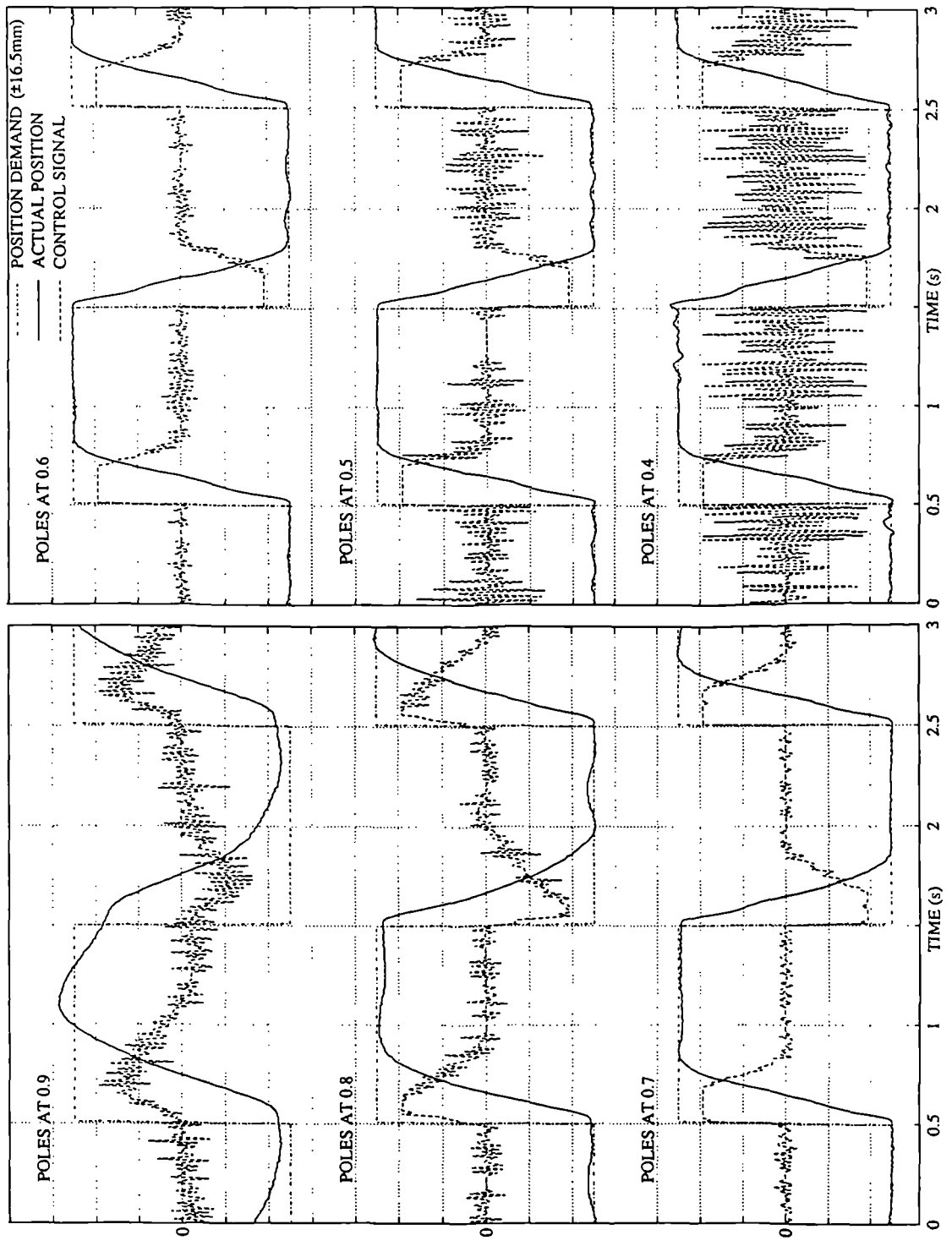

Figure 6.6 Step responses for different desired closed-loop pole positions

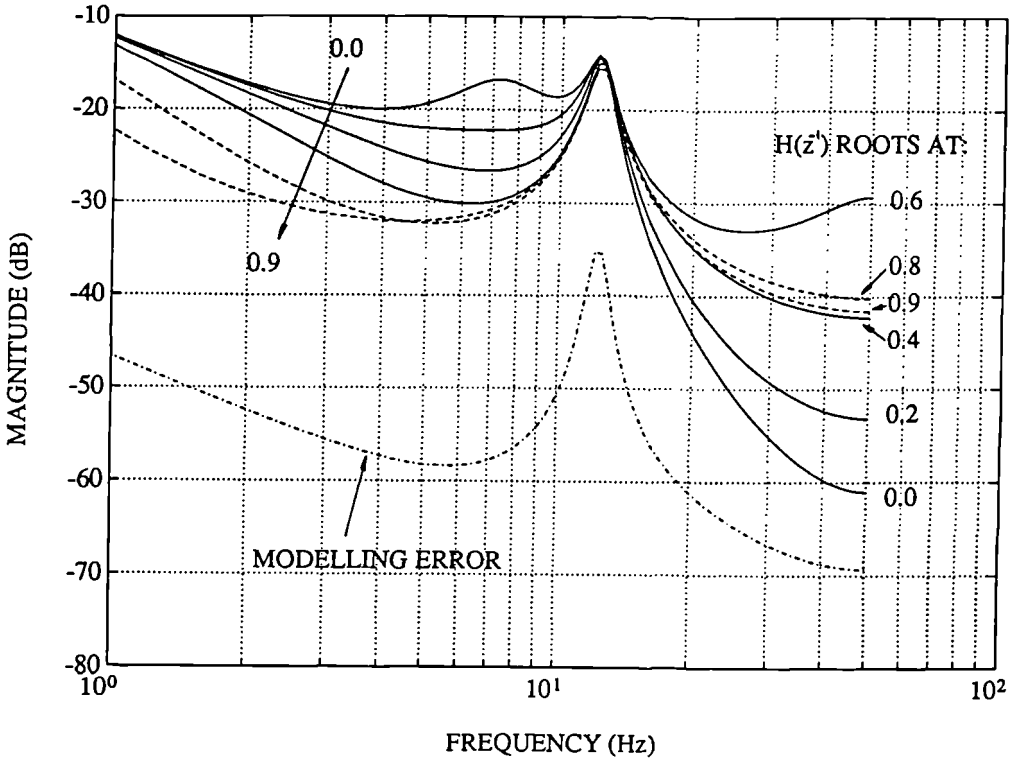

Figure 6.7 Robustness quantity $|R|$ for different demand filter roots (with closed-loop poles at z=0.4), compared to modelling error σ

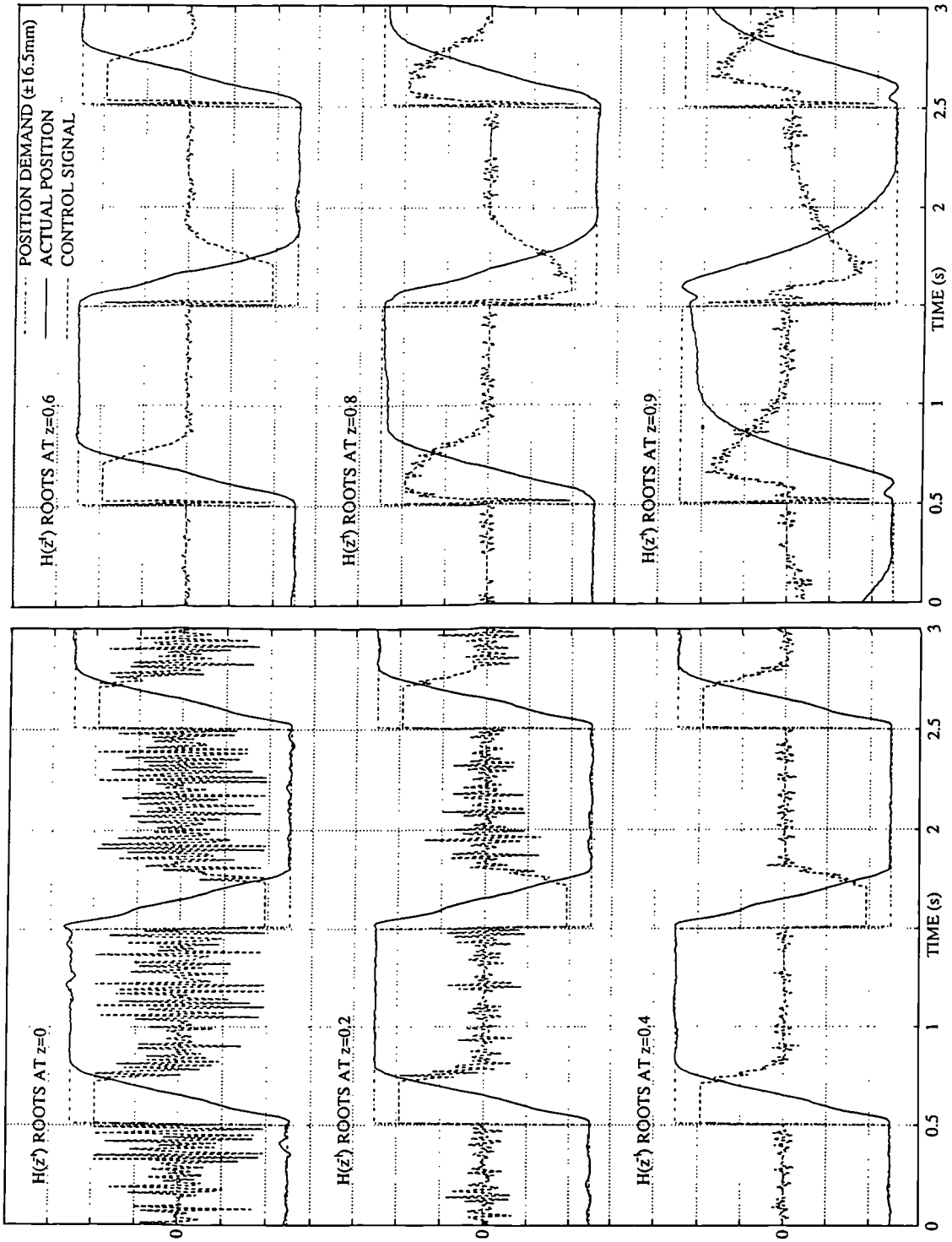

Figure 6.8 Step responses for different demand filter roots (with closed-loop poles at z=0.4)

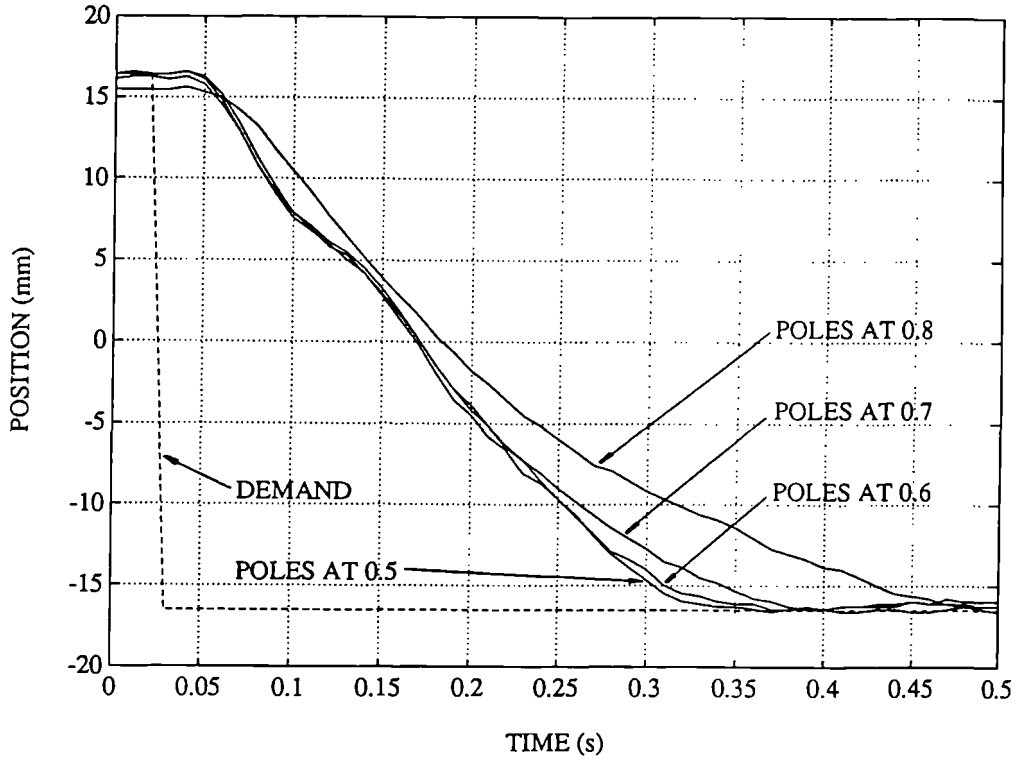

Figure 6.9 Comparison of step responses for different desired closed-loop pole positions

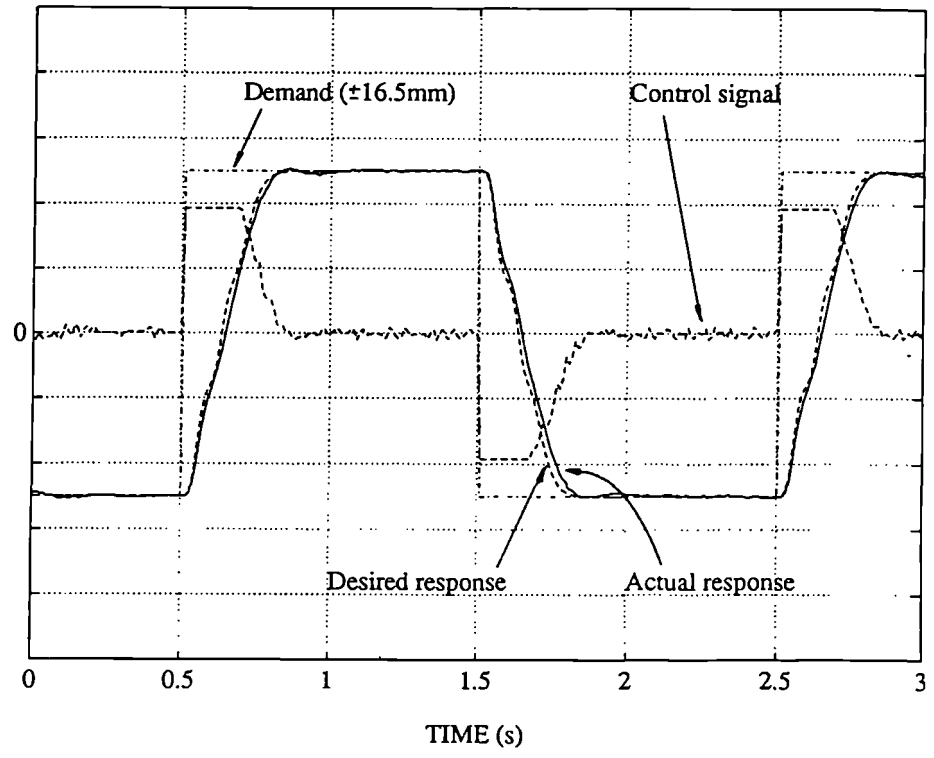

Figure 6.10 Actual and desired step responses with closed-loop poles at z=0.6 and demand filter roots at z=0.2

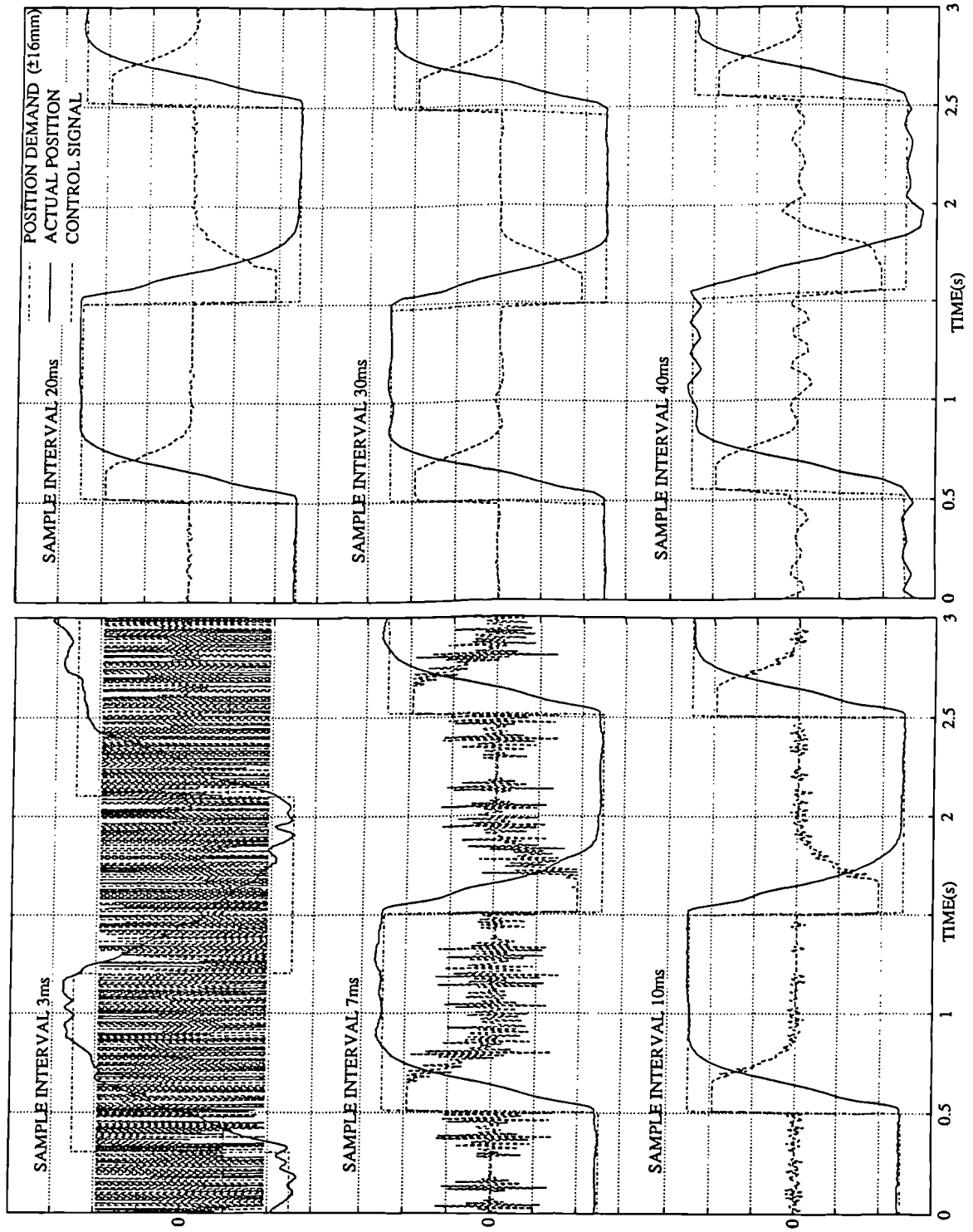

Figure 6.11 Pole-placement control using different sample intervals

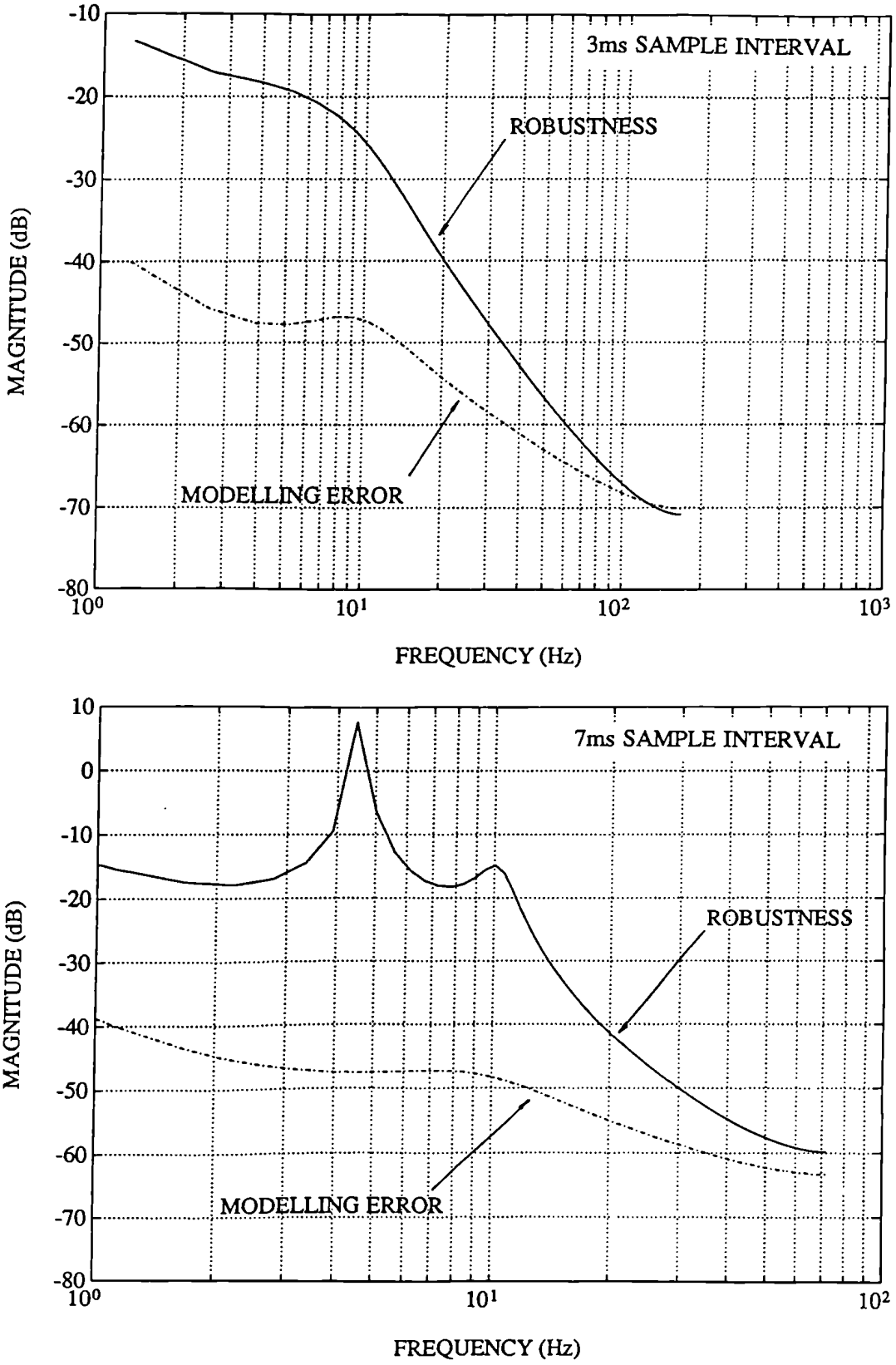

Figure 6.12a Robustness quantity $|R|$ compared to modelling error σ for different sample intervals (3ms and 7ms)

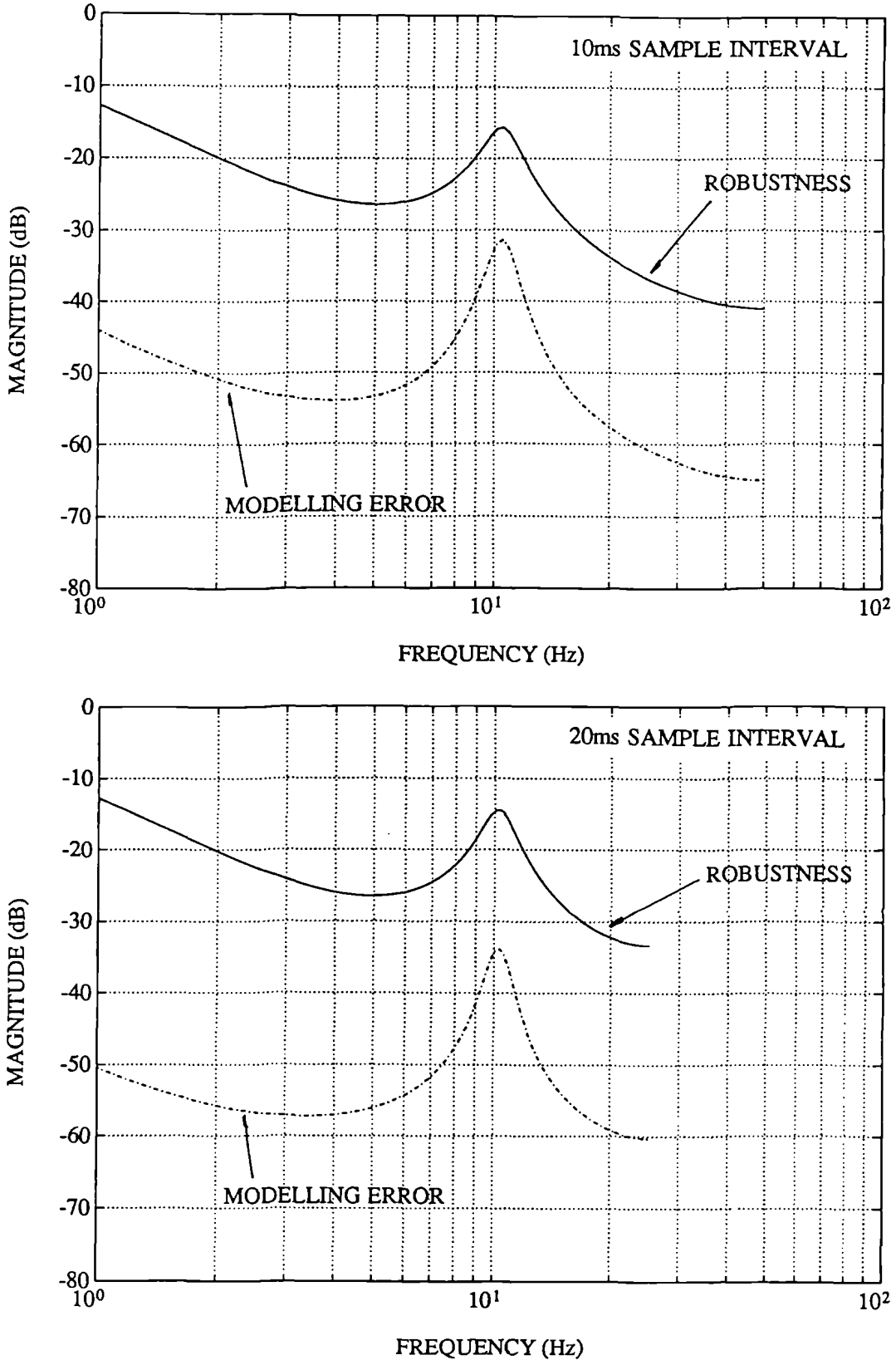

Figure 6.12b Robustness quantity $|R|$ compared to modelling error σ for different sample intervals (10ms and 20ms)

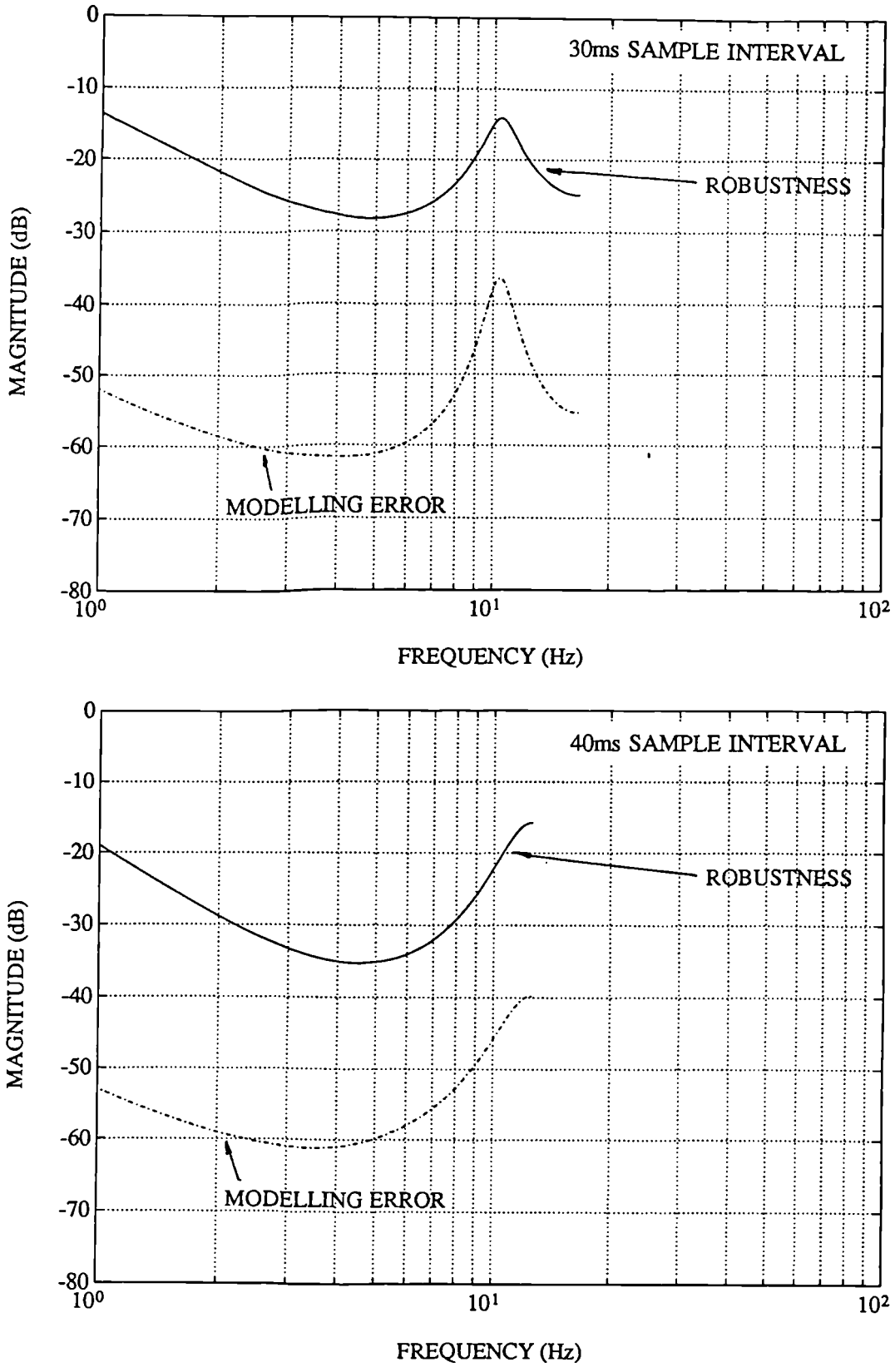

Figure 6.12c Robustness quantity $|R|$ compared to modelling error σ for different sample intervals (30ms and 40ms)

7. Pole-placement with integral action

7.1 Introduction

As described in Section 3.4, in the presence of offsets or low frequency disturbances, such as those resulting from an external load force acting on a position servosystem, integral action is required to reduce steady-state error. The PID controller examined in that Section does not give a very good performance; a pole-placement controller exhibiting integral action may be better. Integral pole-placement has been applied to electro-hydraulic servosystems before (e.g. Figueredo, 1987), but problems have sometimes been encountered (Unbehauen *et al*, 1988). Two ways of incorporating integral action into pole-placement are presented in this Chapter. The first is a well known method, but its application exposes difficulties which are investigated using techniques developed in Chapter 6. The second method has been evolved in an attempt to overcome these difficulties.

7.2 Integral pole-placement

7.2.1 Design

Incorporating integral action into a pole-placement controller can be achieved by forcing $F(z^{-1})$ to have a root at $z=1$:

$$F(z^{-1}) = (1-z^{-1})F_1(z^{-1}) \tag{7.1}$$

The diophantine equation (6.8) now becomes:

$$F_1(z^{-1})(1-z^{-1})\hat{A}(z^{-1}) + G(z^{-1})\hat{B}(z^{-1}) = A_m(z^{-1})H(z^{-1}) \tag{7.2}$$

which can be solved for $F_1(z^{-1})$ and $G(z^{-1})$.

The extra constraint increases the polynomial degrees for the minimal degree solution to:

$$\left.\begin{aligned} \deg F(z^{-1}) &= m \\ \deg G(z^{-1}) &= n \\ \deg A_m(z^{-1})H(z^{-1}) &= n + m \end{aligned}\right\} \tag{7.3}$$

Note that integral wind-up is not a problem with this controller if the control signal is saturated in software in the manner described in *Section 3.6.*

7.2.2 Application to positioning system

Figure 7.1 shows the control system with two disturbance signals. The transfer function between e'_t and the output y_t (assuming exact plant modelling) is contained in equation (6.5); it is:

$$\frac{F(z^{-1})A(z^{-1})}{A_m(z^{-1})H(z^{-1})} \tag{7.4}$$

Even for non-integral pole-placement, if e'_t were a low frequency disturbance it would have little influence on the output due to the natural integrating characteristic of the positioning system in question (i.e. $A(1) = 0$). This is shown in Figure 6.5: the magnitude of the transfer function has an amplitude ratio which diminishes to zero as the frequency reduces. The equivalent transfer function from w_t to the output is:

$$\frac{F(z^{-1})B(z^{-1})}{A_m(z^{-1})H(z^{-1})} \tag{7.5}$$

In this case integral pole-placement is required (i.e. $F(1) = 0$) to ensure that low frequency components of w_t have little effect. As revealed in Appendix 1, a non-zero control signal is needed to compensate for external load forces in the steady-state, so load forces appear as part of w_t.

The magnitude of transfer function (7.5) is plotted against frequency in Figure 7.2. The curve for non-integral control is plotted for comparison, using three closed-loop poles specified at z=0.6, and two demand filter roots at z=0.2, which were the best positions found in Section 6.4. These pole and root positions are retained for the integral controller, but the larger degree of $A_m(z^{-1})H(z^{-1})$ allows an extra demand filter root to be used, and this root is varied. The Figure demonstrates that this root can control the frequency below which integral action is dominant. Figure 7.3 shows the equivalent curves for the robustness quantity $|R|$. Introducing integral action has seriously reduced the robustness, but increasing the additional (third) demand filter root to 0.9 restores the robustness to nearly that of the non-integral controller. The very 'slow' root restricts the influence of the integrator to a low frequency range.

Implementing the controller for the different demand filters gives the responses in Figure 7.4. The responses for a step change in disturbance w_t are shown as well as for step changes in demand. The demand filter chosen using robustness and noise criteria (i.e. with roots at 0.2, 0.2, and 0.9) does give the best performance, but unfortunately saturation prevents adequate cancellation of the filter out of the closed-loop response, and a completely satisfactory performance cannot be achieved.

The problem arises because altering the demand filter is the only way of reducing the integral gain. Motivated by the need for a more easily adjustable integral gain, another integral control method has been developed.

7.3 Model reference integral control

7.3.1 Design

The model reference integral control method uses a plant model running in parallel with the actual plant, as illustrated in Figure 7.5. A disturbance will cause an error between plant and model outputs. The error will integrate up assuming the plant model has an integrating characteristic (otherwise the error should be integrated explicitly). This signal is then scaled by gain k_i and added to the pole-placement control signal to cancel out the effect of the disturbance. The value of k_i can be chosen by trial and error to give a suitable combination of properties. If $k_i = 0$ is used the controller reverts back to the normal non-integral controller, an option which is not available in practice with the previous integral method.

To prevent integrator wind-up with this controller, the software saturation limit for the original control signal u_t must be modified to take into account the additional control signal component u_{it}. Thus the combined control signal u_{ct} is now bounded by the saturation limits, and u_t is limited to $u_{ct} - u_{it}$.

Note that the method has similarities to that used by Figueredo (1987) for electro-hydraulic servosystems. However in that case the reference model was for the whole closed-loop system, and so was driven by the demand signal rather than the control signal.

7.3.2 Application to positioning system

The response of the controller with an integral gain (k_i) value of 5.0 is shown in Figure 7.6. The performance is acceptable, and better than that achievable with the first method. Some responses with different k_i values are shown in Figure 7.7. With k_i=2, the step disturbance has a very prolonged effect. With k_i=10, the position response has signs of ripple which characterized lack of robustness using the previous integral method.

7.4 Conclusions

Incorporating integral action into pole-placement control, in the manner of Section 7.2, has a detrimental effect on robustness and noise response properties. The inclusion of a demand filter is even more important than in the previous Chapter, and probably essential for many plant. Unfortunately, for the positioning system under test, valve saturation prevents a suitably 'slow' demand filter from being used, and satisfactory results cannot be obtained. However this may not be the case for other plant of similar type, as precise values of valve saturation and noise amplitude will vary.

The alternative method uses the error between the actual plant output and the output predicted by a plant model running in parallel to detect disturbances and correct the control signal accordingly. The results obtained using this method are much better than with either the first method or the PID controller of Section 3.4.

Appendix 3 contains a theoretical analysis of the model-reference integral controller. Neglecting the saturation non-linearity, the controller can be rearranged into the same form as the initial integral controller. In fact the methods become identical for first order plant. As shown in the Appendix, the benefits of the model-reference technique still exist with first order plant, so in this case at least they are entirely due to the way in which saturation is handled.

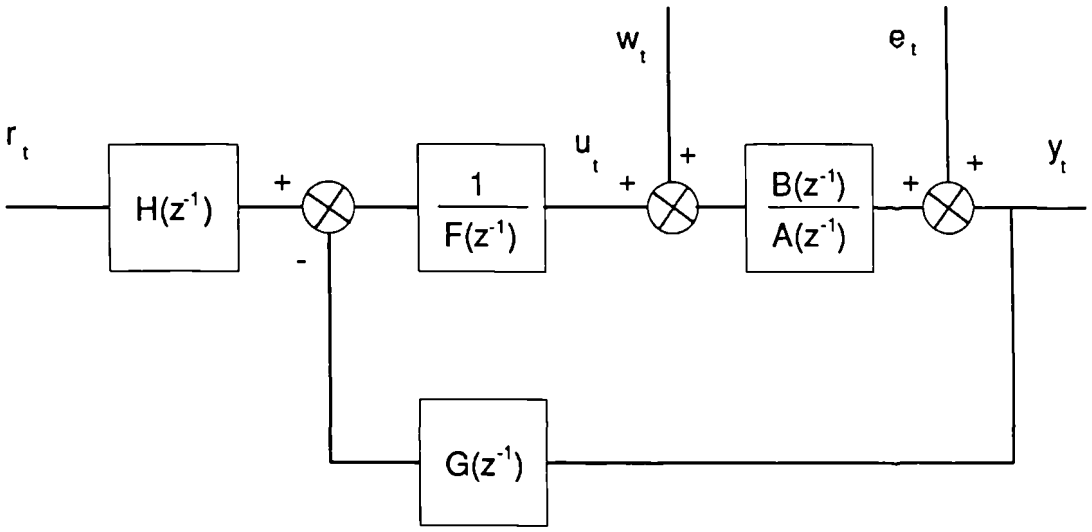

Figure 7.1 Pole-placement controller (with two disturbance signals)

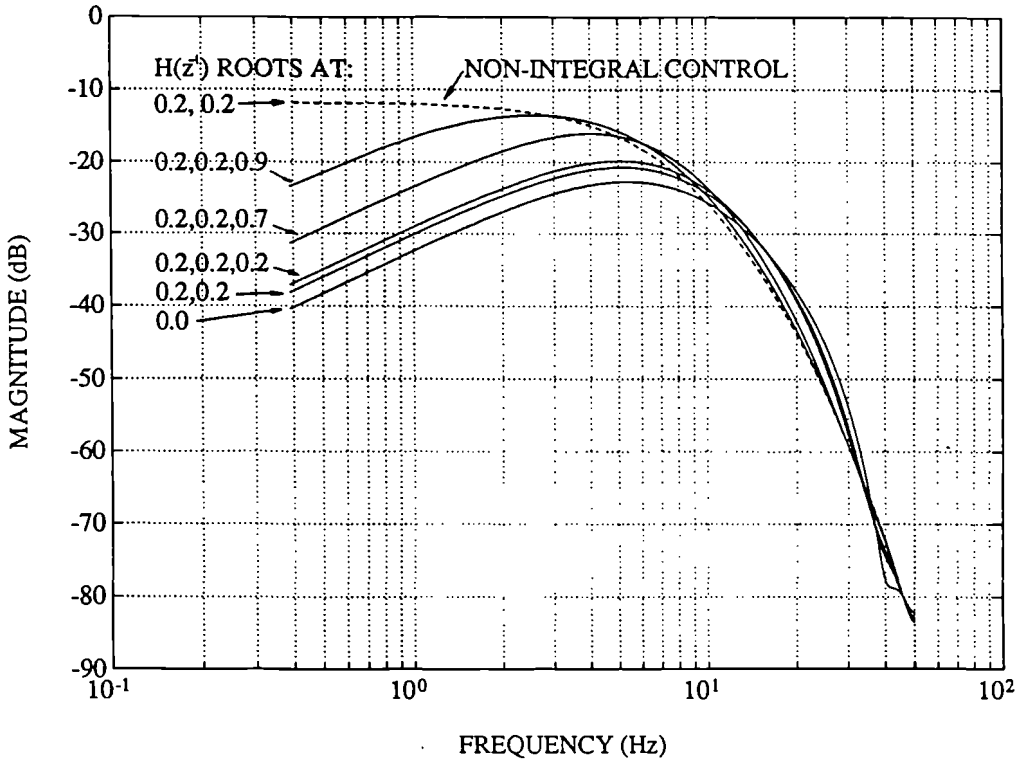

Figure 7.2 Integral pole-placement: Frequency response of load position (y_t) to a disturbance additive at the plant input (closed-loop poles at z=0.6)

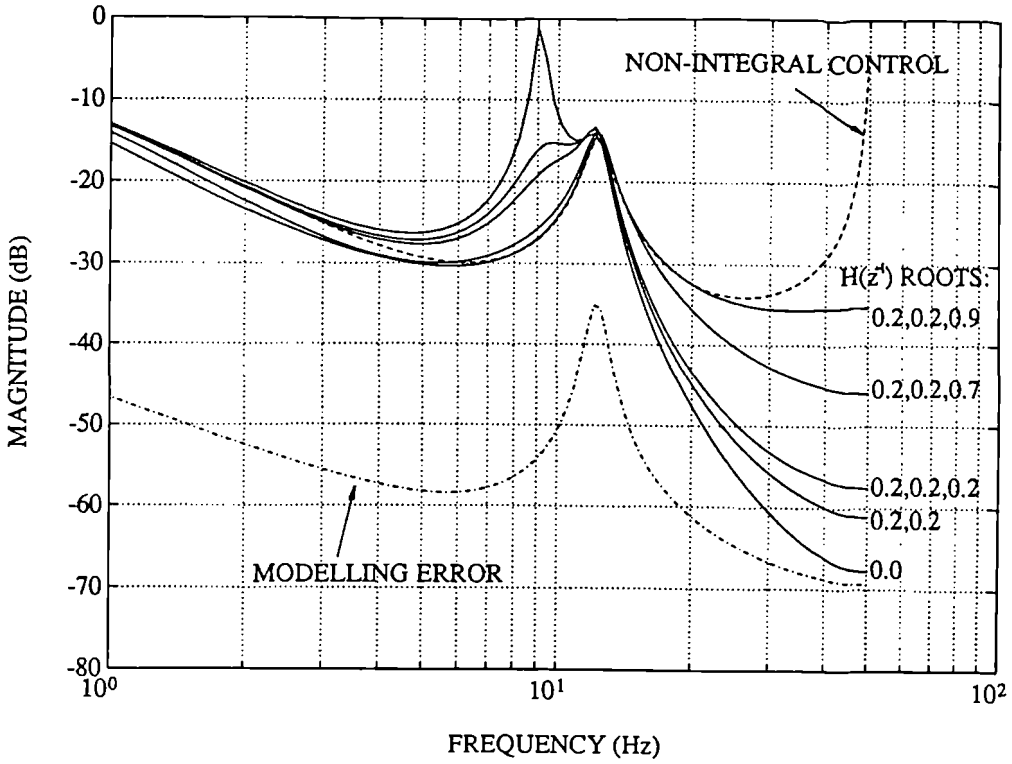

Figure 7.3 Integral pole-placement: Robustness quantity $|R|$ for different demand filter roots (with closed-loop poles at z=0.6), compared to modelling error σ

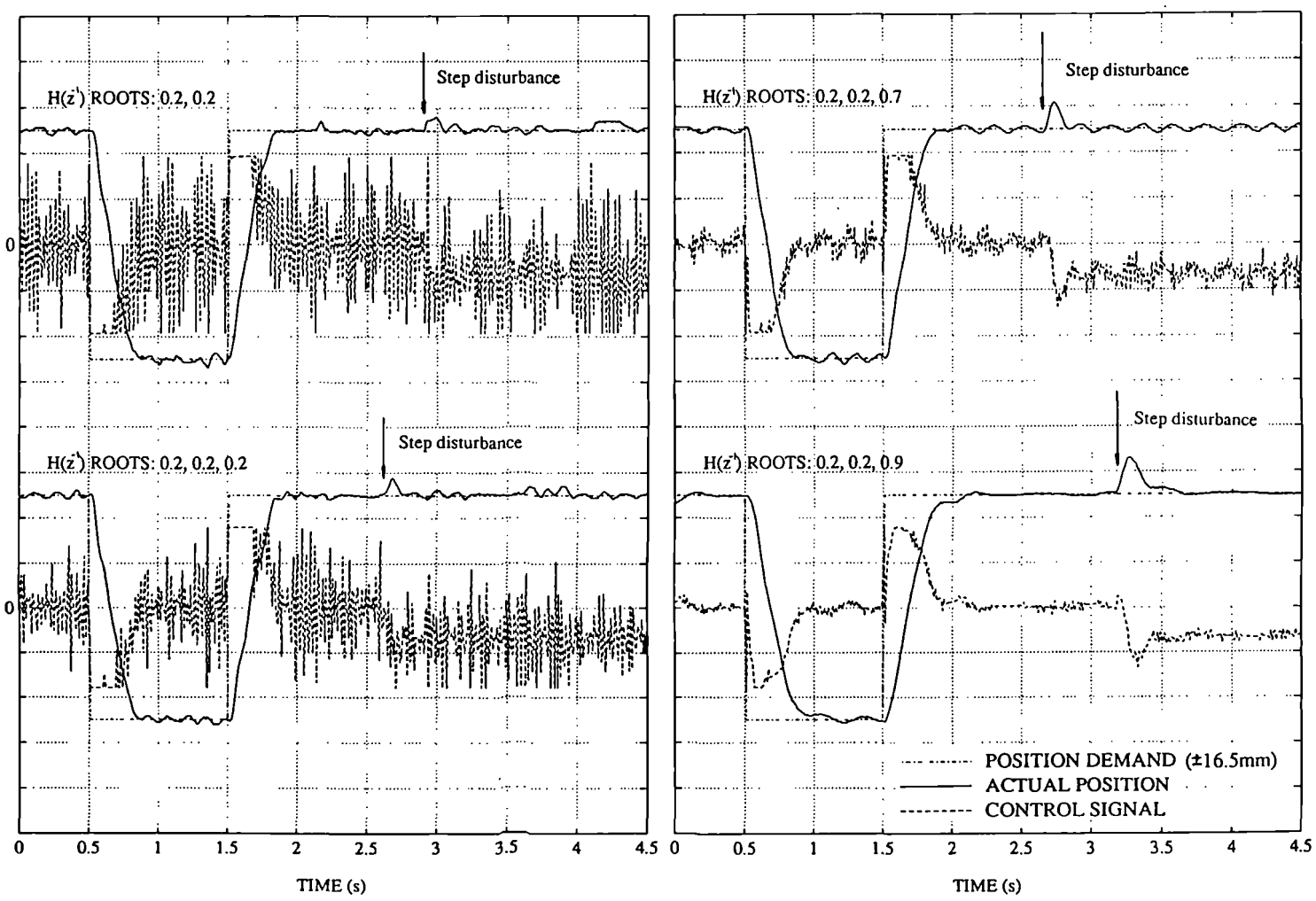

Figure 7.4 Integral pole-placement: Step responses for different demand filter roots (closed-loop poles at z=0.6), with disturbance of 3.3mA at plant input

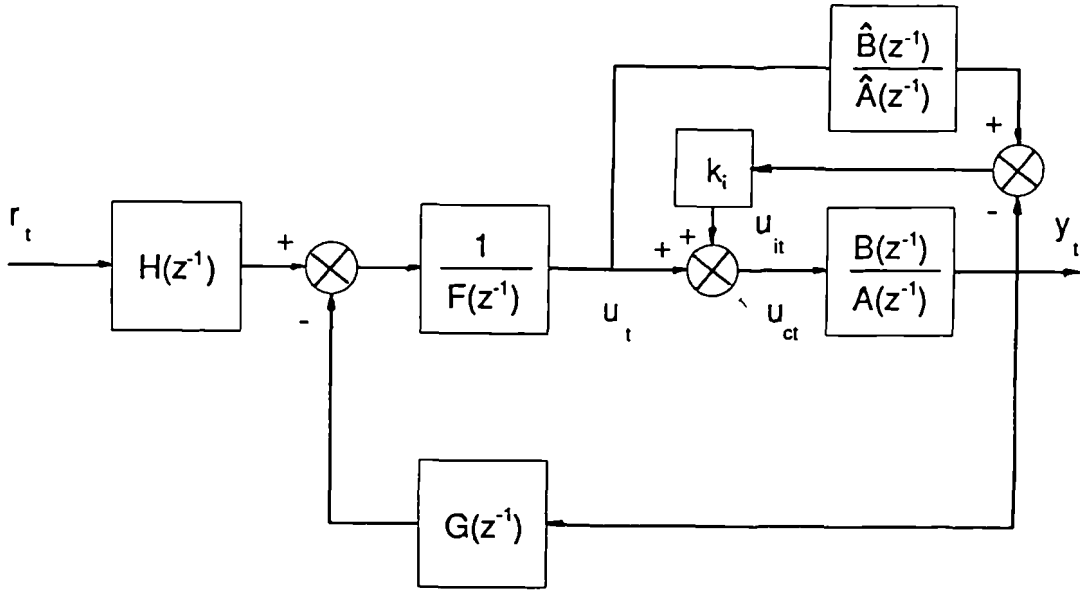

Figure 7.5 Model reference integral controller

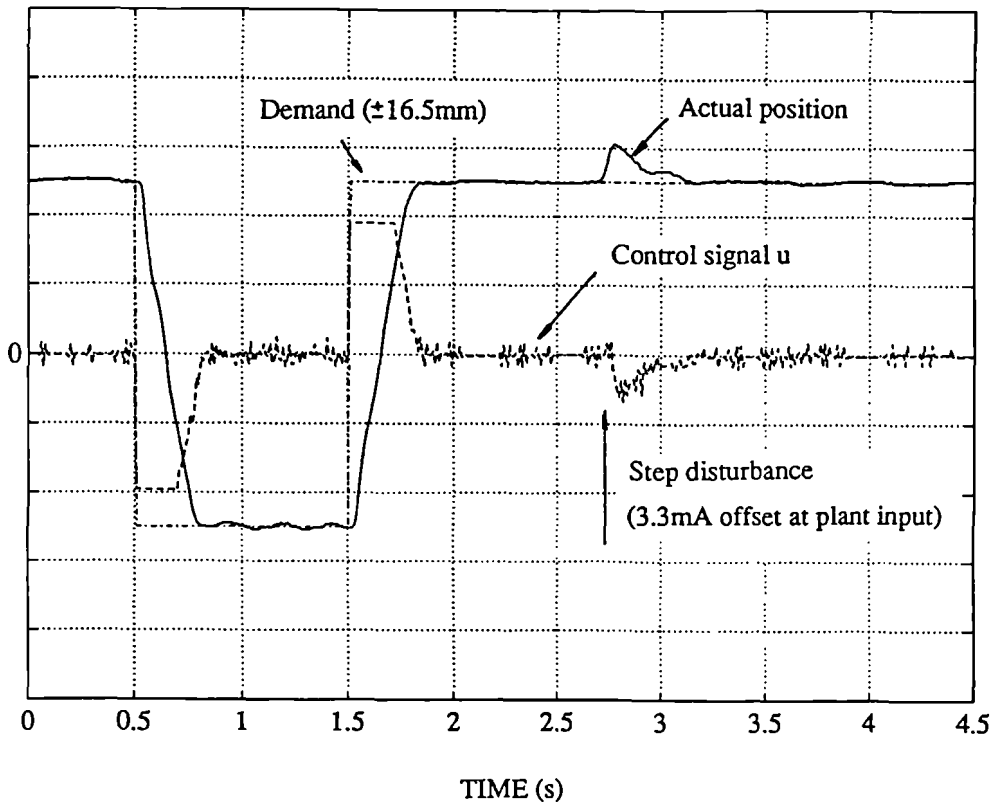

Figure 7.6 Model reference integral controller: step and disturbance responses with k_i=5 (closed-loop poles at z=0.6, demand filter roots at z=0.2)

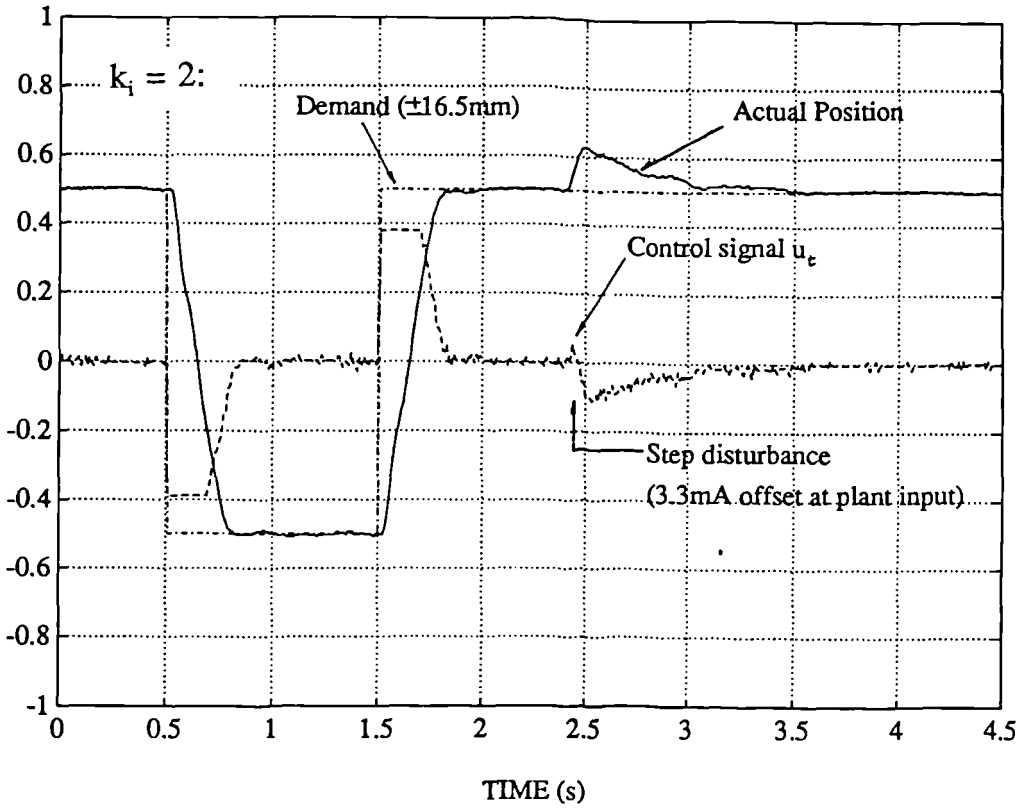

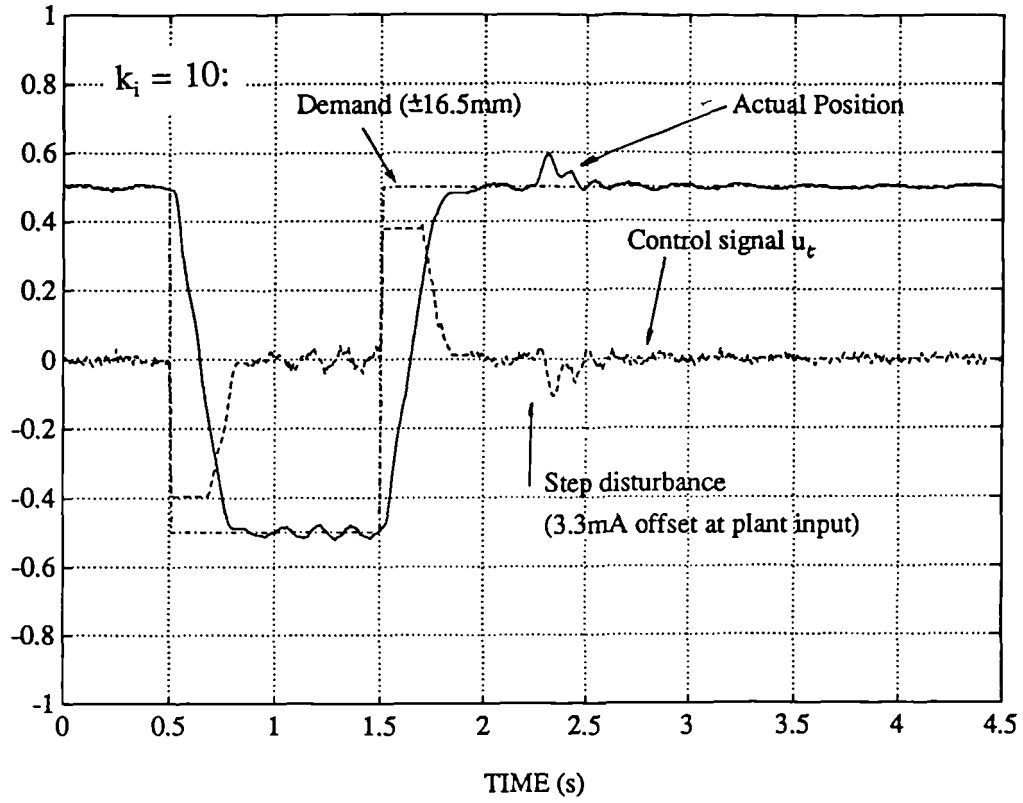

Figure 7.7 Model reference integral control with k_i=2 and k_i=10

8. Adaptive control

8.1 Introduction

In the preceding two Chapters great emphasis has been placed upon designing fixed-coefficient pole-placement controllers which are robust. In some circumstances this consideration of robustness is essential to achieve satisfactory controller performance in the light of model estimation errors, and non-linear plant behaviour. It has also been argued that increasing robustness may endow the controller response with improved insensitivity to unexpected changes in plant behaviour. However, sufficiently large changes in plant parameters *will* cause unacceptable deviations away from the desired response. So in situations where such changes are likely to occur, and where the desired response needs to be adhered to closely, an adaptive version of the pole-placement controller is appropriate. Large plant parameter changes are often caused by variations in load behaviour. These variations are common in a wide range of servo applications, including heavy duty robots, material testing equipment and plastic injection moulding machines.

To tackle the problem of time-varying plant, a number of researchers have applied adaptive controllers to electro-hydraulic servosystems in the past. The first application occurred two decades ago (Porter and Tatnall, 1970). However the analogue computing technology available at the time made the controller implementation cumbersome. The rapid development of digital electronics in recent years, especially the microprocessor, means that adaptive controllers can now be applied to fast servosystems relatively cheaply. The intervening years have also seen significant advancements in the theoretical aspects of adaptive control.

Two distinct approaches have been used for the practical application of adaptive control to electro-hydraulic positioning systems. Indirect (or self-tuning) adaptive control involves the on-line estimation of a plant model, and uses a conventional model-based controller which is repeatedly re-designed using the latest model estimate. In its original form self-tuning control was only used for the initial tuning of controller parameters. This form was implemented by Finney *et al* (1985). For a full adaptive version the estimator must be modified to forget old data, for example by the inclusion of a fixed forgetting factor as used by Vaughan and Whiting (1986). A similar method was used by Daley (1987) for the speed control of a rotary hydraulic system.

Direct (or model reference) adaptive control is the other approach. In this method the controller coefficients required to give a prescribed model-following performance are estimated. They are estimated directly from input-output data, and not calculated from a plant model. A number of applications of this type of adaptive controller to electro-hydraulic position control systems exist, notably those of Edge and Figueredo (1987), Hori *et al* (1988), and Unbehauen *et al* (1988).

Despite these applications, further development is required before adaptive control is widely adopted. Room for improvement is evident in three areas in particular:

- achieving fast adaptation without large tuning transients,
- achieving reliable and consistent performance under a wide range of conditions with any demand signal,
- making adaptive controllers easier to design.

The indirect adaptive method is the subject of the present study. The use of this method has allowed the lessons learnt through work on off-line estimation (Chapter 4) and fixed-coefficient control (Chapter 6) to be incorporated into an adaptive controller with ease. The most significant part of the controller which has not been touched upon in previous chapters is the modification of the estimator so that it forgets old data. Thus a large part of this Chapter is concerned with a comparison of different forgetting strategies.

Pole-placement adaptive control, similar to that presented here, was proposed in the seminal papers of Åström and Wittenmark (1980) and Wellstead and Sanoff (1981).

8.2 Adaptive control schemes

8.2.1 Pole-placement control

At each sample instant the pole-placement controller is re-designed according to the latest plant model. The calculation of the controller coefficients and the control signal is as described in Section 6.2.

8.2.2 Estimation with a fixed forgetting factor

The most successful off-line parameter estimator of Chapter 4 was least squares processing filtered input-output data, and thus this estimator is used on-line for the adaptive controller. The rapid convergence of this method bodes well for fast adaptation.

Using filtered input-output signals, the recursive least squares (RLS) estimate of the model parameter vector θ based on data up to sample time t can be shown to be:

$$\left.\begin{aligned} \hat{\theta}_t &= \hat{\theta}_{t-1} + k_t(y'_t - \psi_t^T \hat{\theta}_{t-1}) \qquad (a) \\ \text{where} \quad k_t &= \frac{P_{t-1}\psi_t}{\lambda_1 + \psi_t^T P_{t-1}\psi_t} \qquad (b) \\ \text{and} \quad P_t &= \frac{P_{t-1} - k_t\psi_t^T P_{t-1}}{\lambda_2} \qquad (c) \end{aligned}\right\} \qquad (8.1)$$

remembering that the parameter vector and regressor vector are defined respectively as:

$$\theta = [-a_1, \ldots, -a_n, b_1, \ldots, b_m]^T \qquad (8.2)$$

$$\psi_t^T = [y'_{t-1}, \ldots, y'_{t-n}, u'_{t-1}, \ldots, u'_{t-m}] \qquad (8.3)$$

where y'_t and u'_t are the filtered output and input signals given by:

$$\left.\begin{aligned} y_t' &= D(z^{-1})\, y_t \\ u_t' &= D(z^{-1})\, u_t \end{aligned}\right\} \qquad (8.4)$$

and $D(z^{-1})$ is the transfer function of the estimation filter.

In equation (8.1), λ_1 and λ_2 determine the relative importance of new and old data. Usually:

$$\lambda_1 = \lambda_2 = \lambda, \qquad 0 < \lambda \leq 1 \qquad (8.5)$$

and λ is called the forgetting factor. If $\lambda = 1$ then equation (8.1) is exactly the same as the off-line RLS estimator described in Section 4.2.2. As indicated in that Section, P_t is a normalised version of the covariance matrix of the estimates.

An alternative formulation for equation (8.1) is contained in Appendix 4. This is the square root algorithm due to Potter (see Ljung and Söderström, 1983), which has improved numerical properties for implementation with finite numerical precision. However no difference in performance between the two formulations was noticed in practice.

If the plant were not time-varying, the forgetting factor would be set to unity. Data at each sample instant would then have the same importance, and the elements of the covariance matrix P_t would reduce in size as more data is introduced, reflecting greater confidence in the accuracy of the estimates. Notice from (8.1a) that k_t acts as a gain determining how much the estimates change for a given error between (filtered) actual and model outputs. In addition, it can be shown that (see Appendix 4):

$$k_t = P_t\, \psi_t \qquad (8.6)$$

so P_t directly influences the rate of change of the estimates, and as it reduces, the estimates converge to steady values.

For time-varying plant, the reduction in P_t means that the model will take progressively longer

to adapt to changes in the plant. Thus traditionally a forgetting factor just below unity has been used for this situation. This has most effect on equation (8.1c), where P_t is scaled up on each recursion to counteract its tendency to diminish. The forgetting factor can also be interpreted as a means of weighting old data to have less importance than new data; the significance of data from a particular sample instant decays exponentially as time progresses with time constant $1/(1 - \lambda)$ sample intervals. Equation (8.1) is derived using this interpretation of the forgetting factor in Appendix 4.

Problems are encountered with the use of a fixed forgetting factor less than unity if the data are not persistently exciting. Lack of persistence of excitation implies that not all the modes of the plant are dynamically active; detailed persistence of excitation conditions can be found in (for example) Norton (1986). During periods of low excitation, new data does not drive P_t any lower, yet the matrix is still being scaled up by the forgetting factor. Thus P_t can become very large, and the estimates are sensitive to small model output errors, often changing drastically in the presence of noise.

8.2.3 Constant trace algorithm

As an alternative to a fixed forgetting factor, the constant trace algorithm has been used — Hori *et al* (1988), Unbehauen *et al* (1988). A number of variants of this algorithm exist (Warwick, 1988). In one version, $\lambda_1 = 1$ is used in equation (8.1b), but λ_2 is varied in (8.1c) to maintain P_t at a constant size. The trace of P_t is used as a scalar measure of the size of the matrix. Thus P_t neither becomes too small (as in the case of $\lambda = 1$), nor too large (as can happen with $\lambda < 1$).

8.2.4 Variable forgetting factor

Another alternative is the variable forgetting factor proposed by Fortescue *et al* (1981). In this method a new value for λ is calculated each sample instant, based on the *a posteriori* prediction error, defined as:

$$\varepsilon_t = y_t - \psi_t^T \hat{\theta}_t \tag{8.7}$$

If this error is small, it may be surmised that either

- the parameter estimates are accurate, or
- the estimator has been sensitive enough (due to a large P_t) to significantly reduce the error for this sample instant, or
- the plant has not been excited.

In all these cases a forgetting factor close to unity is desirable. This is achieved by considering ε_t to be a measure of the information available at the sample instant, and varying the forgetting factor to ensure that the estimates are always based on the same total amount of information. The information content of the estimator is:

$$\Sigma_t = \lambda_t \Sigma_{t-1} + \varepsilon_t^2 \tag{8.8}$$

If Σ_0 is the required total amount of information, then

$$\Sigma_t = \Sigma_{t-1} = \Sigma_0 \tag{8.9}$$

and from equations (8.8) and (8.9) the forgetting factor should be:

$$\lambda_t = 1 - \frac{\varepsilon_t^2}{\Sigma_0} \tag{8.10}$$

Unfortunately equation (8.7) can only be calculated once θ_t is known, i.e. after equations (8.1a) and (8.1b) are calculated, and (8.1b) requires a value for λ_1. However the value of λ_2 is found to be far more important, and the following are used:

$$\left.\begin{aligned} \lambda_1 &= 1 \\ \lambda_2 &= \lambda_t \quad \text{for} \quad \lambda_t > \lambda_{min} \\ \lambda_2 &= \lambda_{min} \quad \text{for} \quad \lambda_t \leq \lambda_{min} \end{aligned}\right\} \tag{8.11}$$

The minimum bound on λ_2 is found to be necessary due to the approximation in using λ_1=1.

8.2.5 Estimator jacketting

Numerous other methods for allowing rapid adaptation yet maintaining reliability in the face of poor data have been suggested (Warwick, 1988). Some involve 'jacketting' the estimator so that adaptation is prevented if some criterion is met. One example is the use of an estimation dead-zone. This stops adaptation if the *a priori* prediction error falls below a limiting value ε_L, i.e. if:

$$|y_t - \psi_t^T \hat{\theta}_{t-1}| < \varepsilon_L \tag{8.12}$$

The justification for this modification is similar to that for the variable forgetting factor described above: a small prediction error indicates either lack of excitation or accurate parameter estimates, and adaptation is undesirable in either case.

8.3 Setting up the adaptive controller

Before an adaptive controller can be applied to any servosystem, choices have to be made regarding the structure of the plant model, which parts of the plant model to adapt, initial parameter and covariance values for the estimator, the estimator forgetting strategy parameters etc. The choices made for the electro-hydraulic positioning system are described in this Section. Many rely heavily on a plant model obtained by off-line system identification, and thus the techniques of Chapters 4 and 5 are still important.

The same off-line plant model was used as that in Chapter 6; the conditions under which the model was estimated are described in Section 6.4. In factorised form the model is:

$$\hat{y}_t = \frac{1.07z^{-1}(1 + 1.50z^{-1})(1 + 2.04z^{-1})10^{-3}}{(1 - 1.00z^{-1})(1 - [0.684 + 0.664j]z^{-1})(1 - [0.684 - 0.664j]z^{-1})} u_t \tag{8.13}$$

In order to design a controller which can adapt as rapidly as possible to changes in the plant,

the number of parameters estimated on-line should be reduced to a minimum. The pole at $z=1$ in the above model represents the inherent integrating nature of the plant, and is unlikely to change. Also the zeros play a very minor role in modelling the dynamics of the plant, so they can be fixed without seriously restricting the time-variations to which the model can adapt. Thus the on-line estimator processes $(1 + 1.50z^{-1})(1 + 2.04z^{-1})u'_t$ as the input signal and $(1 - z^{-1})y'_t$ as the output to estimate a model of the form:

$$\frac{\hat{b}_1 z^{-1}}{1 + \hat{a}_1 z^{-1} + \hat{a}_2 z^{-2}} \tag{8.14}$$

Appropriate initial values for the parameters and the normalised covariance matrix are required so that the adaptive controller is well behaved at start-up. To obtain the normalised covariance matrix for the subset of the model to be estimated on-line, the RLS estimator was run for the model structure (8.14), pre-filtering u'_t by the known zeros and y'_t by the known pole as described. The off-line estimates (from 400 samples of data) were:

$$\begin{aligned} \hat{a}_1 &= -1.37 \\ \hat{a}_2 &= 0.907 \\ \hat{b}_1 &= 1.07\text{x}10^{-3} \end{aligned} \qquad P_t = \begin{bmatrix} 51.3 & -34.4 & -5.66\text{x}10^{-3} \\ -34.4 & 42.3 & 2.61\text{x}10^{-3} \\ -5.66\text{x}10^{-2} & 2.61\text{x}10^{-3} & 3.66\text{x}10^{-3} \end{bmatrix} \tag{8.15}$$

For the pole-placement part of the adaptive controller, three closed-loop poles at $z=0.6$ are specified, and demand filter roots are at $z=0.3$. Although these values are consistent with the good robustness and noise response properties discussed in Chapter 6, accepting that the plant is time-varying means that these off-line techniques are no longer ideal. However, short of varying closed-loop pole positions on-line to maintain minimum levels of robustness (necessitating on-line robustness calculation), there is no alternative.

The same estimation filter was used for on-line estimation as for off-line estimation, i.e.:

$$\frac{(1 + z^{-1})^3}{8} \tag{8.16}$$

8.4 Testing the forgetting strategies

The various forgetting strategies are compared by application to the electro-hydraulic positioning system. The behaviour of the parameter estimates and the consequent controller performance are illustrated under several different operating conditions. A square wave demand is used in one case, with a sudden change in supply pressure (from 100bar to 40bar) allowing the rate of adaptation to be gauged. Two other situations are shown for each strategy, both of which exhibit insufficient persistency of excitation. The first has a constant zero demand signal, and the second a 0.5Hz sinusoidal demand.

The results with a fixed forgetting factor of 0.96 and the square wave demand are shown in Figure 8.1. High values of covariance matrix trace are obtained, and adaptation to the reduction of supply pressure after 6s is very rapid. Note that the ramp part of the response corresponding to control signal saturation inevitably reduces in slope with the reduction in pressure. The way in which the covariance increases during the steady-state part of the response, and is driven downwards by more exciting data, can easily be seen. With the zero demand signal (Figure 8.2), the covariance trace rises rapidly, and the parameter estimates drift, until after about 2s the controller becomes unstable. The resulting movement is sufficient to partly re-tune the model and controller, and the process starts again. The large transient which occurs after 5s causes almost complete re-tuning of the parameters to near their original values. Similar parameter drift occurs with the sinusoidal demand (Figure 8.3),

Figure 8.4 gives equivalent results for the square wave demand with a forgetting factor of 0.99. The rate of adaptation is now reduced, with the parameter estimates slowly re-adjusting for 3s after the pressure change. However the bulk of the parameter change occurs rapidly enough to give an adequate closed-loop response. With insufficient excitation, the rate of covariance rise is reduced, and consequently the rate at which the parameter estimates drift is smaller. Just one parameter estimate is plotted in Figure 8.5, its behaviour being typical; it is plotted every second only, but over a longer (50s) period. In the case of the zero demand signal, a re-tuning transient does not occur until after 7s have elapsed.

Figures 8.6 and 8.7 give the results for a forgetting factor of 0.998. The covariance trace is now quite small, and adaptation is slow. Even with this near-unity forgetting factor, insufficient excitation still causes parameter drift, illustrating that no fixed forgetting factor value achieves a satisfactory overall performance.

In Figures 8.8 and 8.9 the corresponding results for the constant trace algorithm are presented. The trace of the covariance matrix is maintained at 150. The rate of adaptation in Figure 8.8 is good. With insufficient excitation, the covariance matrix can no longer grow indefinitely, but as the parameter values which can fit the model to the data are not unique, the estimates still tend to drift.

The results for the same algorithm, but with a trace of 75, are shown in Figures 8.10 and 8.11. The rate of adaptation is still acceptable, but the parameter estimates still drift, even though the first tuning transient (with zero demand) does not occur for nearly 30s.

For the variable forgetting factor, with $\Sigma_0 = 0.005$ and $\lambda_{min} = 0.94$, the rate of adaptation (Figure 8.12) is about the same as that for the fixed forgetting factor at 0.99, but drifting still occurs with insufficient excitation (Figure 8.13). The main problem is seen in the plot of the forgetting factor in Figure 8.12. The noise component of the *a posteriori* prediction error, and consequently of the forgetting factor, is significant compared to the component due to inaccurate parameter estimates. A larger value of Σ_0 would suppress the noise effects, keeping the forgetting factor nearer unity, but would reduce the rate of adaptation as well. Whatever values are chosen, it is inevitable that noise will keep the forgetting factor below unity on average even without sufficient excitation, and the covariance matrix is unlikely to diminish sufficiently to prevent parameter drift.

The parameter drifting exhibited during periods of insufficient excitation using the above methods can (potentially) be tackled by employing jacketting to switch off the adaptation appropriately. The results for a fixed forgetting factor with an estimation dead-zone are presented in Figures 8.14 and 8.15. λ is 0.96, and ε_L is 0.02. Unfortunately the method is afflicted with the same problem as the variable forgetting factor; noise is a very significant component of the prediction error. It is difficult to choose a dead-zone width which prevents adaptation if excitation is insufficient, yet allows rapid adaptation in other circumstances. In Figure 8.14 adaptation is not frequent, but adequate to adapt to the change in pressure.

However the parameters still drift with the sinusoidal demand (Figure 8.15).

8.5 Trace limiting algorithm

An alternative forgetting strategy has been developed in the light of the difficulties recounted in the previous Section. This uses a fixed forgetting factor, but in addition switches off the estimator if the excitation is insufficient. The excitation is deemed to be insufficient if the trace of P_t reaches some user specified limiting value. Thus trace limited RLS is given by equations (8.1) and (8.4) with the following extension:

$$\left.\begin{aligned} &\text{if} \quad \mathrm{tr}P_t \geq \alpha \quad \text{then} \\ &\qquad P_t = \frac{\alpha}{\mathrm{tr}P_{t-1}} P_{t-1} \\ &\qquad \hat{\theta}_t = \hat{\theta}_{t-1} \end{aligned}\right\} \tag{8.17}$$

where α is the trace limit.

The forgetting factor λ can now be re-interpreted: considering the algorithm in the trace limited state, the lower the value of λ, the more exciting the data must be before adaptation occurs. Also the higher the value of α, the higher P_t (and k_t) can become before adaptation is switched off, allowing the model to adapt more rapidly.

Results for the trace limiting algorithm with $\lambda = 0.92$ and $\alpha = 200$ are presented. The rate of adaptation is very good in Figure 8.16, and the adaptation is permanently switched off in both cases of insufficient excitation (Figure 8.17).

An order of magnitude for α was obtained by inspecting the off-line normalised covariance matrix of equation (8.15), which has a trace of 93.6. However the final values for both α and λ were determined experimentally. The results for some other values are also shown in the Figures. For Figure 8.18 the forgetting factor is increased to 0.96, and now the controller does

not switch-off so rapidly as before in the face of insufficient excitation. This is reflected in Figure 8.19, where the parameter estimate does change for both zero and sinusoidal demands. Figure 8.20 reverts to $\lambda = 0.92$, but now has a higher covariance trace limit of 400. With the higher average covariance, adaptation is slightly faster. However the high limit appears to reduce the readiness of the controller to stop adapting, and the parameter estimate in Figure 8.21 drifts with the sinusoid demand.

The first values presented ($\lambda = 0.92$ and $\alpha = 200$) were found to give the best overall controller performance, with a good rate of adaptation, and reliability in the face of all demand signals tried. These values are used throughout the following Section.

8.6 Adaptive versus fixed-coefficient pole-placement

The adaptive controller with trace limited covariance is explored experimentally in more detail in this Section. In particular it is shown adapting to a variety of plant changes, and its performance is compared with that of an equivalent fixed-coefficient controller in the same situations.

Figure 8.22 illustrates the behaviour of the adaptive controller when there is an increase in supply pressure. The fixed pole-placement controller with the same desired closed-loop poles and demand filter is also shown. Both controllers are initially well tuned for the starting pressure of 40bar. After 2s the pressure is suddenly increased to 160bar. The fixed controller becomes very oscillatory, but the adaptive controller fully adapts to the new pressure within one period of the demand cycle.

Figure 8.23 illustrates a similar effect when the pressure is reduced from 160bar to 40bar, with both fixed and adaptive controllers starting well tuned for the higher pressure. Changing the supply pressure is just a convenient means of changing the plant characteristics, and in practice changes are more likely to originate from the load.

In Figure 8.24 the supply pressure is kept constant at 100bar. After 2s the dead oil volumes are switched into the circuit. This reduces the natural frequency of the plant (from 12Hz to 7Hz) in the same way as an increase of load mass would. The adaptation is again very rapid. Figure 8.25 shows the reverse situation, where the extra oil volume is initially present, and is removed after 2s. The fixed controller develops a high frequency limit cycle (the control signal is oscillating between the two saturation levels), but the adaptive controller performs well. Notice that the estimates do show some adaptation to the difference in plant behaviour between when the cylinder is extending and retracting.

All these examples have demonstrated the improvement of the adaptive controller over the fixed-coefficient controller. However the robustness claimed for the pole-placement control method in Chapter 6 would suggest that some plant time-variations could be accommodated without causing instability, and hopefully with acceptably small excursions from the desired response. Figure 8.26 shows the responses for the fixed and adaptive controllers to a step change in supply pressure from 60bar to 120bar. The fixed controller was designed for a 80bar supply pressure. The adaptive controller responds well, but the change in response of the fixed controller is not great, and would undoubtedly be acceptable for some applications. Figure 8.27 shows the responses for the two controllers when the dead oil volumes are switched out. This is the same situation as depicted in Figure 8.25, but now the sample interval has been increased from 10 to 20ms, with a corresponding increase in robustness (see Section 6.5). This time the fixed-coefficient controller response is hardly affected, and adaptive control is unnecessary.

A final demonstration of the performance of the two controllers is given in Figure 8.28. Previous graphs have shown small amplitude square wave responses for convenience of comparison. In this Figure a more varied demand signal is used, covering a much larger part of the stroke. Despite changes in cylinder oil volumes and consequent changes in plant behaviour, the fixed controller gives a good response. Although the adaptive controller is not required if these are the only plant changes, it can be seen that if it is used a reliable performance is obtained with an irregular demand signal.

8.7 Conclusions

An indirect (self-tuning) adaptive control algorithm based on pole-placement control has been designed and applied to an electro-hydraulic positioning system. The controller shows rapid adaptation to changes in plant characteristics, even when the changes are very significant and virtually instantaneous, and in situations which cause an equivalent fixed-coefficient controller to breakdown. The good performance is achieved despite the presence of many non-linear plant characteristics. The main improvements made over adaptive control algorithms previously applied to similar systems are threefold:

- the use of an estimation filter in the recursive least squares estimator. This not only reduces bias but increases the convergence rate. The poor adaptation of the controller with the estimation filter removed is shown in Figure 8.29.
- the use of a demand filter in the pole-placement part of the controller. For particular pole positions this will suppress noise and improve robustness. The latter is still important for an adaptive controller as modelling errors will always exist, especially before adaptation has caught up following a sudden change in plant characteristics. Figure 8.30 shows the controller with the demand filter removed.
- the use of an algorithm which switches off adaptation if the trace of the covariance matrix becomes too great, overcoming the difficulties caused by lack of excitation — which has been the main subject of this Chapter.

The complete adaptive controller algorithm is summarized in Table 8.1, which is principally an amalgam of equations (8.1), (8.3), (8.4), (8.17), (6.8) and (3.12).

Off-line system identification has been shown to be nearly as important for adaptive controller design as it is for the design of a fixed-coefficient controller. In particular it can be used to determine the structure of the plant model, to reduce the number of parameters to be adapted, and to provide initial estimates and variances for controller start-up.

Even though the adaptive controller performs well, it may not always be necessary, even when significant plant changes are encountered. A fixed-coefficient pole-placement controller, designed with robustness in mind, has been shown to be insensitive to changes in plant

parameters. For the system under test, the adaptive controller requires about 3ms computation time per sample, whilst the fixed controller requires about 0.25ms (both values including the time to read and write signals). Although the computation time for the adaptive controller could be reduced if the implementation were optimised for speed, the computational burden will always be an order of magnitude greater. Thus for any particular application, the likely size of plant variations and the allowable deviation in closed-loop response would both have to be carefully considered in order to justify the use of an adaptive controller. However as computational power becomes ever cheaper the balance swings in favour of adaptive control.

1. $y_t' = D(z^{-1})y_t\ , \qquad u_{t-1}' = D(z^{-1})\ u_{t-1}$

2. Also pre-filter output by any known poles and input by any known zeros

3. $\psi_t^T = [y_{t-1}', \ldots, y_{t-n}', u_{t-1}', \ldots, u_{t-m}']$

4. $$k_t = \frac{P_{t-1}\psi_t}{(\lambda + \psi_t^T P_{t-1}\psi_t)}$$

5. $\hat{\theta}_t = \hat{\theta}_{t-1} + k_t(y_t' - \psi_t^T \hat{\theta}_{t-1})$

6. $$P_t = \frac{(P_{t-1} - k_t\psi_t^T P_{t-1})}{\lambda}$$

7. If $\mathrm{tr}P_t \geq \alpha$ then: $$P_t = \frac{\alpha}{\mathrm{tr}P_{t-1}} P_{t-1}\ , \quad \hat{\theta}_t = \hat{\theta}_{t-1}$$

8. Construct $\hat{A}(z^{-1})$ and $\hat{B}(z^{-1})$ from $\hat{\theta}_t$

9. Solve: $F(z^{-1})\hat{A}(z^{-1}) + G(z^{-1})\hat{B}(z^{-1}) = A_m(z^{-1})H(z^{-1})$

10. $$u_{ft} = \frac{r_t - G(z^{-1})y_t - (F(z^{-1}) - f_0)u_t}{f_0}$$

11. $$\begin{cases} u_t = u_{ft} & \text{for } u_{sat-} < u_{ft} < u_{sat+} \\ u_t = u_{sat-} & \text{for } u_{ft} \leq u_{sat-} \\ u_t = u_{sat+} & \text{for } u_{ft} \geq u_{sat+} \end{cases}$$

12. Modify u_t using static non-linear compensation if required

Table 8.1 Full adaptive control algorithm

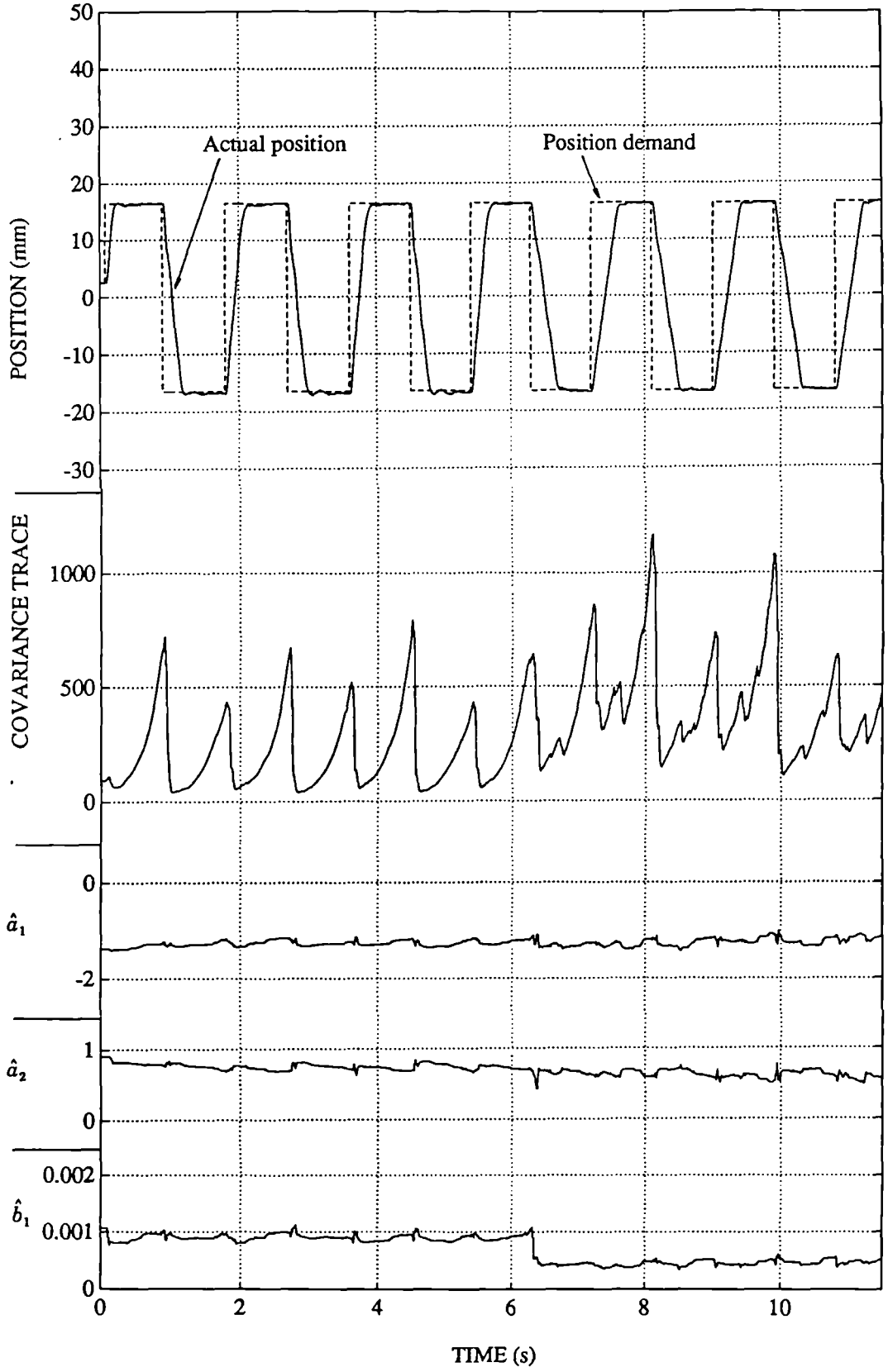

Figure 8.1 Adaptation to a pressure drop from 100bar to 40bar after 6s, using a fixed forgetting factor of 0.96.

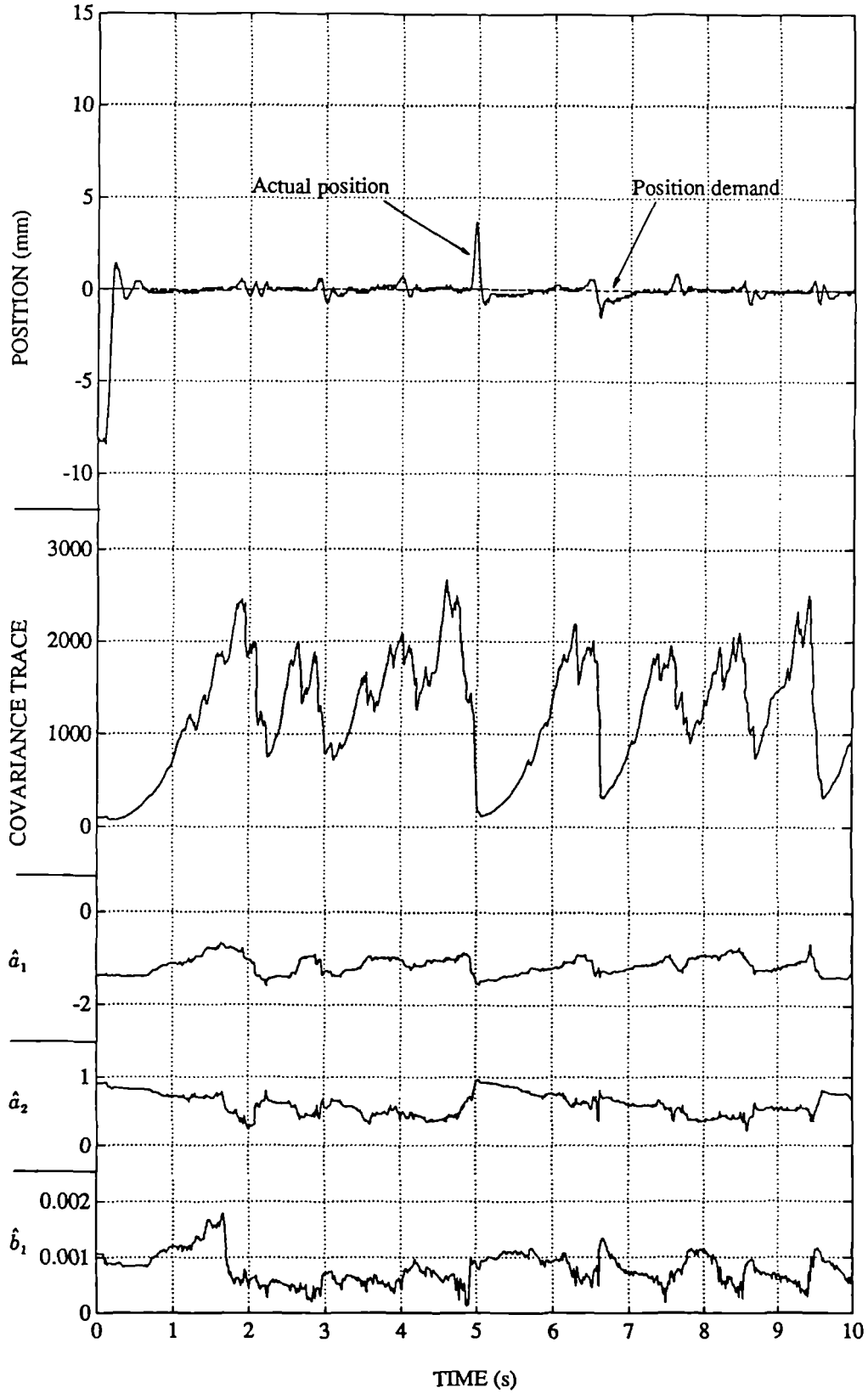

Figure 8.2 Adaptive control with a constant demand signal, using a fixed forgetting factor of 0.96

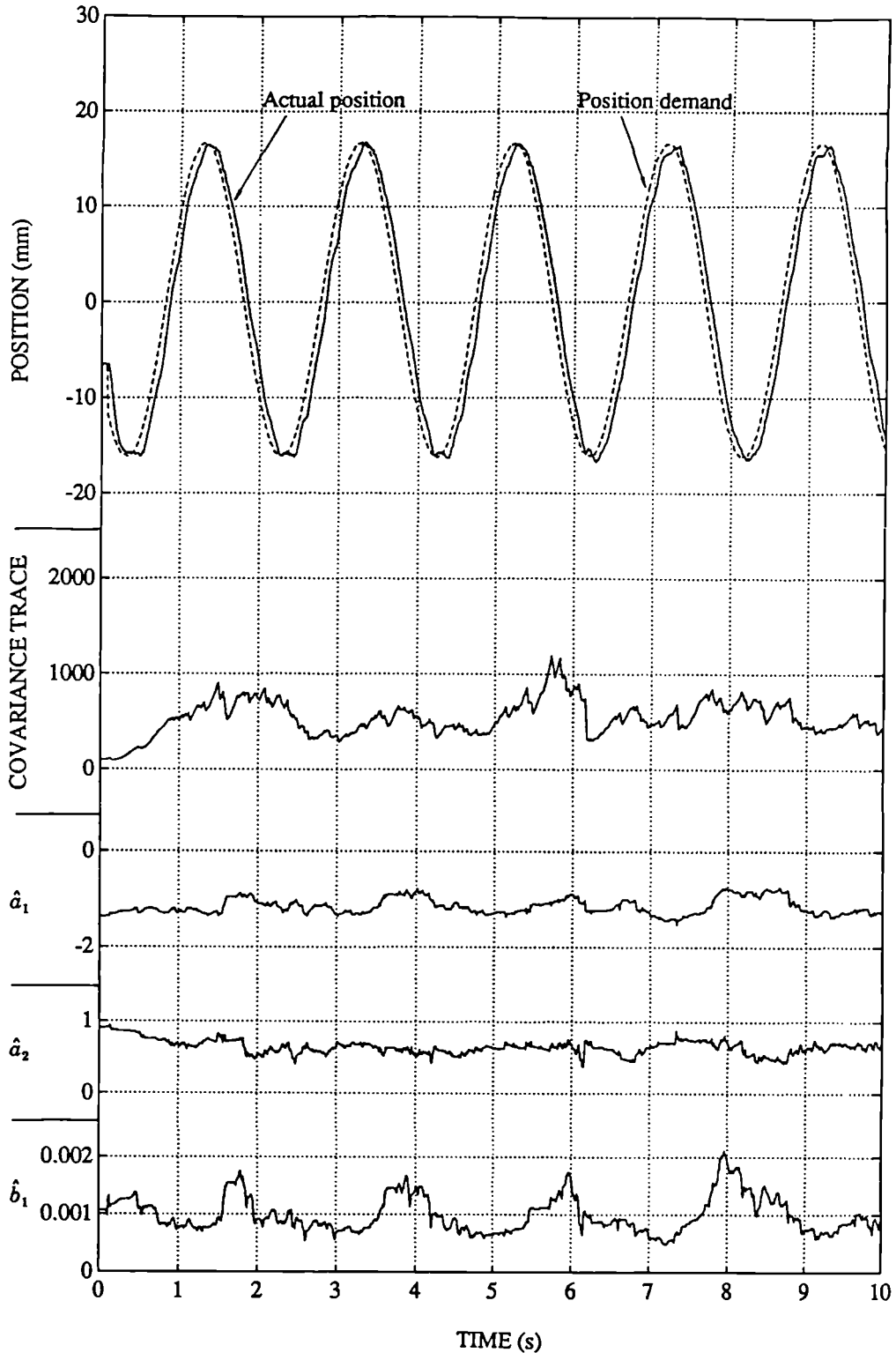

Figure 8.3 Adaptive control with a sinusoidal demand signal, using a fixed forgetting factor of 0.96

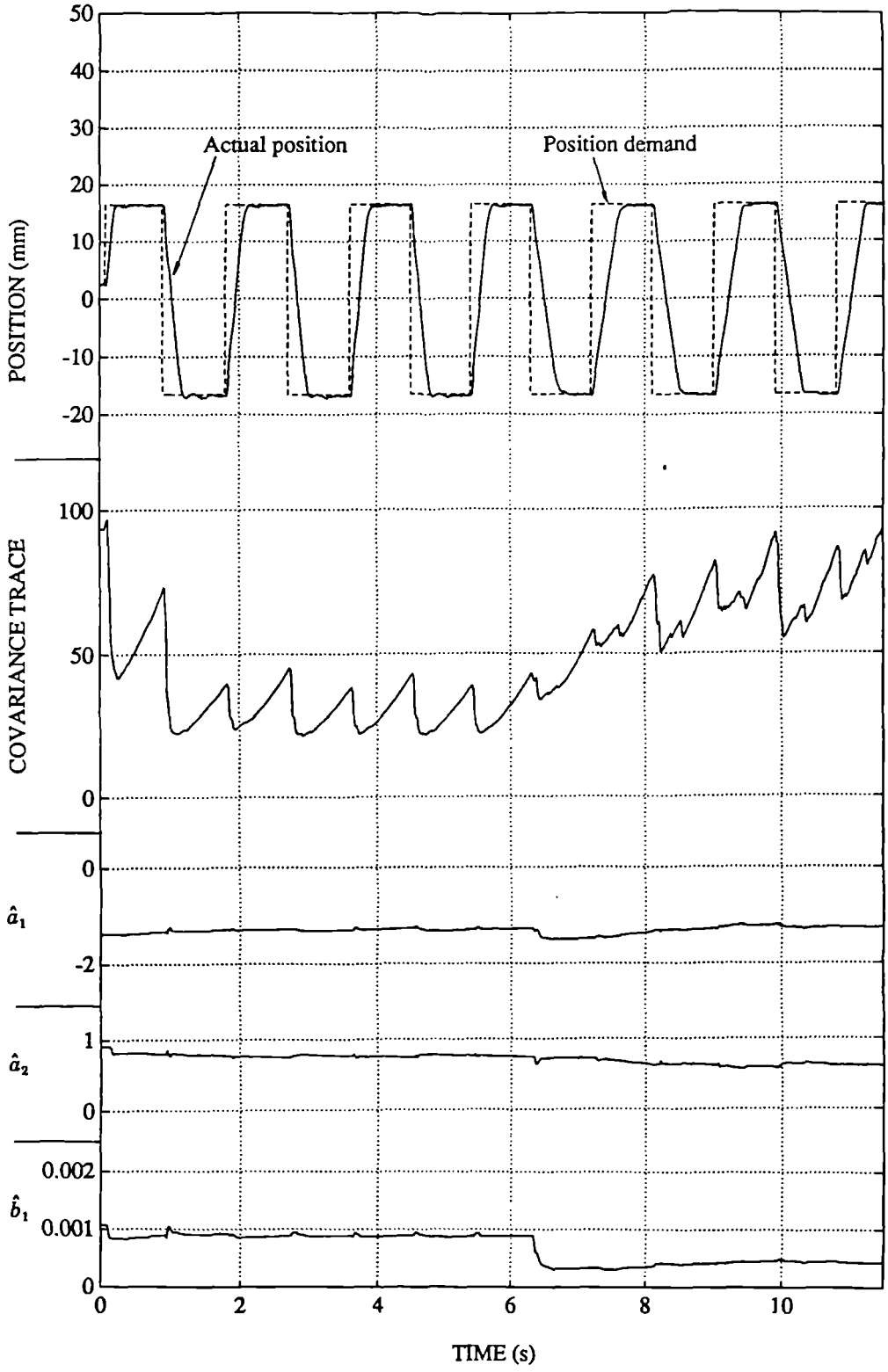

Figure 8.4 Adaptation to a pressure drop from 100bar to 40bar after 6s, using a fixed forgetting factor of 0.99

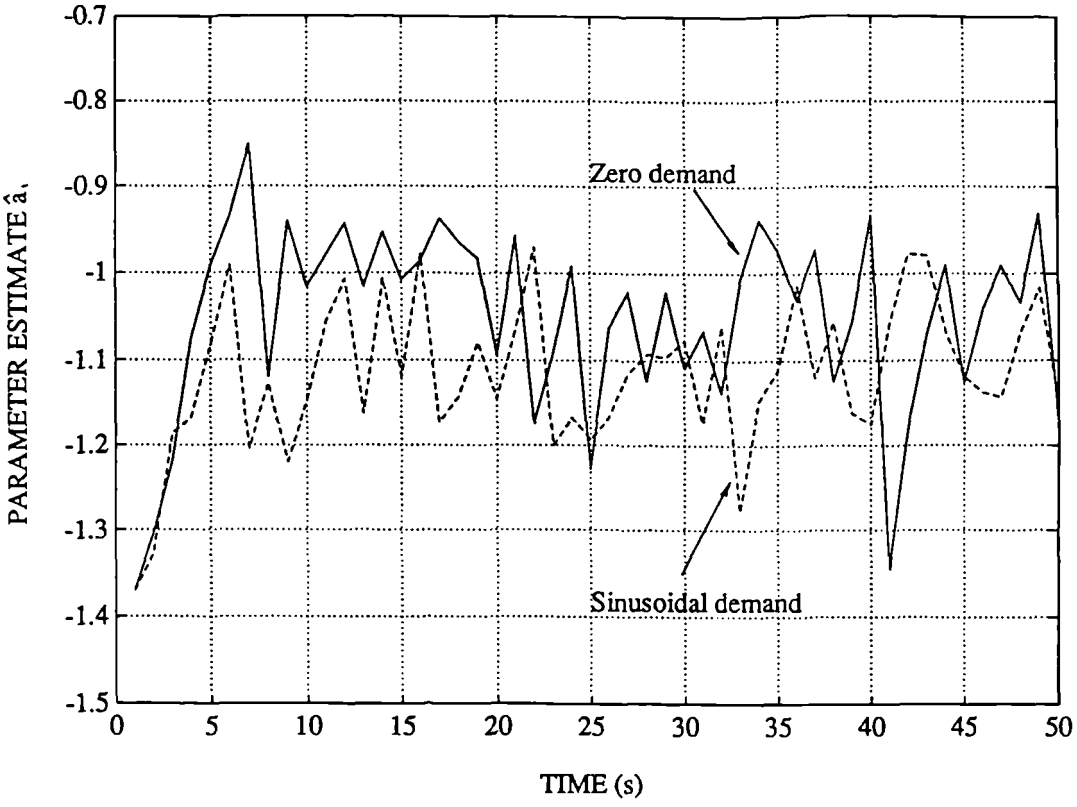

Figure 8.5 Variation of typical parameter estimate using a fixed forgetting factor of 0.99

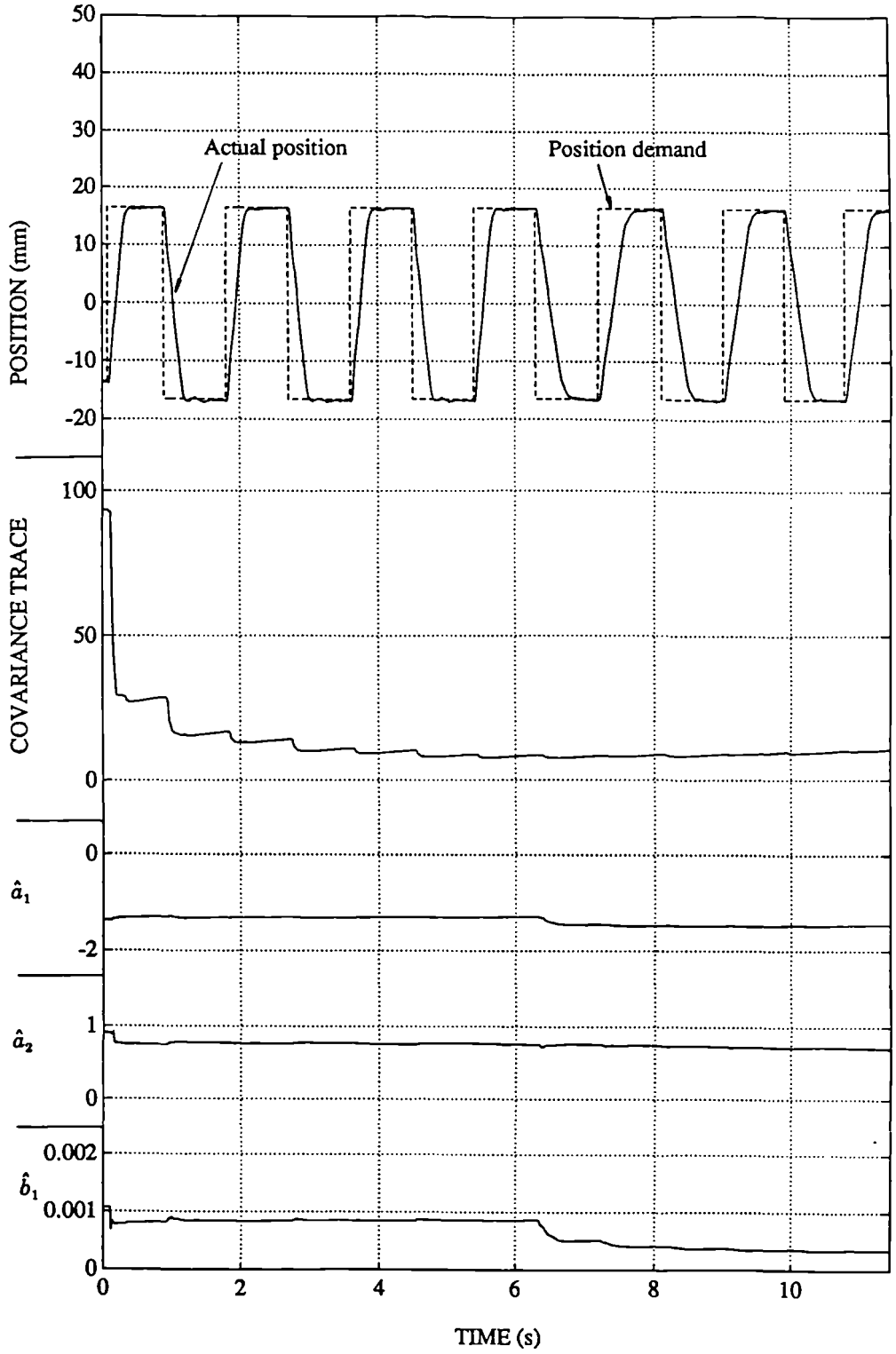

Figure 8.6 Adaptation to a pressure drop from 100bar to 40bar after 6s, using a fixed forgetting factor of 0.998

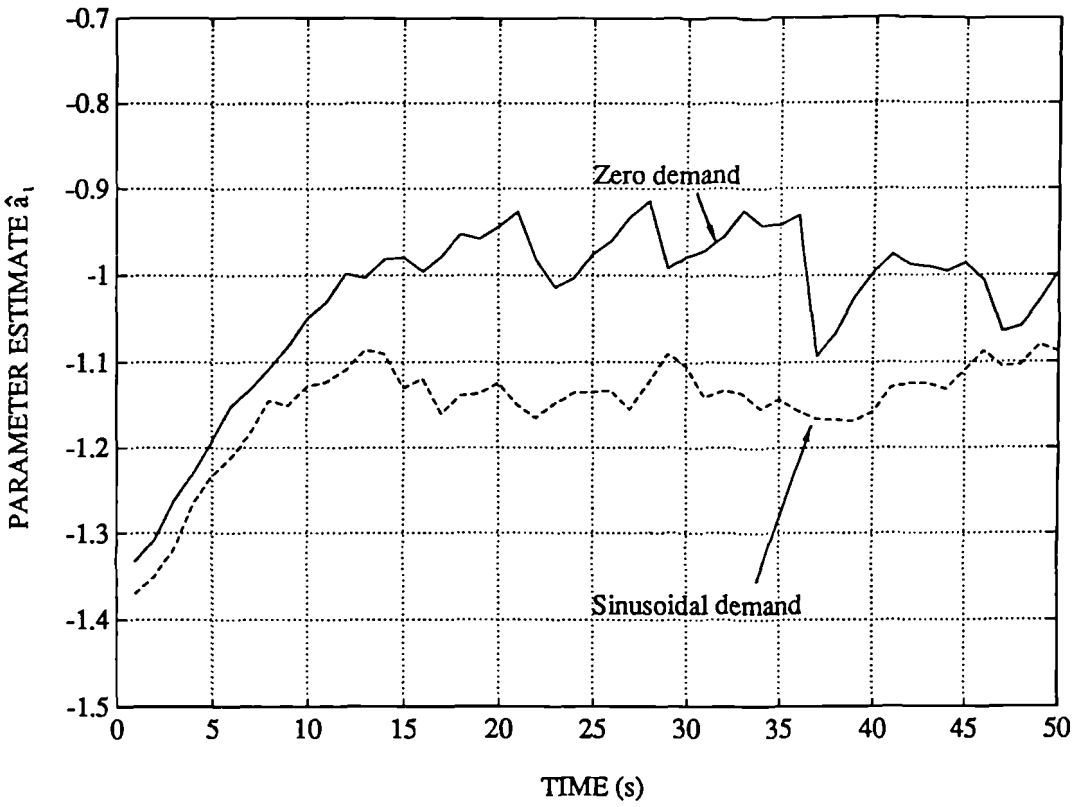

Figure 8.7 Variation of typical parameter estimate using a fixed forgetting factor of 0.998

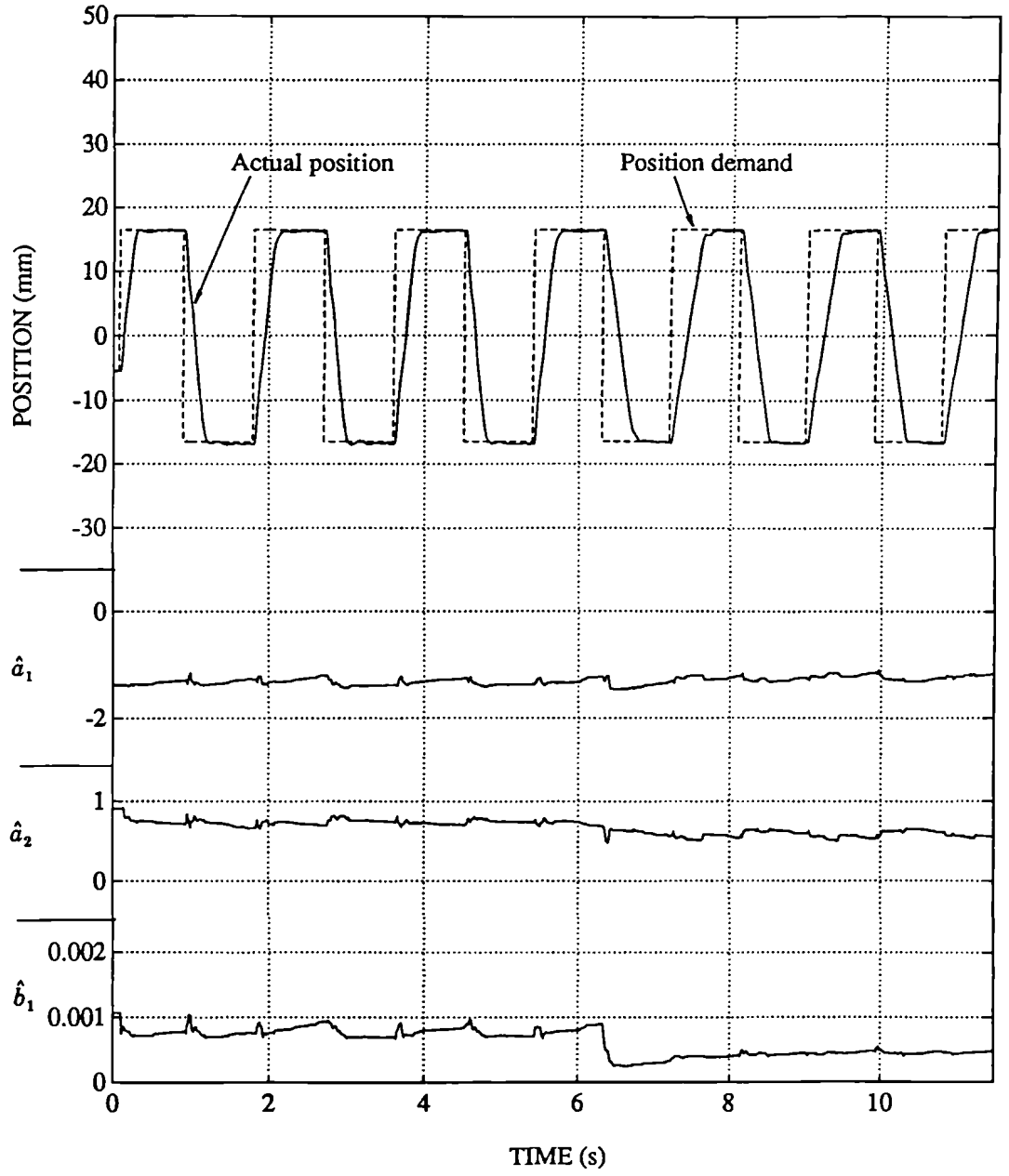

Figure 8.8 Adaptation to a pressure drop from 100bar to 40bar after 6s, using a constant trace of 150

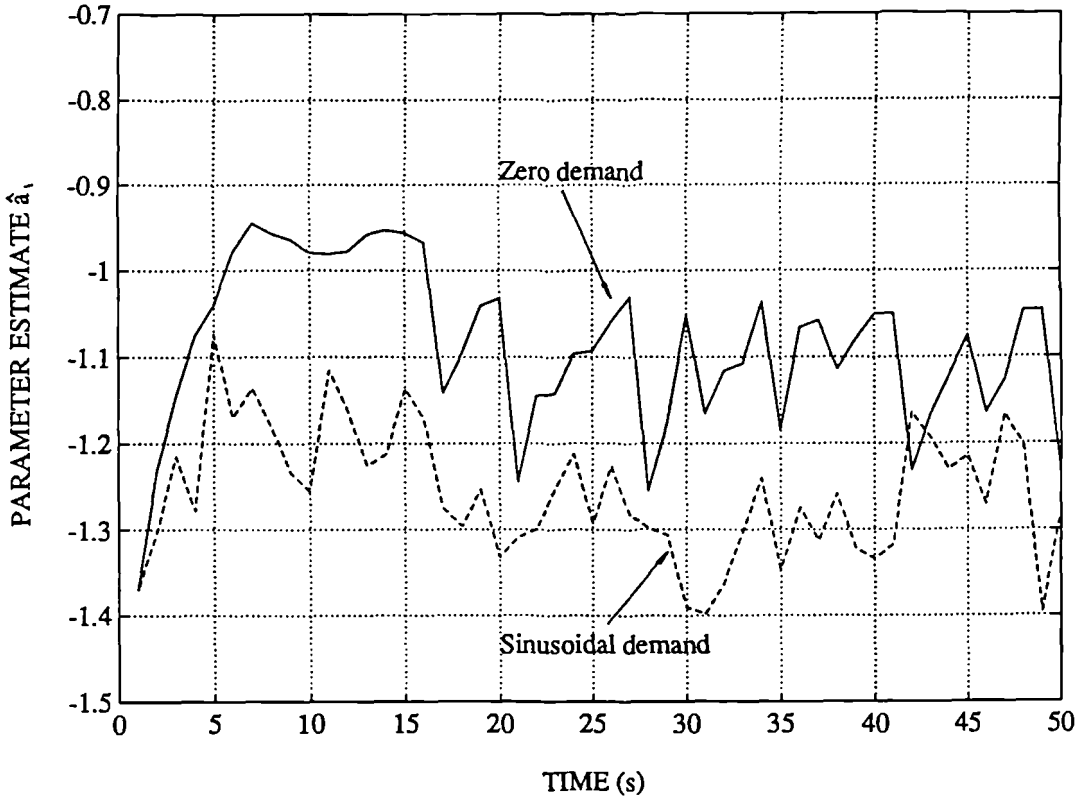

Figure 8.9 Variation of typical parameter estimate using a constant trace of 150

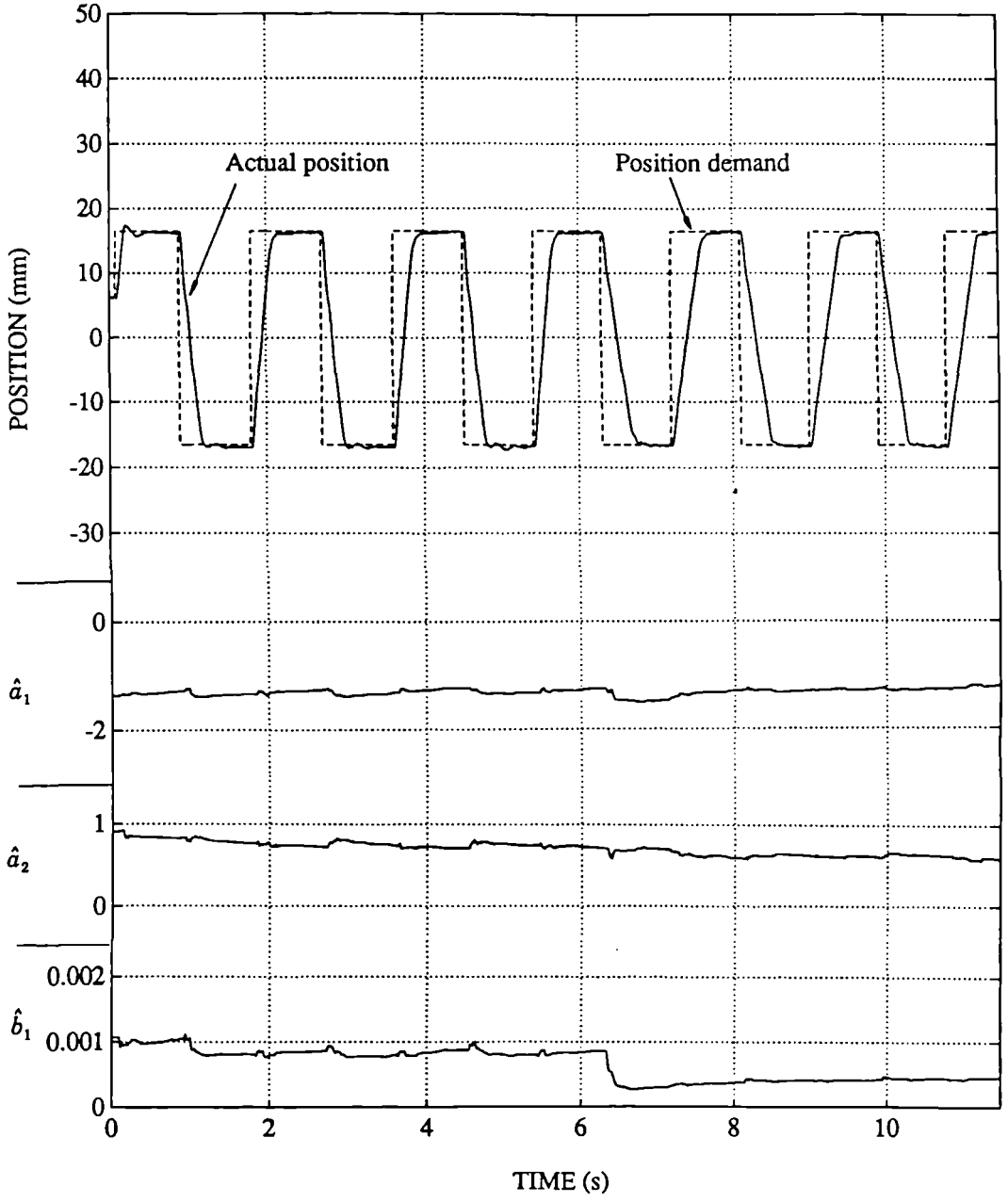

Figure 8.10 Adaptation to a pressure drop from 100bar to 40bar after 6s, using a constant trace of 75

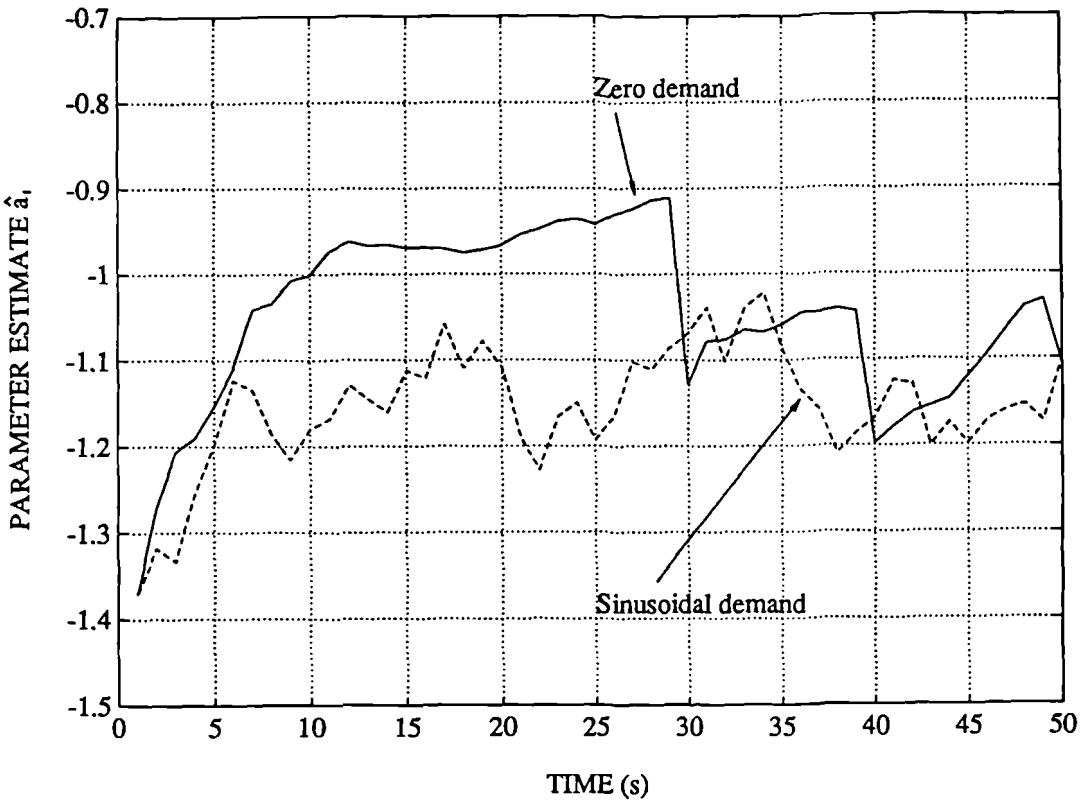

Figure 8.11 Variation of typical parameter estimate using a constant trace of 75

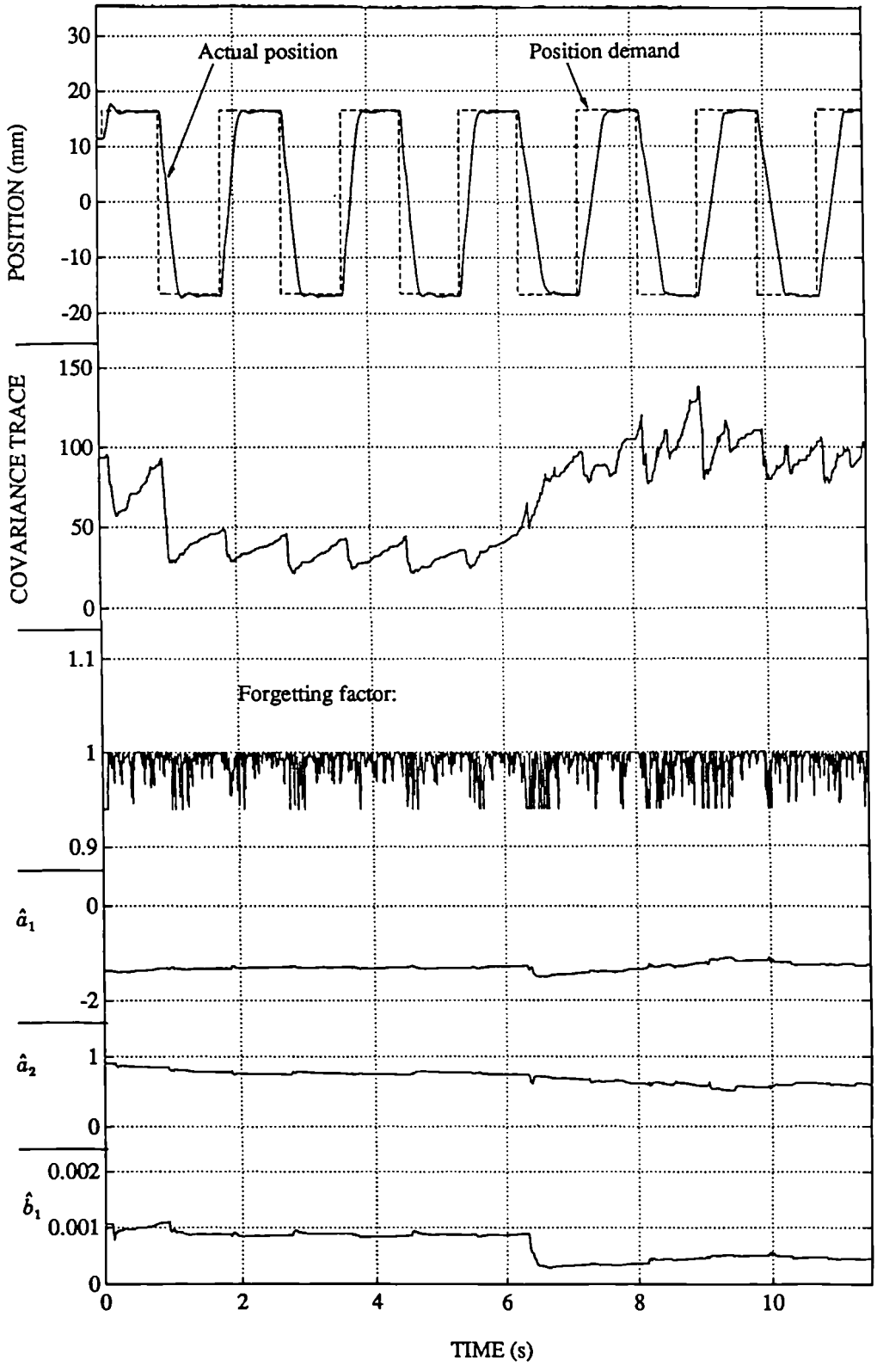

Figure 8.12 Adaptation to a pressure drop from 100bar to 40bar after 6s, using a variable forgetting factor

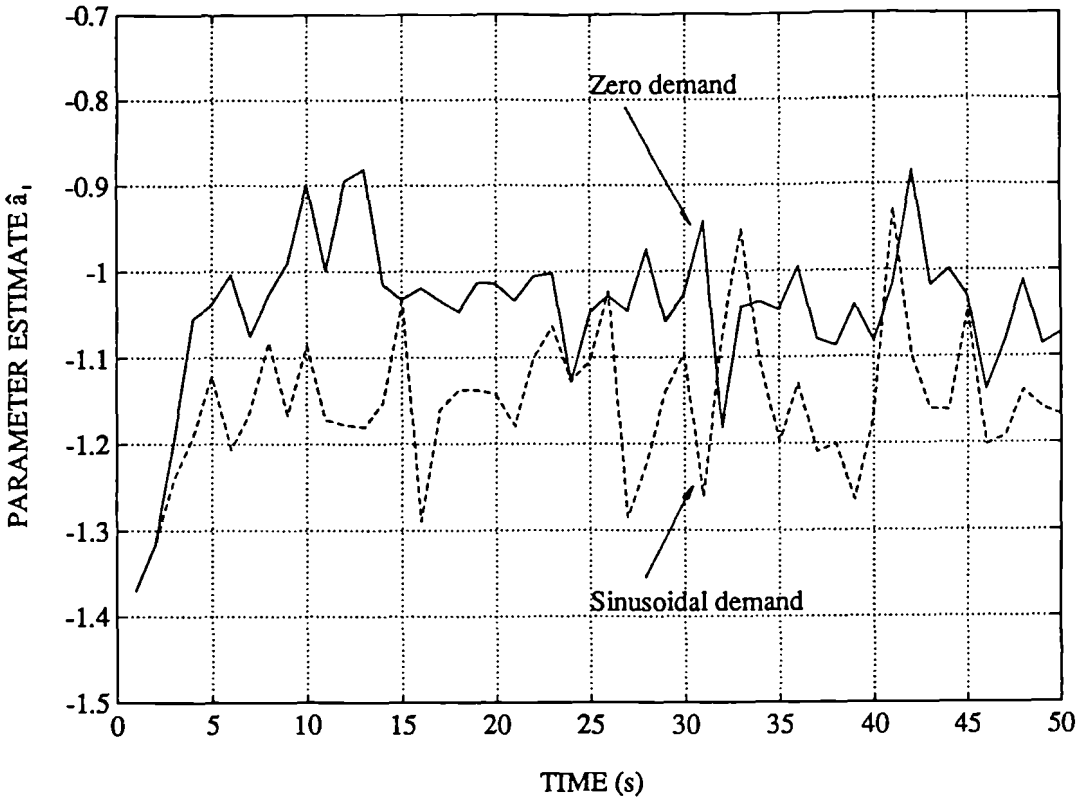

Figure 8.13 Variation of typical parameter estimate using a variable forgetting factor

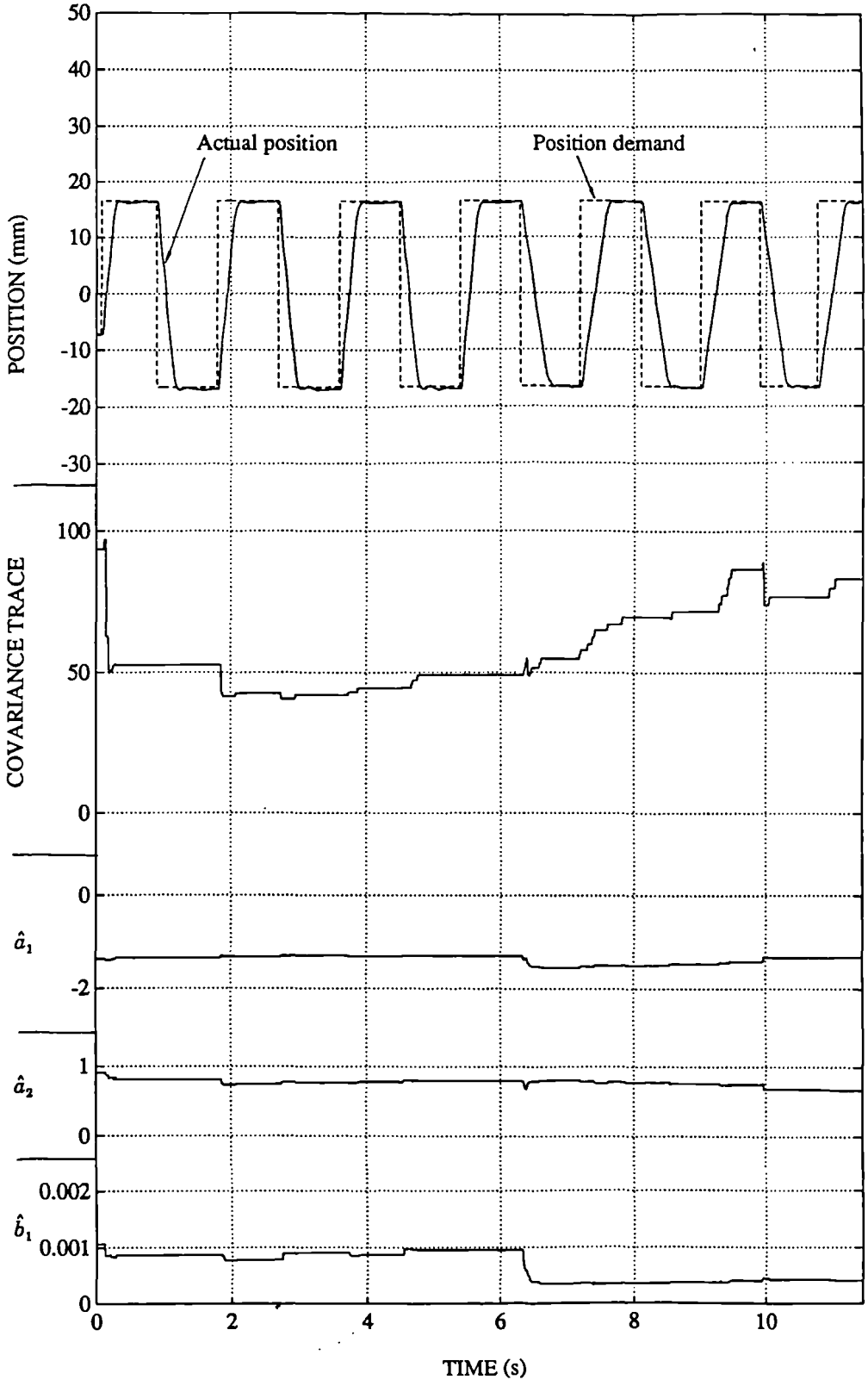

Figure 8.14 Adaptation to a pressure drop from 100bar to 40bar after 6s, using a fixed forgetting factor of 0.96 plus estimation dead zone

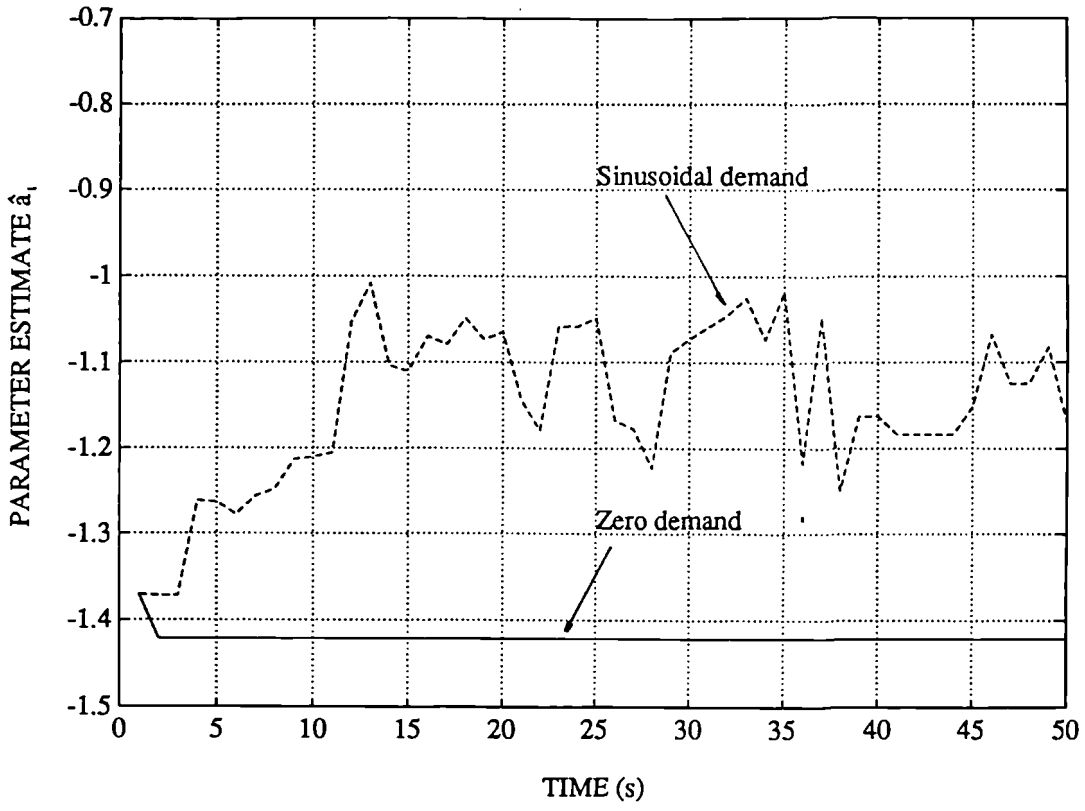

Figure 8.15 Variation of typical parameter estimate using a fixed forgetting factor of 0.96 plus estimation dead zone

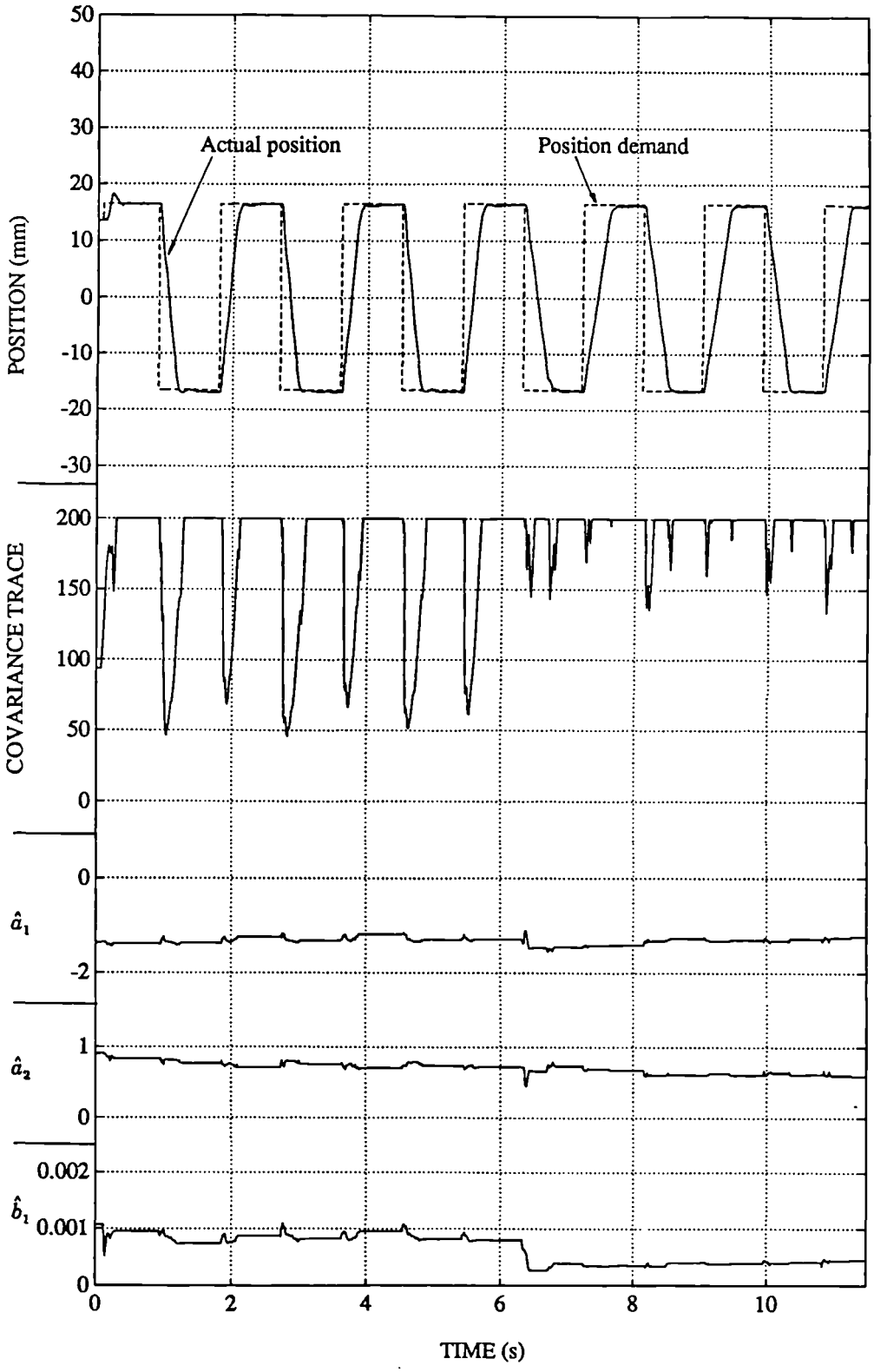

Figure 8.16 Adaptation to a pressure drop from 100bar to 40bar after 6s, using trace limiting algorithm (λ=0.92, α=200)

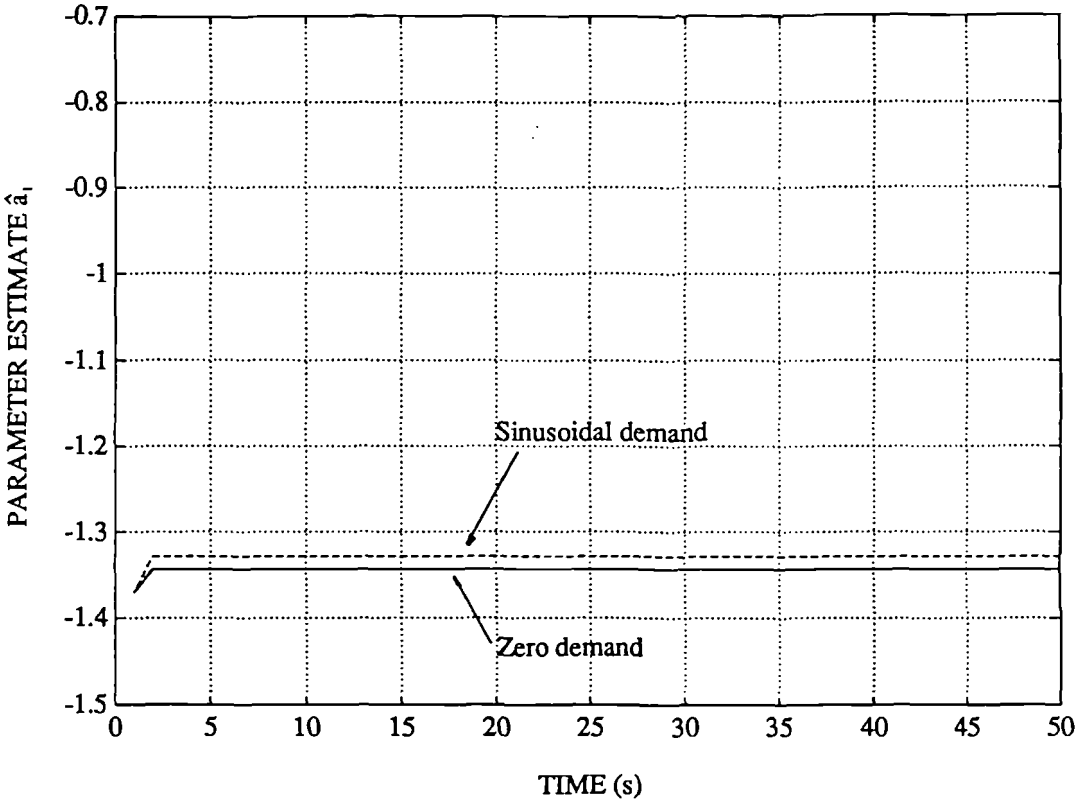

Figure 8.17 Variation of typical parameter estimate using trace limiting algorithm (λ=0.92, α=200)

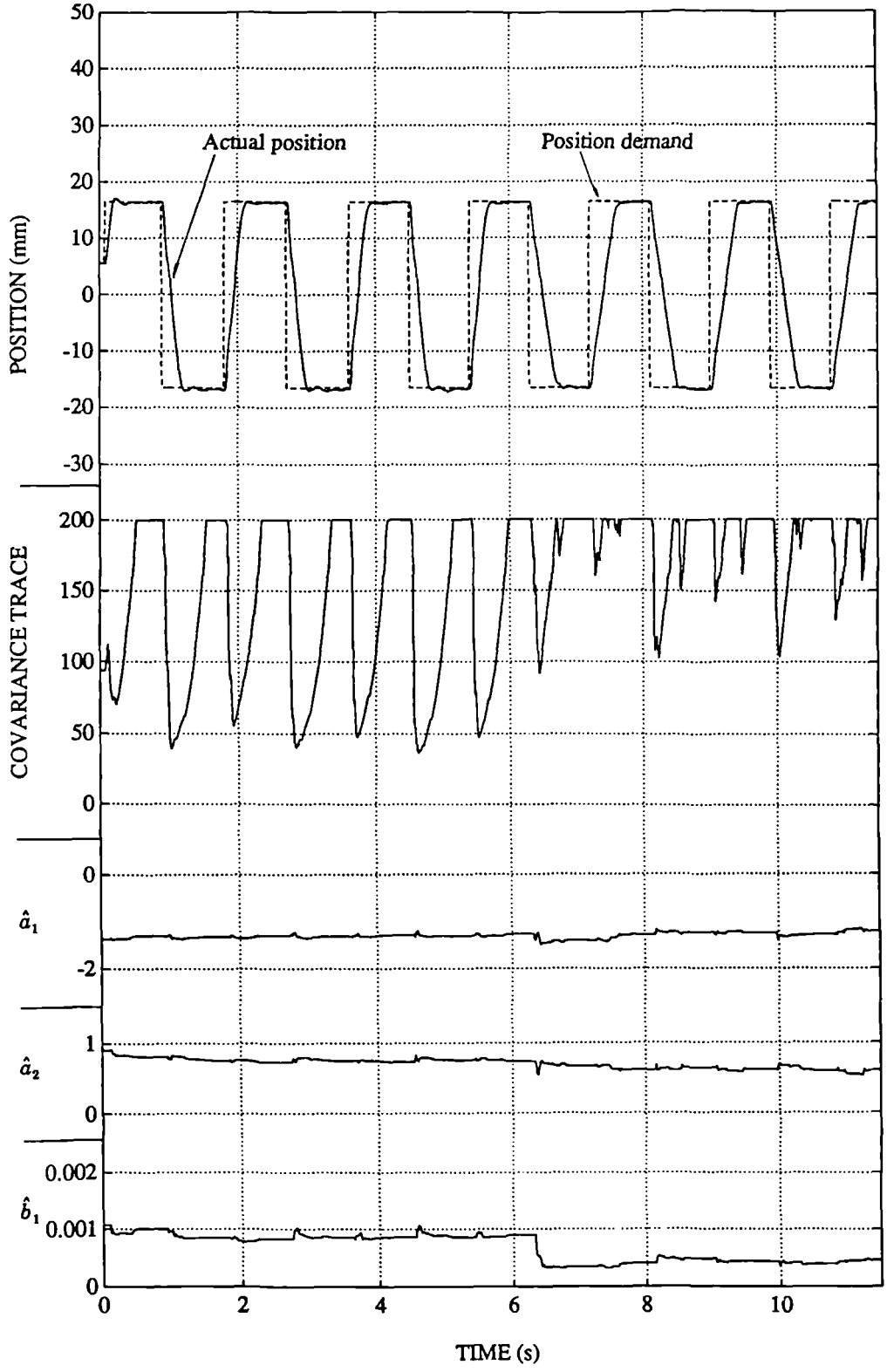

Figure 8.18 Adaptation to a pressure drop from 100bar to 40bar after 6s, using trace limiting algorithm (λ=0.96, α=200)

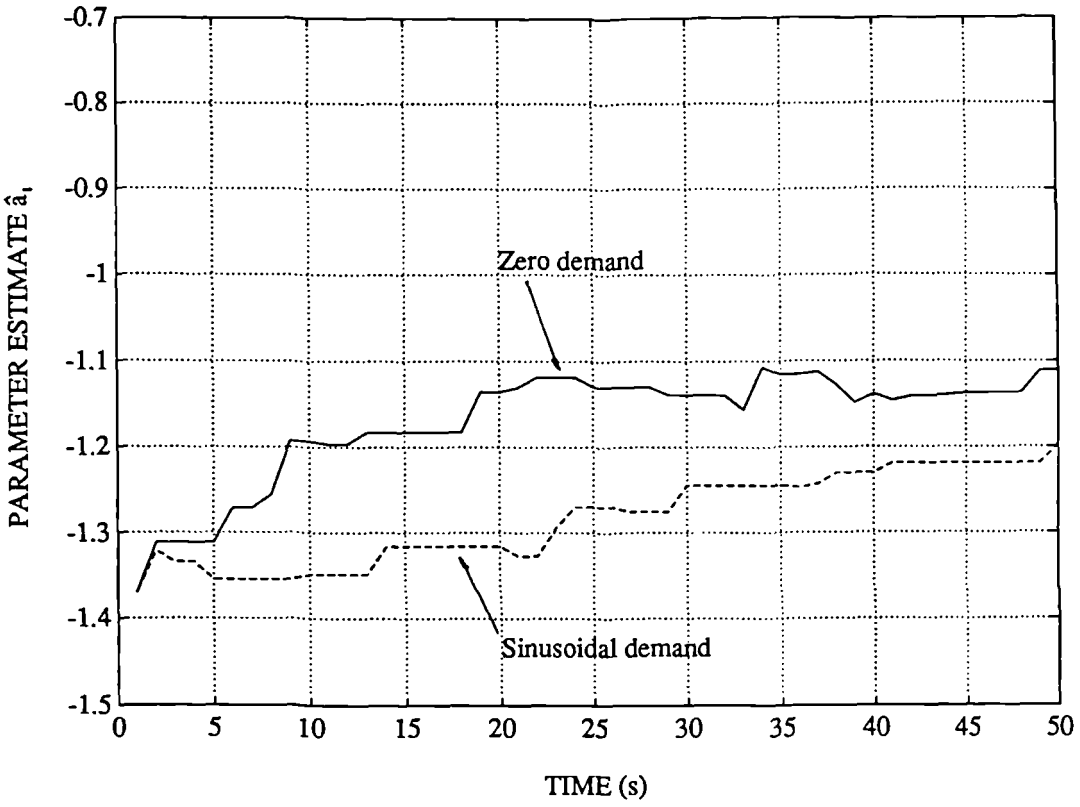

Figure 8.19 Variation of typical parameter estimate using trace limiting algorithm (λ=0.96, α=200)

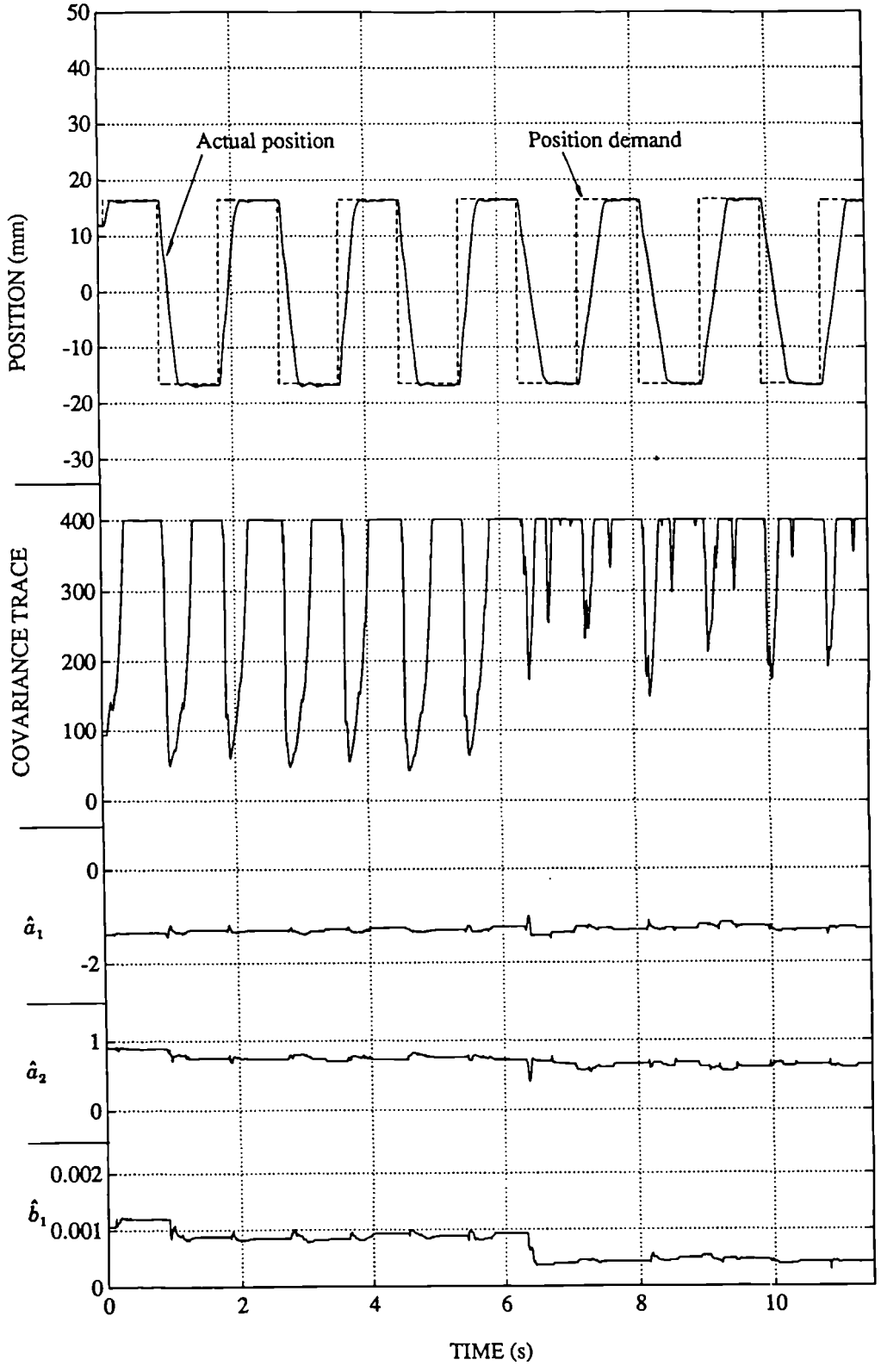

Figure 8.20 Adaptation to a pressure drop from 100bar to 40bar after 6s, using trace limiting algorithm (λ=0.92, α=400)

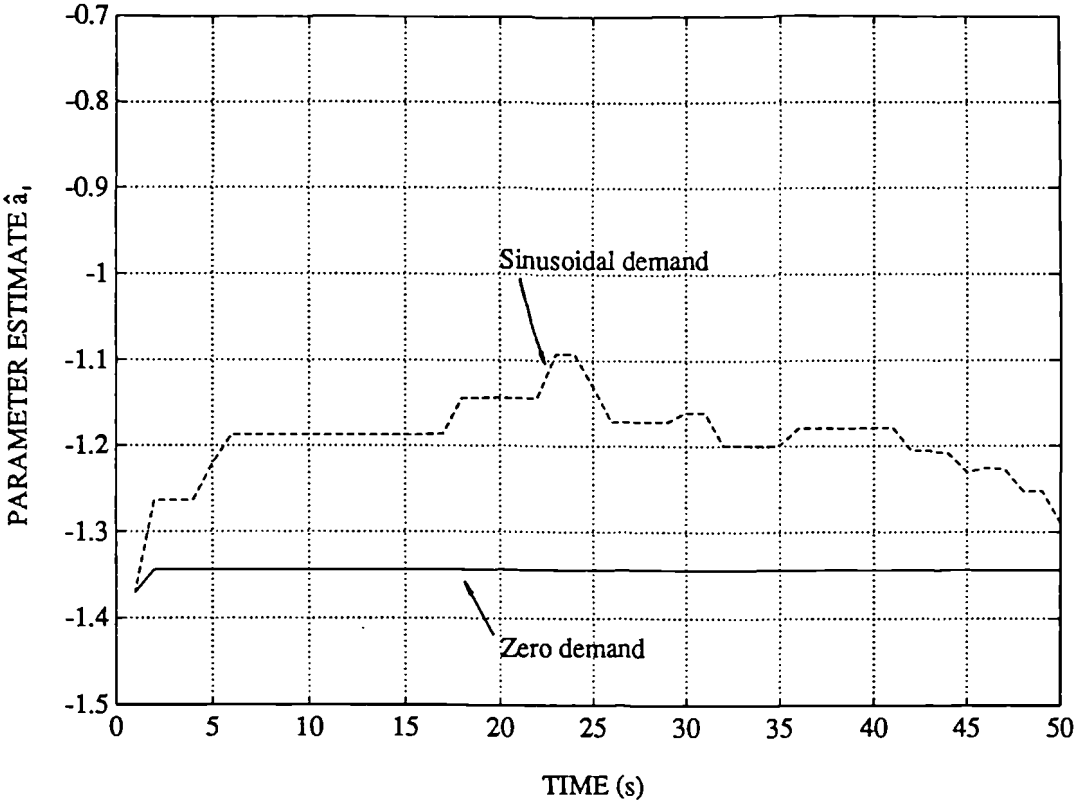

Figure 8.21 Variation of typical parameter estimate using trace limiting algorithm (λ=0.92, α=400)

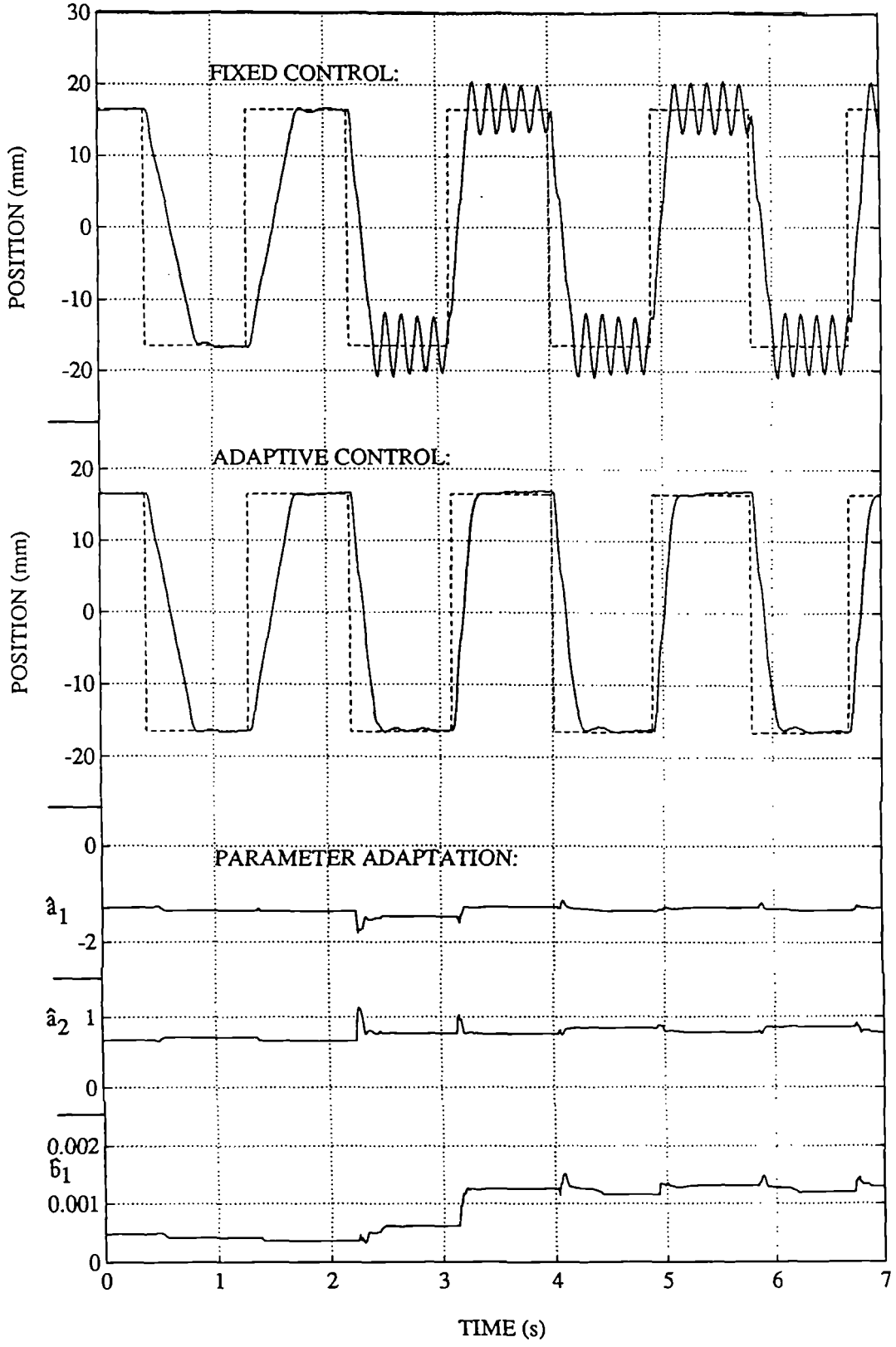

Figure 8.22 Response with increase in supply pressure from 40bar to 160bar after 2s

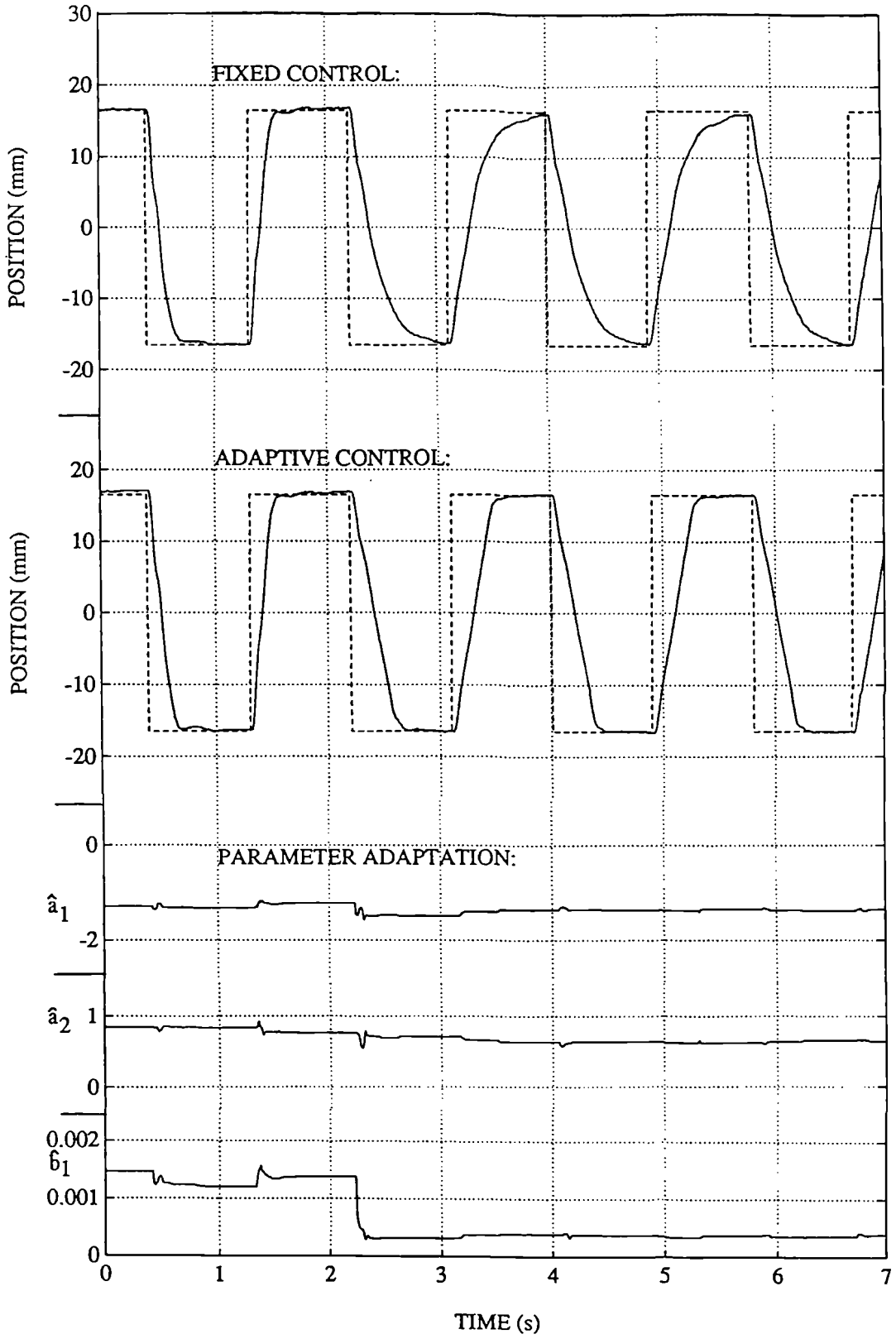

Figure 8.23 Response with decrease in supply pressure from 160bar to 40bar after 2s

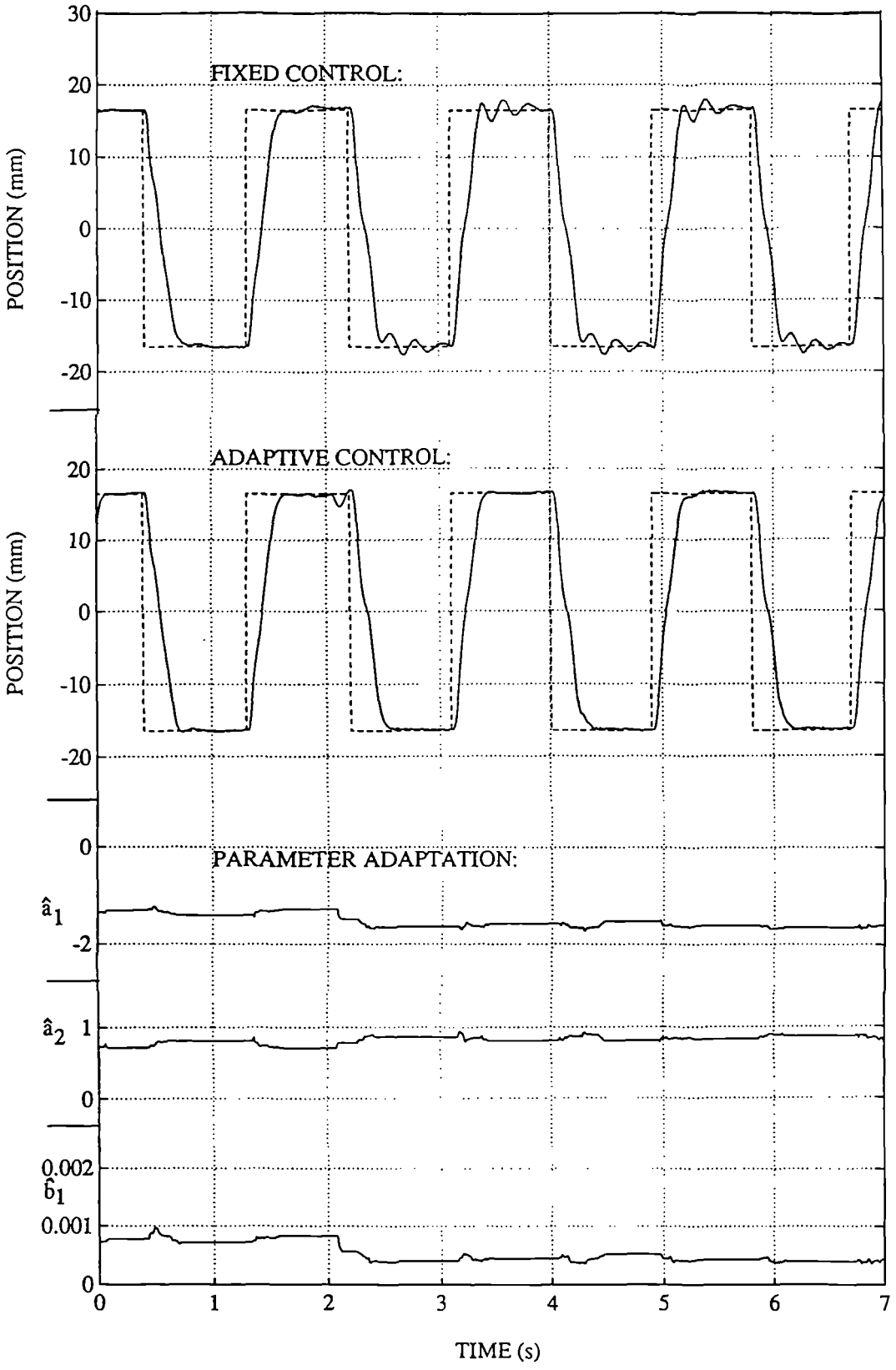

Figure 8.24 Response with dead oil volumes switched in after 2s (100bar supply pressure)

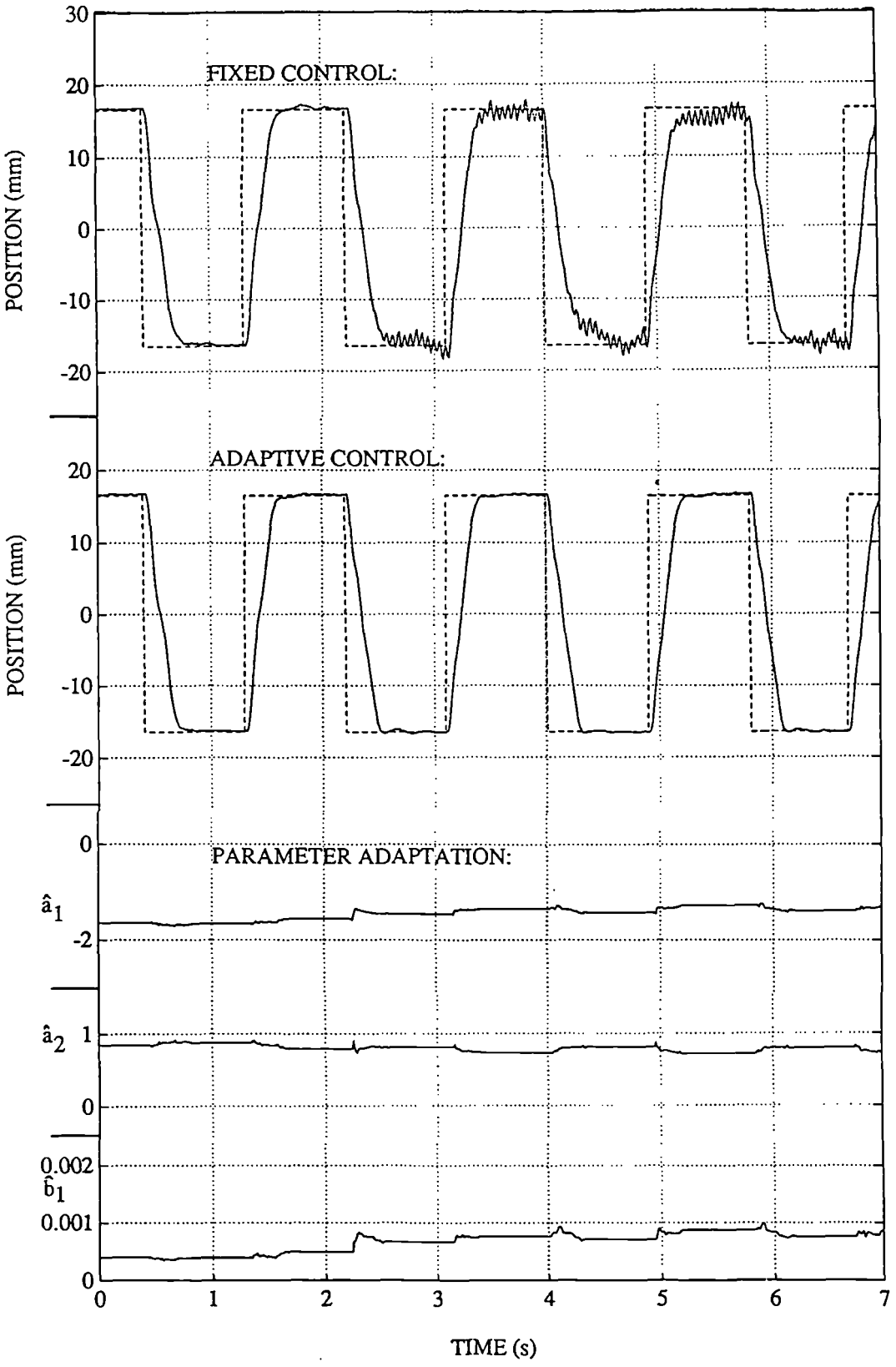

Figure 8.25 Response with dead oil volumes switched out after 2s (100bar supply pressure)

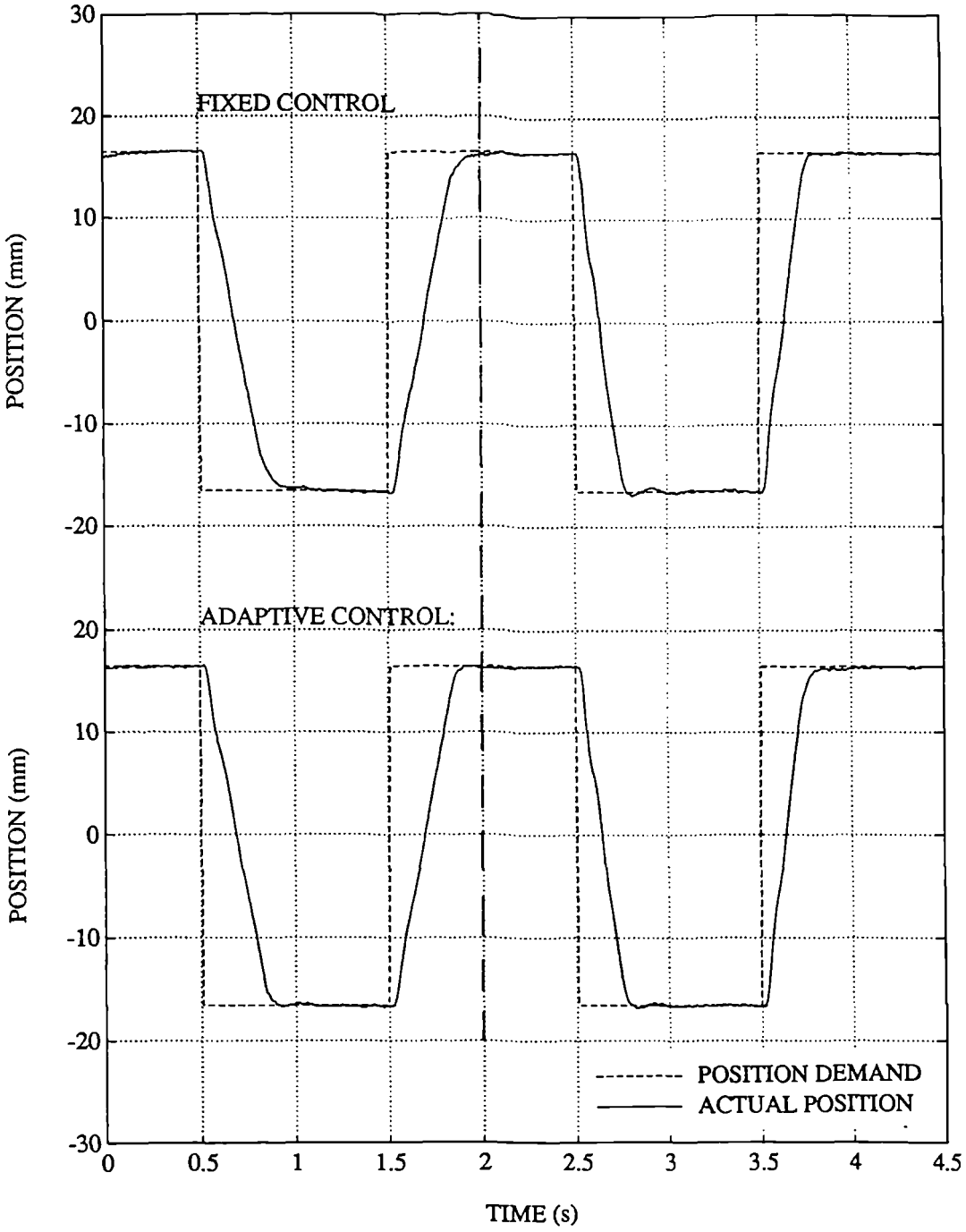

Figure 8.26 Response to increase in supply pressure from 60bar to 120bar after 2s

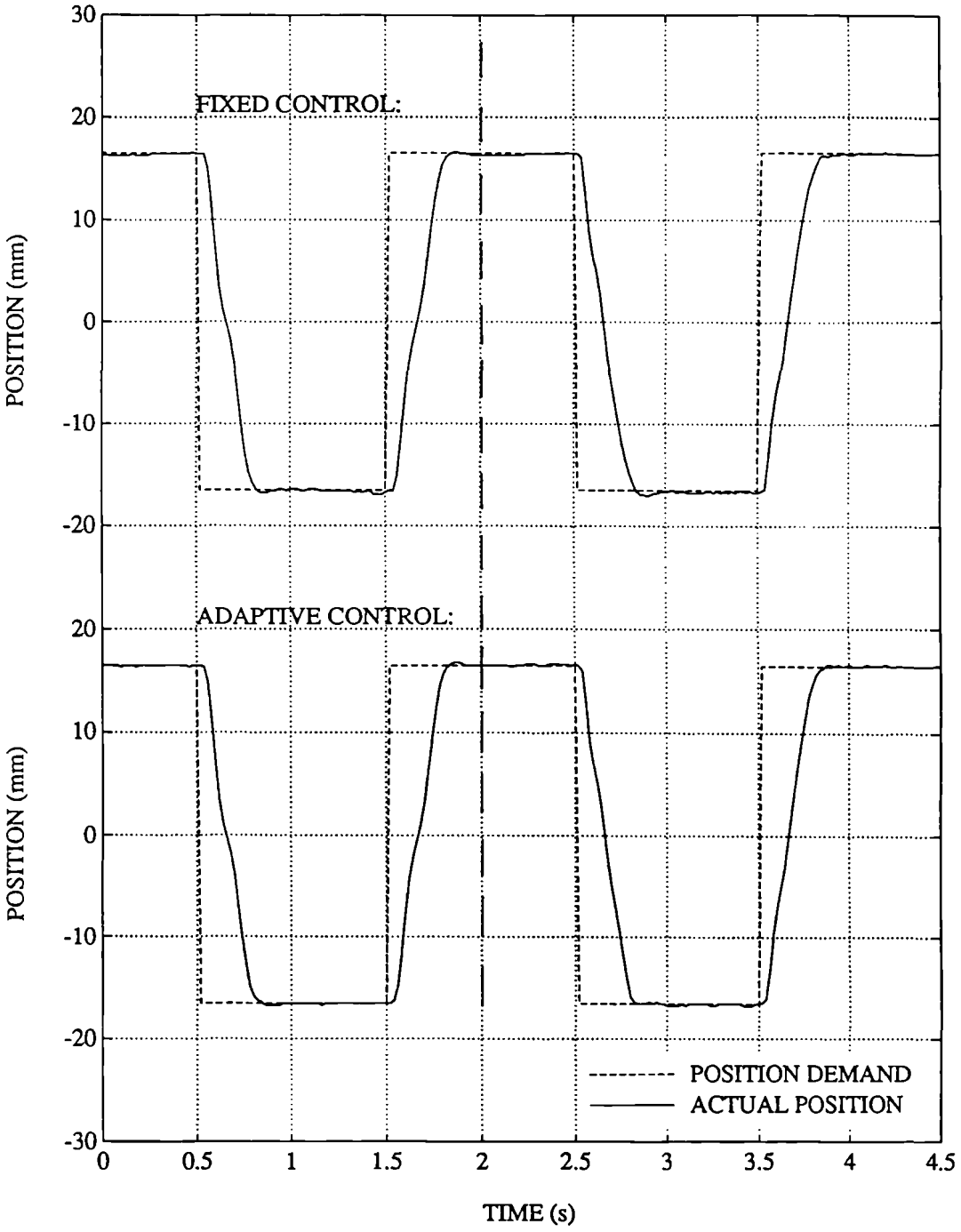

Figure 8.27 Response to switching out dead oil volumes after 2s

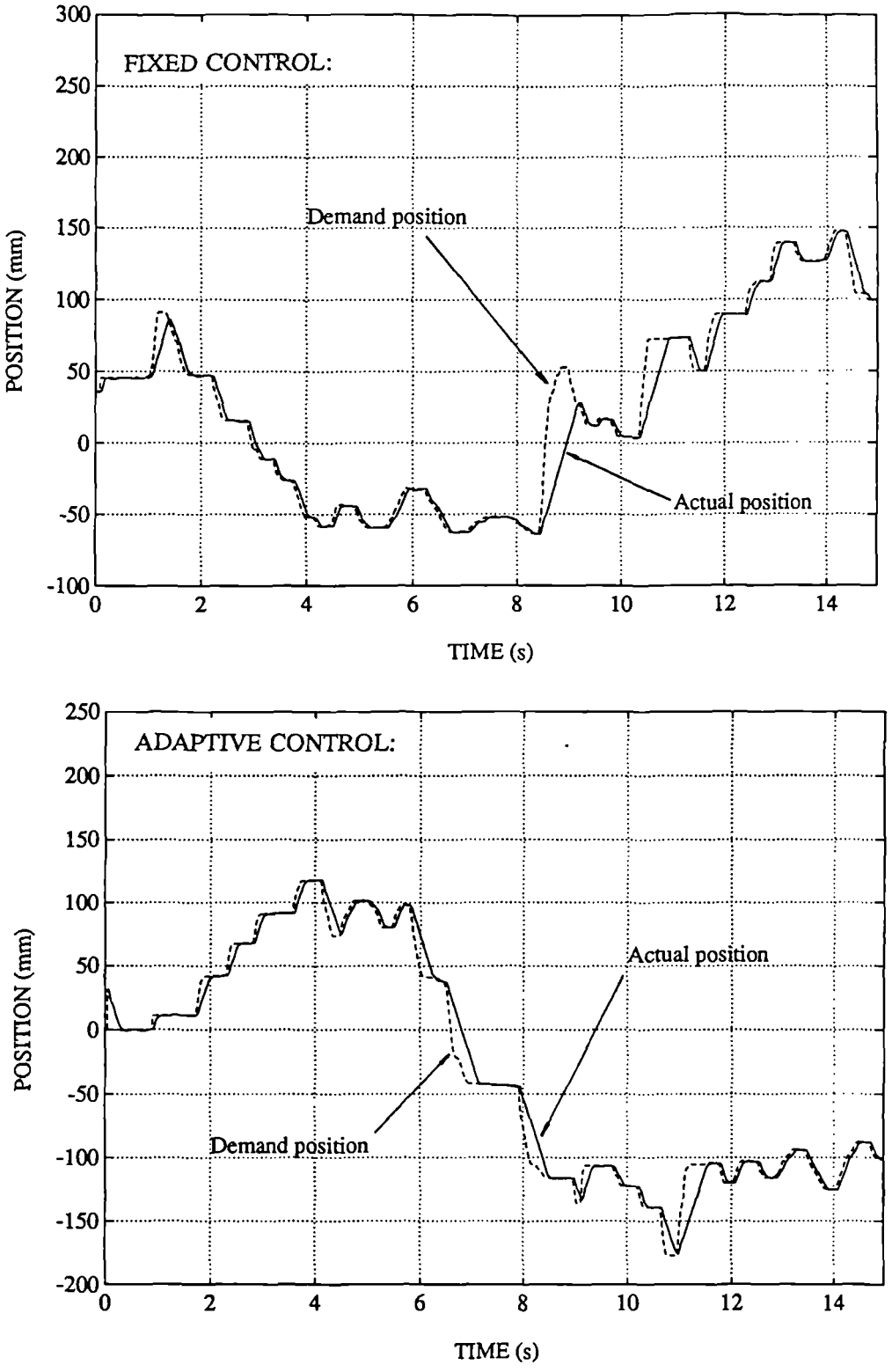

Figure 8.28 Response with an irregular, large amplitude, demand signal

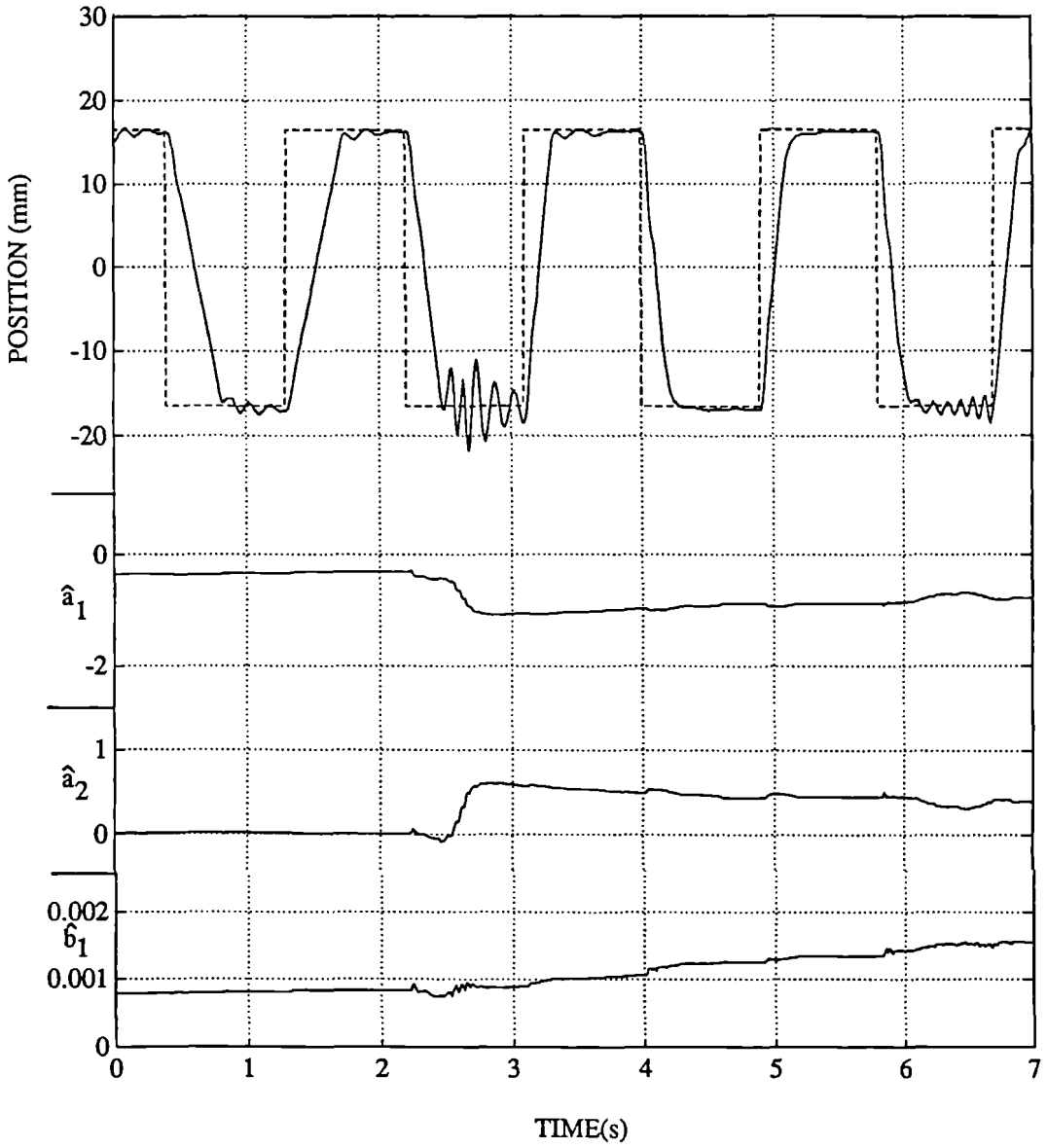

Figure 8.29 No estimation filter: response with increase in supply pressure from 40bar 160bar after 2s (no dead volumes)

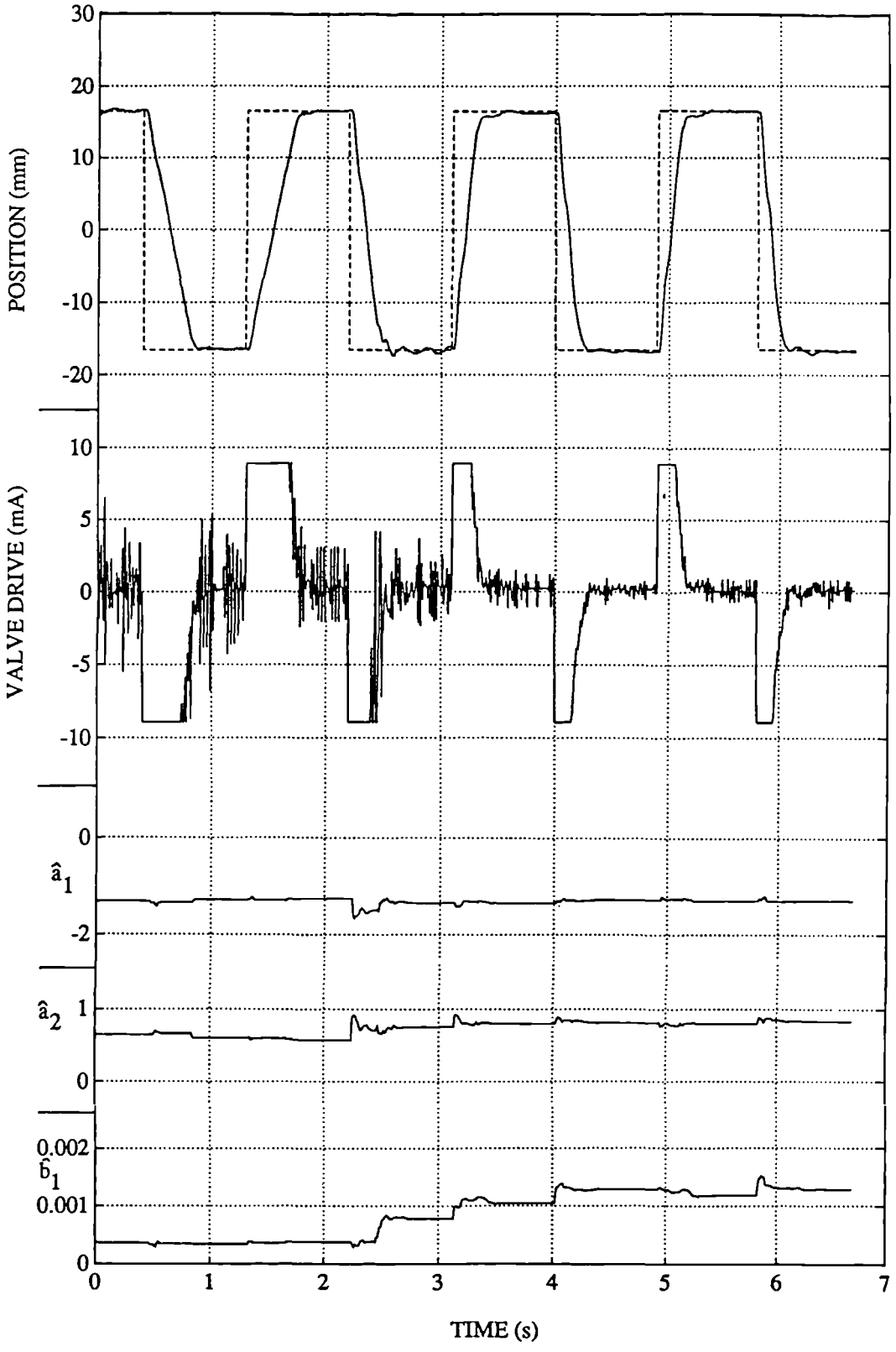

Figure 8.30 No demand filter: response with increase in supply pressure from 40bar 160bar after 2s (no dead volumes)

9. Multivariable control

9.1 Introduction

Many systems exist in which multiple hydraulic actuators act on a common load. These include fatigue test rigs — common in both aerospace and automotive industries — flight simulators, and high performance robots. In all these cases, the actuators are required to work in unison to enable accurate control over a number of forces or displacements.

Using fatigue test rigs as an example, each actuator is positioned on the test component to provide a force representative of that found in normal operation. Force control loops are closed around the individual actuators, commonly using manually-tuned analogue PID controllers. However this approach suffers from dynamic interaction between the channels due to movement of the load, leading to deviations from the demand force profile which can only be reduced by operating the system slowly. A test of many thousands of cycles can take several years, so speeding up operation would provide significant benefits.

The application of the digital modelling and control techniques described in previous chapters to individual channels provides the performance improvements already demonstrated. However extending the techniques to incorporate all channels in one multivariable controller will provide a means of reducing interaction as well. Thus a multivariable pole-placement controller has been developed, using a polynomial matrix fraction description for the plant model. System identification techniques which can estimate such a model from experimental data are also presented.

A multivariable controller has been applied previously to a 2-channel electro-hydraulic force control system by Pannala *et al* (1989). A proportional controller was used, and the controller coefficients were chosen to reduce interaction with the aid of an off-line manual-tuning technique. A sophisticated multivariable controller for speed control of rotary electro-hydraulic drives has been proposed by Schwarz and Guo (1990), giving a decoupling controller based on a non-linear model. However simulation results only have been presented thus far.

Multivariable system identification is discussed in Section 9.2. Filtered least squares is used for parameter estimation, and comparison of prediction errors indicates an appropriate model structure. Both techniques are straightforward extensions of the methods described in Chapters 4 and 5.

The extension of pole-placement control raises some new issues, associated with decoupling the channels and also with manipulating the diophantine equation into a solvable form. These are discussed in Section 9.3. A new method is devised, and this is validated using simulation in Section 9.4.

In Section 9.5, the multivariable identification and control methods are applied to a 2-channel electro-hydraulic servosystem. This comprises one position and one force control channel, and exhibits significant cross-channel interaction.

9.2 Multivariable system identification

The following multivariable input-output equation is used to represent the plant:

$$\boldsymbol{A}(z^{-1})\boldsymbol{y}_t = \boldsymbol{B}(z^{-1})\boldsymbol{u}_t + \boldsymbol{e}_t \tag{9.1}$$

For p channels, the output, input and coloured noise vectors are given by (respectively):

$$y_t = \begin{bmatrix} y_{1,t} \\ \vdots \\ y_{p,t} \end{bmatrix} \qquad u_t = \begin{bmatrix} u_{1,t} \\ \vdots \\ u_{p,t} \end{bmatrix} \qquad e_t = \begin{bmatrix} e_{1,t} \\ \vdots \\ e_{p,t} \end{bmatrix} \tag{9.2}$$

$A(z^{-1})$ and $B(z^{-1})$ are polynomial matrices. Each can be considered to be a matrix with elements which are polynomials, or a polynomial with coefficients which are matrices, as shown below:

$$\left.\begin{aligned} A(z^{-1}) &= \begin{bmatrix} 1 + a_{11,1}z^{-1} + \ldots + a_{11,n}z^{-n} & \cdots & a_{1p,1}z^{-1} + \ldots + a_{1p,n}z^{-n} \\ \vdots & & \vdots \\ a_{p1,1}z^{-1} + \ldots + a_{p1,n}z^{-n} & \cdots & 1 + a_{pp,1}z^{-1} + \ldots + a_{pp,n}z^{-n} \end{bmatrix} \\ &= I + A_1 z^{-1} + \ldots + A_n z^{-n} \end{aligned}\right\} \tag{9.3}$$

$$\left.\begin{aligned} B(z^{-1}) &= \begin{bmatrix} b_{11,1}z^{-1} + \ldots + b_{11,m}z^{-m} & \cdots & b_{1p,1}z^{-1} + \ldots + b_{1p,m}z^{-m} \\ \vdots & & \vdots \\ b_{p1,1}z^{-1} + \ldots + b_{p1,m}z^{-m} & \cdots & b_{pp,1}z^{-1} + \ldots + b_{pp,m}z^{-m} \end{bmatrix} \\ &= B_1 z^{-1} + B_2 z^{-2} + \ldots + B_m z^{-m} \end{aligned}\right\} \tag{9.4}$$

where I is the pxp identity matrix.

Filtered least squares is used for parameter estimation (see Section 4.2.7). Thus where $D(z^{-1})$ is a scalar filter transfer function, the filtered output and input signals are given by:

$$\left.\begin{aligned} y'_t &= D(z^{-1})y_t \\ u'_t &= D(z^{-1})u_t \end{aligned}\right\} \tag{9.5}$$

A regression equation can be formed for each channel. So for channel i ($1 \le i \le p$):

$$y'_{i,t} = \psi_t^T \theta_i + e_{i,t} \tag{9.6}$$

where the regressor and parameter vectors are:

$$\left.\begin{aligned} \psi_t^T &= [y'_{1,t-1}\ldots y'_{1,t-n} \ \ldots \ y'_{p,t-1}\ldots y'_{p,t-n},\ u'_{1,t-1}\ldots u'_{1,t-m} \ \ldots \ u'_{p,t-1}\ldots u'_{p,t-m}] \\ \theta_i &= [-a_{i1,1}\ldots -a_{i1,n} \ \ldots \ -a_{ip,1}\ldots -a_{ip,n},\ b_{i1,1}\ldots b_{i1,m} \ \ldots \ b_{ip,1}\ldots b_{ip,m}]^T \end{aligned}\right\} \tag{9.7}$$

Thus each channel's output signal is modelled in terms of previous samples of all input and output signals. The model parameter vector for any channel output can be estimated by using least squares in the normal way, either batch least squares (equation (4.6)) or recursive least squares (equation (4.7)). Note that the regressor vector is the same, no matter which parameter vector is being estimated. This fact can be used to give considerable computational savings when estimating the entire model, as the common part of the calculation, i.e. the part involving the regressor vector alone, need be performed only once. Note that using a more sophisticated model structure, such as allowing different degrees for the individual polynomials in $A(z^{-1})$ and $B(z^{-1})$, or fixing known factors in the polynomials, would give different regressor vectors in general.

The ability to write the model in terms of conventional regression equations allows any of the structure identification techniques of Chapter 5 to be applied in the normal way. The RMS prediction error technique (see Section 5.2.2) is used for the 2 channel electro-hydraulic servosystem later in this Chapter.

9.3 Multivariable pole-placement

9.3.1 Options

Consider the controller structure of Figure 9.1. This is of the same form as the SISO pole-placement controller, but now polynomial matrices are used instead of scalar controller polynomials. System identification provides a left matrix fraction description for the plant

model, i.e. $A^{-1}(z^{-1})B(z^{-1})$, and thus from the block diagram:

$$\begin{aligned} y_t &= A^{-1}(z^{-1})B(z^{-1})F^{-1}(z^{-1})[H(z^{-1})r_t - G(z^{-1})y_t] \\ [A(z^{-1}) + B(z^{-1})F^{-1}(z^{-1})G(z^{-1})]y_t &= B(z^{-1})F^{-1}(z^{-1})H(z^{-1})r_t \end{aligned} \tag{9.8}$$

In the SISO case, multiplying equation (9.8) through by $F(z^{-1})$ would be the next step in deriving the diophantine equation. However *matrix* multiplication is not commutative, so this cannot be done. Several ways to overcome the problem have been suggested in the past. Wahab and Wellstead (1986) used a right matrix fraction description for the plant. This can be derived from the left matrix fraction description using the pseudo-commutivity transform (Wolowich, 1974):

$$\tilde{B}(z^{-1})\tilde{A}^{-1}(z^{-1}) = A^{-1}(z^{-1})B(z^{-1}) \tag{9.9}$$

Thus now the block diagram gives:

$$\begin{aligned} y_t &= \tilde{B}(z^{-1})\tilde{A}^{-1}(z^{-1})F^{-1}(z^{-1})[H(z^{-1})r_t - G(z^{-1})y_t] \\ [F(z^{-1})\tilde{A}(z^{-1}) + G(z^{-1})\tilde{B}(z^{-1})]\tilde{B}^{-1}(z^{-1})y_t &= H(z^{-1})r_t \\ y_t &= \tilde{B}(z^{-1})A_m^{-1}(z^{-1})r_t \end{aligned} \tag{9.10}$$

where

$$F(z^{-1})\tilde{A}(z^{-1}) + G(z^{-1})\tilde{B}(z^{-1}) = H(z^{-1})A_m(z^{-1}) \tag{9.11}$$

An alternative approach is to rearrange the controller structure, as shown in Figure 9.2, a method used by Bayoumi and Mo (1988), and Porter and Boddy (1989). This gives the following closed-loop transfer function:

$$\begin{aligned} y_t &= A^{-1}(z^{-1})B(z^{-1})[H(z^{-1})r_t - G(z^{-1})F^{-1}(z^{-1})y_t] \\ [A(z^{-1})F(z^{-1}) + B(z^{-1})G(z^{-1})]F^{-1}(z^{-1})y_t &= B(z^{-1})H(z^{-1})r_t \\ y_t &= F(z^{-1})A_m^{-1}(z^{-1})H^{-1}(z^{-1})B(z^{-1})H(z^{-1})r_t \end{aligned} \tag{9.12}$$

where

$$A(z^{-1})F(z^{-1}) + B(z^{-1})G(z^{-1}) = H(z^{-1})A_m(z^{-1}) \tag{9.13}$$

Although the second method avoids the computational expense of the pseudo-commutivity transform, the demand filter no longer cancels out of the closed-loop response, and more zeros are present in the closed-loop.

Neither method decouples the channels in general. Even if the denominator matrix $A_m(z^{-1})$ is specified as diagonal, coupling will still exist due to the non-diagonal numerator. Bayoumi and Mo (1988) suggested a method of decoupling the channels using the demand filter. The method modifies equation (9.12) in the following way:

$$\left.\begin{array}{lll} \text{Use} & A(z^{-1})F(z^{-1}) + B(z^{-1})G(z^{-1}) = T(z^{-1})I\,, & \text{where } T(z^{-1}) \text{ is scalar,} \\ \text{and} & H(z^{-1}) = \text{adj}[B(z^{-1})]\,\text{adj}[F(z^{-1})] & \\ \text{thus} & y_t = \dfrac{|B(z^{-1})|\,|F(z^{-1})|}{T(z^{-1})} r_t & \end{array}\right\} \tag{9.14}$$

Notice that the determinants of the numerator matrices are not cancelled, so that non-minimum phase plant can be controlled without creating unstable hidden modes. A similar technique could be used to decouple the channels with the first approach (equation (9.10)). Either way, however, each of the decoupled channels is obliged to have same set of closed-loop poles.

Another way of decoupling the channels has been suggested by Kineart *et al* (1987). This involves a form of open-loop decoupling for the plant initially, and then a SISO pole-placement controller is used for each channel. However the method is computationally intensive, again restricts each channel to having the same closed-loop pole set, and lacks robustness (Kineart and Hanus, 1988).

9.3.2 Chosen method

A method has been devised which has some advantages over each of the approaches described in the previous Section. It involves using an extra block in the controller forward path, which

enables both decoupling and the derivation of the diophantine equation. The block diagram is shown in Figure 9.3, from which:

$$y_t = A^{-1}(z^{-1})B(z^{-1})E(z^{-1})F^{-1}(z^{-1})[H(z^{-1})r_t - G(z^{-1})y_t] + e_t'$$

$$[A(z^{-1}) + B(z^{-1})E(z^{-1})F^{-1}(z^{-1})G(z^{-1})]y_t = B(z^{-1})E(z^{-1})F^{-1}(z^{-1})H(z^{-1})r_t + A(z^{-1})e_t' \quad (9.15)$$

$E(z^{-1})$ is calculated thus:

$$E(z^{-1}) = \text{adj}[B(z^{-1})]z^d \quad (9.16)$$

where z^d is the maximum forward shift which does not make $E(z^{-1})$ non-causal. Hence:

$$\begin{aligned} B(z^{-1})E(z^{-1}) &= |B(z^{-1})|z^d \\ &= B_d(z^{-1}) \qquad \text{(a scalar polynomial)} \end{aligned} \quad (9.17)$$

From equation (9.15):

$$\begin{aligned} [A(z^{-1}) + B_d(z^{-1})F^{-1}(z^{-1})G(z^{-1})]y_t &= B_d(z^{-1})F^{-1}(z^{-1})H(z^{-1})r_t + A(z^{-1})e_t' \\ [F(z^{-1})A(z^{-1}) + G(z^{-1})B_d(z^{-1})]y_t &= B_d(z^{-1})H(z^{-1})r_t + F(z^{-1})A(z^{-1})e_t' \\ y_t &= A_m^{-1}(z^{-1})B_d(z^{-1})r_t + A_m^{-1}(z^{-1})H^{-1}(z^{-1})F(z^{-1})A(z^{-1})e_t' \end{aligned} \quad (9.18)$$

where

$$F(z^{-1})A(z^{-1}) + G(z^{-1})B_d(z^{-1}) = H(z^{-1})A_m(z^{-1}) \quad (9.19)$$

The method has the following advantageous features:

- the channels will be decoupled if $A_m(z^{-1})$ is specified as diagonal,
- different poles can be assigned to the decoupled channels,
- the demand filter can be used to attenuate noise without affecting the closed-loop response to the demand signal (in the same way as the SISO case),
- open-loop unstable and non-minimum phase plant can be controlled.

All the zeros of the plant are associated with each decoupled channel, which could give high

order closed-loop transfer functions, especially if the number of channels is large (although not as high order as the method of Bayoumi and Mo, 1988). If this were a problem, the controller could cancel some or all of the minimum-phase zeros using an additional forward path term, thus reducing the order.

Equation (9.19) can be solved analogously to the SISO diophantine equation, by multiplying out the matrix polynomials and equating equal powers of z. Defining:

$$V(z^{-1}) = H(z^{-1})A_m(z^{-1}) \tag{9.20}$$

Then the following matrix equation can be formed, where each matrix element is actually a pxp sub-matrix:

$$[F_0,\ F_1,\ldots,\ G_0,\ G_1,\ldots] \begin{bmatrix} I & A_1 & A_2 & \ldots \\ 0 & I & A_1 & \ldots \\ \vdots & \vdots & \vdots & \\ 0 & b_{d1}I & b_{d2}I & \ldots \\ 0 & 0 & b_{d1}I & \ldots \\ \vdots & \vdots & \vdots & \end{bmatrix} = [V_0,\ V_1,\ V_2,\ldots]$$

which can be represented by:

$$\begin{aligned} C\,S &= X \\ S^T\,C^T &= X^T \\ C^T &= (S^T)^{-1}\,X^T \end{aligned} \tag{9.21}$$

This is an appropriate form for solution.

9.3.3 Integral version

An integral version of this controller has been implemented, the integral action being incorporated in a similar way to that of the SISO integral pole-placement controller of Section 7.2. From the block diagram of Figure 9.4, which includes a disturbance signal w_t:

$$y_t = A_m^{-1}(z^{-1})B_d(z^{-1})r_t + A_m^{-1}(z^{-1})H^{-1}(z^{-1})P(z^{-1})B(z^{-1})w_t \quad (9.22)$$

where

$$P(z^{-1})A(z^{-1}) + Q(z^{-1})B_d(z^{-1}) = H(z^{-1})A_m(z^{-1}) \quad (9.23)$$

For integral control:

$$P(z^{-1}) = P_1(z^{-1})(1 - z^{-1}) \quad (9.24)$$

Thus giving the required zero steady-state error:

$$A_m^{-1}(1)H^{-1}(1)P(1)B(1) = 0 \quad (9.25)$$

The demand filter can be used to control the frequency range in which integral action is dominant.

$P_1(z^{-1})$ and $Q(z^{-1})$ can be calculated by modifying the diophantine equation similarly to the SISO case. However a more efficient method is to calculate them from the non-integral controller matrices $F(z^{-1})$ and $G(z^{-1})$. Equations (9.19) and (9.23) are the same except a minimal degree solution is required in the former, whilst a solution which satisfies the additional constraint of integral action is required in the latter. By comparing the two equations, the following relationships are apparent:

$$\left.\begin{aligned} P(z^{-1}) &= F(z^{-1}) - DB_d(z^{-1}) \\ Q(z^{-1}) &= G(z^{-1}) + DA(z^{-1}) \end{aligned}\right\} \quad (9.26)$$

where D is a matrix designed to give $P(1) = 0$, i.e.:

$$D = \frac{F(1)}{B_d(1)} \quad (9.27)$$

A similar technique could be used for the SISO case, but note that the extra degree of $H(z^{-1})A_m(z^{-1})$ cannot be utilized.

9.4 Simulation results

The method has been validated using a simple simulation, without noise or modelling error. The following unstable, non-minimum phase system is used:

$$A(z^{-1}) = \begin{bmatrix} 1 - 0.9z^{-1} & 0.5z^{-1} \\ 0.5z^{-1} & 1 - 0.2z^{-1} \end{bmatrix} \qquad B(z^{-1}) = \begin{bmatrix} 0.2z^{-1} + z^{-2} & z^{-1} \\ 0.25z^{-1} & 0.2z^{-1} + z^{-2} \end{bmatrix} \quad (9.28)$$

The poles of the system, i.e. the roots of $|A(z^{-1})|$, are at z = -0.060 and 1.16, and the zeros of the system, i.e. the roots of $|B(z^{-1})|$, are at z = 3.33 and -1.43. The response of the system with a proportional controller of gain $0.5I$ is shown in Figure 9.5. Using separate SISO pole-placement controllers for each loop, neglecting the off-diagonal terms in the above polynomial matrices, gives the response in Figure 9.6. A closed-loop pole at z = 0.5 is specified for each loop. The response of the multivariable pole-placement controller of the previous Section is shown in Figure 9.7, using $A_m(z^{-1}) = (1 - 0.5z^{-1})I$. The channels are now decoupled, but there is some reverse response associated with the zeros. Figure 9.8 shows the equivalent response for the integral form of the controller. A unity demand filter is used in all cases.

9.5 Application to electro-hydraulic servosystem

9.5.1 System description

The multivariable pole-placement controller has been applied to a 2-channel electro-hydraulic servosystem. The two actuators bear on a common load, which in this case is just a mass, as shown in Figure 9.9. The mass is mounted on a trolley which can move horizontally. Its position is measured by an LVDT, and the force applied by one of the actuators is also available, although only indirectly by differential pressure measurement. This loading actuator is double-ended with equal piston areas, but the other (nominally positioning) actuator is single-ended. A directional gain change is used for the single-ended actuator as described for

the SISO positioning system in Section 3.6. A small bleed orifice is connected across the loading actuator. Table 9.1 contains some specifications, and Figure 9.10 is a photograph of the rig.

The mass is quite low, and the actuators quite short, so that the natural frequency of the positioning channel (channel 1) is high, at about 50Hz. Response of the force channel (channel 2) is faster still, necessitating rapid sampling; a sample interval of 2.3ms was used, which was the fastest achievable with the computer system available (described in Section 2.3). The system is not as oscillatory as before, but considerably more friction is present, as are the other non-linearities usual for such systems (see Section 2.2.2). The friction together with valve offsets rendered integral action essential.

Note that to obtain the results presented below, both control signals were scaled up by a factor of 100 before being output by the computer. This additional gain was treated as part of the plant, thus increasing the gain of the plant models, and gave numerical improvements in the controller design calculations.

9.5.2 Results

Figure 9.11 shows the response of the system with the channels controlled by a proportional controller with the following gain:

$$\begin{bmatrix} 0.1 & 0.0 \\ 0.0 & 0.01 \end{bmatrix} \tag{9.29}$$

Channel 1 is the position channel, and channel 2 the force channel. The dynamic response of both channels is quite good with this controller, but there is considerable interaction between the two, particularly affecting the force channel.

To identify a model of the plant, data were collected whilst operating the plant with this proportional closed-loop controller, using a PRBS demand signal. A portion of the data is shown in Figure 9.12. The following estimation filter was chosen:

$$\frac{(1 - z^{-1})(1 + z^{-1})(1 + z^{-1})}{(1 - 0.8z^{-1})} \tag{9.30}$$

Note that the filter differences the data in order to eliminate steady-state offsets. Using 600 samples of data, filtered batch least squares was used to estimate models for each channel and a variety of model orders. To help choose the best order, the RMS prediction errors are plotted in Figure 9.13. The plots indicate that the third order model is best for each channel, and this model is shown below in factored form:

$$\begin{bmatrix} (1 - 1.01z^{-1})(1 - 1.04z^{-1} + 0.473z^{-2}) & -1.1\text{x}10^{-5}(1 - 1.55z^{-1})(1 - 27.5z^{-1}) \\ -3.24(1 - 1.00z^{-1})(1 - 0.182z^{-1}) & (1-0.814z^{-1})(1 - 0.650z^{-1} + 0.456z^{-2}) \end{bmatrix} y_t$$

$$= \begin{bmatrix} 0.0626(1 - 2.68z^{-1} + 10.0z^{-2}) & -0.0648(1 + 1.55z^{-1})(1 - 27.5z^{-1}) \\ 0.705(1 - 5.45z^{-1})(1 + 1.91z^{-1}) & 0.278(1 - 0.36z^{-1})(1 + 19.25z^{-1}) \end{bmatrix} u_t \tag{9.31}$$

The following closed-loop poles and demand filter are specified for the integral multivariable controller:

$$A_m(z^{-1}) = \begin{bmatrix} (1 - 0.75z^{-1})(1 - 0.75z^{-1})(1 - 0.75z^{-1}) & 0 \\ 0 & (1 - 0.35z^{-1})(1 - 0.35z^{-1})(1 - 0.35z^{-1}) \end{bmatrix} \tag{9.32}$$

$$H(z^{-1}) = \begin{bmatrix} (1 - 0.9z^{-1})(1 - 0.4z^{-1})(1 - 0.4z^{-1})(1 - 0.4z^{-1}) & 0 \\ 0 & (1 - 0.9z^{-1})(1 - 0.4z^{-1})(1 - 0.4z^{-1})(1 - 0.4z^{-1}) \end{bmatrix} \tag{9.33}$$

Note the use of demand filter zeros at $z = 0.9$ to restrict the speed of the integral action.

The resulting step responses are shown in Figure 9.14. The position response is very close to the desired until it approaches the steady-state, where some deviation occurs, possibly due to friction effects. The interaction from the force channel is now very small. The transient force response is also very close to the desired, including the initial reverse response associated with the system zeros. The interaction from the position channel is still large, but causes no more than 0.5kN error, as opposed to 3kN in Figure 9.11.

Figure 9.15 shows the non-integral version of the controller (for which the demand filter zeros at 0.9 are removed). As expected, significant steady-state error is in evidence. Figure 9.16

shows the response of the system when each channel is controlled with a separate (non-integral) pole-placement controller, designed from the same model as before by neglecting the off-diagonal elements. The significant interaction has now reappeared. Returning to the original integral multivariable controller, but removing the first two factors in each of the demand filter polynomials in equation (9.33), the response deteriorates to that of Figure 9.17. This illustrates that an appropriate choice of demand filter is important in multivariable controller just as it is for the SISO case.

With the full third order model, there are 24 model parameters. Also the degree of $B_d(z^{-1})$ is 5, giving the following controller polynomial matrix degrees:

$$\left.\begin{aligned} \deg E(z^{-1}) &= 2 \\ \deg F(z^{-1}) &= 5 \\ \deg G(z^{-1}) &= 3 \end{aligned}\right\} \tag{9.34}$$

In order to reduce the complexity of the controller, the degrees and dead-times in the plant model polynomials can be altered individually, and their effect on the prediction error determined. Using this approach, the following model was estimated:

$$\begin{bmatrix} (1 - 1.00z^{-1})(1 - 1.12z^{-1} + 0.468z^{-2}) & -5.4\text{x}10^{-3}(1 - 1.705z^{-1}) \\ -2.47(1 - 1.00z^{-1})(1 - 0.103z^{-1}) & (1 - 0.765z^{-1})(1 - 0.628z^{-1} + 0.465z^{-2}) \end{bmatrix} y_t \tag{9.35}$$

$$= \begin{bmatrix} 0.475z^{-3} & 0.0939z^{-2} \\ -9.54z^{-3} & -4.497z^{-2} \end{bmatrix} u_t$$

This gives prediction errors of 0.00802 and 0.0810 (for channel 1 and 2 outputs respectively), only slightly higher than the 0.00743 and 0.0775 for the full third order model. The controller degrees of equation (9.34) are now 1, 3, and 3 respectively, and the controller response (Figure 9.18) remains good. The demand filter polynomial matrix degree is also reduced by 2, and each polynomial in the leading diagonal now has a root at $z = 0.9$ and $z = 0.7$.

9.6 Conclusions

Some of the system identification and pole-placement control techniques of previous chapters have been extended to accommodate systems with more than one actuator.

A new technique for decoupling the channels in a multivariable pole-placement controller is proposed. It allows different pole sets to be specified for each decoupled channel, and can cope with non-minimum phase and unstable plant. The method is validated in simulation, and is applied to a highly non-linear 2-channel servosystem. Considerable reductions in interaction are achieved compared to controlling the channels individually. An integral version of the controller is required to give acceptably small steady-state errors, and this is implemented successfully, but an appropriate choice for the demand filter is essential.

Despite the increase in complexity over the SISO plant, filtered least squares is still quite successful, and the prediction error technique for structure selection is also effective. The latter can simply be used to find an overall plant order, or to assess each polynomial individually. The second case is more time consuming, but it can lead to a simpler controller. Also the reduction in the number of model parameters would allow faster adaptation in an adaptive controller. The original 24 parameters has been reduced to 15 in equation (9.35), and if the roots at $z = 1$ in the polynomials in the $\hat{A}(z^{-1})$ matrix (which recognise that the absolute position is not important) are fixed, there are 13 parameters to adapt. As noted in Section 9.2, in general the reduced model will need different regressor vectors to model each output, requiring the full estimator to be run for every channel. However this would naturally lend itself to implementation on a parallel computer of course granularity. A multivariable adaptive controller was not implemented as part of this study as the computer system in use did not possess sufficient computational speed.

A fixed-coefficient controller has been successfully demonstrated for a 2-channel system, and an adaptive controller may also be feasible for such a system, but significantly more channels would give excessively complex controllers. A simpler approach would be desirable for multivariable control of, for example, a 12-channel fatigue test rig.

Valves:	Saturation at 7mA
Load:	46kg mass
	90mm horizontal movement
Channel 1 (position):	Piston area 1140mm^2
	Annulus area 633mm^2
	LVDT position feedback
	Zero position at centre stroke
	Retract is positive position
Channel 2 (force):	Both areas 942mm^2
	Differential pressure force feedback
	Positive force is extend direction
Supply pressure:	70bar

Table 9.1 Two-channel electro-hydraulic servosystem specification

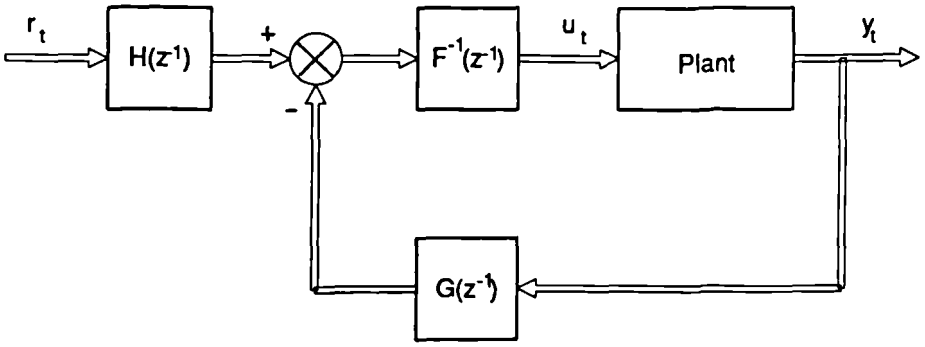

Figure 9.1 A multivariable pole-placement controller

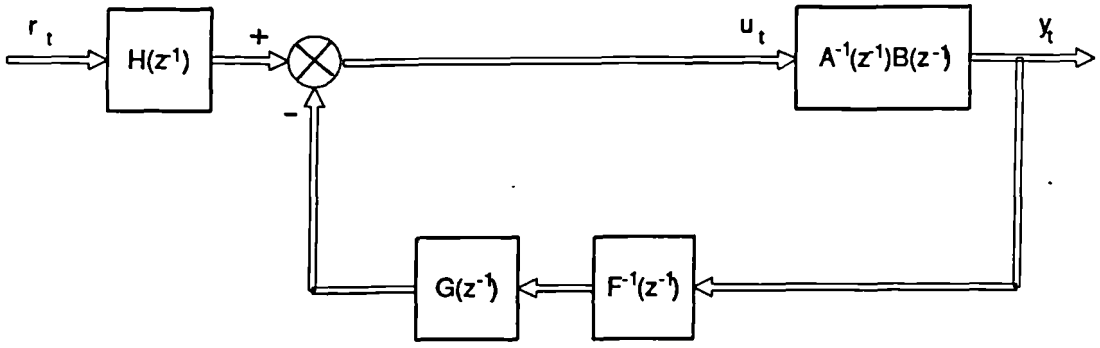

Figure 9.2 Rearranged multivariable pole-placement

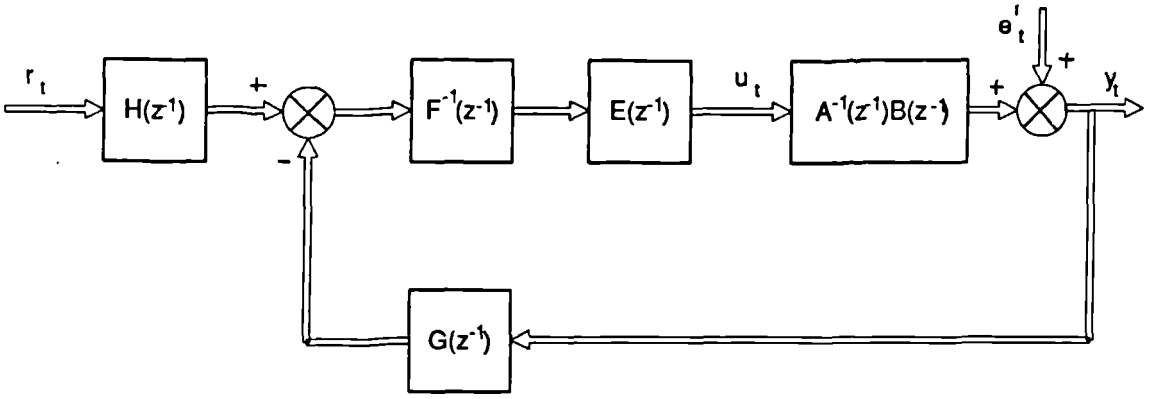

Figure 9.3 Proposed decoupling pole-placement controller

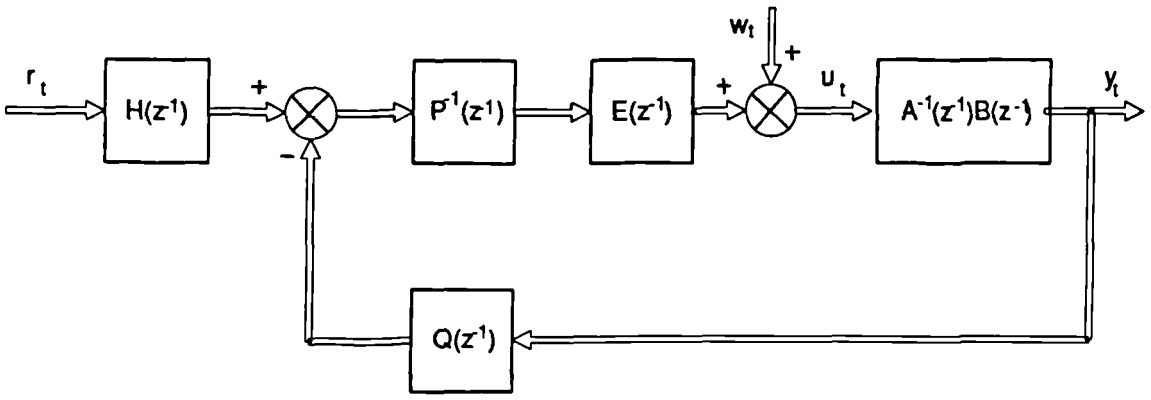

Figure 9.4 Integral decoupling pole-placement controller

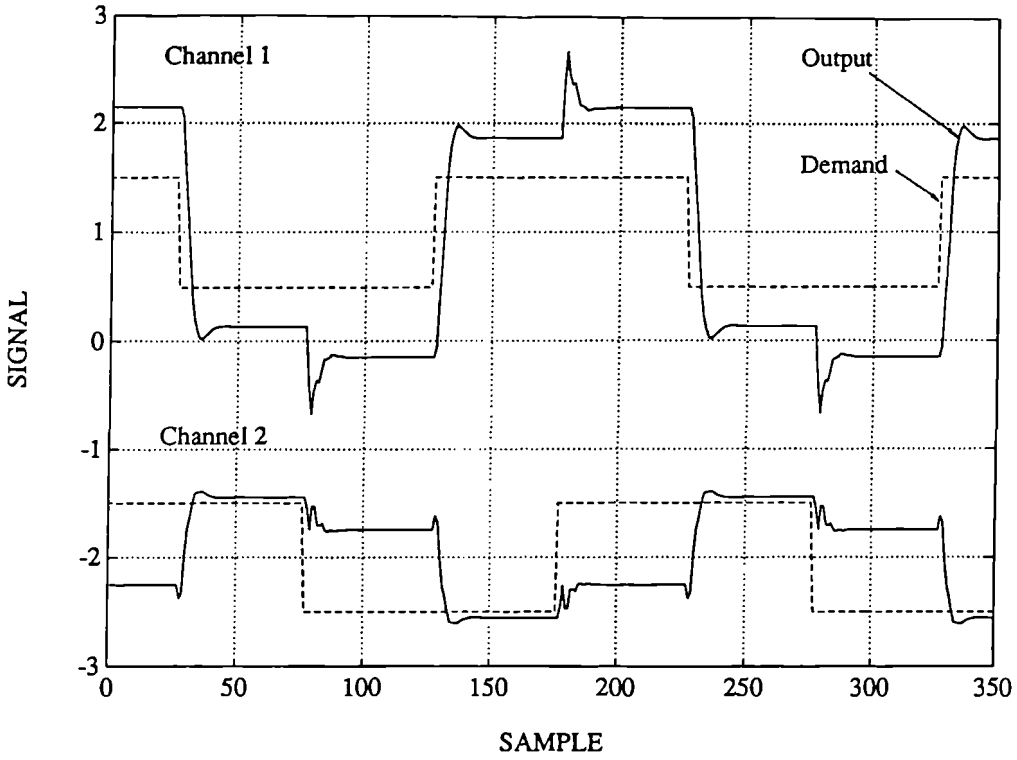

Figure 9.5 Control of simulated multivariable plant using SISO proportional controllers for each channel

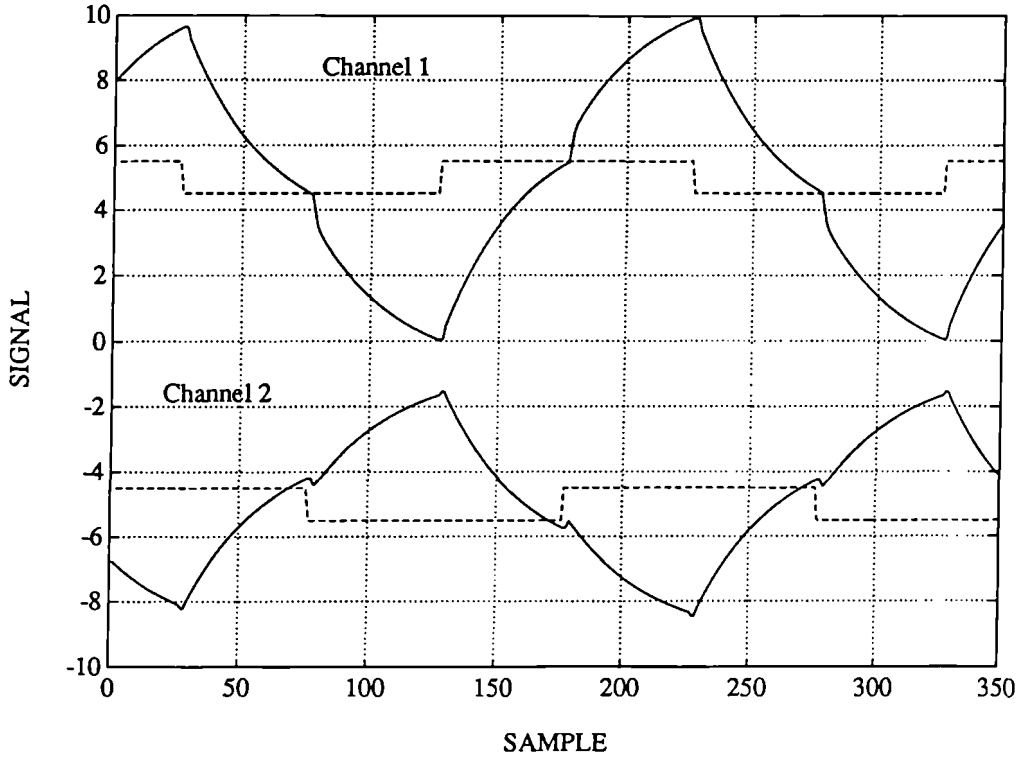

Figure 9.6 Control of simulated multivariable plant using SISO pole-placement controllers for each channel

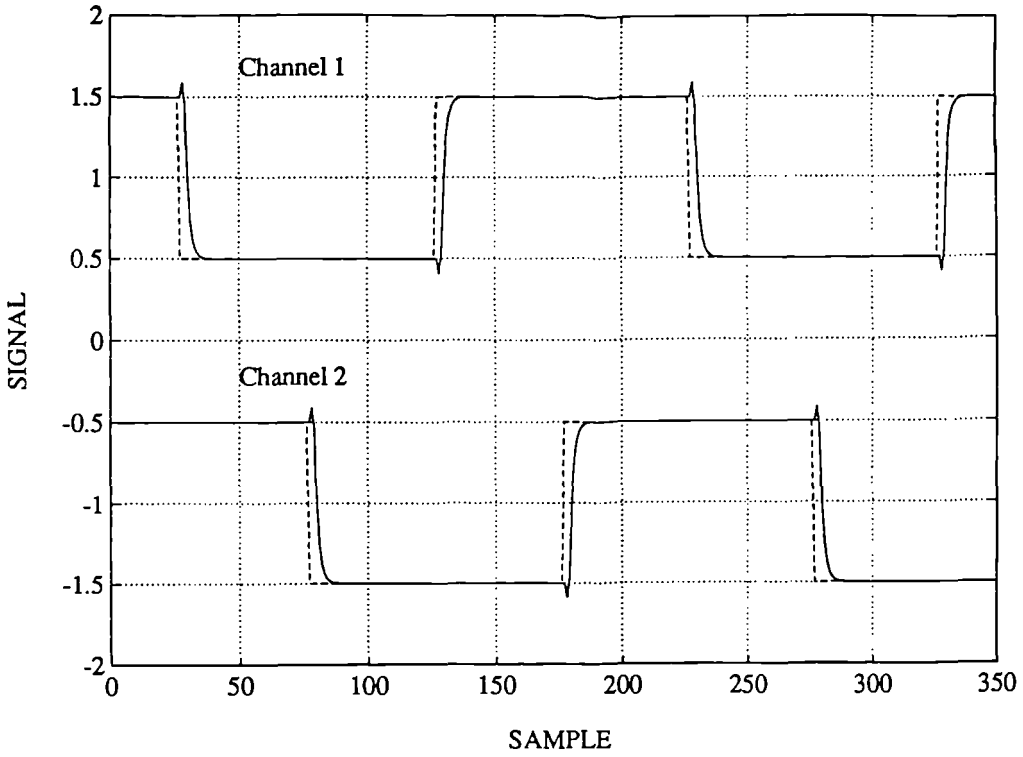

Figure 9.7 Multivariable pole-placement control (simulated plant)

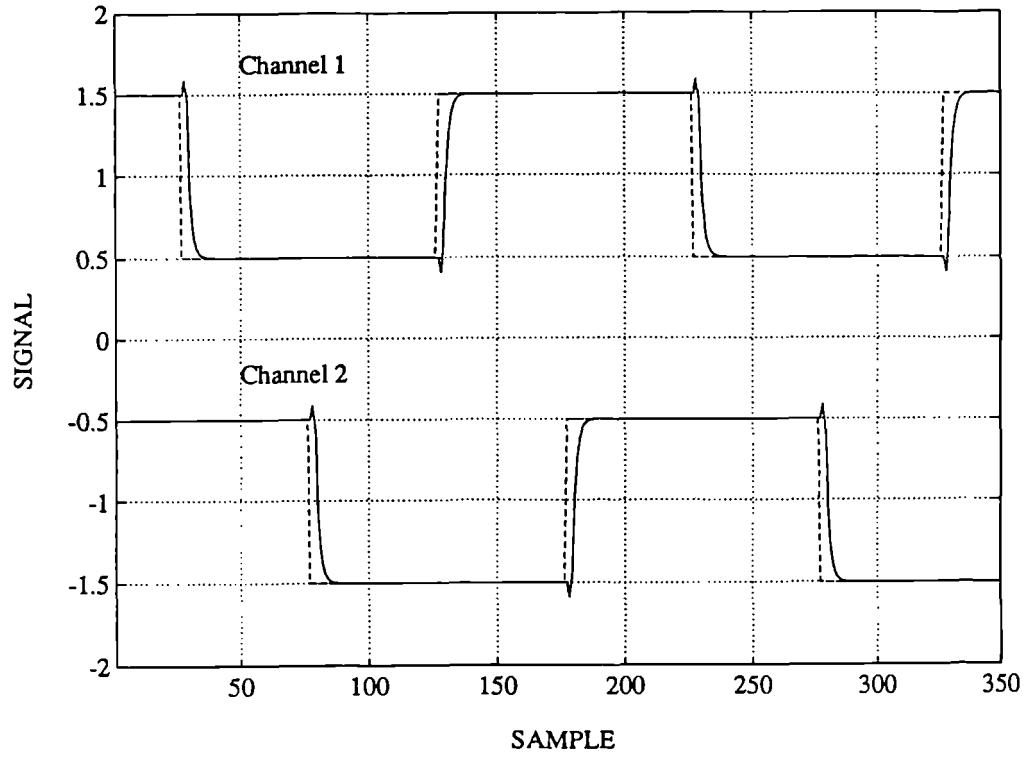

Figure 9.8 Integral multivariable pole-placement control (simulated plant)

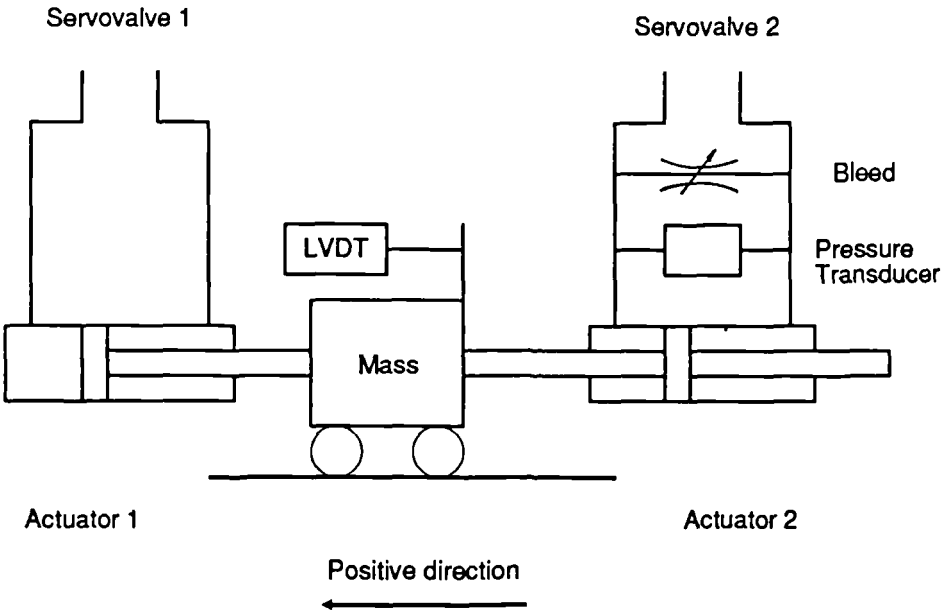

Figure 9.9 2-channel electro-hydraulic test rig schematic

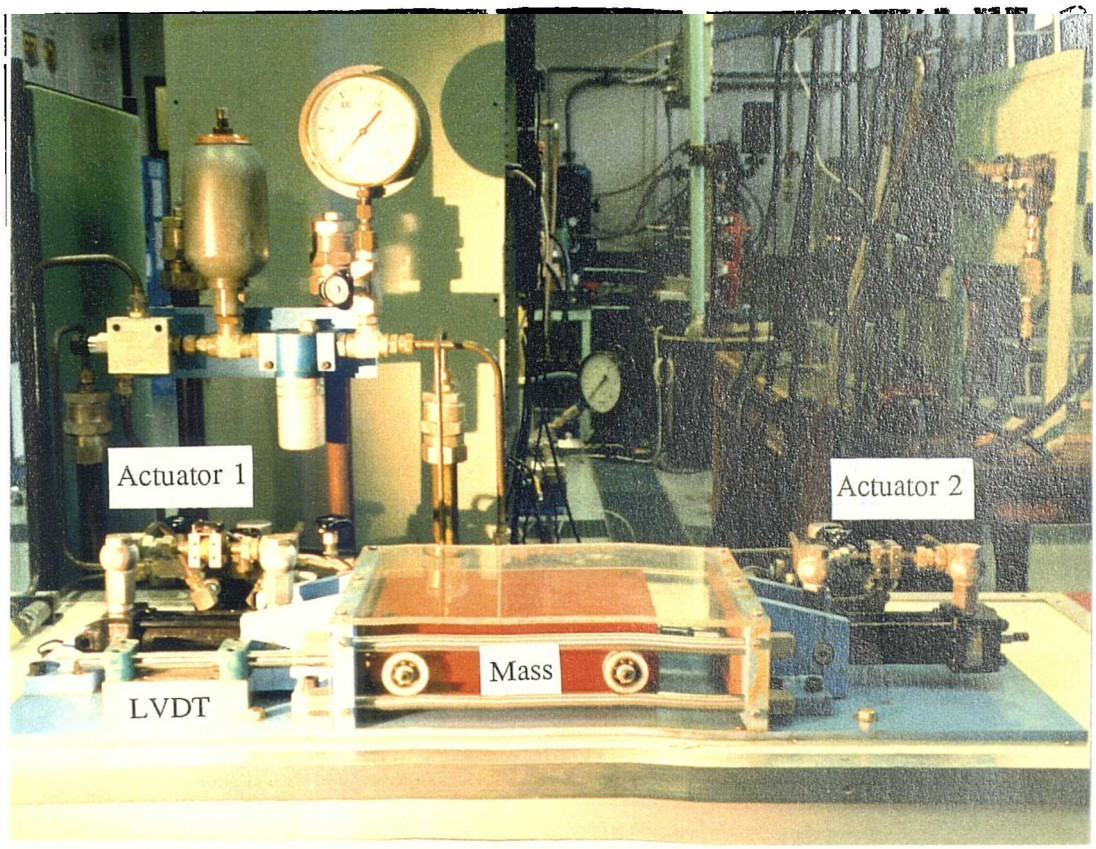

Figure 9.10 2-channel electro-hydraulic test rig

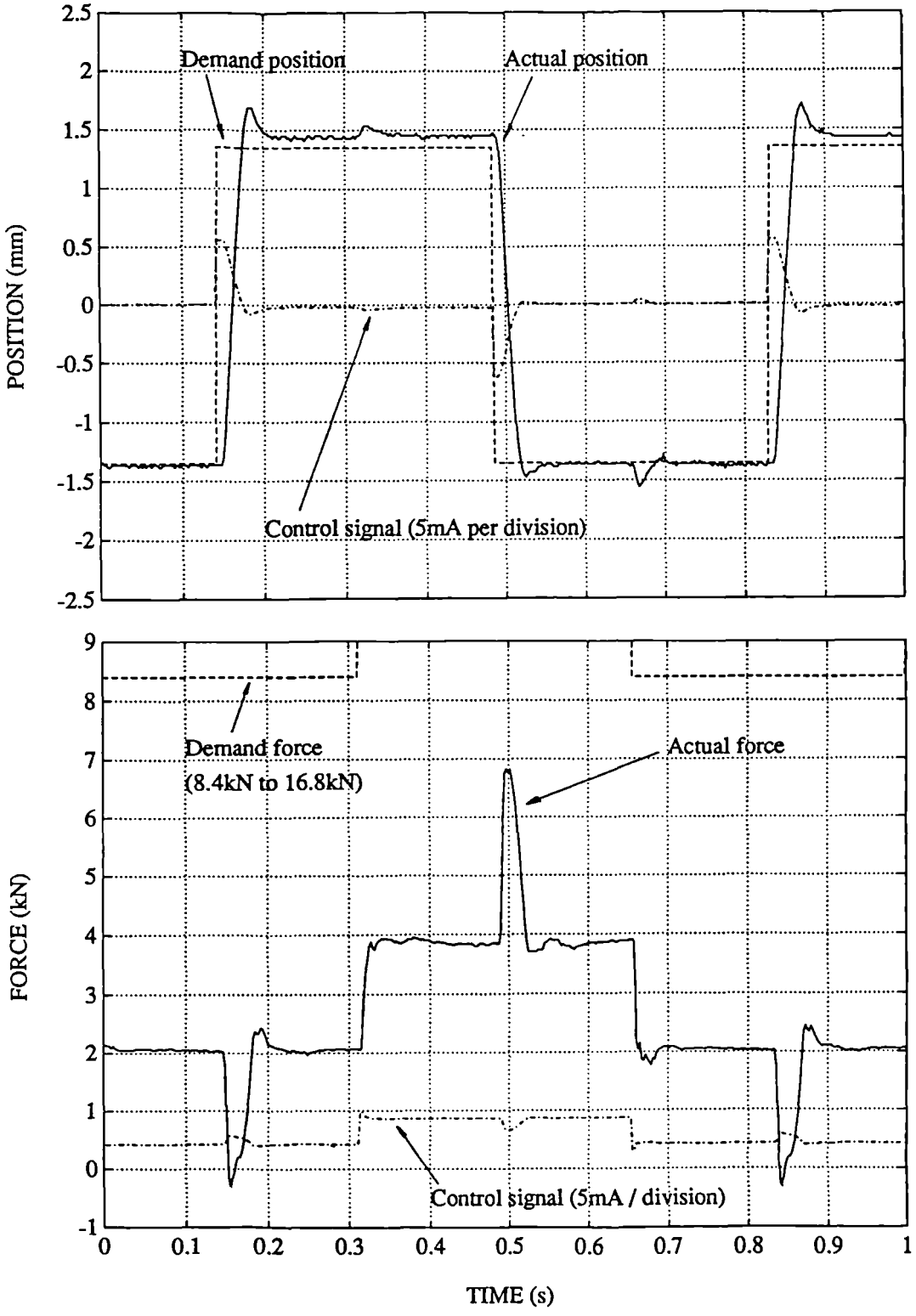

Figure 9.11 Control of test rig using SISO proportional controllers for each channel

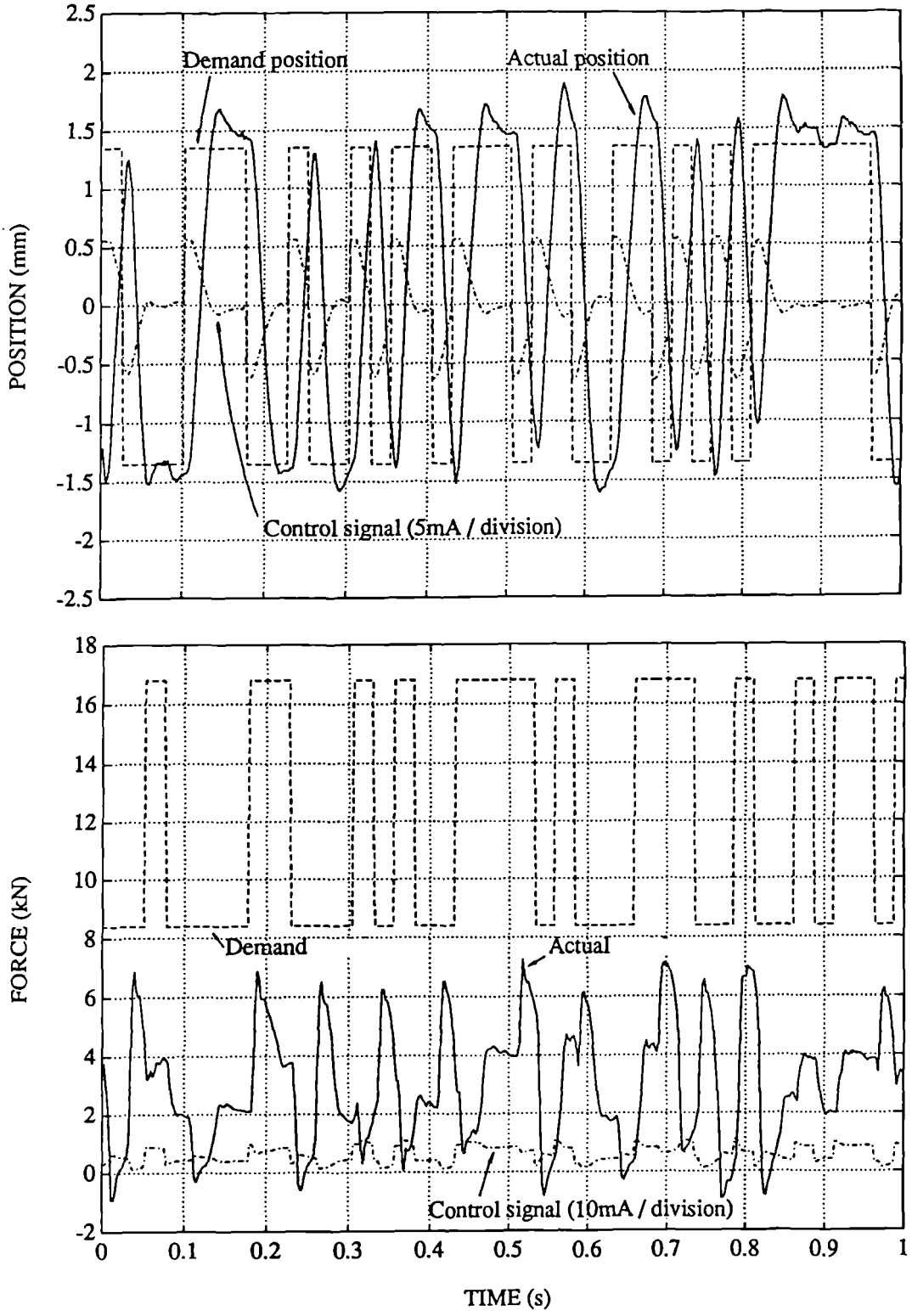

Figure 9.12 Input-output data for estimation

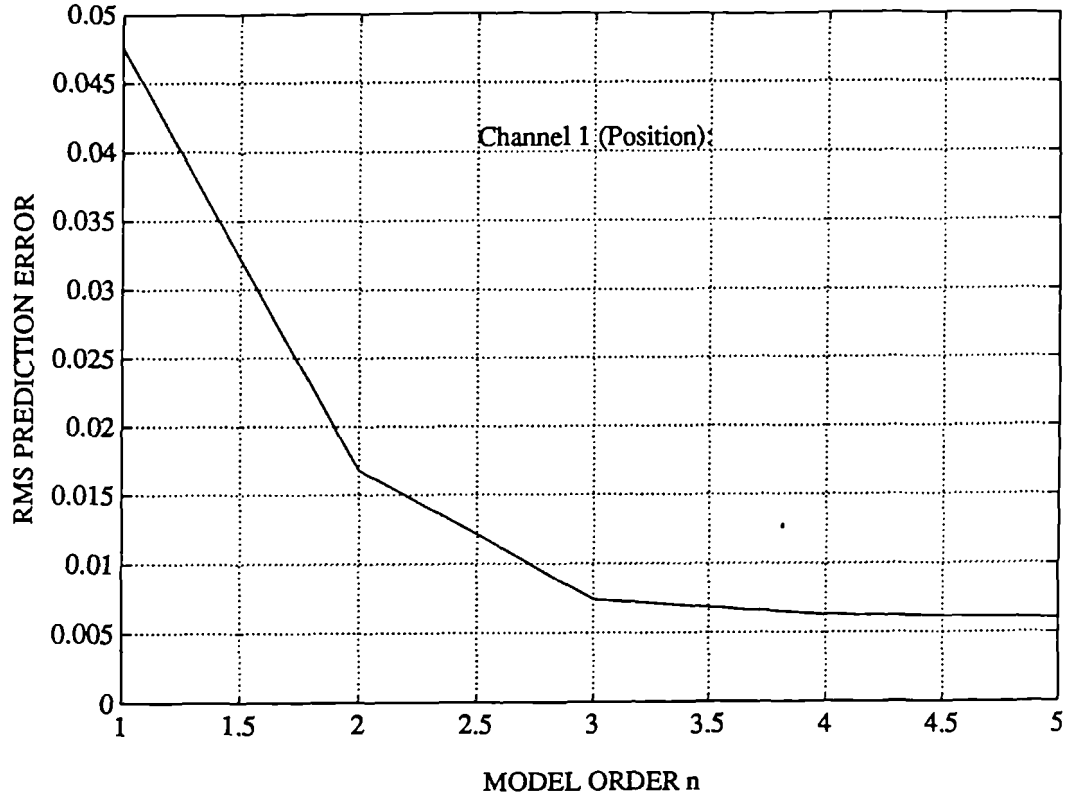

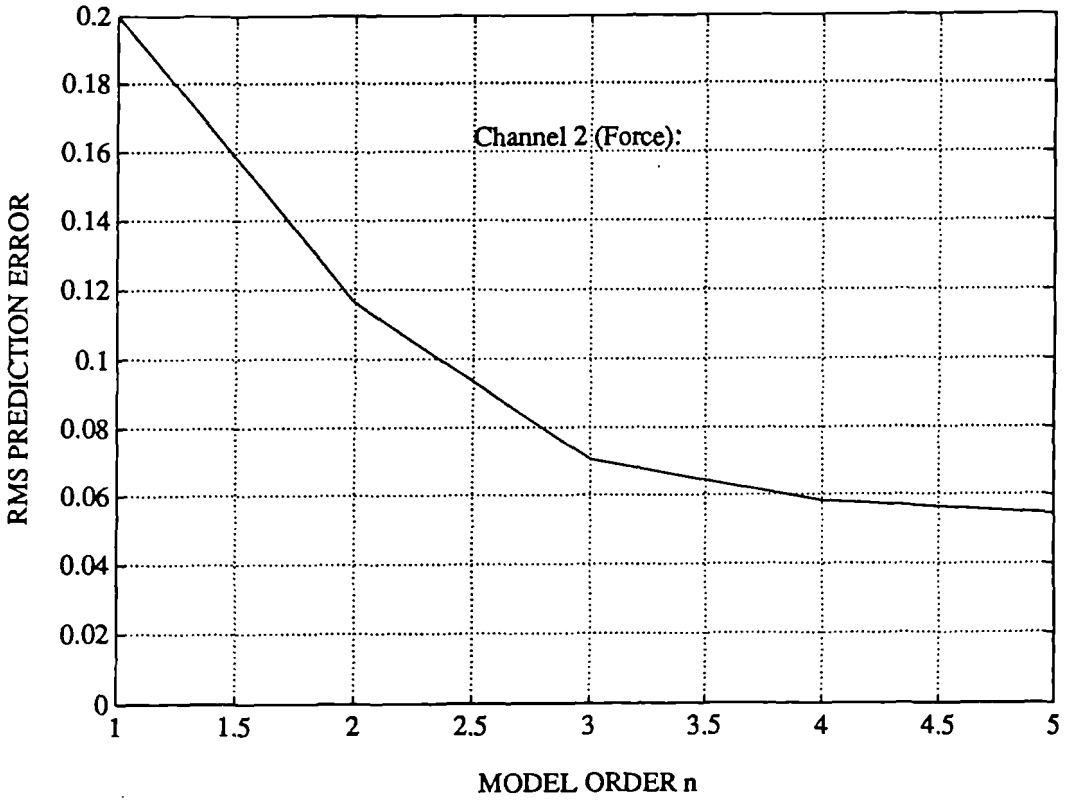

Figure 9.13 Model structure selection

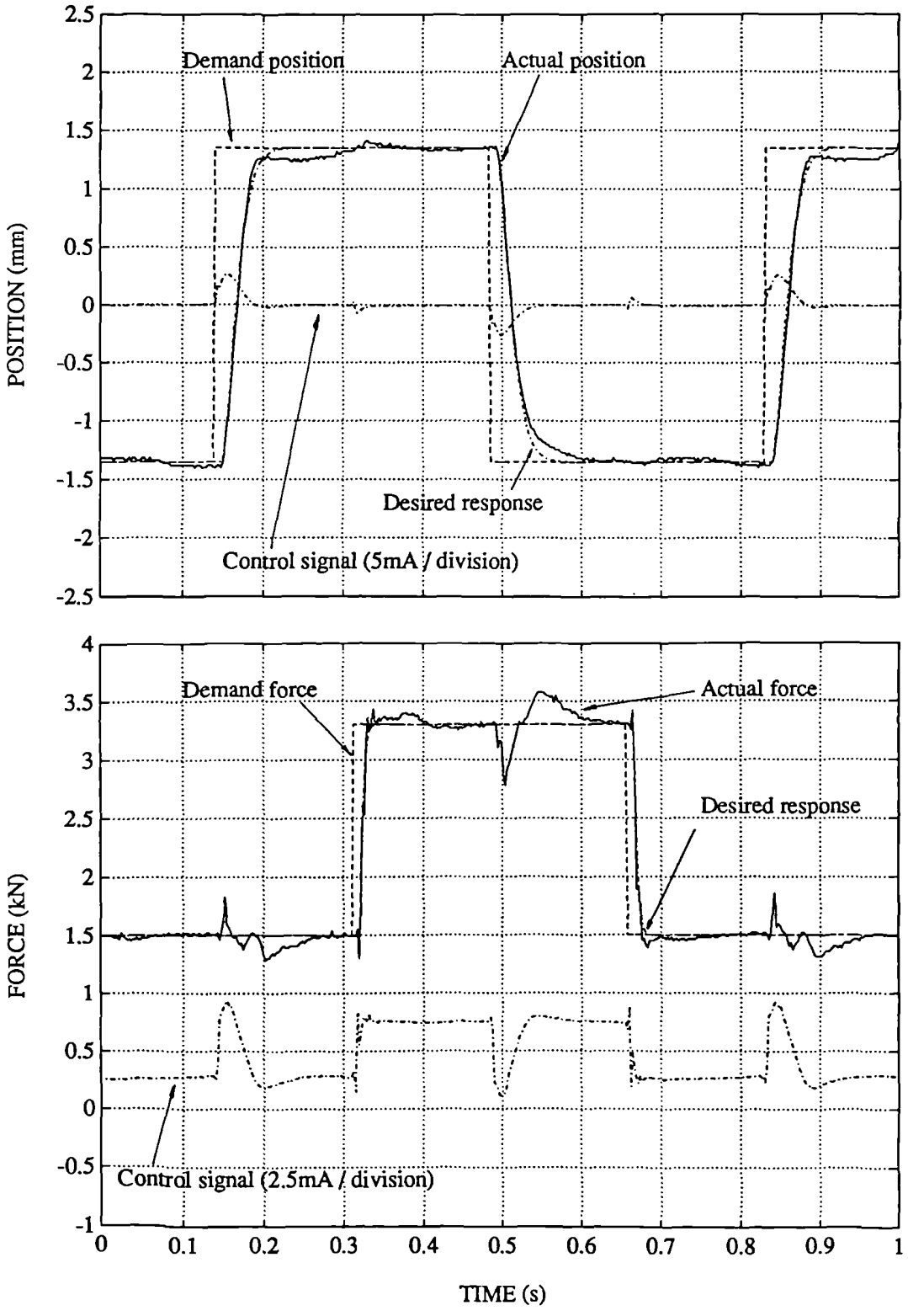

Figure 9.14 Integral multivariable pole-placement control

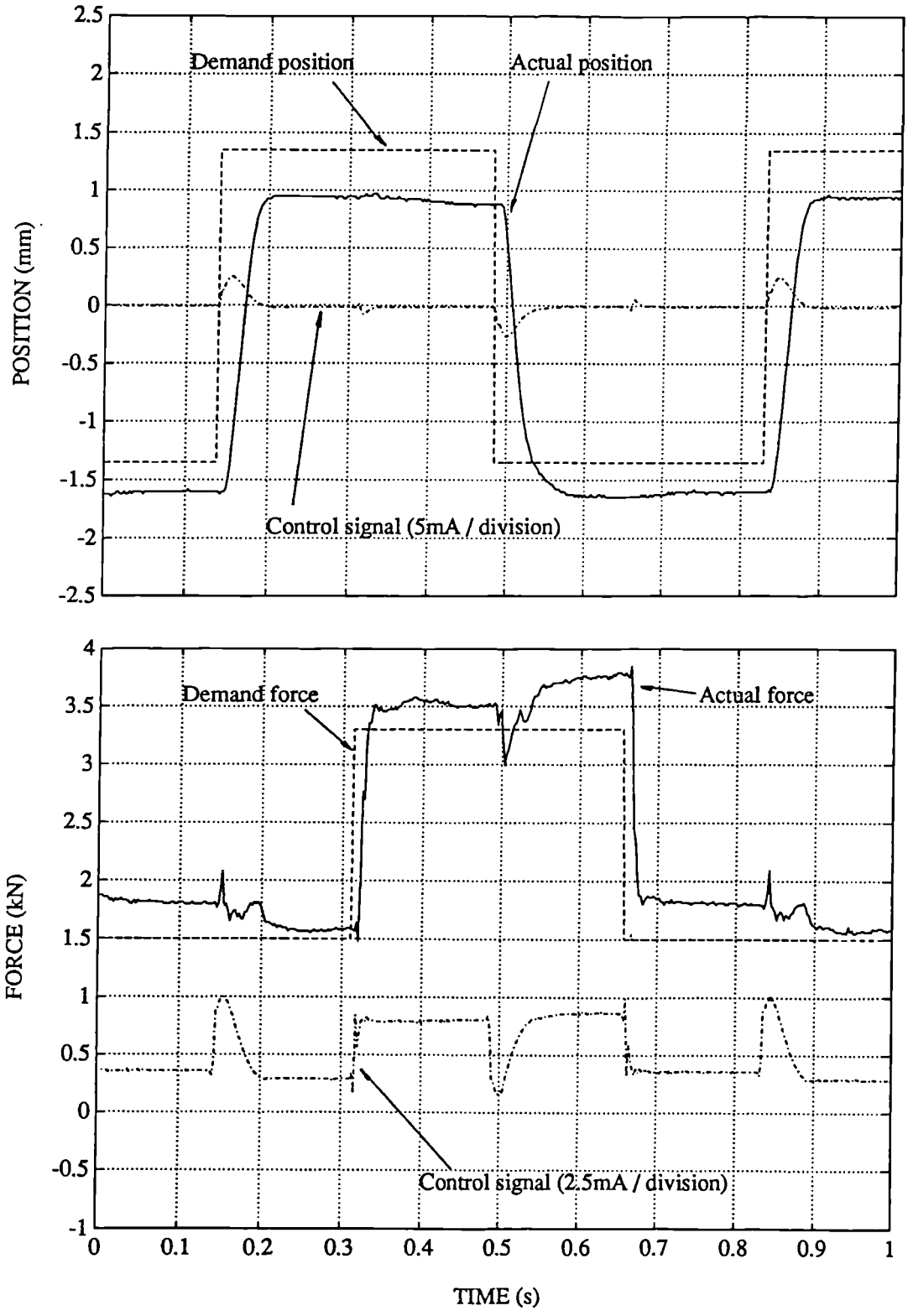

Figure 9.15 Non-integral multivariable pole-placement control

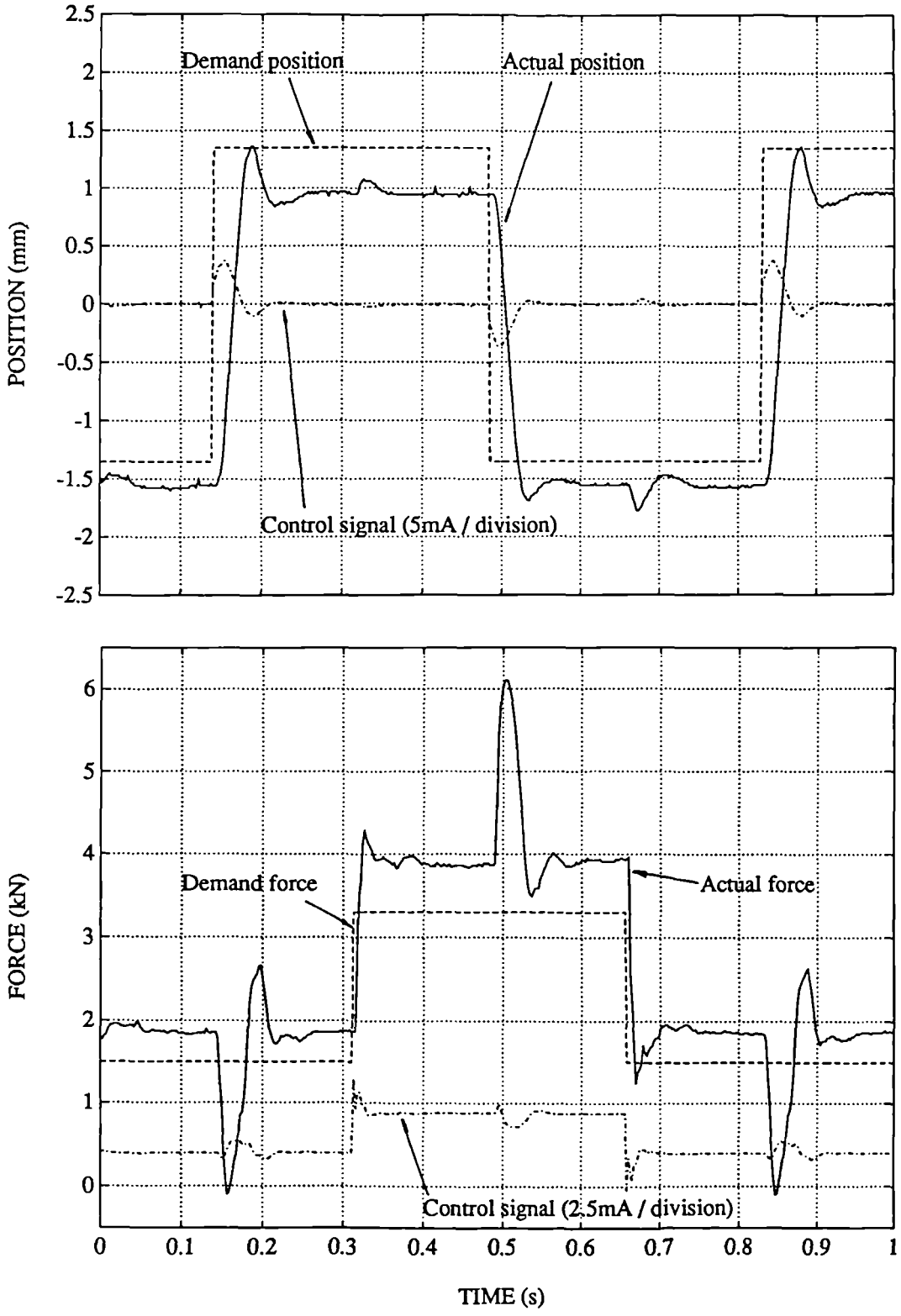

Figure 9.16 SISO pole-placement control for each channel (non-integral)

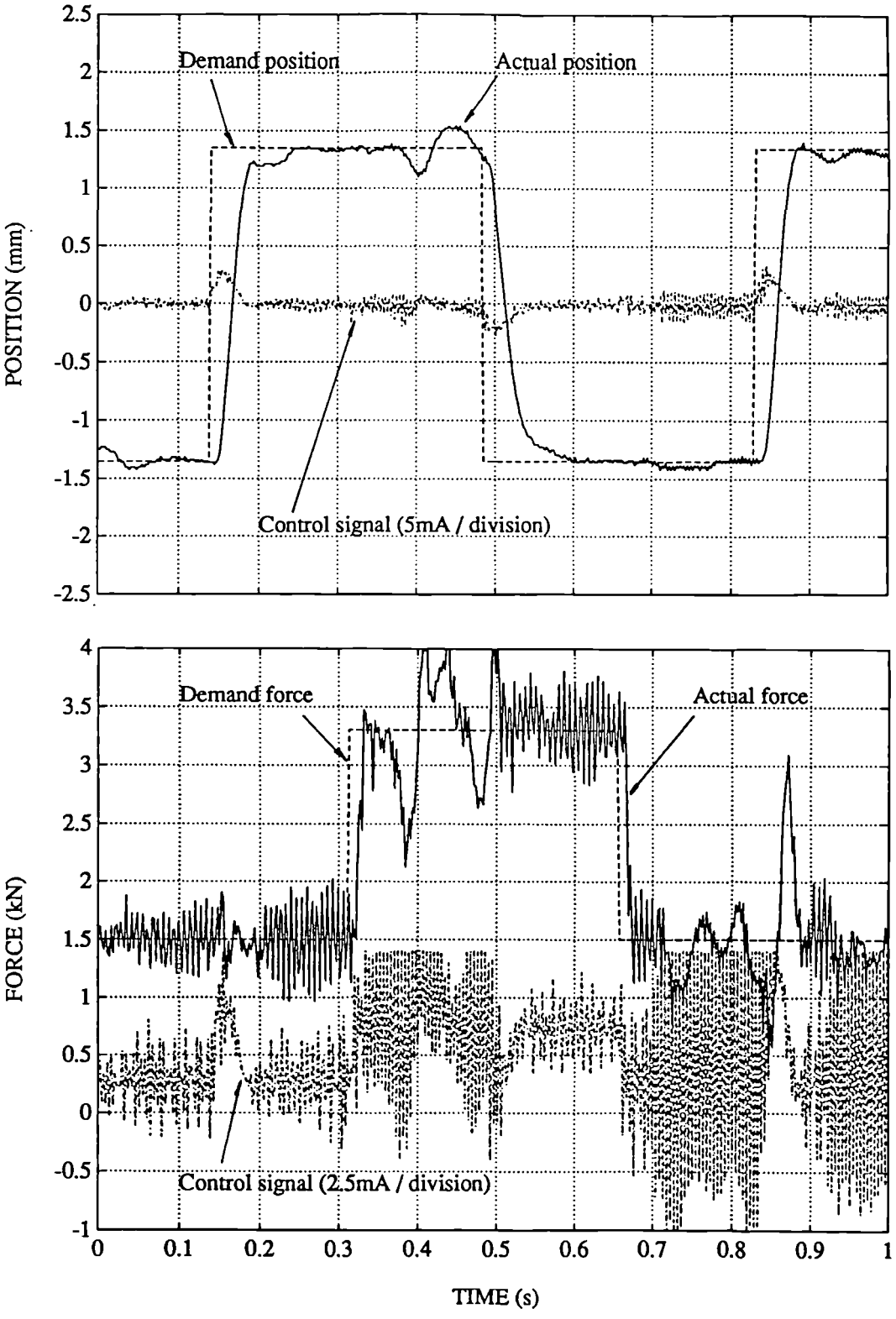

Figure 9.17 Integral multivariable pole-placement control with demand filter of degree 2.

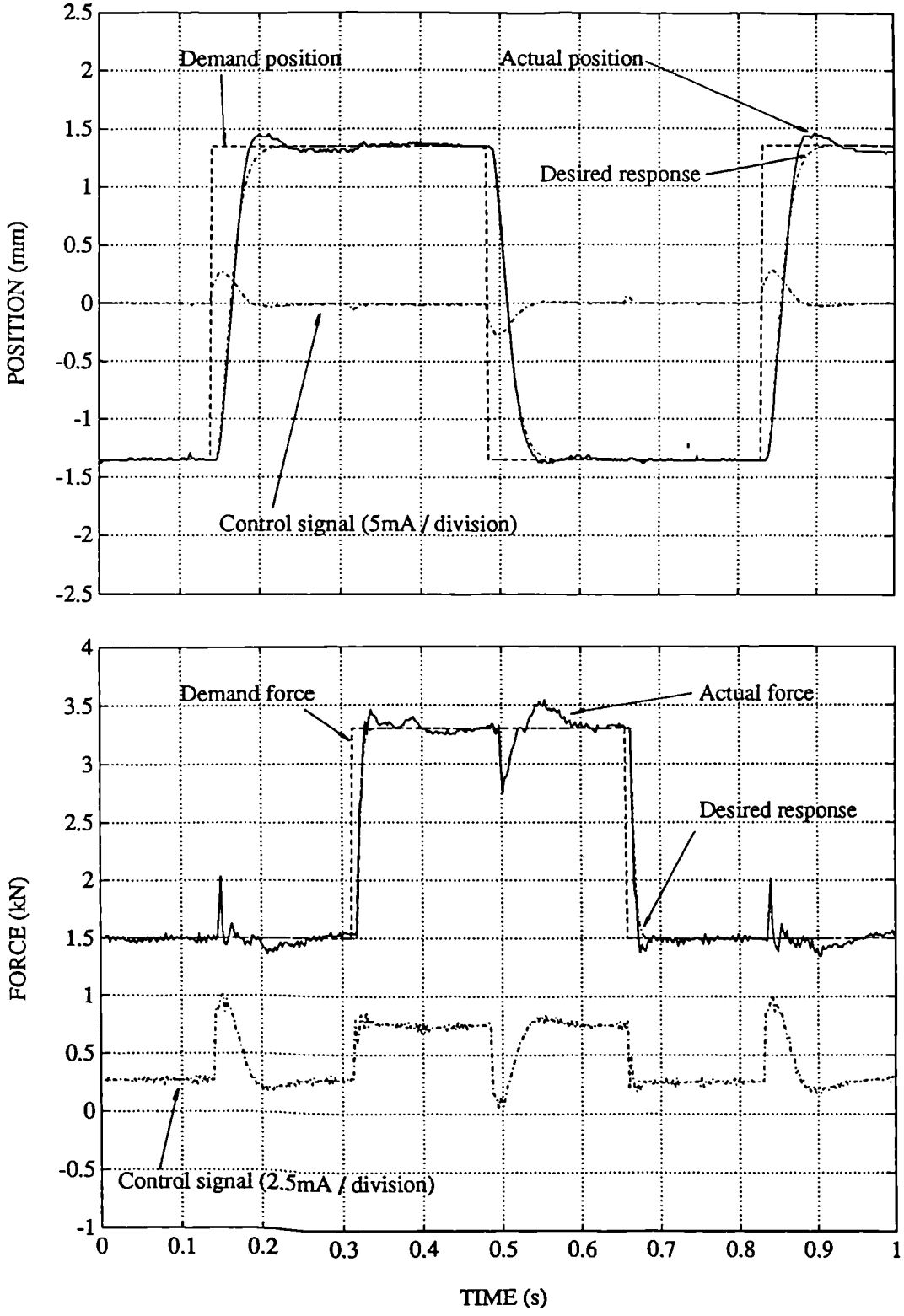

Figure 9.18 Integral multivariable pole-placement using reduced model

10. Conclusions

10.1 Achievements

A variety of digital modelling and control techniques have been applied to electro-hydraulic servosystems. Some techniques are well known in theoretical circles, but have not been practically assessed by application to such servosystems before. Other techniques have been developed in order to overcome particular difficulties encountered in practice and not addressed by established techniques. Some particular achievements are noted below.

System identification has been shown to be a good basis for controller design. Very little work on off-line system identification for such systems has been published, although on-line parameter estimation has been applied on a number of occasions as part of adaptive control schemes. Model structure identification has been particularly neglected, with model orders being selected merely on an experimental trial and error basis, perhaps guided by physical analysis. If model-based controllers are to be adopted widely, a more rigorous approach is needed. Several methods have been compared for selecting structures from input-output data, two of which — the RMS prediction error and instrumental product-moment matrix methods — are very successful. The error variance norm and non-instrumental product-moment matrix methods also tried do not give such a clear indication of the best model structure.

Previous studies involving parameter estimation for electro-hydraulic servosystems have mostly used recursive least squares. However the well-known bias problem associated with least squares has been shown to be a handicap. Several estimators designed to overcome this

problem have been tried, with varying degrees of success. However simply filtering the data before estimation, using a low-pass filter to attenuate noise above the plant bandwidth, is most successful. Using a band-pass filter also reduces the influence of low frequency disturbances. A bonus is the greatly increased convergence rate, especially important for adaptive control. The other estimators — instrumental variables, extended least squares and a correlation-based method — do show a significant improvement over basic least squares, but do not yield such reliable models for controller design.

Pole-placement control is a technique which has been applied a number of times to such systems. It has the advantage of relative simplicity compared to optimal control methods, and allows the designer the freedom to specify the pole positions. A freedom such as this is normally required, as modelling and control of electro-hydraulic servosystems has not yet reached a degree of proficiency which eliminates experimental tuning of design parameters. However previous application studies have been largely deterministic, and have not considered the uncertainties of modelling errors and noise. By assessing the noise response of the closed-loop system, and the robustness to modelling errors, the limitations on the placement of the poles can be readily understood. This understanding allows more intelligent choices to be made.

The consideration of uncertainty also highlights the usefulness of filtering the demand signal. This filter can be cancelled out of the closed-loop response by specifying additional poles which are the roots of the filter, but it still affects the noise response and robustness of the system. So by using an appropriate demand filter, a faster desired response can be specified whilst maintaining adequate noise and robustness properties. The experimental effects of both the demand filter and closed-loop pole positions have been shown to be very close to the theoretical effects.

The noise and robustness properties are also influenced by the sample rate, and by the addition of integral action. They have been shown to deteriorate as the sample rate increases, so that for the system under test, a sample rate above 10 times the plant bandwidth was undesirable. The use of a demand filter with the usual integral pole-placement method (e.g. Åström and Wittenmark, 1990) is essential to control the frequency range over which the integral action is dominant. With a large range the robustness is poor, in the same way as adding high gain integral action to a classical controller is known to reduce stability margins.

Saturation in the servovalve limits the demand filter which can be adequately cancelled out of the closed-loop response. In the case of the SISO system under test, this prevented the use of a demand filter suitable for integral control. Thus an alternative integral control method has been devised, which integrates the error between the plant output and the output of a plant model running in parallel. This worked well for the plant in question.

Combining the lessons learnt from off-line parameter estimation and fixed-coefficient pole-placement control, a very effective indirect adaptive controller has been developed. For an electro-hydraulic position control system, a third order model is used, and the gain and 2 coefficients in the second order lag term are adapted. The demand filter is still important to improve robustness, not least to minimise tuning transients after sudden changes in plant behaviour. Adaptation is very rapid, partly due to the quick convergence of the filtered least squares estimator already mentioned. However this is also as a result of the use of a low forgetting factor, in conjunction with a method which switches off adaptation if the trace of the normalised covariance matrix becomes too great. The algorithm prevents parameter divergence when the data is not persistently exciting. Various other forgetting strategies have been tested without success, mostly because adaptation is just restricted rather than prevented when the excitation is insufficient, and thus the parameter estimates can still drift. These strategies include constant trace, variable forgetting factor, and estimator jacketting techniques.

Previous applications of adaptive control to electro-hydraulic servosystems have shown the feasibility of the approach, but have sometimes exhibited large tuning transients, or slow or incomplete adaptation. Alternatively it has been applied to a low inertia system which can be modelled as an integrator alone, with just the gain to adapt, which is a much simpler task.

The final field of study has been multivariable control, an area of the greatest importance in the numerous situations in which several actuators bear simultaneously on a common load. No comparison of alternative methods has been performed; the best SISO techniques have simply been extended. However new issues are raised with multivariable pole-placement control, notably that of decoupling. A new method has been developed which allows complete dynamic decoupling, the use of a demand filter, and different pole-sets to be specified for the decoupled channels. Multivariable system identification and fixed-coefficient control — with integral action — have been applied to a highly non-linear 2-channel servosystem, with significant interaction. The closed-loop response is not ideal, but interaction is much reduced.

10.2 Further work

Further work to give better guidelines for choosing the estimation filter would be useful, thus simplifying the controller design procedure. It has, however, been demonstrated that a range of filters can give good results. Such work may also have a bearing on the choice of demand filter, as both filters are designed to suppress noise, although in different contexts.

A useful extension to the pole-placement control analysis undertaken would be to include the effect of valve saturation. This could, for example, allow the limits on the demand filters which can be cancelled out of the closed-loop response to be determined. More consideration could also be given to other non-linear effects. However the non-linearities inherent in hydraulic actuation systems seem to allow good approximation by linear models (assuming static non-linear compensation is used where needed). Non-linearities in the load are more likely to be a problem.

The adaptive control method is very successful for the electro-hydraulic positioning system. It would be useful to apply it to a wide range of servosystems to determine how universally applicable it is. An integral adaptive controller has not been implemented, but no significant problems are envisaged.

Multivariable control for electro-hydraulic actuator systems is a relatively new field. Much attention needs to be given to simplifying the controller when many channels are involved. For just two or three channels adaptive control would seem possible, although significant processing power would be required. More channels could be handled, if (say) only selected gains are adapted. It would also be useful to extend the robustness analysis techniques to the multivariable case.

References

Åström, K.J., Wittenmark, B., 1980, "Self-tuning controllers based on pole-zero placement", IEE Proc Pt D, Vol 127 No 3, 120-130.

Åström, K.J., Wittenmark, B., 1990, "Computer-controlled systems: theory and design", 2nd Edition (Prentice-Hall, Englewood Cliffs).

Bayoumi, M.M., Mo, Li, 1988, "Adaptive decoupling control of MIMO system", Proc IFAC Conference on Identification and System Parameter Estimation, Beijing, 109-113.

Bell, R., de Pennington, A., 1969, "Active Compensation of Lightly Damped Electrohydraulic Cylinder Drives using Derivative Signals", Proc Instn Mech Engrs, Vol 184 Pt 1 No 4, 83-98.

Daley, S., 1987, "Application of a fast self-tuning control algorithm to a hydraulic test rig", Proc Instn Mech Engrs, Vol 201 No C4, 285-295.

Daley, S., 1990, "Self-tuning control of a hydraulic test-rig using a personal computer", GEC Journal of Research, Vol 7 No 3, 157-166.

Doyle, J.C., 1978, "Guaranteed Margins for LQG Regulators", IEEE Trans in Automatic Control, Vol 23 No 4.

Edge, K.A., Figueredo, K.R.A., 1987, "An adaptively controlled electrohydraulic servo-mechanism, Part 2: Implementation", Proc Instn Mech Engrs, Vol 201 No B3, 181-189.

Figueredo, K.R.A., 1988, "Application of microprocessor based model reference adaptive control to servosystems", PhD Thesis, University of Bath.

Finney, J.M., 1982, "A study of self-tuning controllers and electrohydraulic cylinder drives",

PhD Thesis, University of Leeds.

Finney, J.M, de Pennington, A., Bloor, M.S., Gill, G.S., 1985, "A Pole-Assignment Controller for an Electrohydraulic Cylinder Drive", ASME J. of Dynamic Systems Measurement and Control, Vol 107, 145-150.

Fortescue, T.R., Kershenbaum, L.S., Ydstie, B.E., 1981, "Implementation of self-tuning regulators with variable forgetting factors", Automatica Vol 17 No 6, 831-835.

Franklin, G.F., Powell, J.D., 1980, "Digital Control of Dynamic Systems" (Addison-Wesley, Massachusetts).

Goodwin, G.C., Sin, K.S., 1984, "Adaptive filtering prediction and control" (Prentice-Hall, Englewood Cliffs).

Goodwin, G.C., 1985, "Some Observations on Robust Estimation and Control". Proc 7th IFAC Symposium on System Identification, 851-859.

Gustavsson, I., 1972, "Comparison of Different Methods for Identification of Industrial Processes". Automatica, Vol 8, 127-142.

Henke, R, 1987, "All Fluid or Electrofluid - that is the Question", Control Engineering, June 1987, 63-67.

Hesse, H., 1973, "Load adaptive electrohydraulic position control systems with near time optimal response", Proc 3rd International Fluid Power Symposium, Turin.

Hori, N., Ukrainetz, P.R., Nikiforuk, P.N., Bitner, D.V., 1988a, "Robust Discrete-Time Adaptive Control of an Electrohydraulic Servo Actuator", Proc 8th Fluid Power Symposium, Birmingham, 495-514.

Hori, N., Ukrainetz, P.R., Nikiforuk, P.N., Bitner, D.V., 1988b, "Simplified Adaptive Control of an Electrohydraulic Servo System", Proc Int Conf on Control 88, Oxford, 165-169.

Hori, N., Pannala, A.S., Ukrainetz, P.R., Nikiforuk, P.N., 1989, "Design of an Electrohydraulic Positioning System using a Novel Model Reference Control Scheme", ASME J. of Dynamic Systems, Measurement and Control, Vol 111, 292-298.

Huckvale, S.A., Chambers, P.G., Jones, N., 1984, "A review of applications of microprocessors to electrohydraulic control systems", IMechE paper C237/84.

Isermann, R., Baur, U., Bamberger, W., Kneppo, P., Siebert, H., 1974, "Comparison of Six On-Line Identification and Parameter Estimation Methods", Automatica, Vol 10, 81-103.

Parkkinnen, R., Järviluoma, M., Nevala, K., 1988, "An Intelligent Hydraulic Actuator for Varying Loads", Proc 8th Fluid Power Symposium, Birmingham, 53-86.

Johnson, R.A., Wichern, D.W., 1990, "Applied Multivariate Statistical Analysis" (Prentice-Hall, Englewood Cliffs).

Keller, R.B., Jiashi, C., 1984, "A High Performance Adaptive Controller for Non-linear Hydraulic Servosystems", ASME paper 83-WA/DSC-17.

Kinnaert, M., Hanus, R., 1988, "Comparative study of adaptive control algorithms for multi-input multi-output linear systems", Proc IFAC Conference on Identification and System Parameter Estimation, Beijing, 127-133.

Kinnaert, M., Hanus, R., Henrotte, J.L., 1987, "A new decoupling precompensator for indirect adaptive control of multi-variable linear systems", IEEE Trans in Automatic Control, Vol 32 No 5, 455-459.

Köckemann, A., 1990, "Ein adaptives regelungskonzept für electro-hydraulische antriebe", Proc Aachen Fluid Power Conference (In German).

Kucera, V., 1979, "Discrete Linear Control" (John Wiley, New York).

Kulkarni, M., Trivedi, D., Chandrasekhar, J., 1984, "An adaptive control of an electrohydraulic position control system", Proc American Control Conference, 443-449.

Ljung. L., Söderström T., 1983, "Theory and practice of recursive identification" (MIT Press, Cambridge Massachusetts).

Ljung, L., 1987, "System Identification: Theory for the User" (Prentice-Hall, Englewood Cliffs).

Maskrey, R.H., 1978, "The role of microprocessors in closed-loop electrohydraulic control systems", ASME Design Engineering Conference, Chicago.

McCloy, D., Martin, H.R., 1980, "Control of Fluid Power" (Ellis Horwood, Chichester).

Middleton, R.H., Goodwin, G.C., Hill, D.J., Mayne D.Q., 1988, "Design Issues in Adaptive Control", IEEE Trans in Automatic Control, Vol 33 No 1, 50-58.

Norton, J.P., 1986, "An Introduction to Identification" (Academic Press, London).

Pannala, A.S., Dransfield, P., Palaniswami, M., Anderson, J.H., 1989, "Controller design for a Multichannel Electro-hydraulic System", ASME J. of Dynamic Systems Measurement and Control, Vol 111, 299-306.

Panossian, H., 1986, "Model reference adaptive direct drive actuation system", from "Fluid Control and Measurement" Vol 1, Ed. Harada, M. (Pergamon).

Parker, G.A., Desjardins, Y.C., 1973, "A comparison of transfer function identification methods for an electrohydraulic speed control system", 3rd Interational Fluid Power Symposium, Turin.

Pietola, M., Vilenius, M., 1989, "Theoretical and experimental study of the effect of varying load on the dynamics of a P, MRC or P+PID/x controlled electrohydraulic position servo system", Proc Instn Mech Engrs, Vol 203 Pt C, 267-273.

Plummer, A. R., 1989, "The Application of System Identification". University of Bath School of Mechanical Engineering, Report No. 1007.

Porter, B., Tatnall, M.L., 1970, "Performance characteristics of an adaptive hydraulic servo-mechanism", Int. J. Control, Vol 11 No 5, 741-757.

Porter, B., Boddy C.L., 1989, "Design of adaptive digital controllers incorporating dynamic pole-assignment compensators for high performance aircraft" Proc IEEE National Aerospace and Electronics Conference, Daytona.

Saffe, P., Feigel, H., 1988, "Non-linear control concepts for servohydraulic drives", Proc 8th Fluid Power Symposium, Birmingham, 479-493.

Saridis, G. N., 1974, "Comparison of Six On-Line Identification Algorithms", Automatica, Vol 10, 69-79.

Schwarz, H., Guo, L., 1990, "Multivariable control of Electrohydraulic drives", Proc Application of Multivariable System Techniques Symposium, Bradford, 304-312.

Söderström, T., 1977, "On Model Structure Testing in System Identification". Int. J. Control, Vol 26 1-18.

Söderström, T., Stoica, P., Trulsson, E., 1987, "Instrumental Variable Methods for Closed Loop Systems". Proc 10th IFAC World Congress, Munich.

Söderström, T., Stoica, P., 1989, "System Identification" (Prentice-Hall, UK).

Takahashi, K., Inoue, M., Ikeo, S., 1985, "Application of the MRAC technique to an electrohydraulic servosystem", Proc International Conference on Fluid Power Transmission and Control, Hangzhou, China, 68-87.

Unbehauen, H., Gohring, B., 1974, "Tests for Determining Model Order in Parameter Estimation", Automatica, Vol 10, 233-244.

Unbehauen, H., Du, P., Keuchel, U., 1988, "Application of a digital adaptive controller to a hydraulic system", Proc Int Conf on Control 88, Oxford, 177-182.

Van Den Boom, A.J.W, Van Den Enden, A.W.M., 1974, "The Determination of the Orders of Process and Noise Dynamics", Automatica, Vol 10, 245-256.

Vaughan, N.D., Whiting, I.M., 1984, "Self-tuning microprocessor control of closed-loop time-variable hydraulic systems", Proc 40th National Conference on Fluid Power, Chicago.

Vaughan, N.D., Whiting, I.M., 1986, "Microprocessor control applied to a nonlinear electrohydraulic position servo system", Proc 7th Fluid Power Symposium, Bath, 187-198.

Wahab, W., Wellstead, P.E., 1986, "Multivariable Self-tuning for Robotic Servo Applications", Proc IFAC Conference on Adaptive Systems in Control and Signal Processing, Lund, 289-295.

Warwick, K. (Ed), 1988, "Implementation of Self-Tuning Controllers" (Peter Peregrinus, London).

Warwick, K., Rees, D. (Eds), 1988, "Industrial Digital Control Systems" (Peter Peregrinus, London).

Watton, J., 1988, "A digital compensator design for electrohydraulic servomotor systems using reduced order observers", Journal of Fluid Control, Vol 19 No 3, 44-58.

Watton, J., 1990, "A digital compensator design for electrohydraulic single-rod cylinder position control systems", ASME J. of Dynamic Systems Measurement and Control, Vol 112, 403-409.

Wellstead, P.E., 1978, "An Instrumental Product Moment Test for Model Order Estimation", Automatica, Vol 14, 89-91.

Wellstead, P.E., Sanoff, S.P., 1981, "Extended self-tuning algorithm", Int. J. Control, Vol 34 No 3, 433-455.

Whiting, I.M., 1987, "Closed loop digital control of electrohydraulic systems", PhD Thesis, University of Bath.

Wolowich, W., 1974, "Linear Multivariable Systems" (Springer Verlag, New York).

Young, P.C., 1970, "An Instrumental Variable Method for Real-Time Identification of a Noisy Process", Automatica, Vol 6, 271-287.

Young, P., Jakeman, A, McMurtrie, R., 1980, "An Instrumental Variable Method for Model Order Identification", Automatica, Vol 16, 281-294.

Young, P.C., 1984, "Recursive Estimation and Time-series Analysis" (Springer-Verlag, New York).

Yufei, X., Guoxian, Z., Yuanzhang, L., 1988, "Time Series Analysis of Hydraulic Position System", Journal of Shanghai Jiatong University, Vol 22 No 2, 1-7 (In Chinese).

Appendix 1

Analysis of electro-hydraulic positioning system

A1.1 Introduction

This appendix contains a small perturbation analysis of the electro-hydraulic system described in Chapter 2. Reference is also made to the effect of external forces (relevant to integral control, see Chapter 7), and the effect of changes in supply pressure and oil volume (which are used to test adaptive control in Chapter 8).

The notation used in this appendix is given below. The exact definition of some of the variables is clarified in the diagram of valve and actuator in Figure A1.1. Note the external force F shown in the Figure is initially assumed to be zero.

A	Area of piston
B	Bulk modulus
c_L	Leakage coefficient
c_p	Valve flow/pressure coefficient
c_x	Valve flow/opening coefficient
f	Small perturbation in F
F	External load force
k	Ratio of small pressure change over volume change for oil volume
k_s	System constant (combination of piston areas and supply pressure)
k_v	Valve gain constant

M	Load and ram mass
p	Small perturbation in P
P	Pressure in cylinder
P_s	Supply pressure
q	Small perturbation in Q
Q	Volume flowrate through valve
R	Ratio of annular over full piston area
s	Differential operator
v	Small perturbation in V
V	Oil volume in one side of cylinder
x	Small perturbation in x
X	Valve opening
y	Small perturbation in Y
Y	Load position

Greek

ζ	Damping ratio
ω_n	Natural frequency

Subscripts

1	Annular side of piston
2	Full side of piston

Miscellaneous

$[\cdot]_{ss}$	Steady-state value of

A1.2 Derivation of general transfer function

A1.2.1 Valve

For a zero-lap valve, if X (the valve opening) is positive, the orifice equation gives:

$$\left.\begin{aligned} Q_1 &= k_v X \sqrt{P_s - P_1} \\ Q_2 &= k_v X \sqrt{P_2} \end{aligned}\right\} \qquad \text{(A1.1)}$$

To linearise these equations, consider small perturbations in X and the pressures around steady values. If lower case indicates size of perturbation, as opposed to the steady value in upper case:

$$\left.\begin{aligned} q_1 &= c_{x1} x - c_{p1} p_1 \\ q_2 &= c_{x2} x + c_{p2} p_2 \end{aligned}\right\} \qquad \text{(A1.2)}$$

where $\quad c_{x1} = \dfrac{\partial Q_1}{\partial X}, \quad c_{p1} = \dfrac{\partial Q_1}{\partial P_1}, \quad c_{x2} = \dfrac{\partial Q_2}{\partial X}, \quad c_{p2} = \dfrac{\partial Q_2}{\partial P_2}$

So **for positive X**, equation (A1.1) gives:

$$\left.\begin{aligned} c_{x1} &= k_v \sqrt{P_s - P_1} \qquad c_{p1} = \frac{k_v X}{2\sqrt{P_s - P_1}} \\ c_{x2} &= k_v \sqrt{P_s - P_1} \qquad c_{p2} = \frac{k_v X}{2\sqrt{P_2}} \end{aligned}\right\} \qquad \text{(A1.3)}$$

Steady pressure values can be found thus (assuming no leakage):

$$\begin{aligned} \frac{Q_1}{A_1} &= \frac{Q_2}{A_2} \\ \sqrt{P_s - P_1} &= \frac{A_1}{A_2}\sqrt{P_2} \qquad (X \neq 0) \end{aligned} \qquad \text{(A1.4)}$$

and solving with the force balance equation $P_1 A_1 = P_2 A_2$ (which assumes no friction), gives

$$\left.\begin{aligned} P_2 &= \frac{RP_s}{R^3 + 1} \\ P_s - P_1 &= \frac{R^3 P_s}{R^3 + 1} \end{aligned}\right\} \qquad \text{(A1.5)}$$

where

$$R = \frac{A_1}{A_2} \qquad \text{(A1.6)}$$

Thus the coefficients of equation (A1.3) become:

$$\left.\begin{aligned} c_{x1} &= Rk_v k_s & c_{p1} &= \frac{k_v X}{2Rk_s} \\ c_{x2} &= k_v k_s & c_{p2} &= \frac{k_v X}{2k_s} \end{aligned}\right\} \qquad \text{(A1.7)}$$

where k_s is constant for any system:

$$k_s = \sqrt{\frac{RP_s}{R^3 + 1}} \qquad \text{(A1.8)}$$

For **negative** X, equation (A1.2) still holds, but now:

$$\left.\begin{aligned} Q_1 &= k_v X\sqrt{P_1} \\ Q_2 &= k_v X\sqrt{P_s - P_2} \end{aligned}\right\} \qquad \text{(A1.9)}$$

and the steady pressure values are:

$$\left.\begin{aligned} P_1 &= \frac{R^2 P_s}{R^3 + 1} \\ P_s - P_2 &= \frac{P_s}{R^3 + 1} \end{aligned}\right\} \quad (X \neq 0) \tag{A1.10}$$

Thus the coefficients equivalent to those in equation (A1.7) are:

$$\left.\begin{aligned} c_{x1} &= \sqrt{R}\, k_v k_s & c_{p1} &= \frac{k_v X}{2\sqrt{R}\, k_s} \\ c_{x2} &= \frac{k_v k_s}{\sqrt{R}} & c_{p2} &= \frac{\sqrt{R} k_v X}{2 k_s} \end{aligned}\right\} \tag{A1.11}$$

A1.2.2 Flow

Assuming no leakage, the valve flow stems from piston movement and oil compression. Let k_1 and k_2 be stiffness constants for the oil volumes, defined by:

$$\left.\begin{aligned} p_1 &= k_1 v_1 \quad \text{and} \quad p_2 = k_2 v_2 \\ \text{Hence} \quad k_1 &= \frac{B}{V_1} \quad \text{and} \quad k_2 = \frac{B}{V_2} \end{aligned}\right\} \tag{A1.12}$$

For k_1 and k_2 to be approximately constant, only small volume changes are allowed.

The flow equations are:

$$\left.\begin{aligned} q_1 &= A_1 s y + \frac{s p_1}{k_1} \\ q_2 &= A_2 s y - \frac{s p_2}{k_2} \end{aligned}\right\} \tag{A1.13}$$

Note that rigid pipes between valve and cylinder give negligible pipe expansion.

A1.2.3 Forces

Assuming no friction or damping in load or cylinder, and that the load is rigidly attached to the piston rod (with total mass M):

$$p_1A_1 - p_2A_2 = Ms^2y \tag{A1.14}$$

A1.2.4 Solution

From equations (A1.2) and (A1.13):

$$\left.\begin{aligned}(c_{p1} + \frac{s}{k_1})p_1 &= c_{x1}x - A_1sy \\ (-c_{p2} - \frac{s}{k_2})p_2 &= c_{x2}x - A_2sy\end{aligned}\right\} \tag{A1.15}$$

Using (A1.15) to substitute for p_1 and p_2 in (A1.14):

$$\frac{A_1c_{x1}x - A_1^2sy}{\frac{s}{k_1} + c_{p1}} + \frac{A_2c_{x2}x - A_2^2sy}{\frac{s}{k_2} + c_{p2}} = Ms^2y \tag{A1.16}$$

$$\frac{y}{x} = \frac{\left(\frac{c_{x1}A_1}{k_2} + \frac{c_{x2}A_2}{k_1}\right)s + (c_{x1}A_1c_{p2} + c_{x2}A_2c_{p1})}{s\left(\frac{M}{k_1k_2}s^3 + M\left(\frac{c_{p2}}{k_1} + \frac{c_{p1}}{k_2}\right)s^2 + \left(\frac{A_1^2}{k_2} + \frac{A_2^2}{k_1} + Mc_{p1}c_{p2}\right)s + (A_1^2c_{p2} + A_2^2c_{p1})\right)} \tag{A1.17}$$

Thus the general small perturbation transfer function is fourth order.

This assumes that the input to the plant is the valve opening, rather then the valve drive amplifier input voltage. Thus valve dynamics have been neglected.

Note that the coefficients in (A1.17) change with changes in the following:

- valve opening X, via c_{p1} and c_{p2} (and c_{x1} and c_{x2} when X changes sign),
- stiffnesses k_1 and k_2, due to oil volume changes (e.g. as the piston moves from one point of the stroke to another),
- supply pressure P_s, via c_{x1}, c_{x2}, c_{p1} and c_{p2}.

The next section considers some cases in which simplifications can be made.

A1.3 Simplified transfer function

The first order lag terms on the left hand side of (A1.16) are due to the oil compressibility — they would disappear if k_1 and k_2 were infinite. The transfer function reduces to third order if these lags have the same time constant, i.e. if:

$$k_1 c_{p1} = k_2 c_{p2} \tag{A1.18}$$

This gives the transfer function:

$$\frac{y}{x}(s) = \frac{\frac{1}{M}(c_{x1}A_1k_1 + c_{x2}A_2k_2)}{s\left(s^2 + c_{p1}k_1 s + \frac{A_1^2k_1}{M} + \frac{A_2^2k_2}{M}\right)} \tag{A1.19}$$

The second order lag term has the following natural frequency and damping ratio:

$$\left.\begin{aligned} \omega_n &= \sqrt{\frac{A_1^2 k_1}{M} + \frac{A_2^2 k_2}{M}} \\ \zeta &= \frac{c_{p1} k_1}{2\omega_n} \end{aligned}\right\} \qquad \text{(A1.20)}$$

Note that the damping ratio varies with valve opening via c_{p1}.

From (A1.7) for positive X or (A1.11) for negative X, (A1.18) becomes:

$$k_1 = R k_2$$

$$\text{or} \qquad \frac{V_1}{V_2} = \frac{A_2}{A_1} \qquad \text{(A1.21)}$$

So (A1.18) is satisfied, and the transfer function reduces to third order, at one particular point in the stroke.

Operating around $X = 0$ also satisfies (A1.18), as this gives $c_{p1} = c_{p2} = 0$ — see (A1.3) for example. The damping is zero with this valve position. The natural frequency expression in (A1.20) can readily be calculated with the valve closed just by considering the interaction of the mass with the stiffnesses of the two oil volumes.

A1.4 Steady-state gain

The steady-state velocity gain can be found from (A1.17):

$$\left[\frac{sy}{x}\right]_s = \frac{c_{x1} A_1 c_{p2} + c_{x2} A_2 c_{p1}}{A_1^2 c_{p2} + A_2^2 c_{p1}} \qquad \text{(A1.22)}$$

Using the relationships between the c_x's and c_p's evident in (A1.7) for positive X or (A1.11) for negative X:

$$\left[\frac{sy}{x}\right]_{ss} = \frac{c_{xl}}{A_1} \tag{A1.23}$$

As c_{x1} is dependent on the sign of X, so is the velocity gain:

$$\left.\begin{array}{lll} \text{for positive } X & \left[\frac{sy}{x}\right]_{ss} & = \frac{k_v k_s}{A_2} \\ \text{for negative } X & \left[\frac{sy}{x}\right]_{ss} & = \frac{k_v k_s}{\sqrt{R}A_2} \end{array}\right\} \tag{A1.24}$$

Thus the gain is constant with respect to valve opening, except that the extend (negative) gain is greater then the retract (positive) gain by the factor:

$$\sqrt{\frac{A_2}{A_1}} \tag{A1.25}$$

The gain will also vary in proportion to the root of the supply pressure (via k_s).

A1.5 Leakage effects: damping and steady-state error

In reality there will be some leakage from each oil volume, likely to be dependent on the oil pressure. Thus the following small perturbation in leakage flow can be introduced:

$$\left.\begin{array}{l} q_{L1} = c_{L1}\, p_1 \\ q_{L2} = c_{L2}\, p_2 \end{array}\right\} \tag{A1.26}$$

The flow equations of (A1.13) are now:

$$\left.\begin{aligned} q_1 &= A_1 sy + \frac{sp_1}{k_1} + c_{L1}p_1 \\ q_2 &= A_2 sy - \frac{sp_2}{k_2} - c_{L2}p_2 \end{aligned}\right\} \qquad \text{(A1.27)}$$

and equation (A1.15) becomes:

$$\left.\begin{aligned} ([c_{p1} + c_{L1}] + \frac{s}{k_1})p_1 &= c_{x1}x - A_1 sy \\ (-[c_{p2} + c_{L2}] - \frac{s}{k_2})p_2 &= c_{x2}x - A_2 sy \end{aligned}\right\} \qquad \text{(A1.28)}$$

The leakage gains c_L simply add to the valve flow/pressure gains c_p. So, for example, the damping ratio given in (A1.20) becomes:

$$\zeta = \frac{(c_{L1} + c_{p1})k_1}{2\omega_n} \qquad \text{(A1.29)}$$

Thus with leakage the damping ratio is not zero when $X = 0$; leakage plays a significant part in determining plant behaviour.

Leakage also dictates what valve opening is required to resist a steady load force (F) whilst keeping the mass stationary. In the steady-state, (A1.28) reduces to:

$$\left.\begin{aligned} (c_{p1} + c_{L1})p_1 &= c_{x1}x \\ -(c_{p2} + c_{L2})p_2 &= c_{x2}x \end{aligned}\right\} \qquad \text{(A1.30)}$$

and the force balance is $p_1A_1 + p_1A_1 = f$, so:

$$x = \frac{f}{\frac{c_{x1}A_1}{c_{p1} + c_{L1}} + \frac{c_{x2}A_2}{c_{p2} + c_{L2}}} \qquad \text{(A1.31)}$$

Consider no leakage ($c_{L1} = c_{L2} = 0$). With the system at rest with no load force, $X = 0$. Thus $c_{p1} = c_{p2} = 0$, and (A1.30) reduces to $x = 0$. Hence whatever load force f is now applied, no valve opening is needed to resist it. However if there is leakage, a valve opening is required. This requirement will lead to a steady-state position error in any non-integral control scheme.

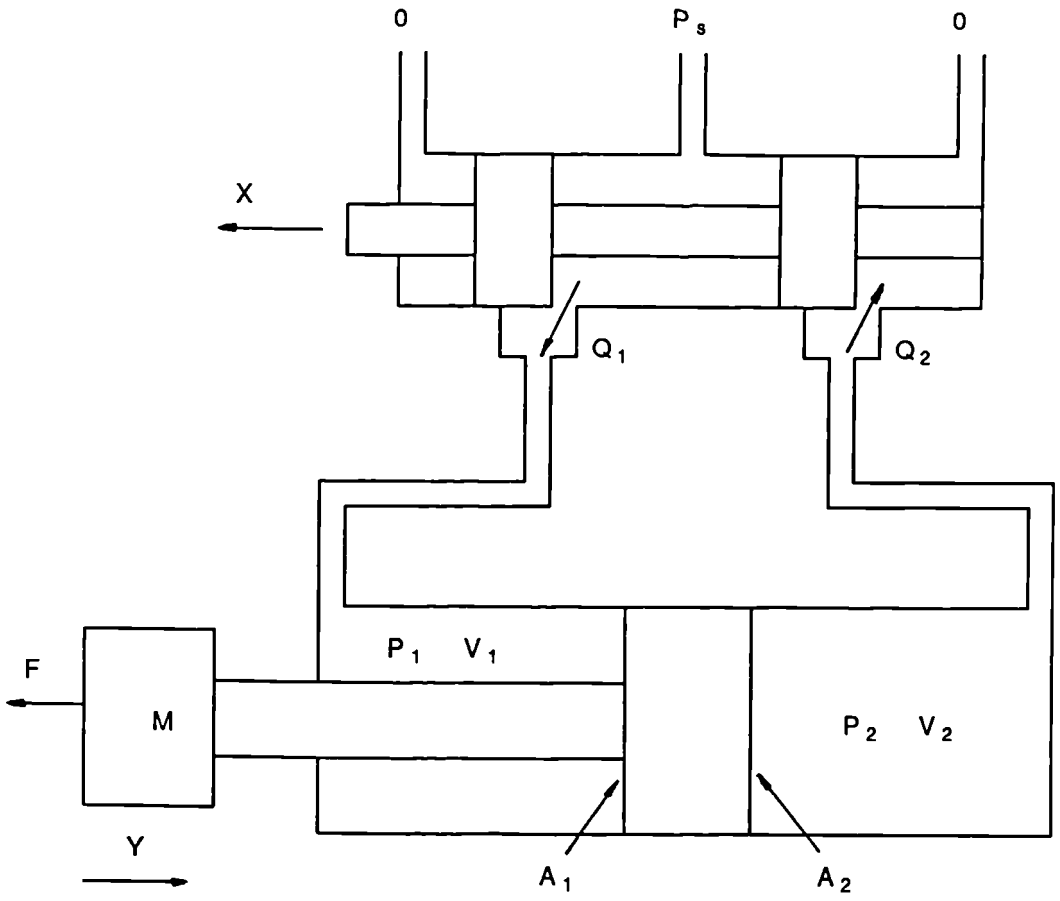

Figure A1.1 Servovalve and actuator

Appendix 2

Pole-placement control: steady-state gain

A pole-placement controller is presented in Section 3.5 for which exact plant modelling is assumed. In the presence of modelling errors, both the transient and steady-state performance of the closed-loop system are likely to be affected. A non-unity steady-state gain is a particularly serious failing for a servosystem. However, many hydraulic servosystems exhibit integral action, and it is shown below that unity steady-state gain can be ensured with such systems. With integral action, $(1 - z^{-1})$ is a factor of $A(z^{-1})$, so $A(1) = 0$. From equation (3.5) this gives the steady-state closed-loop gain as:

$$\frac{1}{G(1)} \tag{A2.1}$$

Recognizing that the controller is designed from approximate plant model polynomials, denoted $\hat{A}(z^{-1})$ and $\hat{B}(z^{-1})$, equation (3.6) can be rewritten:

$$F(z^{-1})\hat{A}(z^{-1}) + G(z^{-1})\hat{B}(z^{-1}) = A_m(z^{-1}) \tag{A2.2}$$

In the steady-state, noting that $A_m(1)$ is equated to $\hat{B}(1)$, this becomes:

$$\frac{F(1)\hat{A}(1)}{\hat{B}(1)} + G(1) = 1 \tag{A2.3}$$

Thus from (A2.1) the steady-state gain is:

$$\frac{1}{1 - \dfrac{F(1)\hat{A}(1)}{\hat{B}(1)}} \tag{A2.4}$$

If the integral action is modelled accurately, then $\hat{A}(1) = 0$, and unity gain has been achieved. If the integrating nature of the plant is recognized at the outset by forcing the factor $(1 - z^{-1})$ in $\hat{A}(z^{-1})$, unity gain is ensured despite the presence of modelling errors.

Appendix 3

Analysis of model-reference integral control

This Appendix contains an analysis of the model-reference integral control method described in Section 7.3. In particular the method is compared with the integral pole-placement method of Section 7.2. The analysis neglects control signal saturation, but the effect of saturation is demonstrated at the end of the Appendix using simulation results.

From Figure 7.5:

$$\begin{aligned} u_{ct} &= u_t + k_i\left[\frac{\hat{B}(z^{-1})}{\hat{A}(z^{-1})}u_t - y_t\right] \\ \hat{A}(z^{-1})u_{ct} &= \left[\hat{A}(z^{-1}) + k_i\hat{B}(z^{-1})\right]u_t - k_i\hat{A}(z^{-1})y_t \end{aligned} \qquad \text{(A3.1)}$$

and u_t is given by:

$$u_t = \frac{H(z^{-1})r_t - G(z^{-1})y_t}{F(z^{-1})} \qquad \text{(A3.2)}$$

Thus from equation (A3.1):

$$\hat{A}(z^{-1})F(z^{-1})u_{ct} = \left[\hat{A}(z^{-1}) + k_i\hat{B}(z^{-1})\right]H(z^{-1})r_t - \left[\hat{A}(z^{-1})G(z^{-1}) + k_i\hat{B}(z^{-1})G(z^{-1}) + k_i\hat{A}(z^{-1})F(z^{-1})\right]y_t$$

$$\hat{A}(z^{-1})F(z^{-1})u_{ct} = \left[\hat{A}(z^{-1}) + k_i\hat{B}(z^{-1})\right]H(z^{-1})r_t - \left[\hat{A}(z^{-1})G(z^{-1}) + k_iA_m(z^{-1})H(z^{-1})\right]y_t \quad \text{(A3.3)}$$

Figure A3.1 is a block diagram of the controller in this form. The closed-loop transfer function is:

$$y_t = \frac{\left[\hat{A}(z^{-1}) + k_i\hat{B}(z^{-1})\right]H(z^{-1})B(z^{-1})r_t + \hat{A}(z^{-1})F(z^{-1})B(z^{-1})w_t}{\hat{A}(z^{-1})F(z^{-1})A(z^{-1}) + \left[\hat{A}(z^{-1})G(z^{-1}) + k_iA_m(z^{-1})H(z^{-1})\right]B(z^{-1})} \quad \text{(A3.4)}$$

The integral action comes from the factor $(1 - z^{-1})$ in $\hat{A}(z^{-1})$, which acts to difference the disturbance signal w_t, attenuating its low frequency components. If modelling is exact, *i.e.* $\hat{A}(z^{-1}) = A(z^{-1})$ and $\hat{B}(z^{-1}) = B(z^{-1})$:

$$y_t = \frac{\left[A(z^{-1}) + k_iB(z^{-1})\right]H(z^{-1})B(z^{-1})r_t + A(z^{-1})F(z^{-1})B(z^{-1})w_t}{\left[A(z^{-1}) + k_iB(z^{-1})\right]A_m(z^{-1})H(z^{-1})}$$

$$y_t = \frac{B(z^{-1})}{A_m(z^{-1})}r_t + \frac{A(z^{-1})F(z^{-1})B(z^{-1})}{\left[A(z^{-1}) + k_iB(z^{-1})\right]A_m(z^{-1})H(z^{-1})}w_t \quad \text{(A3.5)}$$

This confirms that the additions to the pole-placement controller to yield integral action do not interfere with the underlying requirement that the output should follow the demand according to the specified response.

For a first order plant, the degrees of the controller filters in Figure A3.1 are all 1, which is the same as they would be for the integral pole-placement method of Section 7.2, thus the two controllers could be entirely equivalent. For higher order plant the filter degrees do not correspond, so the controllers are different. Taking the first order case, consider the plant:

$$\frac{b_1 z^{-1}}{1 - z^{-1}} \tag{A3.6}$$

which is modelled approximately by:

$$\frac{\hat{b}_1 z^{-1}}{1 - z^{-1}} \tag{A3.7}$$

The desired response will also be first order, i.e.:

$$A_m(z^{-1}) = a_{m0} + a_{m1} z^{-1} \tag{A3.8}$$

and $F(z^{-1})$ and $G(z^{-1})$ are found from the diophantine equation (6.8) to be:

$$F(z^{-1}) = a_{m0}, \qquad G(z^{-1}) = 1 \tag{A3.9}$$

Figure A3.2 shows the block diagram which results for the first order plant, as compared to Figure A3.1 which was for the general case. The controller filters are the same as those for the integral pole-placement controller found from equations (7.1) and (7.2), given that:

$$k_i = \frac{1 + h_1}{\hat{b}_1} \tag{A3.10}$$

where h_1 is the demand filter coefficient used in the integral pole-placement controller, i.e.:

$$H(z^{-1}) = 1 + h_1 z^{-1} \tag{A3.11}$$

Thus neglecting saturation the two controllers are exactly equivalent, with the demand filter in integral pole-placement playing the same role as the integral gain in the model-reference integral controller.

However simulation results for the two controllers *with* control signal saturation are shown in Figure A3.3, illustrating a marked difference in performance. The parameter values used for

the simulation are as follows:

- $b_1 = 0.06, \quad \hat{b}_1 = 0.05$
- $A_m(z^{-1}) = 0.167(1 - 0.7z^{-1})$
- $k_i = 1$, i.e. $h_1 = -0.95$
- saturation at 1V.

Without saturation the simulation confirms that the controllers are identical (Figure A3.4). Although these results are only for first order plant, it seems likely that saturation effects are a major contribution to the difference in performance between the two controllers for higher orders as well.

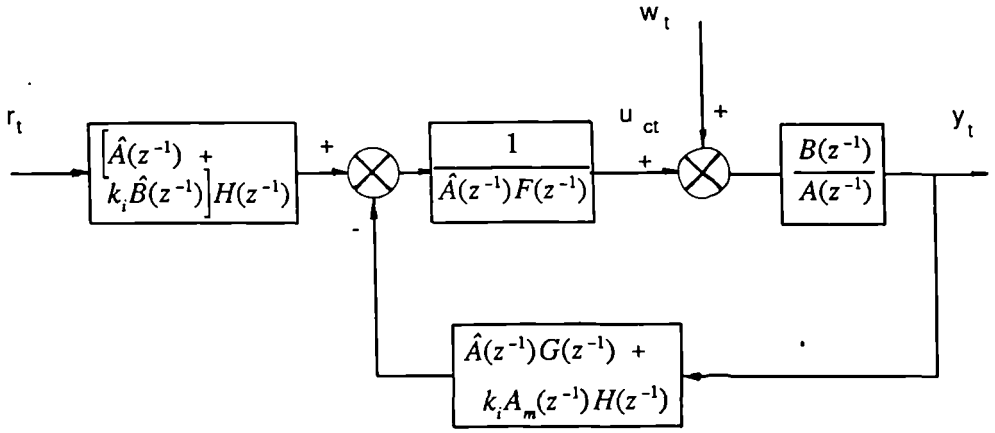

Figure A3.1 Rearranged model-reference integral controller

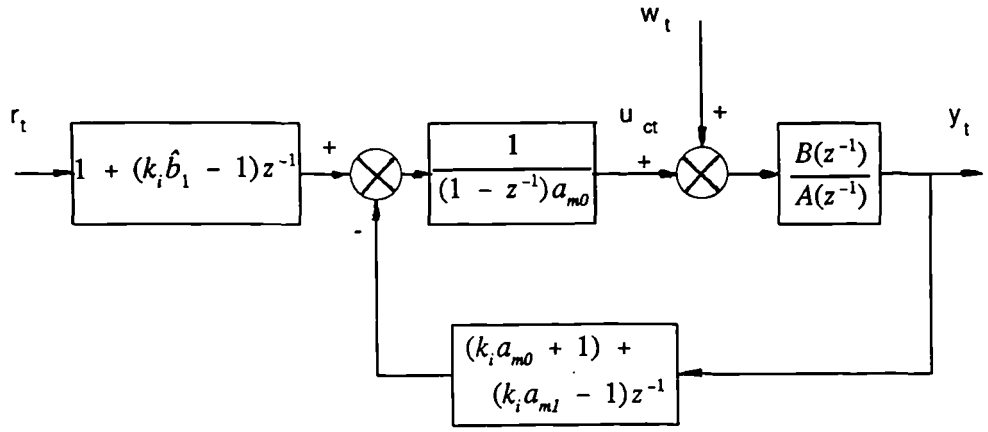

Figure A3.2 Model-reference integral controller
for first order plant

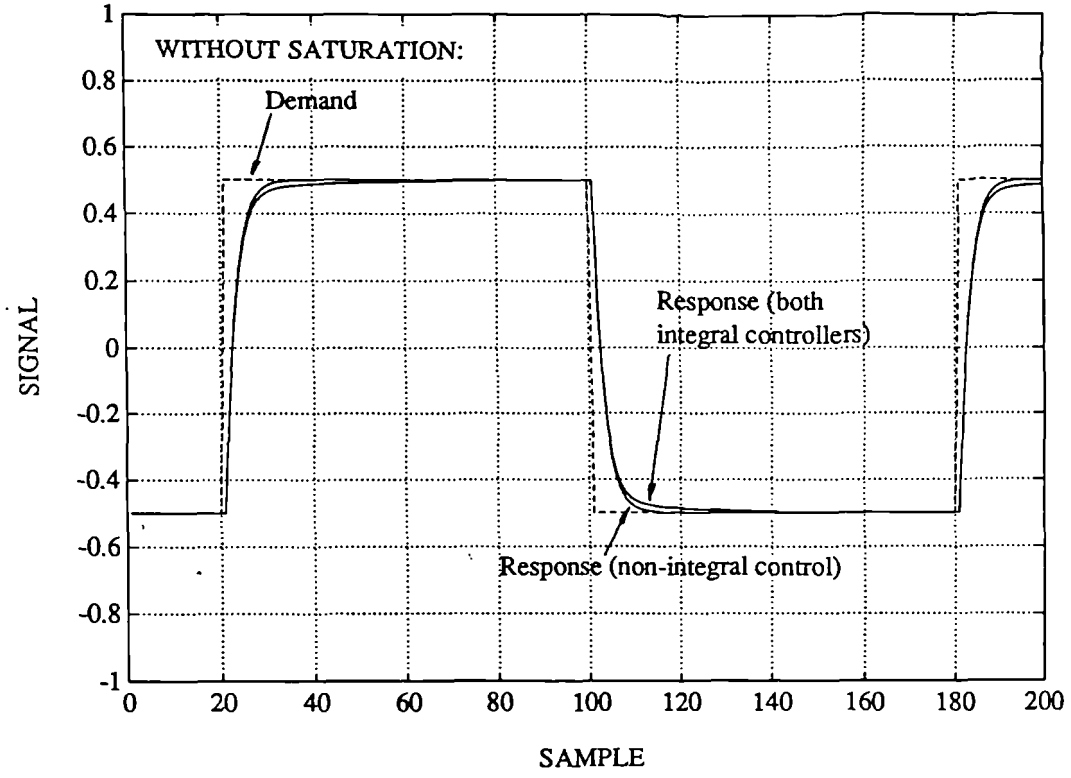

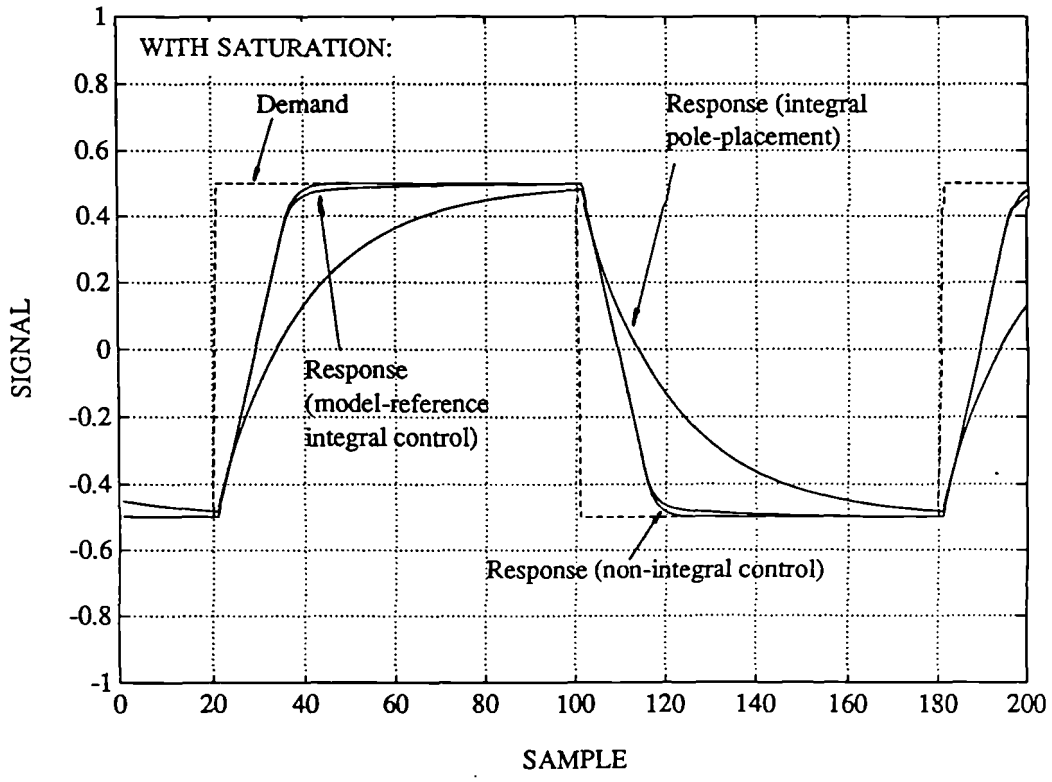

Figure A3.3 Simulated controller responses

Appendix 4

Recursive Least Squares Algorithms

A4.1 Introduction

The derivation of a weighted least squares estimator, leading to the use of a fixed forgetting factor as referred to in Section 8.2.2, is contained in this Appendix. The batch version is derived first from which the recursive estimator is obtained. As ordinary least squares is a special case of weighted least squares — with all the weights equal — its derivation can also be ascertained. A square root version of the recursive covariance update equation is also presented.

A4.2 Batch weighted least squares

Combining the plant model regression equations for each sample instant as in equation (4.4), except based on parameter estimates, gives:

$$y = \Psi\hat{\theta} + \hat{e} \qquad \text{(A4.1)}$$

In ordinary least squares the parameter vector is calculated to minimise the sum of the squares of the elements in vector $\hat{e}$. In weighted least squares the square of the element is scaled

(weighted) before being summed so that the errors at some sample instants can be given more prominence than those at others. Thus the following cost function is minimised:

$$J = \hat{e}^T W \hat{e} \tag{A4.2}$$

where W is a diagonal matrix of weights. If Q is a diagonal matrix with elements which are the square roots of those in W, equation (A4.2) can be rewritten:

$$\begin{aligned} J &= \hat{e}^T Q^T Q \hat{e} \\ \text{or} \quad J &= \hat{e}^{*T} \hat{e}^* \\ \text{where} \quad \hat{e}^* &= Q\hat{e} \end{aligned} \tag{A4.3}$$

Thus from equation (A4.1):

$$\begin{aligned} \hat{e}^* &= Qy - Q\Psi\hat{\theta} \\ \hat{e}^* &= y^* - \Psi^*\hat{\theta} \end{aligned} \tag{A4.4}$$

The cost function in equation (A4.3) can be minimised in the same way as for ordinary least squares. Hence substituting for $\hat{e}^*$ using equation (A1.4), and differentiating with respect to $\hat{\theta}$:

$$\frac{\partial J}{\partial \hat{\theta}} = -2\Psi^{*T}y^* + 2\Psi^{*T}\Psi^*\hat{\theta} \tag{A4.5}$$

Setting to zero to minimise gives the batch weighted least squares estimate:

$$\begin{aligned} \hat{\theta} &= [\Psi^{*T}\Psi^*]^{-1}\Psi^{*T}y^* \\ \hat{\theta} &= [\Psi^T W \Psi]^{-1}\Psi^T W y \end{aligned} \tag{A4.6}$$

A4.3 Recursive weighted least squares

The recursive form of the estimator will now be derived. If equation (A4.6) is based on data up to and including sample instant t, it can be expressed as:

$$\hat{\theta}_t = P^*_t q_t \tag{A4.7}$$

where

$$\begin{aligned} P_t^* &= [\Psi(t)^T W(t) \Psi(t)]^{-1} \\ P_t^{*-1} &= \sum_{i=d+1}^{t} \psi_i w_i \psi_i^T \\ P_t^{*-1} &= P_{t-1}^{*-1} + \psi_t w_t \psi_t^T \end{aligned} \tag{A4.8}$$

and

$$\begin{aligned} q_t &= \Psi(t)^T W(t) y(t) \\ q_t &= \sum_{i=d+1}^{t} \psi_i w_i y_i \\ q_t &= q_{t-1} + \psi_t w_t y_t \end{aligned} \tag{A4.9}$$

In these equations w_i is a weight forming element ii in matrix W.

Equations (A4.7), (A4.8) and (A4.9) are the basis of a recursive estimator as only the current data and the values of P^* and q from the previous step are required to update the estimate. The equations can be rationalised by substituting (A4.9) into (A4.7):

$$\begin{aligned} \hat{\theta}_t &= P_t^*(q_{t-1} + \psi_t w_t y_t) \\ \hat{\theta}_t &= P_t^*(P_{t-1}^{*-1}\hat{\theta}_{t-1} + \psi_t w_t y_t) \\ \hat{\theta}_t &= P_t^*(P_t^{*-1} - \psi_t w_t \psi_t^T)\hat{\theta}_{t-1} + P_t^* \psi_t w_t y_t \\ \hat{\theta}_t &= \hat{\theta}_{t-1} + k_t(y_t - \psi_t^T \hat{\theta}_{t-1}) \end{aligned} \tag{A4.10}$$

where

$$k_t = P^*_t \psi_t w_t \tag{A4.11}$$

The matrix inversion to get P^*_t from equation (A4.8) can be avoided by rearranging the equation using the matrix inversion lemma (Norton, 1986), giving:

$$P^*_t = P^*_{t-1} - \frac{P^*_{t-1}\psi_t \psi_t^T P^*_{t-1} w_t}{1 + \psi_t^T P^*_{t-1} \psi_t w_t} \tag{A4.12}$$

Thus equations (A4.10), (A4.11) and (A4.12) form the recursive weighted least squares estimator. However the weights remain to be chosen. A common choice for an adaptive estimator is weights which exponentially increase with time, i.e.:

$$w_t = \frac{w_{t-1}}{\lambda} \tag{A4.13}$$

where λ is a constant which satisfies $0 < \lambda < 1$, known as the forgetting factor. By putting $P_t = w_t P^*_t$, equations (A4.11) and (A4.12) can be rewritten:

$$k_t = P_t \psi_t \tag{A4.14}$$

$$P_t = \frac{1}{\lambda}\left(P_{t-1} - \frac{P_{t-1}\psi_t \psi_t^T P_{t-1}}{\lambda + \psi_t^T P_{t-1} \psi_t}\right) \tag{A4.15}$$

These two equations are often used as they stand, but a further computational saving can be made as shown below. Substituting (A1.15) into (A1.14):

$$k_t = \frac{1}{\lambda}\left(\frac{P_{t-1}\psi_t(\lambda + \psi_t^T P_{t-1}\psi_t) - P_{t-1}\psi_t\psi_t^T P_{t-1}\psi_t}{\lambda + \psi_t^T P_{t-1}\psi_t}\right)$$

$$k_t = \frac{P_{t-1}\psi_t}{\lambda + \psi_t^T P_{t-1}\psi_t} \qquad \text{(A4.16)}$$

and hence

$$P_t = \frac{P_{t-1} - k_t\psi_t^T P_{t-1}}{\lambda} \qquad \text{(A4.17)}$$

The complete recursive estimator is given by equations (A4.10), (A4.16) and (A4.17).

A4.4 Square root algorithm

The square root approach to updating P_t ensures that it remains positive definite in the face of rounding errors. The method due to Potter is as follows (Ljung and Söderström, 1983):

$$\left.\begin{aligned} c_t &= \lambda + \psi_t^T P_{t-1}\psi_t \\ S_t &= \frac{1}{\sqrt{\lambda}}\left(S_{t-1} - \frac{P_{t-1}\psi_t\psi_t^T S_{t-1}}{c_t + \sqrt{c_t\lambda}}\right) \\ P_t &= S_t S_t^T \end{aligned}\right\} \qquad \text{(A4.18)}$$